

Ministry of Natural Resources

34

CLIMATE
CHANGE
RESEARCH
REPORT
CCRR-34



*Responding to
Climate Change
Through Partnership*

Effects of a Changing Climate on Peatlands in Permafrost Zones: A Literature Review and Application to Ontario's Far North



Sustainability in a Changing Climate: An Overview of MNR's Climate Change Strategy (2011-2014)

Climate change will affect all MNR programs and the natural resources for which it has responsibility. This strategy confirms MNR's commitment to the Ontario government's climate change initiatives such as the Go Green Action Plan on Climate Change and outlines research and management program priorities for the 2011-2014 period.

Theme 1: Understand Climate Change

MNR will gather, manage, and share information and knowledge about how ecosystem composition, structure and function – and the people who live and work in them – will be affected by a changing climate.

Strategies:

- Communicate internally and externally to build awareness of the known and potential impacts of climate change and mitigation and adaptation options available to Ontarians.
- Monitor and assess ecosystem and resource conditions to manage for climate change in collaboration with other agencies and organizations.
- Undertake and support research designed to improve understanding of climate change, including improved temperature and precipitation projections, ecosystem vulnerability assessments, and improved models of the carbon budget and ecosystem processes in the managed forest, the settled landscapes of southern Ontario, and the forests and wetlands of the Far North.
- Transfer science and understanding to decision-makers to enhance comprehensive planning and management in a rapidly changing climate.

Theme 2: Mitigate Climate Change

MNR will reduce greenhouse gas emissions in support of Ontario's greenhouse gas emission reduction goals. Strategies:

- Continue to reduce emissions from MNR operations through vehicle fleet renewal, converting to other high fuel efficiency/low-emissions equipment, demonstrating leadership in energy-efficient facility development, promoting green building materials and fostering a green organizational culture.

- Facilitate the development of renewable energy by collaborating with other Ministries to promote the value of Ontario's resources as potential green energy sources, making Crown land available for renewable energy development, and working with proponents to ensure that renewable energy developments are consistent with approval requirements and that other Ministry priorities are considered.
- Provide leadership and support to resource users and industries to reduce carbon emissions and increase carbon storage by undertaking afforestation, protecting natural heritage areas, exploring opportunities for forest carbon management to increase carbon uptake, and promoting the increased use of wood products over energy-intensive, non-renewable alternatives.
- Help resource users and partners participate in a carbon offset market, by working with our partners to ensure that a robust trading system is in place based on rules established in Ontario (and potentially in other jurisdictions), continuing to examine the mitigation potential of forest carbon management in Ontario, and participating in the development of protocols and policies for forest and land-based carbon offset credits.

Theme 3: Help Ontarians Adapt

MNR will provide advice and tools and techniques to help Ontarians adapt to climate change. Strategies include:

- Maintain and enhance emergency management capability to protect life and property during extreme events such as flooding, drought, blowdown and wildfire.
- Use scenarios and vulnerability analyses to develop and employ adaptive solutions to known and emerging issues.
- Encourage and support industries, resource users and communities to adapt, by helping to develop understanding and capabilities of partners to adapt their practices and resource use in a changing climate.
- Evaluate and adjust policies and legislation to respond to climate change challenges.

Effects of a Changing Climate on Peatlands in Permafrost Zones: A Literature Review and Application to Ontario's Far North

Jim McLaughlin^{1*} and Kara Webster^{1,2}

¹ Ontario Forest Research Institute, Ontario Ministry of Natural Resources, Sault Ste Marie, Ontario

² Present address, Canadian Forest Service, Great Lakes Forestry Centre, Sault Ste Marie, Ontario

* Corresponding author, jim.mclaughlin@ontario.ca

2013

Library and Archives Canada Cataloguing in Publication Data

McLaughlin, Jim W.

Effects of a changing climate on peatlands in permafrost zones : a literature review and application to Ontario's far north [electronic resource] / Jim McLaughlin and Kara Webster.

(Climate change research report ; CCRR-34)

Electronic monograph in PDF format.

Issued also in printed form.

Includes some text in French.

Includes bibliographical references.

ISBN 978-1-4606-1438-9

1. Peatland ecology – Ontario, Northern. 2. Peatland ecology – Hudson Bay Region. 3. Peat bog ecology – Ontario, Northern. 4. Carbon cycle (Biogeochemistry) – Ontario, Northern. 5. Carbon cycle (Biogeochemistry) – Hudson Bay Region. 6. Climatic changes – Environmental aspects – Ontario, Northern. I. Webster, Kara L. (Kara Liane), 1972 – II. Ontario. Ministry of Natural Resources. Applied Research and Development Branch. III. Title. IV. Series: Climate change research report (Online) ; CCRR-34

S592.85 M34 2013

577.687097131

C2013-964013-4

© 2013, Queen's Printer for Ontario
Printed in Ontario, Canada

Single copies of this publication
are available from:

Applied Research and Development
Ontario Forest Research Institute
Ministry of Natural Resources
1235 Queen Street East
Sault Ste. Marie, ON
Canada P6A 2E5

Telephone: (705) 946-2981
Fax: (705) 946-2030
E-mail: information.ofri@ontario.ca

Cette publication hautement spécialisée *Effects of a Changing Climate on Peatlands in Permafrost Zones: A Literature Review and Application to Ontario's Far North* n'est disponible qu'en Anglais en vertu du Règlement 411/97 qui en exempte l'application de la Loi sur les services en français. Pour obtenir de l'aide en français, veuillez communiquer avec le ministère de Richesses naturelles au information.ofri@ontario.ca.

Abstract

The Far North of Ontario encompasses 45.2 million hectares of land, with peatlands—defined here as non-forested bogs and fens—as the dominant land class, accounting for nearly 50% of the landscape and storing approximately 36 Gt (1 Gt = 10^{15} g) of carbon. The Hudson Bay Lowlands (HBL) account for nearly 50% of the land area and stores about 75% of the peatland carbon in the Far North. The HBL is the largest peatland complex with the southernmost distribution of non-alpine permafrost in North America. More than 75% of the HBL occurs in Ontario, where the provincial Far North Act mandates that the vulnerability of ecosystems to climate change, and their carbon storage and sequestration potential, be considered in land use planning. Because peatlands account for nearly 75% of the HBL landscape, we reviewed the peatland literature and identified peatland succession, permafrost thaw, hydrology, and fire as potential climate change indicators that drive peatland carbon budgets. As well, remote sensing can be used to scale these indicators to estimate current and project future states of the HBL landscape and the strength of its carbon sink. We propose two hypotheses of potential climate change effects on peatland carbon in the HBL: (1) in northern ecoregions accelerated permafrost thawing and wetter peat enhances methane emissions and (2) in southern ecoregions increased evapotranspiration and drier peat accelerates carbon dioxide losses through peat decomposition (and possible fire). We also propose a climate change vulnerability and adaptation assessment framework for HBL peatlands and discuss challenges to its development and application in land use planning.

Resumé

Effets d'un climat changeant sur les tourbières dans les zones pergélisolées : Revue de la littérature et application au Grand Nord de l'Ontario

Le Grand Nord de l'Ontario englobe 45,2 millions d'hectares de terres, dont la majeure partie, soit près de 50 p. 100 de la surface terrestre de la région, est formée de tourbières – définies ici comme étant les baissières et les marais non boisés – lesquelles stockent environ 36 Gt (1 Gt = 10^{15} g) de dioxyde de carbone. Les basses-terres de la baie d'Hudson (BTBH) représentent près de 50 p. 100 de ce territoire et stockent environ 75 p. 100 du carbone séquestré par les tourbières du Grand Nord. Les BTBH constituent la zone de tourbières la plus vaste, située le plus au sud du pergélisol non alpin en Amérique du Nord. Plus de 75 p. 100 des BTBH se trouvent en Ontario, où la *Loi de 2010 sur le Grand Nord* provinciale exige que l'aménagement du territoire tienne compte de la vulnérabilité des écosystèmes au changement climatique, de même que de leur potentiel de séquestration et de stockage du dioxyde de carbone. Vu que les tourbières forment près de 75 p. 100 de la superficie des BTBH, nous avons étudié la littérature pertinente et repéré la succession écologique des tourbières, le dégel du pergélisol, l'hydrologie et les incendies comme indicateurs possibles du changement climatique et de son influence sur le bilan de carbone des tourbières. Par ailleurs, la télédétection peut servir à hiérarchiser ces indicateurs, de sorte à pouvoir estimer l'état présent et prévisionnel des BTBH et de leur robustesse en tant que puits de carbone. Nous proposons deux hypothèses concernant les effets possibles du changement climatique sur le dioxyde de carbone stocké dans les tourbières des BTBH : (1) l'accélération du dégel du pergélisol et l'humidité accrue des tourbières accroît les émissions de méthane dans les écorégions les plus au nord et (2) l'évapotranspiration des tourbières et leur plus grande sécheresse accélère les pertes de dioxyde de carbone liée à la décomposition des tourbières (voire à des incendies) dans les écorégions les plus au sud. Nous proposons aussi un cadre d'évaluation de la vulnérabilité et de l'adaptation au changement climatique des tourbières des BTBH, et nous discutons des obstacles à son perfectionnement et son application aux fins de l'aménagement du territoire.

Acknowledgements

Support for this project was provided by the Ontario Ministry of Natural Resources' Applied Research and Development Branch under the auspices of projects CC-008 and CC-021, and Far North Branch under the auspices of project FNIKM 028, to McLaughlin and Natural Resources Canada-Canadian Forest Service A-base to Webster. The authors also thank Lisa Buse, Sandra Wawryszyn, Benoit Hamel, Trudy Vaitinen, Ngaire Eskelin, John Ralston, Adam Kinnunen, Mark Crofts, Sheri-Ann Kuiper, Ravi Kanipayor, and Paul Gray for their assistance with various aspects of the project.

I. Acronyms

AFFES – Aviation, Forest Fire and Emergency Services
 ALL – allogenic
 ALT – active layer thickness
 AMSR – advanced microwave sensing radiometer – Earth observing system
 ASAR – advanced synthetic aperture radar
 AUT – autogenic
 AVHRR – advanced very high resolution radiometer
 BERN-CC – Bern Carbon Cycle-Climate Model
 BREB – Bowen ratio energy balance
 C – carbon
 CAI – cellulose absorption index
 CALM – Circumpolar Active Layer Monitoring program
 CASI – compact airborne spectrographic imager
 CCSMS - Community Climate System Model
 CCSR – Japanese Center for Climate Research Studies
 CGCM – Canadian Global Climate Model
 CLIMBER2 - Coupled Climate-Carbon Cycle Model
 CM2C – climate model version 2
 CM4 – climate model version 4
 CPZ – continuous permafrost zone
 CRCM – Canada Regional Climate Model
 CSIRO – Australian Commonwealth Scientific and Industrial Research Organization
 DEM – digital elevation model
 DIC – dissolved inorganic carbon
 DMSP – Defense Meteorological Satellite Program
 DNDC – denitrification and decomposition
 DOC – dissolved organic carbon
 DPZ – discontinuous permafrost zone
 ECHAM4 – German Max-Planck-Institut für Meteorologie
 EM – electromagnetic induction mapping
 ER – ecosystem respiration
 ERS – European remote sensing
 ERT – electrical resistivity tomography
 ET – evapotranspiration
 ET_a – actual evapotranspiration
 ET_p – Potential evapotranspiration
 ETM+ – Enhanced Thematic Mapper Plus
 FPTGC – federal, provincial, and territorial governments of Canada
 FRCGC – The Frontier Research Center for Global Change
 GCM – general circulation model

GEP – gross ecosystem photosynthesis
GFDL – United States Geophysical Fluid Dynamics Laboratory
GHG – greenhouse gas
GPR – ground penetrating radar
GWP – global warming potential
HadCM3 – Hadley British Climate Model Version 3
HBL – Hudson Bay Lowlands
HJUB – Hudson-James-Ungava bays
IGSM - Integrated Global Systems Model
IPSL – Institut Pierre Simon Laplace
IPZ – isolated permafrost zone
JBL – James Bay Lowland
JSBACH – Jena Scheme for Biosphere-Atmosphere Coupling in Hamburg
LAI – leaf area index
LIDAR – light detection and ranging airborne images
LORCA – long-term rate of carbon accumulation
LULUCF – land use, land use change and forestry
LPJ – Lund-Postdam-Jena Dynamic Global Model
MAAT – mean annual air temperature
MAGT – mean annual ground temperature
MAP – mean annual precipitation
MIRCO3.2 – Model for Interdisciplinary Research on Climate
MIR – Mid-infrared
MODIS – Moderate resolution imaging spectroradiometer
MPI – Max Planck Institute for Meteorology
mTMF – mixed tune match filtering
MWM – McGill Wetland Model
N – nitrogen
NCAR – United States Center for Atmospheric Research
NDVI – normalized difference vegetation index
NEE – net ecosystem exchange
NEST – northern ecosystem soil temperature
NIR – near infrared
NOAA – National Oceanic and Atmospheric Administration
NPP – net primary production
NSCAT – NASA scatterometer
ORCHIDEE – Organizing Carbon and Hydrology in Dynamic Ecosystems Model
P – precipitation
PAN – panchromatic
PCI – peatland cover index
PFT – plant functional type
PISCES – Pelagic Interactions Scheme for Carbon and Ecosystems Studies

POC – particulate organic carbon
Q* – net radiation
Q_b – heat flux through bottom of the lake
Q_e – latent heat flux
Q_h – sensible heat flux
Q_g – ground heat flux
Q_w – lake heat storage
RECA – recent rate of carbon accumulation
R – runoff
S – sulphur
SAR – synthetic aperture radar
SiBCASA - Simple Biosphere/Carnegie-Ames-Stanford Approach Model
Sim-CYCLE - Simulation model of Carbon Cycle in Land Ecosystems
SLAVE – Scheme for Large-Scale Atmosphere Vegetation Exchange
SOC – soil organic carbon
SPOT – System Pour Observation de la Terre
SPZ – sporadic discontinuous permafrost zone
SSM/I – special sensor microwave/imager
SMMR – scanning multichannel microwave radiometer
SWIR – shortwave infrared
TEM – Terrestrial Ecosystem Model
TIR – thermal infrared
TM – thematic mapper
TRIFFID – Top-Down Representation of Interactive Foliage and Flora Including Dynamics
TTOP – temperature at top of permafrost
UMD – University of Maryland
UVic – University of Victoria
VEGAS – VEgetation Global Atmosphere and Soil Model

Sample notation meaning

IPSL-CM4-LOOP-PISCES-ORCHIDEE comprises a coupling among the IPSL-CM4 model and two carbon cycle models: PISCES ocean biogeochemical model and ORCHIDEE terrestrial biogeochemical model

II. Scientific Notation

Al^{3+} – aluminium ion

^{13}C and ^{14}C – stable- and radio-isotopes of carbon, respectively

CH_4 – methane

CO_2 – carbon dioxide

HCO_3 – bicarbonate

Gt – gigatonne

H^+ – hydrogen ion

H_2 – hydrogen

H_2CO_3 – carbonic acid

MJ m^3 – megajoule per cubic metre

^{210}Pb – lead radiotracer

pH – measure of acidity/alkalinity of a substance

SO_4^{2-} – sulphate ion

$\delta^2\text{H}$ – isotope of hydrogen

$\delta^{18}\text{O}$ – isotope of oxygen

Wm^{-2} – watts per square metre

μm – wavelength

dB – decibels

GHz – gigahertz

BP – before present

Mt – megaton

Pg – petagram

Example meaning of notation

Tg C yr⁻¹ – teragram of carbon per year

III. Relevant Peatland Carbon Terminology

Successful communication among researchers, policymakers, and land managers requires common terminology.

For this report, we defined **peat carbon content** as mass of C contained in a unit area (e.g., kg C m²) of dry peat. **Carbon content** was calculated as the product of C concentration, peat bulk density, and sample increment thickness. **Peat C storage** was defined as the product of C content and area of peatland in a landscape. **Carbon dioxide sequestration** was defined as short-term (annual to decadal) balance of atmospheric CO₂ uptake by plants and its release through plant respiration and organic matter decomposition. Carbon dioxide sequestration is commonly measured using gas flux chambers and eddy covariance flux towers. **Carbon accumulation** was defined as net C gain in peat at century to millennial scales. **Peat C accumulation** is measured by: (1) dating of surface peat with specified tracers, such as ^{210}Pb and ^{137}Cs that provide decadal to century (e.g., 50 to 200 years) timescales of peat accumulation [e.g., recent C accumulation (RECA) rates; Oldfield et al. 1995] and (2) radiocarbon (^{14}C) dating of basal peat and peat profile age/depth relationships to estimate century to millennial C accumulation [e.g., long-term C accumulation (LORCA); Kuhry 1994] rates. These rates are considered apparent because without intensively dating individual peat cores and identifying wetness using paleoecological indicators, timelines for and causes of LORCA changes during peatland development cannot be inferred (Yu 2012). However, differentiating sequestration from accumulation is critical in climate change vulnerability assessments because CO₂ sequestration in plant biomass and surface litter does not equate to long-term C accumulation as peat.

Contents

Abstract	i
Resumé	ii
Acknowledgements	ii
I. Acronyms	iii
II. Scientific notation	vi
III. Relevant peatland carbon terminology	vi
1. Introduction	1
2. Peatland development and plant associations	2
3. Permafrost patterns	3
4. Peatland hydrology	4
5. Peatland carbon cycling	4
6. Fire regimes	6
7. Mapping, monitoring, and modelling permafrost peatlands	7
8. Climate change and peatland carbon in the Hudson Bay Lowlands	8
9. Uncertainties, challenges, and science priorities in assessing peatland carbon storage and sequestration	8
2. Peatland Development and Plant Associations	9
Background	9
Peatland types	9
Peatland classification methods	9
Bogs	10
Fens	17
Peatland succession	18
Plant functional types	18
Vegetation dynamics and peatland succession	19
Vegetation and peatland carbon accumulation relationships	26
Effects of climate change on peatland succession	28
Summary and conclusions	29
3. Permafrost Patterns	31
Background	31
Permafrost dynamics	31
Permafrost soil layers	31
Aggrading permafrost features	31
Degrading permafrost features	35
Environmental controls of permafrost dynamics	36
Temperature	36
Thaw dynamics	37
Permafrost and climate change	39
Twentieth-century permafrost dynamics	39
Twenty-first century permafrost dynamics	39
Summary and conclusions	44

4. Peatland Hydrology	45
Background	45
Water balance.....	45
Evapotranspiration	45
Energy balance in northern peatlands	48
Climate influence on evapotranspiration.....	51
Sedge wetlands.....	51
Bogs	51
Permafrost features.....	52
Upland/heath and shrub tundra	52
Runoff	52
Hydrogeological settings in large peatland complexes.....	53
Peatland hydrological connectedness.....	54
River discharge.....	57
Climate change effects on runoff	59
Twenty-first century runoff patterns.....	59
Role of permafrost in future runoff patterns	60
Summary and conclusions	61
5. Peatland Carbon Cycling	63
Background	63
Carbon accumulation and storage.....	63
Net ecosystem exchange.....	66
General patterns	66
Spatial and temporal patterns.....	70
Methane.....	72
Ponds.....	76
Dissolved carbon and nutrient export	76
Carbon and climate change	77
General patterns	77
Carbon sequestration.....	78
Vegetation and succession	78
Summary and conclusions	80
6. Fire Regimes	81
Background	81
Boreal and subarctic biome fire patterns	81
Cover types and fire dynamics.....	82
Black spruce forests	82
Peatlands.....	86
Climate change and fire behaviour	89
Coupled carbon-climate change model projections for northern (>45°N) biomes	89
Uncertainties and challenges in predicting peatland carbon.....	93
Summary and conclusions	95

7. Mapping, Monitoring, and Modelling Permafrost Peatlands	96
Background	96
Mapping permafrost peatlands and their properties	96
Remote sensing of peatlands	96
Remote sensing of vegetation using optical and near-infrared sensors	99
Mapping peatland hydrology using active and passive microwave sensors	103
Challenges and future work in mapping peatlands using remote sensing	105
Under-representation of wetland area	105
Mixed spectral signals	107
Narrow or out-of-range spectral bands	108
Changing spectral signals	108
Mapping permafrost	109
General patterns	109
Traditional methods	109
Geophysical methods	109
Remote sensing methods	110
Terrain analysis	110
Numerical modelling	111
Empirical and semi-empirical models	111
Physical models	113
Monitoring permafrost peatlands	114
Vegetation	115
Hydrology	115
Permafrost	116
Modelling permafrost peatland carbon dynamics	121
Representation of processes	122
Accuracy of regional climate drivers	122
Changes in the extent of peatlands and permafrost	122
Summary and conclusions	123
8. Climate Change and Peatland Carbon in the Hudson Bay Lowlands	124
Background	124
Hudson Bay Lowlands climate	127
Peatland succession	129
Permafrost	130
Carbon	130
Carbon accumulation	130
Climate, environmental, and microbiological controls on carbon cycling	131
Remote sensing and carbon scaling	132
Fire	132
Summary and conclusions	136
9. Uncertainties, Challenges, and Science Priorities to Assess Peatland Carbon Storage and Sequestration	137
Literature Cited	140

1. Introduction

The Far North of Ontario (located between approximately 50 and 57 °N, 79 and 94 °W) is a highly variable landscape that contains elements of arctic, boreal, and temperate biomes. It consists of 45.2 million hectares distributed relatively evenly between the Canadian Shield and Hudson Bay Lowlands (HBL) (Table 1.1). Peatlands—defined here as non-forested bogs and fens—are the dominant land class in the Far North, accounting for approximately 21 million hectares, or 47%, of the landscape. Peatlands here store about 36 Gt (1 Gt = 1 Pg = 10¹⁵g) of carbon (C) as peat (Far North Science Advisory Panel 2010), which is approximately one-quarter of the C stored in all of Canada's peatlands. The HBL, accounting for three fourths of the C stored in the Far North, is the largest peatland complex in North America and second largest in the world (Martini 2006). This region provides many economic opportunities, as well as a variety of ecosystem services; such as water storage, stream flow regulation, water quality, and biodiversity. By steadily accumulating C, peatlands in the HBL also perform an important climate-regulating ecosystem service, one that has been ongoing since their inception following deglaciation.

Bill 191, the Far North Act (http://www.ontla.on.ca/bills/bills-files/39_Parliament/Session2/b191ra.pdf), which achieved Royal assent in October 2010 includes a land use planning goal of “protecting the unique ecology and vast boreal environment of the Far North of Ontario while enabling the region's resources to contribute to a more prosperous, healthy and sustainable future for its people, communities, and the entire province.” The act describes five land use planning objectives, one of which is “the maintenance of biological diversity, ecological processes and ecological functions, including the storage and sequestration of carbon in the Far North.” It also requires the Ontario Ministry of Natural Resources (MNR) to develop eight policy statements, one of which concerns “Ecological systems processes and functions, including considerations for cumulative effects and for climate change adaptation and mitigation.” Achieving the Act's planning objective and developing the required policy statement for land use planning requires an understanding of how climate change affects C storage and sequestration in local and regional landscapes. For example, important controls of C storage and sequestration in the Far North are soil temperature regimes, permafrost presence, hydrological processes, and vegetation community structure, all of which are regulated by interactions among isostatic rebound, air temperature, and precipitation amounts. Permafrost is defined as subsurface earth materials, including mineral and organic soil, rock, and ice, that remain below 0 °C for two or more consecutive years (Brown 1967).

Peatlands in the HBL have been important in Holocene climate cooling because since deglaciation they have sequestered large amounts of atmospheric carbon dioxide (CO₂) (van Bellen et al. 2011, Bunbury et al. 2012). However, when disturbed these peatlands may release large quantities of this CO₂ back to the atmosphere, which may speed global warming (Frolking et al. 2006, Tarnocai 2006). Air temperature and precipitation changes may enhance permafrost thawing, which can alter ecological processes and functions, including: (1) plant community structure and peatland succession (Klinger and Short 1996, Benscoter et al. 2005) and (2) evapotranspiration (ET), water runoff (Boike et al. 1998, Woo and Young 2006), and subsequent C sequestration (Tarnocai 2006, Schuur et al. 2007, Turetsky et al. 2007) and global warming potential [GWP: CO₂ plus methane (CH₄)] fluxes (Wickland et al. 2006, Prater et al. 2007).

In addition to the potential effects of climate change, multiple economic opportunities such as mining and alternative energy (bioenergy and hydroelectric power) exist in the HBL, as well as the Far North as a whole (Far North Science Advisory Panel 2010). Moreover, ‘managed wetlands,’ in which management includes mining and alternative energy, may become important to provincial and national C accounting for land use, land use change and forestry (LULUCF) in future international agreements (IPCC 2007). Developing and implementing sustainable land use plans requires an understanding of how interactions between land use practices and climate change control peatland C cycling across landscapes. However, understanding of, and projections for, peatland conditions across permafrost zones in the HBL, and Far North in general, are limited by lack of empirical data. As such, research on and monitoring of climate and management controls on peatland C across the Far North is needed.

In this report, we summarize current knowledge of processes occurring across permafrost zones in peatlands, focusing on peatland development and plant associations (section 2), permafrost patterns (section 3), peatland hydrology (section 4), peatland carbon cycling (section 5), fire regimes (section 6), and approaches for mapping,

monitoring, and modelling permafrost peatlands (section 7). In section 8, climate change and peatland carbon in the Hudson Bay Lowlands, we summarize what is known about peatlands in permafrost zones specific to the HBL. In section 9, about uncertainties, challenges, and science priorities in assessing peatland carbon storage and sequestration, we identify research and monitoring needs related to land use planning in this region in a changing climate. Below we briefly introduce these topics and identify the specific goals of each section.

Table 1.1. General physical and biological characteristics and ecological processes of Ontario's Far North (adapted from OMNR 2010).

Description	Far North (Total)	Canadian Shield	Hudson Bay Lowlands
Physical and biological			
Total area (million ha)	45.2	20.6	24.6
Open water (%)	10	13	7
Marsh (freshwater and tidal) (%)	0.3	0	0.5
Bog and fen (%)	47	20	69
Tundra, palsas, and peat plateau (%)	0.6	0.0	1.0
Forest, woodland, and swamp (%)	35	53	20
Rock barren (%)	0.2	0.5	0
Burns and early regeneration (%)	7	12	2
Ecological processes			
Total stored peatland carbon (billion tons)	35.3	9.3	26.0
Estimated stored forest carbon (billion tons)	2.6	-	-
Estimated annual stored carbon (million tons)	3.36	-	-
Wildfires (average area burned from 1980-2007) (ha)	150,000	125,000	25,000

2. Peatland development and plant associations

Peatland development occurs via two processes (Lavoie et al. 2005, Simard et al. 2009): terrestrialization (filling in of ponds and lakes by peat accumulation) and paludification (lateral spreading of peat-forming mosses). Terrestrialization is important in confined basins and thermokarst features (see section 3, Permafrost Patterns for definitions), including collapse scars, ponds, and lakes (NWWG 1997). Paludification dominates peatland formation in unconfined basins and is the most important peat-forming process in the HBL (Simard et al. 2009).

Peatlands have developed since deglaciation, with peat accumulation dominating during periods of inundation due to more precipitation or flooding (Arlen-Pouliot and Bhiry 2005). Peat and C accumulation then steadily decreased as peatlands dried. Studies in western Canada indicate that recent (i.e., past 1,000 years) C accumulation continues to decrease significantly (Kuhry 1994). In contrast, results from eastern Canada are inconsistent, with increased (Turunen et al. 2004, Bunbury et al. 2012) and decreased (van Bellen et al. 2011) recent C accumulation rates reported. These differences may be the result of increasing atmospheric nitrogen (N) deposition and warmer temperatures enhancing peatland C accumulation rates in boreal relative to subarctic regions (Vitt et al. 2003, Turunen et al. 2004). However, the subarctic biome may be experiencing wetter peat than in the past, also enhancing C accumulation rates (Bunbury et al. 2012). Differences in recent peatland C accumulation rates have been correlated with presence of plant functional types (PFTs), with sedges, tall shrubs, and wet-adapted *Sphagnum* mosses correlated with rapid C accumulation rates. In contrast, trees (e.g., black spruce, *Picea mariana*), dwarf shrubs, and dry-adapted *Sphagnum* mosses have been correlated with low C accumulation rates (Arlen-Pouliot and Bhiry 2005).

Air and soil warming affects vegetation communities directly through temperature effects on photosynthesis and indirectly by altering soil acidity, nutrient availability, and permafrost features (Camill 1999a, Beilman 2001, Schuur et al. 2007). Understanding these responses is important to predict future C storage and sequestration resulting from environmental changes in permafrost regions (Camill 2000, Vitt et al. 2000b).

Combining charcoal, radiocarbon (^{14}C), macrofossil, and pollen analyses allows relationships to be established among plant associations, hydrology, fire, permafrost features, and C accumulation (Kuhry 2008). These

relationships have been used to identify the general sequence of peatland succession from open water to marsh (saltwater or freshwater) to fen and eventually to bog (Kuhry 1994, Camill et al. 2009) and provide estimates for apparent long-term C accumulation rates (LORCA) across northern peatlands (Gorham et al. 2003, Tarnocai and Stolbovoy 2006). Coupling stratigraphic studies with those of vegetation and C sequestration on current landscapes will increase the certainty of model projections and spatial scaling of peatland C storage and sequestration to confidently prescribe land use plans. Therefore, in this section, we explore the role of vegetation in peatland C dynamics by (1) peatland type, including general peatland characteristics and classification methods, and bog and fen vegetation and biogeochemical characteristics; (2) peatland succession, including plant functional types (PFTs) and peatland C accumulation relationships; and (3) effects of climate change on peatland succession, including the effects of temperature and water table and soil moisture levels on peatland vegetation structure.

3. Permafrost patterns

Using physiographic and climatic data, Heginbottom et al. (1995) divided Canada into five permafrost zones based on the amount of area underlain by permafrost (Figure 1.1a):

- Continuous permafrost: >90%
- Extensive discontinuous permafrost: 51 to 90%
- Sporadic discontinuous permafrost: 11 to 50%
- Isolated permafrost patches: 1 to 10%
- No permafrost: 0%

Within those zones, permafrost exists as a variety of features (Table 1.2), each with unique hydrology (Washburn 1980). Pingos and polygonal peatlands are common in the continuous permafrost zone (CPZ), while internal lawns are generally restricted to the discontinuous permafrost zone (DPZ). The remaining features occur in both permafrost zones.

Mean annual air temperature (MAAT) and permafrost distribution are correlated (Brown 1967, Anisimov and Nelson 1996, Smith and Riseborough 2002). The CPZ occurs north of the $-8\text{ }^{\circ}\text{C}$ MAAT isotherm, which is commonly associated with mean annual ground temperature (MAGT) colder than $-5\text{ }^{\circ}\text{C}$ (Figure 1.1a, b). The transition between the CPZ and the northern (i.e., extensive) DPZ occurs between MAATs of -6 to $-8\text{ }^{\circ}\text{C}$ and MAGTs between -2 and $-5\text{ }^{\circ}\text{C}$, with the DPZ extending south to a MAAT of about $-1\text{ }^{\circ}\text{C}$ and ground surface temperatures warmer than $-2\text{ }^{\circ}\text{C}$. Permafrost is generally absent at sites with mineral soil at MAATs above $-2\text{ }^{\circ}\text{C}$, but can persist in organic soils at MAATs of 1 to $1.5\text{ }^{\circ}\text{C}$ (Brown 1967).

Table 1.2. Features common in the continuous (CPZ) and discontinuous (DPZ) permafrost zones in Ontario's Far North.

Permafrost feature	Characteristics	Zone of occurrence
Aggrading to mature		
Pingo	Land elevated due to ice-wedge growth	CPZ
Polygonal peatland	Land elevated due to cracks in shrinking permafrost	CPZ
Palsa	Peat elevated due to ground ice expansion; ice penetration into mineral sediment	CPZ, DPZ
Peat plateau	Peat elevated due to ground ice expansion; ice core only in peat; coalesced palsas	CPZ, DPZ
Lithalsa	Mineral sediment elevated due to ground ice expansion	CPZ, DPZ
Degrading		
Thermokarst		
Pond	Surface inundated due to ice melt	CPZ, DPZ
Thaw lake	Ground collapsed following thawing of ground ice in regions underlain by permafrost resulting in shallow body of water	CPZ, DPZ
Internal lawn	Area inundated outside peat plateau or palsa due to melting of ice	DPZ
Collapse scar	Internal regions of a peat plateau collapse where ice has melted	CPZ, DPZ
Talik	Patch of permanently unfrozen ground underneath thaw lakes	CPZ, DPZ

Although MAAT provides a good indication of where permafrost is expected to occur, the relationship between climate and ground temperature is relatively complex and data describing climate, ground temperature, and related permafrost dynamics are sparse. For example, in the DPZ, local variations in vegetation, topography, snow cover, and soil conditions result in differences in MAGT that contribute significantly to the presence or absence of permafrost (Riseborough 2002, Zhang 2005). These local variations are referred to as *n* (nival)-factors. When MAAT is within a few degrees of 0 °C (i.e., southern DPZ), the *n*-factors thought to be primarily responsible for permafrost occurrence are variations in snow cover and peatland area (and its vegetation cover) (Smith and Riseborough 2002, Overduin et al. 2006). In addition to influencing distribution, *n*-factors control the active layer thickness (ALT) of permafrost (Boike et al. 2008). This layer is where most of the processes, such as biogeochemical cycles, water flow, and trace gas exchange with the atmosphere occur, which in turn control C balances (Hinkel et al. 2001, Woo and Young 2006). In the permafrost patterns section, we discuss aggrading and degrading permafrost features, their controlling processes, and responses to changes in climate.

4. Peatland hydrology

Peatlands in permafrost zones are characterized by cold, frozen, and waterlogged soils with low decomposition rates and thick organic deposits, constituting unique hydrologic features. For example, because it has low water storage capacity, frozen peat promotes shallow water flow paths to draining streams and lakes (Hayashi et al. 2004). In contrast, thawed peat has deeper water flow paths and higher water storage capacity that supports evapotranspiration (ET). Climate change is expected to affect peatland hydrology via permafrost degradation (Anisimov and Nelson 1996), increased ET rates (Rouse 1998), reduced soil moisture storage (Riordan et al. 2006), and deeper or modified groundwater flow paths (Quinton et al. 2005). In addition, the amount, nature, and seasonal timing of precipitation may change, further affecting peatland ET and runoff rates (Gagnon and Gough 2005).

Hydrologic changes directly and indirectly affect local and regional C budgets through effects on photosynthesis (Hobbie et al. 2000, Malmer et al. 2005), peat decomposition (Hobbie et al. 2000, Rodinow et al. 2006, Uhlirva et al. 2007), and the forms and amounts of C (e.g., CO₂, CH₄, dissolved organic C – DOC, and dissolved inorganic C – DIC) (Kawahigashi et al. 2004, Corradi et al. 2005, Dutta et al. 2006) released from peatlands. Hydrology is also important in regional C dynamics, influencing fire frequency, area burned, and severity, and potentially enhancing CO₂ emissions through peat combustion. Therefore, understanding and projecting climate change effects on peatland C in permafrost zones requires documentation of hydrologic processes and their responses to changes in climate (Gough and Leung 2002, Martini 2006).

Evidence that permafrost regions—including the Far North of Ontario—are undergoing changes in temperature and precipitation that will affect hydrology is convincing (Gough and Leung 2002, Gagnon and Gough 2005, Tarnocai 2006). For example, long-term flow records for large, non-human-affected rivers in the Hudson-James-Ungava bays (HJUB) in Canada—which includes Ontario's Far North—show decreasing annual flow trends since the 1960s (Déry et al. 2005). Furthermore, overall groundwater contribution to river flow appears to be increasing across North American permafrost zones (Walvoord and Striegl 2007, St. Jacques and Sauchyn 2009).

Changes in runoff rates in expansive peat complexes are largely the result of changes in ET (Gagnon and Gough 2005) and higher ET can dry peatlands, leading to an increase in peatland fire frequency (e.g., Turetsky et al. 2002a, 2004). To develop projections for climate change effects on Far North peatland hydrology, data are needed for water balances, flow paths, and headwater stream to large basin river discharge from various peat-dominated landscapes. In the peatland hydrology section, we provide background information about how water balances are calculated and how water flow is assessed. We further describe what's known about water balances and flows to identify gaps and uncertainties that require further study to allow better projections of the effects of climate change on hydrology in Far North peatlands.

5. Peatland carbon cycling

The northern permafrost region contains approximately 1,670 Gt C, of which 88% occurs in perennially frozen soils and deposits (Tarnocai et al. 2009). This C pool accounts for about one-half of the estimated global C pool, twice the current atmospheric C pool (730 Gt C), and more than three times the amount of global forest biomass

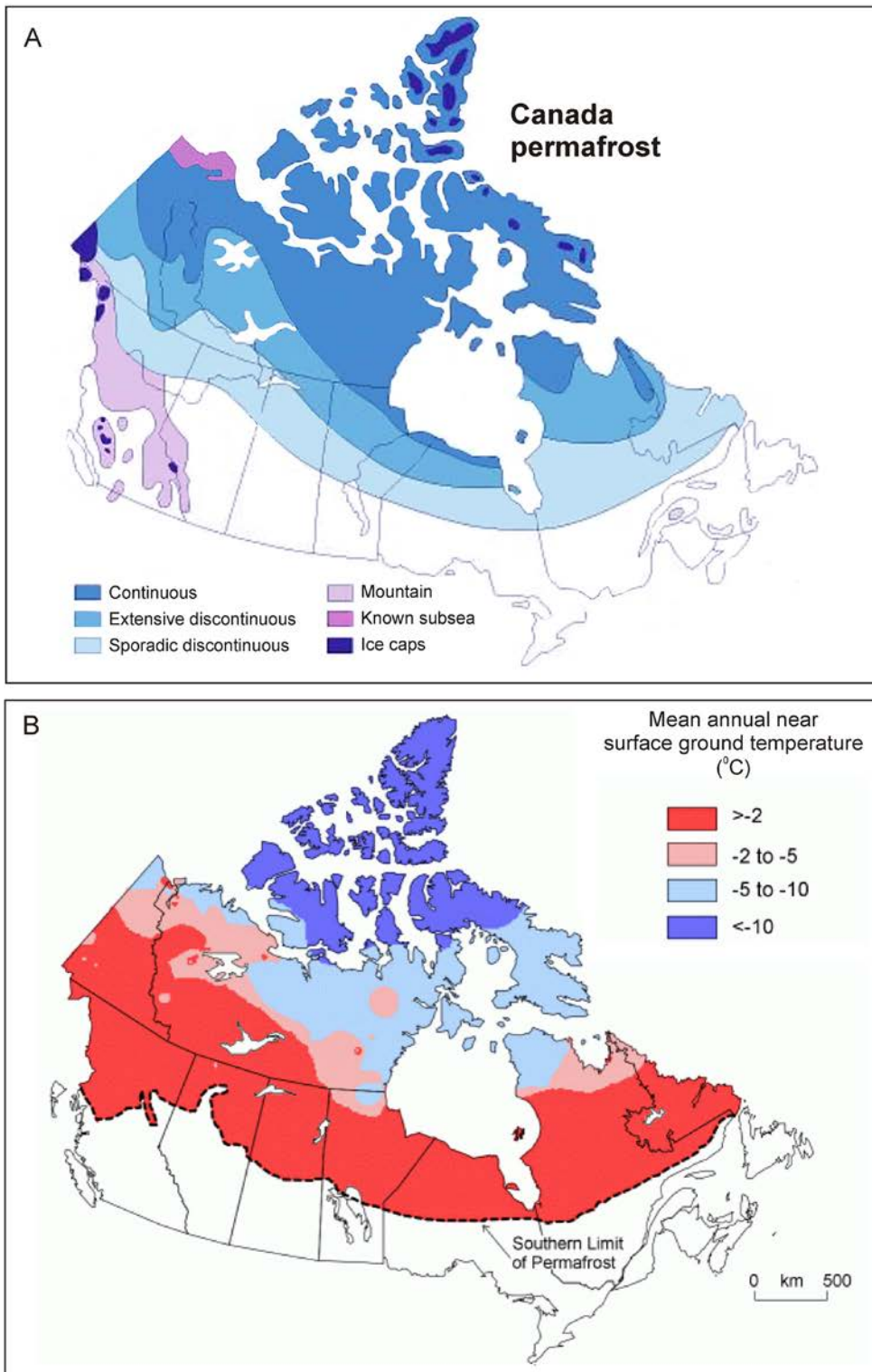


Figure 1.1. (a) Permafrost distribution across Canada illustrating permafrost zones, which are defined by the proportion of area underlain by permafrost. **(b)** Mean annual near surface temperature distribution across Canada. (Image reprinted from <http://www.socc.ca/cms/en/socc/permafrost/futurePermafrost.aspx>.)

C (450 Gt C) (Schoor et al. 2008, Tarnocai et al. 2009). Soils in the North American permafrost region contain 316 Gt C, accounting for approximately 60% of C stored in all soils in North America, and sequester approximately 11 Mt (1 Mt = 1 Tg = 10^{12} g) of C annually (Tarnocai et al. 2007). Canada's permafrost region contains 196 Gt C, of which 57% occurs in peatlands (Figure 1.2) and perennially frozen peatlands account for 42% of the peatland C pool in Canadian permafrost zones (Tarnocai et al. 2007). The CPZ stores the most C in Canada (predominately in mineral sediments); containing nearly twice as much C as the other permafrost zones (Figure 1.2). Soil C storage is relatively equal in the discontinuous, sporadic, and isolated permafrost zones but C is mainly stored in peatlands (Figure 1.2). Approximately 50% of the peatland C pool in Canada is deemed sensitive to climate change. Of this C, 57% occurs in non-permafrost and the other 43% is in permafrost peatlands (Tarnocai 2006).

Under a warming climate, release of C from permafrost to the atmosphere will occur primarily through accelerated microbial decomposition of organic matter (Schoor et al. 2008). Because C was incorporated into permafrost by different mechanisms, its quality (e.g., decomposability) varies (Zimov et al. 2006a,b; Kaiser et al. 2007). Compared to mineral soils, peat is thought to have been subjected to microbial decomposition for longer periods before being incorporated into permafrost. Therefore, C occurring in peat is likely to decompose more slowly than organic matter mixed with or adsorbed onto mineral soil surfaces (Turetsky 2004, Rodionov et al. 2006, Turetsky et al. 2007). A key unknown about the effects of climate change on permafrost thawing is the resulting amount and rate of C transfer to the atmosphere. Atmospheric emissions are controlled by the size of the C pool and continuous (microbial decomposition) and episodic (e.g., fire) processes that control the rate of C release to the atmosphere after thaw (Turetsky et al. 2004, Limpens et al. 2008). Moreover, permafrost thaw can increase DOC and particulate organic C (POC) export to aquatic environments (Hagedorn et al. 2008, Waldron et al. 2009) and DOC export from thawing permafrost may increase by 29 to 46% in future years (Frey and Smith 2005). Some of that exported DOC and POC will decompose anaerobically due to anoxic conditions in thermokarst features (e.g., collapse scars, ponds and lakes) and stimulate CH_4 fluxes to the atmosphere (Blodau et al. 2008). As such, on decadal timeframes permafrost landscapes may be a net C sink, but due to enhanced CH_4 emissions also a GWP source (Johansson et al. 2006). However, changes in CO_2 emissions will affect GWP over centuries to millennia (Frolking et al. 2006). In the peatland carbon cycling section, we discuss processes involved in (1) C accumulation and storage, (2) net ecosystem exchange of CO_2 , (3) CH_4 cycling and flux, (4) DOC and nutrient exports, and (5) peatland C and climate change.

6. Fire regimes

In North America, burning of black spruce forests accounts for most C released from fires, while peatlands account for 10 to 30% of the total C released from natural fires (Zoltai et al. 1998, Turetsky et al. 2010). Fires in western Canada emit approximately 80% of the annual C released from fires across Canada (Balshi et al. 2007). As such, literature on fire in North American peatlands and permafrost is limited primarily to western Canada and Alaska, with minimal published data on fire and forest and peat C combustion in eastern Canada. This needs to be rectified because (1) the current C sequestration potential of eastern Canadian peatlands is largely unknown and (2) increased peatland area burned and deeper peat combustion are expected to emit more C to the atmosphere in future relative to current landscapes.

Fire return intervals in temperate and boreal peatlands historically ranged from 80 to greater than 1,000 years (Zoltai et al. 1998) and are considerably longer than return intervals in neighbouring boreal forests (e.g., 50 to 500 years) (Kuhry 1994, Zoltai et al. 1998). Turetsky et al. (2004) estimated that fire return intervals of 123 and 105 years were likely for bogs and fens, respectively, in central Alberta. These shorter fire return intervals are because these continental peatlands are at the dry end of bog and fen climatic ranges. Longer fire return intervals are more consistent with the wetter Maritime climate of the HBL (Zoltai et al. 1998, Martini 2006), where area burned is low (Balshi et al. 2007).

Combustion of peat C stocks leads to large C emissions to the atmosphere. The amount of C released in a fire is a function of the area burned and peat combustion rate. Although variability in peat combustion rates is high, leading to large errors in estimated C emissions from peat fires, they appear to be important contributors to the total estimated C emissions from fire in natural systems across Canada (Zoltai et al. 1998). From the 1960s to the

1990s, the frequency of large fire events increased across western boreal and subarctic Canada, and these fires occurred progressively later in the growing season (Kasischke and Turetsky 2006). Because burning is more likely to occur during the period of maximum water table drawdown and fuel exposure peatlands may be more vulnerable to deep soil combustion (Flannigan et al. 2009). Combined with the changes in peatland C dynamics expected with changed climate, fires are anticipated to further influence climate through additions of greenhouse gases to the atmosphere, trapping additional heat. In the fire regimes section, we discuss the role of fire and its interaction with permafrost in relation to (1) boreal and subarctic biome fire patterns, including area burned, fire return intervals, and fire severity in black spruce forest and peatland cover types and (2) model projections of fire and C sequestration to identify uncertainties and challenges in assessing peatland C.

7. Mapping, monitoring, and modelling permafrost peatlands

Quantifying C pools for regional landscapes and understanding how they are affected by climate requires knowledge of (1) extent and depth of peatland distribution, (2) peatland plant species composition and its biomass and productivity, and (3) environmental drivers (e.g., climate, water table, soil temperature, and active layer depth) controlling peatland C fluxes (Klinger et al. 1994, Limpens et al. 2008). Collecting the necessary data can be achieved by direct field measurements or indirectly by airborne or satellite remote sensing (Vitt et al. 2000a,b; Beilman et al. 2009). Direct measurements provide accurate local characterization but logistical constraints and cost limit temporal and spatial sampling intensity. Furthermore, extrapolating highly detailed, fine-scale point-based measurements across vast expanses of peatland complexes does not capture regional-landscape heterogeneity, thereby biasing estimates of peatland properties (Frolking et al. 2009).

Observations from remote sensing provide detailed, non-invasive and spatially explicit data over large areas, reducing the need to extrapolate small-scale point data (Vitt et al. 2000b, Sheng et al. 2004). However, the accuracy of remote sensing for characterizing peatlands depends on the type of sensor, its resolution, and how well the resulting data represent the property of interest (Beilman et al. 2008). Use of high resolution remote sensing data is practical at local landscapes, but at regional to global scales cost and computing power become prohibitive. On the other hand, coarse resolution satellite sensors (e.g., 1° by 1° grid square) can bias estimates of peatland properties, particularly where conditions are heterogeneous (Harris and Bryant 2009a,b). This dichotomy needs to be resolved to productively map and model attributes of interest. In the mapping, monitoring, and modelling section, we explore approaches to map permafrost peatlands and discuss the role of mapping in assessing changes in permafrost biophysical properties.

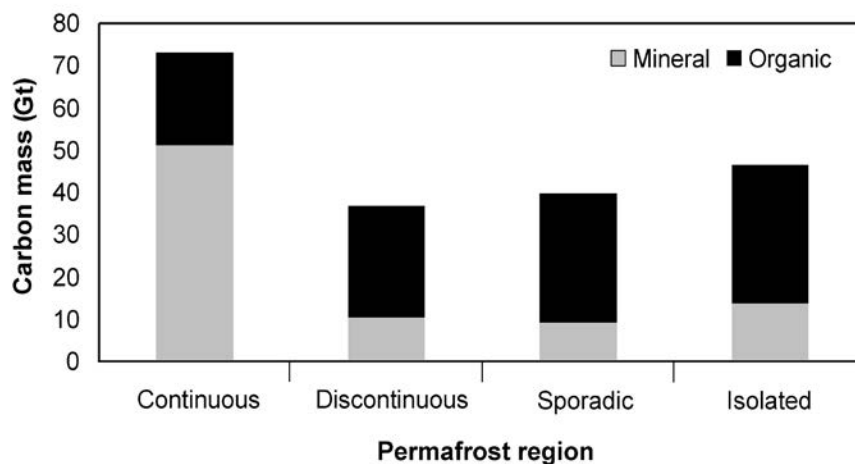


Figure 1.2. Organic carbon mass in mineral and organic layers of permafrost zones in Canada (adapted from Tarnocai et al. 2007).

8. Climate change and peatland carbon in the Hudson Bay Lowlands

Permafrost in the HBL is relatively young, with development initiated between 500 and 2000 cal yr BP (Arlen-Pouliot and Bhiry 2005, Kuhry 2008). In the HBL, MAAT is projected to rise between 2.5 and 8.0 °C, with most rapid warming occurring during the winter months in the northern HBL (Table 8.2, Figure 8.2). This is the most permafrost-dense location and models project that the HBL has already surpassed its temperature threshold for maintaining permafrost (Koven et al. 2011), or will do so by 2020 (Zhang et al. 2008). Although mean monthly precipitation varies widely, it is projected to increase in the HBL (Table 8.2). However, these increases are expected to be less than 25% of current amounts, indicating a potential overall drying of peatlands.

The HBL peatland complex is spatially diverse and composed of various types, amounts, and proportions of permafrost and non-permafrost bogs and fens and aggrading and degrading permafrost features (e.g., Zoltai 1995, Beilman 2001). To understand this heterogeneity, a combination of field, laboratory, remote sensing, and modelling studies at multiple landscapes and covering long timeframes are needed to estimate C storage and sequestration in response to changes in climate and various management regimes. Improved knowledge of spatial and temporal patterns in air temperature and precipitation trends is needed before confident assessments of future greenhouse gas (GHG; CO₂ and CH₄) exchange between peat surfaces and the atmosphere are possible. This includes temperature and precipitation interactions with permafrost thawing, successional processes, and subsequent control on ET rates. Furthermore, intensified peatland and permafrost C inventories are needed. Few inventories exist and though we have collated data from published reports and our field sites, small sample sizes result in significant variation in C storage calculations. Because of these data deficiencies, confidence in calculated current and future C storage and sequestration is low, hindering its application to Far North land use planning. In section 8, we summarize previous chapters and discuss current understanding of ecological processes, their effects on C storage and sequestration, and how this information, with data from our research sites in the HBL, can be used to successfully link peatland C science to Far North land use planning.

9. Uncertainties, challenges, and science priorities in assessing peatland carbon storage and sequestration

Achieving the Far North Act's planning objective of maintaining ecosystem processes and C storage and sequestration and developing the required policy statement for land use planning requires an understanding of how climate change affects peatland C storage and sequestration at landscape scale. In section 9, we discuss current capacity to assess permafrost, ET and peat wetness, and PFTs as scalable climate change indicators that drive peatland C budgets. We further discuss uncertainties and challenges that impede the use of climate and C indicators in climate change vulnerability and adaptation assessments. We end the report by emphasizing that data limitations in (1) air temperature and precipitation effects on permafrost thaw, successional processes, ET, and subsequent GHG exchange between peat surfaces and the atmosphere, and (2) intensified peatland and permafrost C inventories must be overcome before confident projections of long-term peatland C sink strengths are possible, and peatland climate change vulnerability and adaptation assessment can be completed with acceptable levels of uncertainty.

2. Peatland Development and Plant Associations

Background

Net C accumulation in peatlands has primarily been a function of cold and waterlogged soils, but this may change as peatlands warm and dry in future years, in part due to changes in plant communities (Riutta et al. 2007). Warmer and drier conditions across North America, Scandinavia, and Russia have contributed to increases in shrubs and trees at the expense of sedges and mosses (Gunnarsson et al. 2002, Malmer et al. 2005, Tape et al. 2006), while warmer and wetter conditions have produced opposite results (Weltzin et al. 2003, Belyea and Malmer 2004). Increased drying and shrub biomass have been positively correlated with higher photosynthesis, root respiration (and exudation of DOC), and microbial organic matter decomposition rates (Lafleur et al. 2005, Aerts 2006); the net effect on the C budget, however, is unclear. In contrast, increased wetness results in more CH₄ being emitted (relative to dry peat) (Ström et al. 2005). Methane has a 23 times larger GWP (sum of CO₂-C and CH₄-C expressed as CO₂ equivalents) than CO₂ over a 100-year timeframe (IPCC 2007). Thus, although they were net C sinks during the Holocene, peatlands have also been a net GWP source over the same period (Frolking and Roulet 2007). In this section, we explore the role of vegetation in peatland C dynamics by (1) peatland type, including general peatland characteristics and classification methods, and bog and fen vegetation and biogeochemical characteristics; (2) peatland succession, including PFTs, vegetation, and C accumulation relationships; and (3) effects of climate change on peatland succession, including the effects of temperature and water table levels on vegetation structure.

Peatland types

Peatland classification methods

A variety of methods have been used to classify peatlands. The Canadian Wetland Classification System (NWWG 1997) and the Ontario Wetland Evaluation System for northern peatlands (OMNR 1993) are hierarchical classification methods (Figure 2.1). Both systems separate wetlands using combinations of landscape, soil, water, and vegetation characteristics.

The Canadian system separates wetlands into classes (wetland types), forms (e.g., basin bog; Table 2.1), and vegetation types (e.g., low shrub bog) based on landscape features. Wetland classes in the Canadian system are defined relative to the genetic origin of the landscape. Formations are differentiated using combinations of site morphology (elevation above surrounding terrain, surface form and pattern), water source and chemistry (nutrient levels, base saturation, and pH), and basin depth and shape. The Canadian Wetland Classification System recognizes 20 bog and 19 fen forms and subforms (NWWG 1997) that can be subdivided into various wetland types (e.g., tall shrub, low shrub) based on plant communities and their structure, ranging from open, sedge fens to treed and forested bogs (NWWG 1988).

The Ontario system separates wetlands into four formations (i.e., wetland types); (1) bog, (2) fen, (3) swamp, and (4) marsh, with the latter including marsh and shallow open water. Two subformations are defined by the presence and density of trees as open or treed (tree species taller than 150 cm and covering 10 to 25% of area). Treed peatlands may be separated by level of tree cover, with low-density peatlands having 10 to 15% cover and medium-density peatlands having 15 to 25% cover. Subformations are divided into seven physiognomic groups (e.g., low shrub) by the plant communities and their structure, ranging from open, sedge fens to treed and forested bogs (OMNR 1993), which are similar to the wetland types in the Canadian classification system (NWWG 1988).

The Ontario Land Classification system uses remote sensing (of 1:50 000 to 1:100 000 images) to classify wetlands for land use planning (Hogg 2010). Here, wetlands are categorized into (1) marsh (intertidal, supertidal, and freshwater), (2) treed peatland (ecotones between treed fens and bogs that cannot be differentiated based on remote sensing data alone), (3) bog (open and treed), (4) fen (open and sparsely treed), and (5) open water (clear and turbid). The Ontario government's five-year state of the forest report uses wetland (e.g., marshes, open fens, open bogs), treed bog/fen, and swamp as reporting categories

(Watkins 2011). Therefore, to allow comparisons among peatland C research and monitoring studies, results need to accommodate and be aligned with the various federal and provincial peatland classification systems.

Peatland classification often involves gradient analysis, which relies on peatland soil and water chemistry, water table levels, and vegetation community field sampling at the site level (Glaser et al. 1990, Vitt and Chee 1990, Gignac et al. 2004). Statistical procedures, such as canonical correspondence, and detrended and cluster analyses, are used to separate peatland ecological types along acidity, nutrient, or water table level gradients. Species community associations are useful for separating moss layers by acidity and vascular plants along nutrient gradients (Vitt and Chee 1990, Anderson et al. 1996). Gradient analyses have successfully been used to differentiate peatlands into bog and fen, with the latter further classified as poor (e.g., treed fen), intermediate (e.g., moderately-rich; tall shrub fen), and rich (e.g., open, sedge fen) fen ecological groups. In this classification, bogs are acidic (pH less than 4.5) and generally nutrient poor. In contrast, fens occur along a gradient of pH values, with poor fens restricted to areas with values between 4.5 and 5.5, intermediate fens to between 5.5 and 6.5, and rich fens occupying areas with values greater than 6.5 (Vitt and Chee 1990).

Bogs

Classification and vegetation: Bogs are ombrotrophic peatlands that receive most of their water from precipitation (Glaser et al. 1981) and have low peat base saturation (Gorham et al. 1984, Urban et al. 1995, Gunnarsson et al. 2000). They are classified as ombrotrophic because their surface peat has limited connection to local or regional groundwater sources and their nutrient input is primarily from atmospheric deposition (Glaser et al. 1981).

Bogs are divided into domed, flat, and basin bogs (Table 2.1) and open (dominated by *Sphagnum* mosses), shrub (dominated by dwarf shrubs and *Sphagnum* mosses), and treed and forested (dominated by black spruce, dwarf shrubs, and *Sphagnum* and feather mosses) ecological types (NWWG 1997). The highest water table levels are generally associated with open bogs, followed by shrub, treed, and forested bogs, respectively. Net primary production (NPP) is highest in forested, followed by treed and open bogs, respectively (Campbell et al. 2000). *Sphagnum* mosses account for 10 to 90% of NPP across bog types, with *Sphagnum* contributing more to NPP in open bogs and than in forested bogs (Campbell et al. 2000).

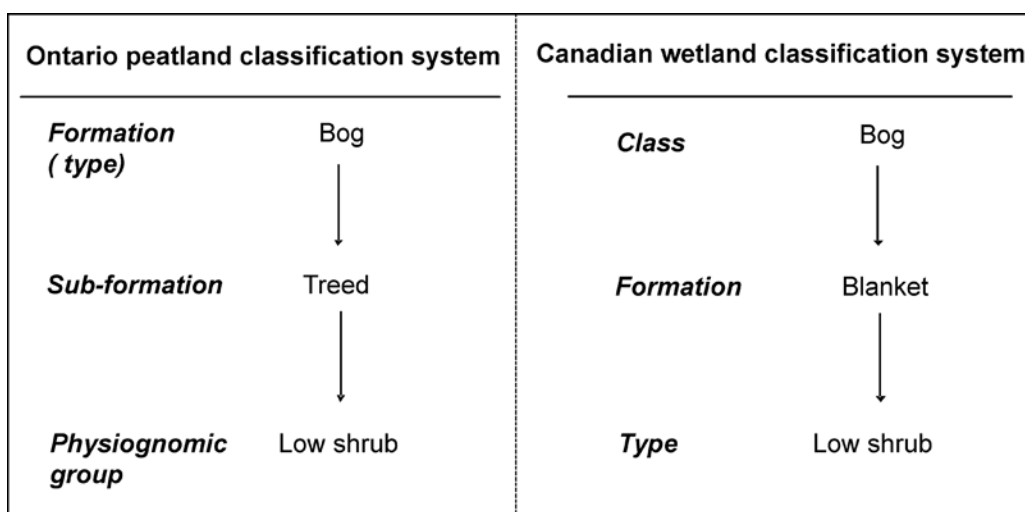


Figure 2.1. Example of bog classification based on the Ontario Ministry of Natural Resources' (OMNR 1993) and Canadian Wetland Classification (NWWG 1997) systems.

Table 2.1. Vegetation characteristics of boreal bogs and fens (from NWWG 1988).

Peatland type	Tree layer	Shrub layer	Grass/herb/forb layer	Moss layer
Domed bogs	<i>Picea mariana</i> <i>Larix laricina</i>	<i>Chamaedaphne calyculata</i> <i>Ledum groenlandicum</i> <i>Kalmia polifolia</i> <i>Vaccinium vitis-idaea</i> <i>Vaccinium oxycoccus</i>	<i>Cornus canadensis</i> <i>Anemone quinquefolia</i> <i>Mitella nuda</i> <i>Trientalis borealis</i> <i>Coptis trifolia</i>	<i>Sphagnum neroreum</i> <i>Sphagnum fuscum</i> <i>Sphagnum girgensohnii</i> <i>Sphagnum magellanicum</i> <i>Pleurozium schreberi</i>
Peat plateaus/palsas	<i>Picea mariana</i>	<i>Chamaedaphne calyculata</i> <i>Ledum groenlandicum</i> <i>Kalmia polifolia</i> <i>Vaccinium vitis-idaea</i> <i>Vaccinium oxycoccus</i> <i>Rubus chamaemorus</i>		<i>Sphagnum fuscum</i> <i>Pleurozium schreberi</i> <i>Hylocomium splendens</i> <i>Cladina</i> spp. (lichens)
Flat bogs	<i>Picea mariana</i>	<i>Chamaedaphne calyculata</i> <i>Ledum groenlandicum</i> <i>Kalmia polifolia</i> <i>Rubus chamaemorus</i> <i>Vaccinium vitis-idaea</i> <i>Vaccinium oxycoccus</i>	<i>Smilacina trifolia</i> <i>Oxycoccus quadripetalus</i> <i>Carex oligosperma</i> <i>Sarracenia purpurea</i> <i>Andromeda glaucophylla</i>	<i>Sphagnum fuscum</i> <i>Sphagnum angustifolium</i> <i>Pleurozium schreberi</i> <i>Dicranum polysetum</i> <i>Dicranum undulatum</i>
Basin bogs	<i>Picea mariana</i>	<i>Chamaedaphne calyculata</i> <i>Ledum groenlandicum</i> <i>Kalmia polifolia</i> <i>Rubus chamaemorus</i>	<i>Eriophorum vaginatum</i> <i>Smilacina trifolia</i> <i>Oxycoccus quadripetalus</i>	<i>Sphagnum fuscum</i> <i>Sphagnum magellanicum</i> <i>Sphagnum fallax</i> <i>Pleurozium schreberi</i> <i>Hylocomium splendens</i> <i>Sphagnum angustifolium</i> <i>Polytrichum strictum</i>
Horizontal fens	<i>Larix laricina</i>	<i>Betula pumila</i> <i>Rhamnus alnifolia</i> <i>Myrica gale</i>	<i>Carex exilis</i> <i>Carex lasiocarpa</i> <i>Scripus caespitosus</i> <i>Menyanthes trifolia</i> <i>Scripus hudsonianus</i> <i>Equisetum fluviatile</i> <i>Habenaria dilatata</i>	<i>Sphagnum teres</i> <i>Sphagnum warnstorffii</i> <i>Sphagnum fallax</i> <i>Campyllum stellatum</i> <i>Drepanocladus revolvens</i> <i>Scorpidium scorpiodes</i>
Basin fens	<i>Larix laricina</i>	<i>Betula pumila</i>	<i>Carex aquatilis</i> <i>Carex lasiocarpa</i>	<i>Drepanocladus exannulatus</i> <i>Drepanocladus revolvens</i> <i>Campyllum stellatum</i> <i>Calliergon giganteum</i> <i>Calliergon richardsonii</i> <i>Sphagnum angustifolium</i>
Spring fens	<i>Larix laricina</i>	<i>Betula pumila</i> <i>Andromeda polifolia</i> <i>Salix pedicellaris</i>	<i>Carex interior</i> <i>Carex lasiocarpa</i> <i>Scripus caespitosus</i> <i>Eleocharis quinqueflora</i> <i>Muhlenbergia glomerata</i>	<i>Scorpidium scorpiodes</i> <i>Drepanocladus revolvens</i> <i>Campyllum stellatum</i>
Northern ribbed fens	<i>Larix laricina</i> <i>Picea mariana</i>	<i>Betula pumila</i> <i>Salix candida</i> <i>Salix pedicellaris</i> <i>Andromeda polifolia</i> <i>Lonicera villosa</i> <i>Rhamnus alnifolia</i> <i>Ledum groenlandicum</i> <i>Chamaedaphne calyculata</i>	<i>Carex diandra</i> <i>Carex disperma</i> <i>Carex chordorrhiza</i> <i>Carex lasiocarpa</i> <i>Carex limosa</i> <i>Menyanthes trifolata</i>	<i>Scorpidium scorpiodes</i> <i>Drepanocladus revolvens</i> <i>Messia triquetra</i> <i>Cinclidium stygium</i> <i>Sphagnum fuscum</i> <i>Sphagnum magellanicum</i> <i>Pleurozium schreberi</i> <i>Dicranum undulatum</i>
Feather fens	<i>Larix laricina</i>	<i>Picea mariana</i> <i>Chamaedaphne calyculata</i>	<i>Carex</i> spp.	<i>Sphagnum warnstorffii</i>

Sphagnum species composition differs depending on whether mosses grow on dry features, such as hummocks and palsas/peat plateaus, or wet features, such as lawns, carpets, collapsed scars, and pools (Table 2.2). For example, *Sphagnum capillifolium*, *Sphagnum magellanicum*, and *Sphagnum fuscum* are hummock and *Sphagnum lindbergii* are wet-moss preferential bog species, respectively (Table 2.2). Associate bog-hummock mosses include *Sphagnum balticum* and *Aulacomnium palustre*, while associate wet area (e.g., hollow / lawn) species include *Sphagnum angustifolium*, *Sphagnum fallax*, *Sphagnum jensenii*, and *Sphagnum riparium* (Table 2.2). Associate species are generally adapted to wider pH ranges and also occur in poor fens. Diversity of sedges is low in bogs, with *Carex limosa*, *Carex pauciflora*, *Eriophorum vaginatum*, and *Eriophorum virginicum* occurring on hummocks, lawns, or carpets (Table 2.2), depending on water table level and nutrient conditions. Dwarf shrubs (*Chamaedaphne calyculata*, *Ledum groenlandicum*, *Kalmia polifolia*, *Vaccinium* spp.) are common on hummocks, palsas, and peat plateaus. Tall shrubs (*Betula* spp., *Andromeda* spp., *Alnus* spp., *Salix* spp.) are common along bog margins, collapsed scars, and lawns in palsa fields (Beilman 2001).

Table 2.2. Habitat characteristics of common vegetation in northern Canadian peatlands.

Plant species	Habitat characteristics				Ecological amplitude ^b	Peatland preference
	pH range	Microtopography	Nutrient regime ^a	Shade tolerance		
Sphagnum mosses						
<i>Sphagnum capillifolium</i>	3.5 – 4.5	Hummock	Poor	Moderate	Narrow	Bog
<i>Sphagnum fuscum</i>	3.5 – 4.5	Hummock, palsa	Poor	Intolerant	Narrow	Bog
<i>Sphagnum magellanicum</i>	3.5 – 4.5	Hummock	Poor	Tolerant	Narrow	Bog
<i>Sphagnum lindbergii</i>	3.5 – 4.5	Carpet, lawn, collapse scar	Poor	Intolerant	Narrow	Bog
<i>Aulacomnium palustre</i>	3.5 – 6.5	Hummock, palsa	Poor to intermediate	Tolerant	Wide	Bog
<i>Sphagnum balticum</i>	4.5 – 5.5	Hummock	Poor to intermediate	Intolerant	Narrow	Poor fen
<i>Sphagnum angustifolium</i>	4.5 – 5.5	Carpet, lawn	Poor to intermediate	Intolerant	Narrow	Poor fen
<i>Sphagnum fallax</i>	4.5 – 5.5	Carpet, lawn	Poor to intermediate	Intolerant	Narrow	Poor fen
<i>Sphagnum jensenii</i>	4.5 – 5.5	Carpet, pool	Poor to intermediate	Intolerant	Narrow	Poor fen
<i>Sphagnum riparium</i>	4.5 – 6.5	Lawn, pool, collapsed scar	Poor to intermediate	Intolerant	Wide	Intermediate fen, poor fen
<i>Sphagnum teres</i>	5.5 – 6.5	Carpet, lawn	Intermediate	Tolerant	Wide	Intermediate fen
<i>Sphagnum warnstorffii</i>	5.5 – 6.5	Hummock, lawn	Intermediate	Tolerant	Narrow	Intermediate fen
Non-sphagnum mosses						
<i>Pleurozium schreberi</i>	3.5 – 5.5	Hummock, palsa	Poor to intermediate	Tolerant	Wide	Bog, poor fen
<i>Hypnum</i> spp.	3.5 – 5.5	Hummock, palsa	Poor to intermediate	Tolerant	Wide	Bog, poor fen
<i>Hylocomium splendens</i>	3.5 – 5.5	Hummock, palsa	Poor to intermediate	Tolerant	Wide	Bog, poor fen
<i>Drepanocladus aduncus</i>	6.5 – 7.5	Carpet, pool	Rich	Tolerant	Narrow	Rich fen, intermediate fen
<i>Drepanocladus revolvens</i>	6.5 – 7.5	Carpet, pool	Rich	Tolerant	Narrow	Rich fen, intermediate fen
<i>Brachythecium mildeanum</i>	6.5 – 7.5	Carpet, lawn	Rich	Tolerant	Narrow	Rich fen, intermediate fen
<i>Calliergonella cuspidate</i>	6.5 – 7.5	Carpet, lawn	Rich	Tolerant	Narrow	Rich fen, intermediate fen
<i>Tomenthypnum nitens</i>	6.5 – 8.5	Hummock	Rich	Tolerant	Wide	Intermediate fen, rich fen
<i>Calliergon giganteum</i>	6.5 – 8.5	Carpet, pool	Rich	Moderate	Wide	Intermediate fen, rich fen

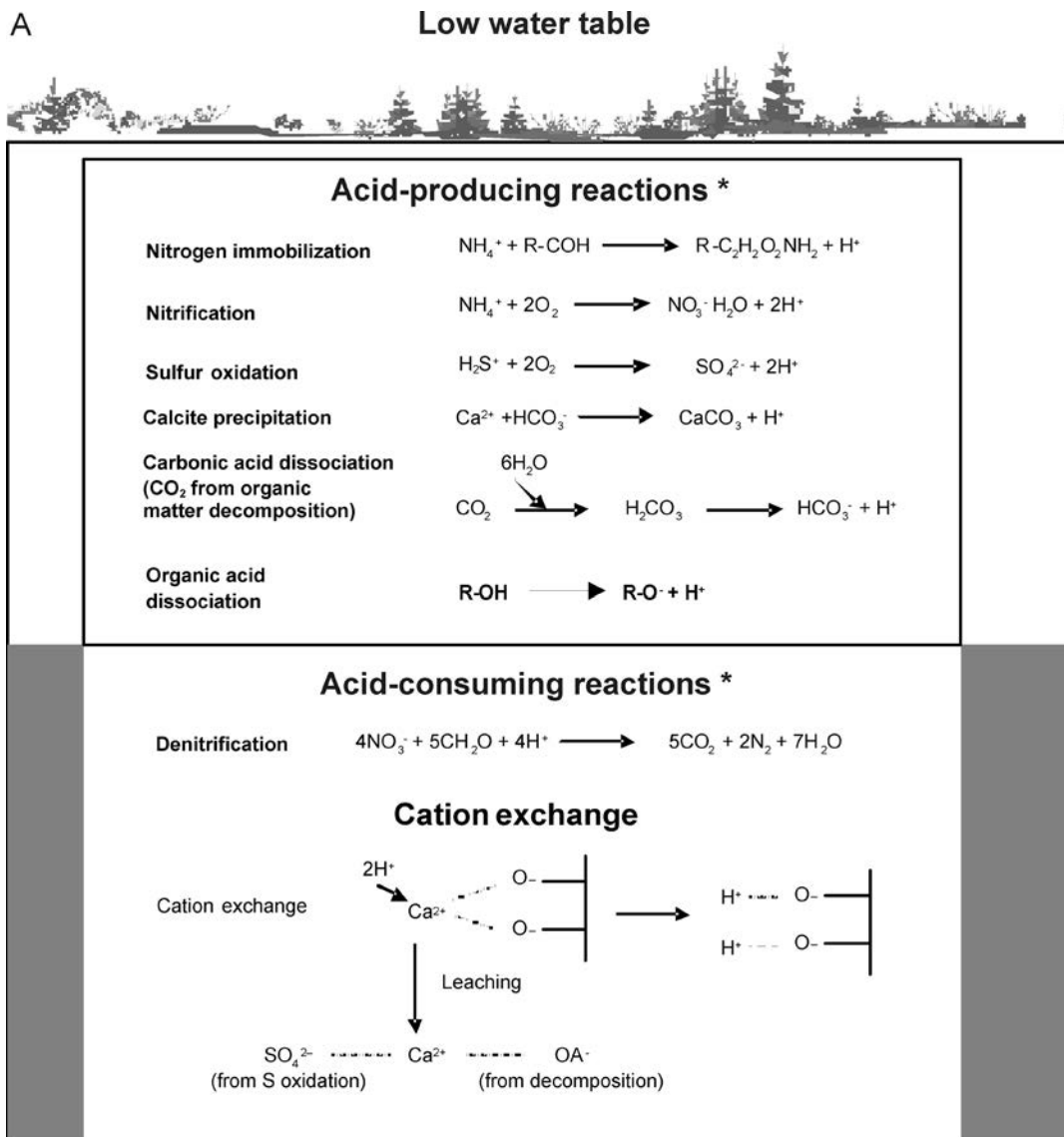
Table 2.2. Con't.

Plant species	Habitat characteristics					
	pH range	Microtopography	Nutrient regime ^a	Shade tolerance	Ecological amplitude ^b	Peatland preference
<i>Scorpidium cossonii</i>	6.5 – 8.5	Hummock, lawn	Rich	Moderate	Wide	Intermediate fen, rich fen
<i>Calliergon richardsonii</i>	7.5 – 8.5	Pool	Rich	Tolerant	Narrow	Rich fen
<i>Scorpidium scorpiodes</i>	7.5 – 8.5	Carpet, pool	Rich	Moderate	Narrow	Rich fen
<i>Scorpidium revolvens</i>	7.5 – 8.5	Carpet, lawn	Rich	Moderate	Narrow	Rich fen
Grasses						
<i>Carex limosa</i>	3.5 – 7.5	Hummock, lawn	Poor to rich	Intolerant	Wide	Bog, poor fen
<i>Carex pauciflora</i>	4.5 – 5.5	Hummock, carpet, lawn	Poor to intermediate	Moderate	Narrow	Poor fen, bog
<i>Eriophorum vaginatum</i>	4.5 – 5.5	Hummock, carpet	Poor to intermediate	Tolerant	Narrow	Poor fen, bog
<i>Eriophorum virginicum</i>	4.5 – 5.5	Hummock, carpet	Poor to intermediate	Intolerant	Narrow	Poor fen, bog
<i>Carex aquatilis</i>	4.5 – 6.5	Hummock, carpet, lawn	Poor to intermediate	Intolerant	Wide	Poor fen, intermediate fen
<i>Carex stricta</i>	4.5 – 6.5	Hummock, carpet, lawn	Poor to intermediate	Moderate	Wide	Poor fen, intermediate fen
<i>Carex exilis</i>	4.5 – 7.5	Carpet	Poor to rich	Tolerant	Wide	Poor fen, intermediate fen, rich fen
<i>Carex chordorhiza</i>	4.5 – 7.5	Carpet	Poor to rich	Intolerant	Wide	Intermediate fen, rich fen
<i>Scirpus hudsoniana</i>	6.5 – 7.5	Carpet	Rich	Intolerant	Narrow	Rich fen, intermediate fen
<i>Scirpus cespitosus</i>	4.5 – 7.5	Carpet	Poor to rich	Intolerant	Wide	Poor fen, intermediate fen, rich fen
<i>Carex diandra</i>	6.5 – 7.5	Carpet	Rich	Moderate	Narrow	Rich fen
<i>Carex lasiocarpa</i>	6.5 – 7.5	Carpet	Rich	Intolerant	Narrow	Rich fen
<i>Carex livada</i>	6.5 – 7.5	Carpet	Rich	Moderate	Narrow	Rich fen
<i>Carex interior</i>	6.5 – 7.5	Carpet	Rich	Moderate	Narrow	Rich fen
Shrubs						
<i>Chamaedaphne calyculata</i>	3.5 – 5.5	Hummock, carpet, lawn	Poor to intermediate	Moderate	Wide	Bog, poor fen
<i>Ledum groenlandicum</i>	3.5 – 5.5	Hummock	Poor to intermediate	Intolerant	Wide	Bog, poor fen
<i>Kalmia polifolia</i>	3.5 – 5.5	Lawn	Poor to intermediate	Tolerant	Wide	Bog, poor fen
<i>Rubus chamaemorus</i>	3.5 – 5.5	Hummock	Poor to intermediate	Moderate	Wide	Bog, poor fen
<i>Vaccinium oxycoccus</i>	3.5 – 5.5	Hummock	Poor to intermediate	Moderate	Wide	Bog, poor fen
<i>Vaccinium vitis-idaea</i>	3.5 – 5.5	Hummock	Poor to intermediate	Intolerant	Narrow	Bog, poor fen
<i>Betula pumila</i>	4.5 – 6.5	Carpet, lawn, collapse scar	Poor to intermediate	Intolerant	Wide	Poor fen, intermediate fen, bog
<i>Andromeda polifolia</i>	4.5 – 5.5	Carpet, lawn, collapse scar	Poor to intermediate	Tolerant	Wide	Poor fen, intermediate fen, bog
<i>Salix</i> spp.	4.5 – 6.5	Carpet, lawn, collapse scar	Poor to intermediate	Intolerant	Wide	Intermediate fen, poor fen
<i>Alnus</i> spp.	4.5 – 6.5	Carpet, lawn, collapse scar	Poor to intermediate	Moderate	Wide	Intermediate fen, poor fen
<i>Rhamnus alnifolia</i>	4.5 – 6.5	Carpet, lawn, collapse scar	Poor to intermediate	Tolerant	Wide	Intermediate fen, poor fen
<i>Myrica gale</i>	4.5 – 6.5	Carpet, lawn	Poor to intermediate	Tolerant	Wide	Intermediate fen, poor fen

^a Nutrient regime = available soil nutrition (mainly N).^b Ecological amplitude = the degree of adaptation of a plant to changes in its environment, which is expressed quantitatively as the range of environmental changes within which the species is able to carry out its normal vital activities.

Peat acidification: A low water table level in bogs contributes to aerobic respiration dominating organic matter decomposition in surface peat (Lafleur et al. 2005). Acid [i.e., proton (H^+)]-producing reactions then dominate those producing bicarbonate (HCO_3^-) alkalinity (Figure 2.2a), of which sulphur (S) oxidation, organic acid dissociation, and nitrogen (N) immobilization are important reactions (Figure 2.2a) (McLaughlin and Webster 2010, McLaughlin et al. 2011). During peat decomposition under aerobic conditions, aluminum ions (Al^{3+}) are also released (Hemond 1980, McKnight et al. 1985). Hydrogen ions (and solubilized Al^{3+}) exchange with base cations on peat exchange sites, which are then flushed from the peat by rain (Siegel et al. 1995) with SO_4^{2-} as the major counter ion for base cation export. This process depletes base cations and results in net peat acidification, ultimately manifesting itself in stream and lake acidification (Lazerte 1993).

Bog carbon dynamics: Presence of various microtopographic features in bogs complicates C budget estimations. For example, in addition to rapid CO_2 production and efflux, aerobic decomposition in hummocks results in highly decomposed (i.e., recalcitrant) C entering anaerobic peat layers for long-term storage (Turetsky et al. 2007, Dorrepaal et al. 2009). In contrast, fermentation and anaerobic respiration in wet zones contribute poorly decomposed organic C to storage in anaerobic zones (Reiche et al. 2010).



B

High water table

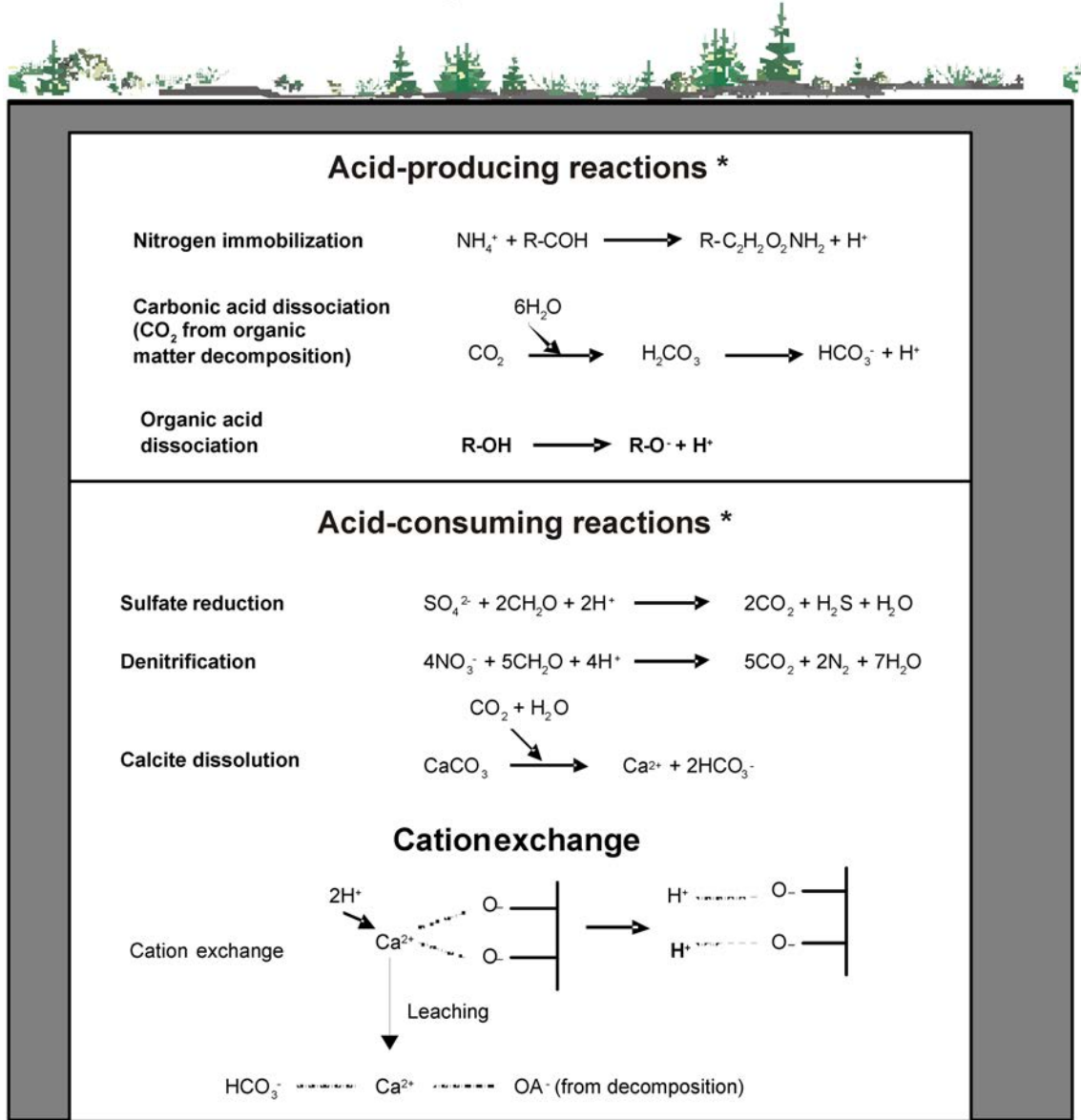


Figure 2.2. Conceptual model for hydrogen ion (H⁺) production and consumption for an intermediate fen peatland in northern Ontario. (A) High water table – dominated by H⁺ consuming reactions – and (b) low water table – dominated by H⁺ producing reactions; * indicates dominant reaction types (from McLaughlin and Webster 2010).

No consensus has been reached about C balances and landscape integration of hummocks and hollows into C models. For example, in the northern boreal zone of Alberta, low water table levels and drier conditions of hummocks supported rapid decomposition rates, inhibiting C sequestration (Turetsky et al. 2008a). This occurred despite the slow decomposition of hummock-*Sphagnum* mosses (Table 2.3). In contrast to hummocks, wet features inhibited litter decomposition even though *Sphagnum* occurring in wet areas decomposed faster than hummock-forming mosses when incubated under common experimental conditions. Moreover, *Sphagnum* mosses growing in wet features had relatively high NPP, contributing more litter to the peat surface than those in hummocks. Turetsky et al. (2008a) proposed that wet features may support rapid C accumulation rates that may be inhibited during drought periods, when the more labile wet-adapted *Sphagnum* mosses are exposed to oxygen. Conversely, in

the temperate region of Ontario, hummock-*Sphagnum* litter decomposition was slower than that of *Sphagnum* mosses growing in wet features (Moore et al. 2007). Net primary production was also higher in hummocks than wet areas, suggesting that hummocks may be C sinks and lawns/hollows C sources. In another study, LORCA values were similar among hummock, hollow, and peat plateau features in the Northwest Territories (Robinson and Moore 2000). Thus, C dynamics of hummocks and hollows are not clear, nor is it possible to adequately integrate hummock and hollow microtopography into landscape-level C assessments or predict their role in C sequestration along spatial and temporal gradients (Dorrepaal 2007).

Table 2.3. Litter decay coefficients for common northern peatland plants.

Growth form/species	Peatland type	Study location	Linear decay coefficient (k)	Exponential decay coefficient (k)	Reference
Mosses					
<i>Sphagnum fuscum</i>	Bog	Alberta	0.14	0.15	Thormann et al. 1999
	Bog	Alberta	-	0.02	Turetsky et al. 2008a
<i>Sphagnum magellanicum</i>	Poor fen	Ontario	0.14	-	Rocheffort et al. 1990
	Poor fen	Ontario	0.18	-	Rocheffort et al. 1990
<i>Sphagnum capillifolium</i>	Poor fen	Alberta	-	0.05	Turetsky et al. 2008a
	Poor fen	Ontario	-	0.14	Moore et al. 2007
<i>Sphagnum lindbergii</i>	Bog	Ontario	-	0.02	Moore et al. 2007
	Peatland pond	Ontario	-	0.19	Moore et al. 2007
<i>Sphagnum angustifolium</i>	Poor fen	Quebec	0.11	0.12	Bartsch and Moore 1985
	Rich fen	Quebec	0.08	0.08	Bartsch and Moore 1985
<i>Sphagnum jensenii</i>	Bog	Alberta	-	0.08	Turetsky et al. 2008a
	Poor fen	Alberta	0.16	0.17	Thormann et al. 1999
	Poor fen	Ontario	0.25	-	Rocheffort et al. 1990
<i>Sphagnum teres</i>	Poor fen	Ontario	-	0.08	Moore et al. 2007
	Poor fen	Alberta	-	0.07	Turetsky et al. 2008a
<i>Sphagnum riparium</i>	Poor fen	Alberta	0.16	0.17	Thormann et al. 1999
<i>Tomenhypnum nitens</i>	Internal lawn	Alberta	-	0.16	Turetsky et al. 2008a
<i>Scorpidium scorpioides</i>	Rich fen	Alberta	-	0.08	Turetsky et al. 2008a
	Rich fen	Alberta	0.22	0.25	Thormann et al. 1999
<i>Scorpidium scorpioides</i>	Rich fen	Alberta	-	0.05	Turetsky et al. 2008a
	Grasses				
<i>Carex oligosperma</i>	Poor fen	Ontario	-	0.21	Moore et al. 2007
	Peatland pond	Ontario	-	0.24	Moore et al. 2007
<i>Carex limosa</i>	Poor fen	Quebec	0.18	0.20	Bartsch and Moore 1985
	Rich fen	Quebec	0.17	0.18	Bartsch and Moore 1985
	Floating fen	Quebec	0.25	0.28	Bartsch and Moore 1985
<i>Carex rostrata</i>	Poor fen	Quebec	0.20	0.23	Bartsch and Moore 1985
	Rich fen	Quebec	0.13	0.17	Bartsch and Moore 1985
	Rich fen	Quebec	0.13	0.14	Bartsch and Moore 1985
<i>Carex aquatilis</i>	Rich fen	Quebec	0.16	0.17	Bartsch and Moore 1985
	Rich fen	Quebec	0.27	0.31	Bartsch and Moore 1985
<i>Carex chorodorrhiza</i>	Rich fen	Quebec	0.21	0.22	Bartsch and Moore 1985
<i>Scripus cespitosus</i>	Poor fen	Quebec	0.12	0.13	Bartsch and Moore 1985
	Rich fen	Quebec	0.12	0.13	Bartsch and Moore 1985
	Rich fen	Quebec	0.16	0.17	Bartsch and Moore 1985
Deciduous shrubs					
<i>Betula glandulosa</i>	Poor fen	Quebec	0.22	0.24	Bartsch and Moore 1985
	Rich fen	Quebec	0.20	0.22	Bartsch and Moore 1985
	Rich fen	Quebec	0.17	0.18	Bartsch and Moore 1985
<i>Betula pumila</i>	Poor fen	Alberta	0.36	0.45	Thormann et al. 1999
	Intermediate fen	Alberta	0.37	0.46	Thormann et al. 1999
<i>Salix pedicellaris</i>	Poor fen	Quebec	0.14	0.15	Bartsch and Moore 1985
	Rich fen	Quebec	0.18	0.20	Bartsch and Moore 1985
Ericaceous shrubs					
<i>Chamaedaphne calyculata</i>	Poor fen	Ontario	-	0.31	Moore et al. 2007
	Bog	Ontario	-	0.18	Moore et al. 2007
	Peatland pond	Ontario	-	0.13	Moore et al. 2007

Uncertainties in hummock and hollow C cycling are attributed to the fact that most litter decomposition study results are based on short-term (<5 years) dynamics (Hobbie et al. 2000, Laiho 2006). Short-term studies have contributed an understanding of litter decomposition patterns and inherent peat processes (autogenic) as well as climate (allogenic) control on C cycling. They have also provided evidence that initial litter decomposition rates are higher for vascular plants than for *Sphagnum* mosses (Table 2.3). However, short-term studies do not provide relevant decadal to century data on C dynamics (Latter et al. 1998, Moore et al. 1998). Therefore, coefficients used to model litter decomposition rates may not be valid over long periods (Moore et al. 2008).

Fens

Fens vary from small spring and basin fens, located at local topographically-constrained groundwater discharge zones, to expansive areas of horizontal and ribbed fens (Table 2.1). Fens are further classified into ecological types, such as (i) open, sedge (e.g., rich), (ii) open, low shrub or tall shrub (e.g., poor and intermediate fens), and (iii) treed and forested poor fens (NWWG 1997). Variation in water table level and soil pH occurs across fens, with circumneutral (pH = 6.0 to 8.0) groundwater consistently located near peat surfaces of rich fens, and lower pH and water table levels in intermediate and poor fens, respectively (Webster and McLaughlin 2010). Poor fens generally have the highest NPP because they support trees, followed by shrub fens, and open fens, respectively. The contribution of mosses to NPP is inversely proportional to total NPP and tree and shrub biomass (Campbell et al. 2000).

Poor fens: Poor fens share a variety of vegetative and biogeochemical features with bogs (Glaser et al. 1990, Vitt and Chee 1990). Vegetation on poor fens includes *S. balticum* and *A. palustris* on hummocks and *S. fallax*, *S. jensennii*, and *S. riparium*, with *Sphagnum teres* and *Sphagnum warnstorffii* occurring on wet microtopographic positions (the latter two *Sphagnum* species are uncommon in bogs). Dominant sedges in poor fens are also similar to those found in bogs, although *Carex aquatilis*, *Carex stricta*, and *Carex exilis* also occur in poor fens where pH values are higher (Table 2.2). Poor fens are also vegetated by dwarf shrubs and trees (black spruce and larch, *Larix laricina*) on hummocks (Table 2.2). Tall shrubs, such as *Betula* spp. and *Alnus* spp., may prevail in lawns and carpets of poor fens, which is similar to bogs (Table 2.2). Acidification and organic matter decomposition processes in poor fens are also similar to those described for bogs (Webster and McLaughlin 2010). However, peat in poor fens is less acidic and water flow is shallower than that in bogs (Glaser et al. 1997).

Intermediate fens: Intermediate fens have the highest plant diversity and most variable biogeochemical reactions of all peatland ecological types as a result of large fluctuations in water table levels, rapid peat decomposition, and higher nutrient availability (Webster and McLaughlin 2010). Since the peat acidifies rapidly, intermediate fens are a transient state between poor and rich fens, with a relatively short life span for fen types, ranging from 50 to 200 years (Gorham et al. 1984, Vitt and Chee 1990, McLaughlin and Webster 2010).

The moss layer of intermediate fens consists of both non-*Sphagnum* (e.g., brown mosses) and *Sphagnum* mosses, with *S. riparium* and *S. teres* common in wet microtopographic positions and *S. warnstorffii* occurring in either hummock or wet positions (Table 2.2), depending on water table levels. *Carex chorderhiza*, *C. aquatilis*, *C. stricta*, and *C. exilis* are common sedges and *Betula* spp., *Alnus* spp., *Salix* spp., *Rhamnus alnifolia*, and *Myrica gale* are common shrubs (Table 2.2). In addition, dwarf shrubs may occur where pH is low.

Fluctuating water table levels in intermediate fens result in combinations of acidity-producing and consuming reactions (McLaughlin and Webster 2010, McLaughlin et al. 2011). At high water table levels, anaerobic SO_4^{2-} reduction and denitrification consume H^+ and produce HCO_3^- alkalinity (Figure 2.2b). Moreover, carbonate mineral dissolution occurs rapidly when the water table is high, producing HCO_3^- . When water table levels are low, aerobic respiration consumes HCO_3^- and produces H^+ , similarly to processes described for bogs (Figure 2.2a). The balance of aerobic and anaerobic respiration, therefore, determines net acidification and thus the timeframe within which an intermediate fen will succeed to a poor fen. For example, McLaughlin and Webster (2010) reported a net loss of 0.8% of base cations (calcium, magnesium, potassium) in the upper 25 cm of peat of an intermediate fen in northern Ontario during a climatically 'average' year, compared to a net loss of 3.0% during a 'dry' year. Based on those data, McLaughlin and Webster (2010) estimated that given an 'average' climate, about 125 years would be required to completely strip the base cations from surface peat cation exchange sites. However, under increased drought this period may decrease to about 30 years. These calculated years are consistent with the 50- to 200-year timeframes reported for the longevity of intermediate fens in northern regions (Gorham et al. 1984, Vitt and Chee 1990).

Although the highest plant diversity and the most widely fluctuating water table levels occur in intermediate fens, few decomposition and C budget studies have been conducted on this peatland type. Fluctuating water table levels can contribute to rapid litter decomposition and deposition of recalcitrant C to long-term storage, as in bogs. For example, Webster and McLaughlin (2010) reported that an intermediate fen had more humified DOC, indicating more complete peat decomposition compared to a rich and a poor fen. Furthermore, presence of sedges in intermediate fens facilitates CH₄ flux from the peat, as CH₄ diffuses through aeranchyma cells (Chanton 2005, Ström et al. 2005) and CH₄ fluxes may be highest when sedge biomass peaks (Godin et al. 2012). Sedge-mediated CH₄ flux is important during (1) high water table levels when diffusion through water is slow and (2) low water table levels because sedge roots can penetrate deeper than one metre below the peat surface. This provides a conduit for CH₄ transport through aeranchyma cells that bypasses aerobic surface peat, where CH₄ can be oxidized to CO₂ (Chanton 2005). Further details are provided in section 5, Peatland Carbon Cycling.

High water table levels also allow CO₂ and CH₄ produced from respiration to dissolve in water (see section 5, Peatland Carbon Cycling). Some dissolved CO₂ is converted to carbonic acid (H₂CO₃) and HCO₃⁻ in peat porewater, depending on pH (Cirimo et al. 2000, Siegel et al. 2006). In addition, rapid water flow in the upper 25 cm of peat exports large amounts of CO₂ and CH₄ (and DOC) to draining streams and lakes where their roles are uncertain. Some CO₂ is emitted to the atmosphere from streams and lakes (Huttunen et al. 2002, Billett and Moore 2007), but some is also retained in the surface water systems through HCO₃⁻ formation, which may serve as a CO₂ source for aquatic vegetation (Dodds 2002).

Rich fens: Of all peatland ecological types, rich fens have the highest pH and water table level, and shallowest and fastest water flow. Combinations of acidity consumption, high dissolved CO₂ concentrations, and carbonate mineral concentrations lead to HCO₃⁻ formation and subsequent circumneutrality of peat and its porewater (Siegel et al. 2006).

Rich fen vegetation is composed primarily of sedges, with *Scripus hudsoniana*, *Scripus cespitosus*, *Carex diandra*, *Carex lasiocarpa*, *Carex livada*, and *Carex interior*, and brown mosses, with *Calliergon richardsonii*, *Scorpidium scorpioides*, *Scorpidium revolvens*, and *Scorpidium cossonii* also present (Table 2.2). Sedges, including *C. stricta* and *C. exilis*, and tall shrubs, including *Betula* spp., *Alnus* spp., and *M. gale* occur as associate species. Rich fens also have the least variable microtopography of all peatland ecological types. However, when microtopography occurs, *S. cossonii* and *C. stricta* occur on hummocks, while the remaining sedges occur in wet areas (Gignac et al. 2004).

In addition to net alkalinity production, anaerobic respiration and fermentation contribute poorly decomposed peat that is high quality (Turetsky and Ripley 2005, Reiche et al. 2010). As such, peat in rich fens is the most sensitive to decomposition when water table drawdown occurs and aerobic reactions dominate surface peat respiration, as in bogs and intermediate fens (Turetsky et al. 2008b). Furthermore, fermentation of organic matter produces fatty acids, such as acetate, that are substrates for CH₄ formation (McLaughlin 2004). High water table levels and rapid water flow in rich fens contribute to large exports of CO₂, CH₄, and DOC, with uncertainties similar to those described for intermediate fens (see section 5, Peatland Carbon Cycling).

Peatland succession

Plant functional types

Plant functional types are commonly used to assess peatland C storage and GHG fluxes at various spatial and temporal scales (St.-Hilaire et al. 2010). Combining (1) remote sensing of peatland PFTs, (2) peat depth and its organic C content and quality, along with (3) GHG fluxes measured at research sites (or atmospheric GHG concentrations measured via remote sensing) allows landscape C budgets to be estimated using calibrated and validated C models (Krankina et al. 2008, Fuchs et al. 2009, Schneider et al. 2009). Different PFTs are used for spatial and temporal C modelling: (1) vegetated and non-vegetated conditions at global scales, (2) vascular (e.g., treed bogs and fens) and non-vascular (e.g. open bogs and fens) plant groups at national scales, (3) broad vegetation classes, such as mosses, grasses, shrubs, and trees at regional scales, and (4) genera and species-level data at local levels (Figure 2.3; Dorrepaal 2007). Although CO₂ uptake and litter quality differ within broad-based PFTs, they are assumed to balance over larger landscapes and are considered amenable for remote sensing and large landscape modelling (Dorrepaal 2007). Further details are provided in section 7, Mapping, Monitoring, and Modelling Peatlands.

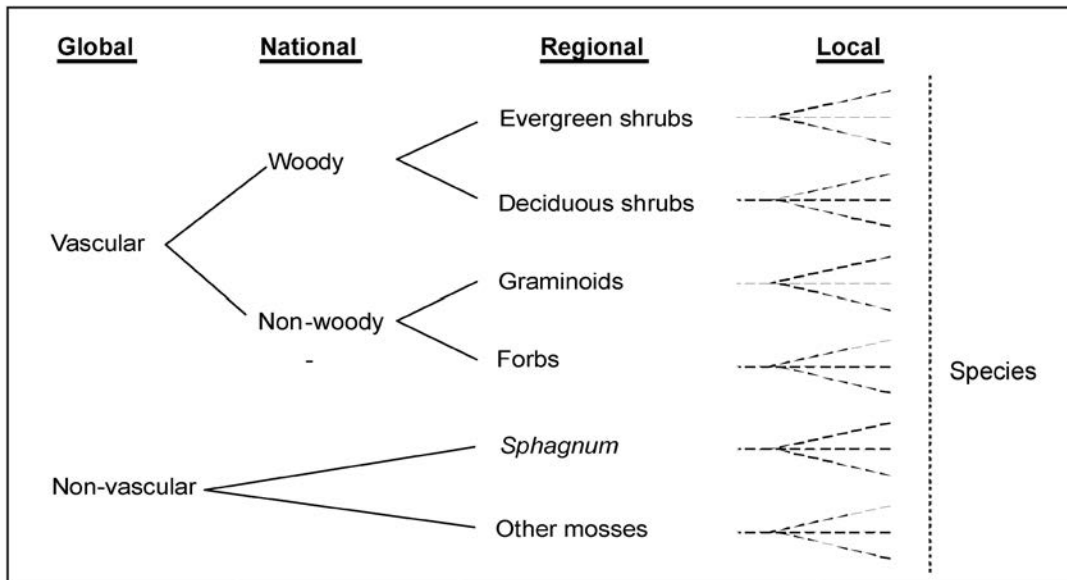


Figure 2.3. Simplified plant functional group classification used for northern peatlands at various scales (adapted from Dorrepaal 2007).

Vegetation dynamics and peatland succession

Various methods have been used to study plant vegetation dynamics and peatland development in boreal and subarctic zones and their responses to climate change. The most common methods include (1) paleoecology (Glaser et al. 2004a, Arlen-Pouliot and Bhiry 2005), (2) long-term sampling of research plots (Gunnarsson et al. 2000, 2002; Johansson et al. 2006), (3) chronosequence studies substituting space for time (Klinger and Short 1996, Wieder et al. 2009), (4) small- to large-scale experimental manipulations (Weltzin et al. 2003), and (5) meta-analysis of experimental data from various studies (Van Wijk et al. 2003). All methods have advantages and disadvantages, but all produce common patterns of vegetation changes and peatland succession from open marsh (salt or freshwater) to various fen stages and ultimately to bogs or palsa/peat plateaus (Table 2.4, Figure 2.4).

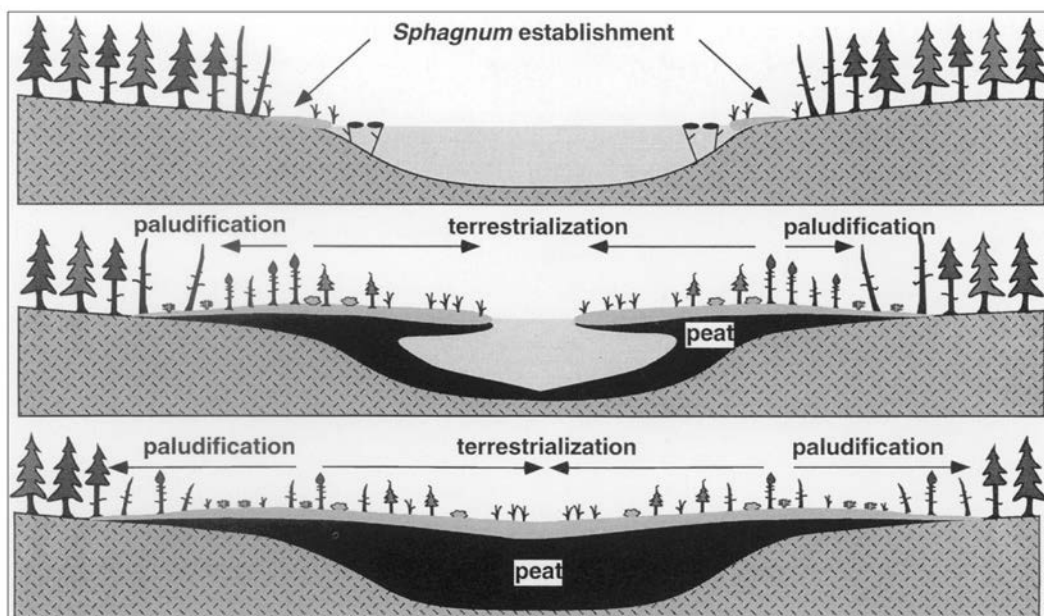


Figure 2.4. Schematic representation of peatland development and expansion (from Klinger 1996; reprinted with permission from Arctic, Antarctic, and Alpine Research).

Table 2.4. Peat stratigraphy in Canadian peatlands.

Province	Latitude/ longitude (N,W)	Permafrost feature	Total peat depth (cm)	Key stratigraphic zone characteristics zone:depth (cm)	Key fossil indicators	Site conditions	Reference
Ontario	49°59', 79°54'	Non- permafrost	120	1 : 120-90	Calliergnella cuspidata, Drepanocladus verticosus, Carex exilis, Carex canescens, Carex oligosperma, Typha latifolia, Pedastrum spp., Larix laricina	Inundated	Kettles et al. 2000
				2a : 90-70	Picea mariana, L. laricina, Carex spp., Sphagnum spp.	Wet/mesotrophic	
				2b : 70-70	P. mariana, Betula spp., Alnus spp., Sphagnum magellanicum, Carex trisperma	Mesotrophic to ombrotrophic	
				2c : 40-20	P. mariana, Betula spp., Alnus spp., Ericaceae, Pteridophyta, C. trisperma, Carex disperma	Low-shrub, tree-covered ombrotrophic bog	
			3 : 20-0	P. mariana, S. magellanicum, Ericaceae	Forested, predominately stunted P. mariana ombrotrophic bog		
Ontario	51°33', 81°49'	Non- permafrost	254	1 : 254-245	P. mariana, Carex spp., Ericaceae, Sphagnum fuscum, Pedastrum spp.	Wet/minerotrophic evolving to drier ombrotrophic bog	Kettles et al. 2000
				2a : 245-220	M. gale, S. fuscum, Eriophorum spissum	Wet/ombrotrophic	
				2b : 220-50	P. mariana, S. fuscum, Ericaceae, Sphagnum capillifolium, Chamaedaphne calyculata	Drier/ombrotrophic	
				3 : 50-0	S. capillifolium, Ericaceae	Open, saturated bog, fluctuating water table	
Ontario	51°04', 84°30'	Non- permafrost	445	4 : 445-430	Typha spp., Equisetum spp., Chenopodiaceae, Cyperaceae, Poacea	Tidal marsh	Glaser et al. 2004a
				3c : 430-425	Calliergon giganteum, Phragmites sp., Equisetum spp.	Wet/minerotrophic	
				3b : 425-340	L. laricina, Equisetum sp., Carex sp., brown mosses, Betula spp., Ericaceae	Forested fen	
				3a : 340-294	L. laricina, S. subsecundum	Forested fen	
				2b : 294-255	L. laricina, P. mariana	Forested bog, L. laricina-dominated	
				2a : 235-97	P. mariana, S. fuscum, S. magellanicum	Forested bog, P. mariana-dominated	
				1 : 97-0	S. fuscum, S. capillifolium, C. calyculata	Non-forested bog	
Ontario	51°15', 83°35'	Non- permafrost	275	4 : 275-266	Typha spp., Equisetum spp., Chenopodiaceae, Cyperaceae, Poacea	Tidal marsh	Glaser et al. 2004a
				3 : 266-182	L. laricina, Equisetum sp., Carex spp., brown mosses, Betula spp., Ericaceae	Forested fen	
				2b : 182-172	L. laricina, P. mariana	Forested bog, L. laricina-dominated	
				2a : 172-66	P. mariana, S. fuscum, S. magellanicum	Forested bog, P. mariana-dominated	
			1 : 66-0	S. fuscum, S. capillifolium, C. calyculata	Non-forested bog		

Table 2.4. Cont.

Province	Latitude/ longitude (N,W)	Permafrost feature	Total peat depth (cm)	Key stratigraphic zone characteristics zone:depth (cm)	Key fossil indicators	Site conditions	Reference
Ontario	51°37', 82°17'	Non- permafrost	236	4 : 236-228 3960±60 ^b 3: 228-197 3960±60-3430±110 ^b 2b : 197-185 3430±110 ^b 2a : 185-83 3430±110-2280±50 ^b 1 : 83-0 2280±50 ^b -present	<i>Typha</i> spp., <i>Equisetum</i> spp., <i>Chenopodiaceae</i> , <i>Cyperaceae</i> , <i>Poaceae</i> <i>L. laricina</i> , <i>Equisetum</i> sp., <i>Carex</i> sp., brown mosses, <i>Betula</i> spp., <i>Ericaceae</i> <i>L. laricina</i> , <i>P. mariana</i> , <i>Betula</i> spp., <i>Sphagnum</i> spp. <i>P. mariana</i> , <i>S. S. magellanicum</i> <i>S. S. capillifolium</i> , <i>C. calyculata</i>	Tidal marsh Forested fen Forested bog, <i>L. laricina</i> - dominated Forested bog, <i>P. mariana</i> - dominated Non-forested bog	Glaser et al. 2004a
Quebec	57°44', 76°05'	Non- permafrost	200	1 : 200-190 6800-6610 ^a 2: 190-158 6610-6390 ^a 3a : 158-115 6390-6190a 3b : 115-80 6190-5620 ^a 4a : 80-50 5620-4850 ^a 4b : 50-22 4850-3670 ^a 5 : 22-5 3670-2420 ^a	<i>Carex aquatilis</i> , <i>Scorpidium scorpioides</i> , <i>Sphagnum</i> <i>recurvum</i> <i>Sphagnum</i> spp., <i>P. mariana</i> , brown mosses, <i>Salix</i> , <i>Empetrum nigrum</i> <i>Carex limosa/paupercula</i> , <i>Viola</i> sp., <i>E. nigrum</i> , <i>Potentilla palustris</i> , brown mosses, <i>P. mariana</i> , <i>Betula</i> <i>glandulosa</i> <i>C. aquatilis</i> , <i>P. palustris</i> , <i>Salix</i> , <i>B. glandulosa</i> , <i>P.</i> <i>mariana</i> , <i>E. nigrum</i> , <i>Sphagnum teres</i> , <i>Sphagnum</i> <i>warnstorffii</i> <i>C. limosa/paupercula</i> , <i>Myrica gale</i> , <i>C. aquatilis</i> , brown mosses, <i>Salix</i> spp. <i>P. mariana</i> , <i>S. teres</i> <i>P. mariana</i>	Peat accumulation initiated through paludification Drier than Zone 1 Wet/minerotrophic Wet/minerotrophic Wet/minerotrophic Drier than sub-zone 4a, but presence of shallow ponds Drier than Zone 4, but presence of shallow ponds Shallow pond Fluctuating water tables Wet/minerotrophic Wet/minerotrophic but drier than Zone 3 Drier conditions	Bhiry et al. 2007
Quebec	57°44', 76°05'	Non- permafrost	120	1 : 120-110 4960-4680 ^a 2 : 110-60 4680-3300 ^a 3 : 60-24 3300-1580 ^a 4a: 24-7 1580-480 ^a 4b : 7-0 480 ^a - present	<i>P. mariana</i> , <i>B. glandulosa</i> , <i>Salix</i> spp., <i>E. nigrum</i> , <i>P.</i> <i>palustris</i> , <i>C. aquatilis</i> <i>P. mariana</i> , <i>B. glandulosa</i> , <i>E. nigrum</i> , <i>Hylocomium</i> <i>splendens</i> , <i>S. teres</i> , <i>S. subsecundum</i> <i>Salix</i> spp., <i>C. aquatilis</i> , <i>C. limosa/paupercula</i> , brown mosses <i>C. aquatilis</i> , <i>Salix</i> spp., <i>C. limosa/paupercula</i> , <i>Menyanthes trifoliata</i> , brown mosses <i>P. mariana</i> , <i>B. glandulosa</i> , <i>Carex</i> spp., <i>Dicranum</i> spp.	Shallow pond Fluctuating water tables Wet/minerotrophic Wet/minerotrophic but drier than Zone 3 Drier conditions	Bhiry et al. 2007
Quebec	55°20', 77°40'	Palsa	225	1 : 225-210 5790-5640 ^a 2a: 210-178 5640-5170 ^a	<i>Potamogeton alpinus</i> , <i>Hippuris vulgaris</i> , <i>M. trifoliata</i> , <i>P.</i> <i>palustris</i> , <i>C. aquatilis</i> , <i>C. paleaceasalina</i> , <i>Alnus vrdis</i> <i>crispa</i> , <i>B. glandulosa</i> , brown mosses Brown mosses, <i>C. aquatilis</i> , <i>Carex rariflora</i> , <i>D. disperma</i> , <i>Salix</i> spp., <i>M. gale</i> , <i>Andromeda</i> spp., <i>E. nigrum</i>	Salt marsh Wet/minerotrophic with many ponds (rich fen)	Arlen-Pouliot and Bhiry 2005

Table 2.4. Con't.

Province	Latitude/ longitude (N,W)	Permafrost feature	Total peat depth (cm)	Key stratigraphic zone characteristics zone:depth (cm)	age (¹⁴ C yr BP)	Key fossil indicators	Site conditions	Reference
Quebec	55°20', 77°40'	Thermokarst pond	50	2b : 178-155	5170-4610 ^a	Brown mosses, <i>L. laricina</i> , <i>S. warnstorffii</i> , <i>C. aquatilis</i>	Wet/minerotrophic with fewer ponds than Sub-zone 2a (rich fen)	Arien-Pouliot and Bhiry 2005
				3 : 155-100	4610-4200 ^a	Brown mosses, <i>S. warnstorffii</i> , <i>S. teres</i> , <i>C. aquatilis</i> , <i>Trichophorum alpinum</i> , <i>M. trifoliata</i> , <i>M. gale</i>	Intermediate fen	
				4a : 100-55	4200-3100 ^a	<i>C. giganteum</i> , <i>L. laricina</i> , <i>P. mariana</i> , <i>M. gale</i> , <i>S.</i> <i>capillifolium</i> , <i>Trichophorum caespitosum</i>	Poor fen with high water table	
				4b : 55-25	3100-1760 ^a	<i>L. laricina</i> , <i>C. aquatilis</i> , <i>C. rariflora</i> , <i>C. disperma</i> , <i>T.</i> <i>caespitum</i> , <i>Viola incognita</i> , <i>T. nitens</i>	Poor fen with low water table	
				5 : 25-0	1760-400 ^a	<i>L. laricina</i> , <i>S. capillifolium</i> , <i>S. angustifolium</i> , <i>B.</i> <i>glandulosa</i> , <i>C. calyculata</i>	Forested bog, permafrost initiation	
				Palsa	400 ^a -present	<i>S. angustifolium</i> , <i>Vaccinium uliginosum</i>	Sphagnum-dominated palsa	
				1 : 50-30	525-480	<i>C. giganteum</i> , <i>S. riparium</i>	Thermokarst pond, maximum depth	
				2 : 30-21	120-40 ^a	<i>S. riparium</i> , <i>C. giganteum</i>	Thermokarst pond, partly filled, rapid peat accumulation	
				3 : 21-0	40 ^a -present	<i>S. lindbergii</i> , <i>S. riparium</i>	Thermokarst pond, filled, rapid peat accumulation	
				Quebec	55°20', 77°40'	Palsa	200	
2 : 170-120	3630-2880 ^a	<i>P. mariana</i> , <i>B. glandulosa</i> , <i>S. lindbergii</i> , <i>Calliergon</i> <i>stramineum</i>	Intermediate to poor fen					
3a : 120-85	2880-1970 ^a	<i>P. mariana</i> , <i>B. glandulosa</i> , <i>S. capillifolium</i> , <i>Cenococcum graniforme</i>	Stunted <i>P. mariana</i> bog					
3b : 85-30	1970-1630 ^a	<i>S. capillifolium</i> <i>Pohlia nutans</i> , <i>Calliergonella cuspidata</i>	Non-treed bog					
4a : 30-10	1630-740 ^a	<i>E. nigrum</i> , <i>S. capillifolium</i>	Palsa formation, substantial decrease in peat accumulation					
4b : 10-0	740-360 ^a	<i>B. glandulosa</i> , <i>E. nigrum</i> , <i>V. vitis-idaea</i> , <i>Dicranum</i> <i>fuscescens</i>	Palsa growth					
A : 171-60	6900-2100 ^a	<i>P. mariana</i> , <i>L. laricina</i> , <i>Juncus</i> spp., brown mosses	Peatland formation through paldification – treed rich fen					
B : 60-33	2100-500 ^a	<i>C. epidermis</i> , brown mosses, <i>S. magellanicum</i>	Open rich fen					
C : 33-15	500 ^a -AD 1960	<i>P. mariana</i> , <i>L. laricina</i> , <i>C. calyculata</i> , <i>S. lindbergii</i> , <i>S.</i> <i>riparium</i> , <i>S. magellanicum</i>	Treed poor fen					
D : 15-0	AD 1960-AD 1993	Lichens, <i>Polytrichum</i> spp., <i>S. acutifolia</i> , <i>S.</i> <i>magellanicum</i> , <i>Ericaceae</i> , <i>P. mariana</i>	Palsa formation					
Manitoba	57°23', 94°11'	Palsa	171	A : 171-60 B : 60-33 C : 33-15 D : 15-0	6900-2100 ^a 2100-500 ^a 500 ^a -AD 1960 AD 1960-AD 1993		Kuhry 2008	

Table 2.4. Con't.

Province	Latitude/ longitude (N,W)	Permafrost feature	Total peat depth (cm)	Key stratigraphic zone characteristics zone:depth (cm)	age (¹⁴ C yr BP)	Key fossil indicators	Site conditions	Reference
Quebec	47°41', 70°36'	Peat plateau	172	A : 172-111	6700-5000 ^a	B. glandulosa, Carex spp., L. laricina, Calliergon spp., Salix spp., Juncus spp.	Shrubby, wet rich fen	Kuhny 2008
				B : 111-71	5000-2250 ^a	L. laricina, P. mariana, S. , S. warnstorffii, Polytrichum spp.	Peat plateau formation	
				C : 71-28	2250-800 ^a	Ericaceae, S. lindbergii, S. riparium	Open, wet intermediate to per fen with in-situ permafrost-free conditions	
				D : 28-16	800-400 ^a	S. magellanicum, S. , Dicranum spp., P. mariana, Ericaceae	Dry treed bog with permafrost	
				E : 16-0	400-0 ^a	L. laricina, P. mariana, C. calyculata, S. jensenii/balticum, S. lindbergii	Permafrost formation under wet conditions, lack of dry vegetation elements almost complete lacking	
Quebec	47°41', 70°36'	Peat plateau	227	I : 227-195	5800-5380 ^a	Drepanocladus spp., Carex lasiocarpa	Rich, humid treed fen	Zimmerman and Laviole 2001
				II : 195-150	5380-4820 ^a	C. trisperma, charcoal composed of wood fragments and charred Abies balsamea, P. mariana, L. laricina	Rich fen – poor fen transition	
				III : 153-130	4280-4060 ^a	Sphagnum spp., C. limosa, E. vaginatum, C. calyculata, L. groenlandicum	Poor and humid treed fen	
				IV : 130-50	4060-1720	Andromeda glaucophylla, C. calyculata, L. groenlandicum, Sphagnum spp., charcoal assemblages composed of P. mariana and ericaceous shrubs	Open bog with ericaceous shrubs	
				V : 50-10	1720-recent	Sphagnum spp., C. trisperma, E. variantum, charcoal assemblages composed of P. mariana and ericaceous shrubs	Open Sphagnum bog	
Nunavut	60°50', 101°33'	Peat plateau	186	I : 186-180	5900-5700	P. mariana, L. laricina, V. vitis-idaea. S. fuscum, P. schreberi, Dicranum spp.	Dry permafrost forest	Sannel and Kuhny 2008
				II : 180-137	5700-4800	Carex spp., brown mosses, S. riparium, S. teres, S. cuspidatum, S. balticum, S. lindbergii	Local permafrost degradation of dry upland forest resulting in wetter, non-permafrost fen	
				III : 137-123	4800-4700	L. laricina, P. mariana, C. calyculata	Renewed permafrost aggradation	
				IV : 123-9	4700-2900	P. mariana, Polytrichum spp., Oxycoccus microcarpus, Ledum spp., charcoal fragments	Peat plateau and fire did not cause permafrost to collapse	
				V : 9-0	<2900	Ledum spp., fungal sclerotia, Carex spp.	Open peat plateau	
Saskatchewan	59°53', 104°12'	Peat plateau	197	I : 197-159	6600-4600	P. mariana, O. microcarpus, A. polifolia, Ledum spp., charcoal	Permafrost aggradation	Sannel and Kuhny 2008
				II : 159-119	4600-3700	Sphagnum cf. jensenii, Carex sp., charcoal, S. , Polytrichum spp., O. microcarpus, Ledum spp.	Permafrost collapse followed by permafrost aggradation	
				III : 119-0	<3700	O. microcarpus, V. vitis-idaea, P. mariana, Polytrichum spp., Ledum spp., charcoal	Treed peat plateau with fire occurrences. However, fire did not degrade the permafrost	

a-Calibrated years before present

b-Uncalibrated C years before present

Peatlands develop through either paludification or terrestrialization, with the former process important in large peatland complexes, such as the HBL (Lavoie et al. 2005, Simard et al. 2009). Peatland and permafrost ages vary from less than 100 to greater than 7000 cal yr BP (Table 2.5). By the time peatland succession has proceeded to the forested bog stage, generally more than two metres of peat have accumulated (Table 2.6), isolating the surface peat from the groundwater (Arlen-Pouliot and Bhiry 2005). In addition, *S. fuscum* presence creates a tight cushion at the peat surface, cooling peat temperatures and slowing decomposition rates, thereby promoting hummock establishment and growth. As hummocks continue to grow, they are further isolated from the groundwater, stimulating ice growth and palsa development when appropriate climatic conditions prevail (see section 3, Permafrost Patterns). Continued surface peat drying in palsas can lead to increases in abundance of *Cladina* spp. and other lichens and decreasing populations of *S. fuscum*, altering the albedo and reflecting more energy from the peat surface during snow-free periods, further enhancing ice growth (Malmer et al. 2005). Colder conditions also slow NPP and decomposition on palsas, where they can be C neutral or sinks or sources to the atmosphere (Robinson and Moore 2000, Bäckstrand et al. 2010). Palsa degradation can lead to either drier or wetter conditions, depending on the degree of thaw, amount of permafrost, and changes in ALT. Drying and active layer deepening shifts vegetation composition to shrubs and trees and exposes litter to oxygen for longer periods, thereby more completely decomposing litter (Malmer et al. 2005, Schuur et al. 2007).

Table 2.5. Basal peat ages in peatlands in permafrost zones of Canada.

Peatland type/province	Latitude/ Longitude (N,W)	Permafrost feature	Peat depth (cm)	Age (¹⁴ C yr BP)	Reference
Bogs					
Ontario	49°59', 79°54'	Non-permafrost	150	7280 + 70	Kettles et al. 2000
Ontario	51° 04', 84°30'	Non-permafrost	445	5920 ± 90	Glaser et al. 2004a
Ontario	51°15', 83°35'	Non-permafrost	266	4810 ± 70	Glaser et al. 2004a
Ontario	51°15', 83°20'	Non-permafrost	220	5220 ± 80	Glaser et al. 2004a
Ontario	51°23', 83°22'	Non-permafrost	127	3700 ± 70	Glaser et al. 2004a
Ontario	51°37', 82°17'	Non-permafrost	236	3960 ± 60	Glaser et al. 2004a
Ontario	51°43', 83°14'	Non-permafrost	223	3730 ± 50	Glaser et al. 2004a
Ontario	51°33', 81°49'	Non-permafrost	264	4000 ± 80	Kettles et al. 2000
Ontario	51°43', 83°38'	Non-permafrost	209	4500 ± 70	Glaser et al. 2004a
Quebec	57°45', 76°15' to 58°10', 76°30'	Palsa (tundra)	1 to 12	630 ± 60 to 3040 ± 70	Lavoie and Payette 1997
Quebec	57°45', 76°15'	Peat plateau	102 to 260	4400 ± 90 to 6480 ± 120	Bhiry et al. 2007
Quebec	57°44', 76°05'	Palsa	-	280 ± 60 to 3410 ± 100	Bhiry et al. 2007
Manitoba	57°23', 94°11'	Palsa	169	5970 ± 90	Kuhry 2008
Manitoba	57°50', 94°12'	Peat plateau	166	5810 ± 90	Kuhry 2008
Fens					
Ontario	51°14', 83°02'	Non-permafrost	149 to 234	5200 ± 60 to 5370 ± 80	Glaser et al. 2004a
Ontario	51°23', 83°22'	Non-permafrost	104 to 127	3910 ± 80 to 4550 ± 70	Glaser et al. 2004a
Ontario	51°37' 82°17'	Non-permafrost	98 to 109	3840 ± 70 to 4010 ± 80	Glaser et al. 2004a
Quebec	55°20', 77°40'	Palsa	225 to 252	4880 ± 100 to 5100 ± 100	Arlen-Pouliot and Bhiry 2005
Quebec	55°20', 77°40'	Filled thermokarst pond	37	350 ± 60	Arlen-Pouliot and Bhiry 2005
Quebec	55°18', 77°34'	Palsa	200	4070 ± 70	Bhiry and Robert 2006
Polygonal peatlands					
Nunavut	66°27', 104°80'	Peat plateau	184	7170 ± 100	Vardy et al. 2005
Nunavut	66°27o, 104°80'	Peat plateau	255	5820 ± 70	Vardy et al. 2005
Nunavut	64°43', 105°35'	Peat plateau	202	5710 ± 70	Vardy et al. 2005
Nunavut	64°43', 105°35'	Peat plateau	196	6370 ± 80	Vardy et al. 2005
Nunavut	60°50', 101°33'	Peat plateau	186	5065 + 70	Sannel and Kuhry 2008
Saskatchewan	59°53', 104°21'	Peat plateau	196	5780 ± 90	Sannel and Kuhry 2008
Nunavut	63°39', 95°50'	Peat plateau	152	3850 ± 400	Zoltai 1993
Nunavut	62°07', 96°32'	Peat plateau	204	3890 ± 160	Zoltai 1993
Nunavut	61°38', 97°12'	Peat plateau	177	4380 ± 130	Zoltai 1993
Northwest Territories	67°28', 134°35'	Peat plateau	104	1720 + 100	Zoltai 1993
Nunavut	72°58', 93°37'	Peat plateau	135	6280 + 80	Zoltai 1993

Table 2.6. Holocene history for a *palsa* peatland in Quebec (adapted from Arlen-Pouliot and Bhiry 2005).

Age (cal yr BP)	Paleoenvironment	Characteristic plant species	Developmental factors (ALL = allogenic; AUT = autogenic)
0	Thermokarst pond	Filled	<i>S. lindbergii</i> , <i>S. riparium</i>
		Partly filled	<i>S. riparium</i> , <i>C. giganteum</i>
		Maximum water depth	<i>C. giganteum</i> , <i>S. riparium</i>
200			Modern climate warming and precipitation increase (ALL)
400	Palsa	<i>S. capillifolium</i> , <i>S. angustifolium</i> , <i>Andromeda</i> spp., <i>C. calyculata</i>	Limited peat accumulation (AUT) Climate cooling during Little Ice Age (ALL) Accumulation of insulating <i>Sphagnum</i> peat cap (AUT)
1,760	Forested bog	<i>S. capillifolium</i> , <i>S. angustifolium</i> , <i>Andromeda</i> spp., <i>C. calyculata</i>	Lowest peat accumulation, acidification (AUT) Total Holocene accumulation of >2 m of peat (AUT) Neoglacial climate deterioration (ALL)
4,200	Poor fen	Afforested	<i>T. nitens</i> , <i>P. squarrosa</i> , <i>Drepanocladus</i> spp., <i>L. laricina</i> , <i>Vaccinium</i> spp.
		Shrubby	<i>C. giganteum</i> , <i>Andromeda</i> spp., <i>M. gale</i> , <i>C. calyculata</i> , <i>L. laricina</i> , <i>Carex</i> spp.
			Low water table associated with decreased precipitation (ALL) Limited peat accumulation, acidification (AUT) High water table associated with increased precipitation (ALL) Limited peat accumulation (AUT)
4,610	Intermediate fen with ponds and forested stands	<i>P. squarrosa</i> , <i>S. warnstroffii</i> , <i>S. teres</i> , <i>L. laricina</i> , <i>P. mariana</i> , <i>Carex</i> spp.	High water table associated with increased precipitation (ALL) Very rapid peat accumulation (AUT)
5,640	Rich fen	Ponds moderately disappeared	<i>P. squarrosa</i> , <i>S. nitidum</i> , <i>L. laricina</i> , <i>C. aquatilis</i>
		With many ponds	<i>C. giganteum</i> , <i>S. scorpioides</i> , <i>Andromeda</i> spp., <i>Salix</i> spp., <i>M. gale</i> , <i>Carex</i> , <i>Eriophorum</i>
			Low water table associated with warm and dry climate during mid-Holocene (ALL) Rapid peat accumulation (AUT) High water table associated with isostatic uplift (ALL) Rapid peat accumulation (AUT)
5,800	Marsh	<i>C. stellatum</i> , <i>Salix</i>	Rapid relative sea level fall (isostatic uplift) (ALL) Rapid peat accumulation (AUT)
6,000	Tyrrell Sea	No macrofossils found	Depressed continent (ALL)

Vegetation succession following permafrost thaw depends on the position of the peat collapse in relation to the water table and location of the collapse (internal, lateral, or edge). For example, lateral and edge scars receive circumneutral groundwater from regional fens, supporting poor to intermediate fen vegetation (Camill 1999a, Beilman 2001). Edge and lateral scars may succeed to (1) *Sphagnum*-dominated bogs or poor fens or (2) brown moss, sedge (*C. aquatilis*, *C. exilis*, and *C. lasiocarpa*), and tall shrub fens, depending on when the collapse scar contacted circumneutral groundwater (Schoor et al. 2007). An internal collapse scar surrounded by permafrost does not receive groundwater from surrounding fens (Beilman 2001). These situations support acidic (hummock) mosses (e.g., *S. fuscum* and *S. capillifolium*) and re-initiation of hummock and hollow microtopography. Where permafrost degradation leads to improved drainage and surface peat drying, feathermosses or lichens become more important hummock plants; combined with appropriate climatic conditions this vegetation change can reinitiate ice growth (Malmer et al. 2005).

Vegetation and peatland carbon accumulation relationships

During Holocene peatland development, long-term climatic conditions have contributed to significantly different C accumulation rates (Borren et al. 2004, Arlen-Pouliot and Bhiry 2005, Yu 2006). Generally, rapid peat accumulation rates are associated with fens during periods of high water table levels and with collapsed scars due to saturated peat that inhibits organic matter decomposition (Tables 2.4 and 2.6). Common species occurring during these periods include brown mosses, sedges (*S. hudsoniana*, *S. cespitosus*, *C. diandra*, *C. lasiocarpa*), and *Sphagnum* species (*S. warnstorffii*, *S. teres*, *S. riparium*) adapted to wet conditions (Arlen-Pouliot and Bhiry 2005, Sannel and Kuhry 2009). Belyea and Malmer (2004) reported that peat height growth and LORCA rates were highest as mosses shifted from dry-to-wet adapted *Sphagnum* species and then steadily decreased until the next vegetation shift (Figure 2.5). Similar results were reported in a permafrost fen in subarctic Québec, where wet-adapted tall shrubs and larch trees were correlated with rapid C accumulation (Arlen-Pouliot and Bhiry 2005). Both studies, as well as others (e.g., Yu et al. 2003, Borren et al. 2004), confirm the role of water table levels in peatland C accumulation. Although rapid peat accumulation occurs when water table levels are high, the accumulated peat is easily decomposed when dry, releasing CO₂ to the atmosphere (Turetsky et al. 2008a).

Throughout the Holocene, C accumulation rates have generally decreased across the boreal and subarctic zones (Yu et al. 2003, Belyea and Malmer 2004, Beilman et al. 2009), even though increases in precipitation or thermokarst formation have been shown to stimulate accumulation rates (Meyers-Smith et al. 2007). Lowest C

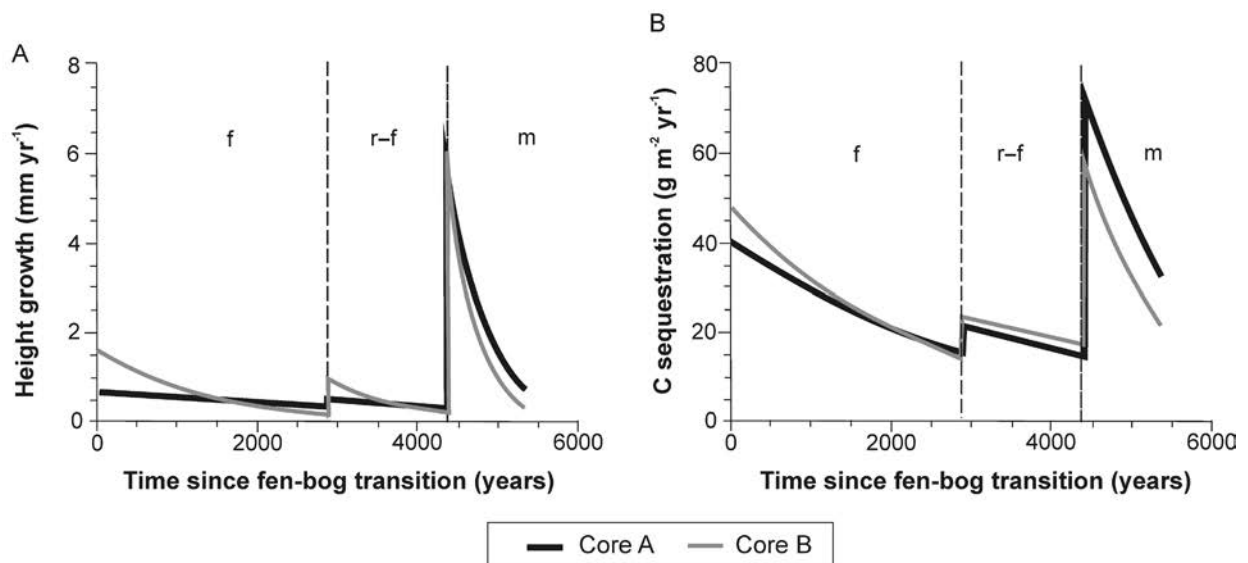


Figure 2.5. Rates of (a) peat height growth and (b) carbon (C) sequestration, for the past 5,400 years at Store Mosse mire, southern Sweden (Belyea and Malmer 2004; reprinted with permission from John Wiley and Sons). Broken vertical bars show dates separating three bog stages: f (*Sphagnum fuscum*), r-f (*Sphagnum rubellum*–*Sphagnum fuscum*) and m (*Sphagnum magellanicum*).

accumulation rates occur in poor fens, bogs, and palsa/peat plateaus (Table 2.6) with the lowest water table levels (Arlen-Pouliot and Bhiry 2005). Here, LORCA varied from less than 0 to approximately $12 \text{ g m}^{-2} \text{ yr}^{-1}$ compared to 19 to $69 \text{ g m}^{-2} \text{ yr}^{-1}$ in fens (Robinson and Moore 2000, Turunen et al. 2001, Borren et al. 2004). Fens show more variation in Holocene C accumulation rates and similar fen types in the same region can differ in their long-term C accumulation rates (Figure 2.6a,b) (Yu et al. 2003, Yu 2006).

Bogs and fens also have different patterns of peat accumulation: bogs have a concave pattern, which is an important assumption for C accumulation modelling (Clymo 1984), whereas fens commonly have a convex pattern (Yu et al. 2003, Robinson 2006, Yu 2006), which inhibits accurate projections of C accumulation rates. Non-conformance of fens to concave peat accumulation patterns needs to be considered in C accumulation modelling because fens are important to peatland C dynamics and seem more sensitive to hydrological changes than bogs (Robinson 2006, Yu 2006). Further research on Holocene C accumulation patterns in fens is warranted.

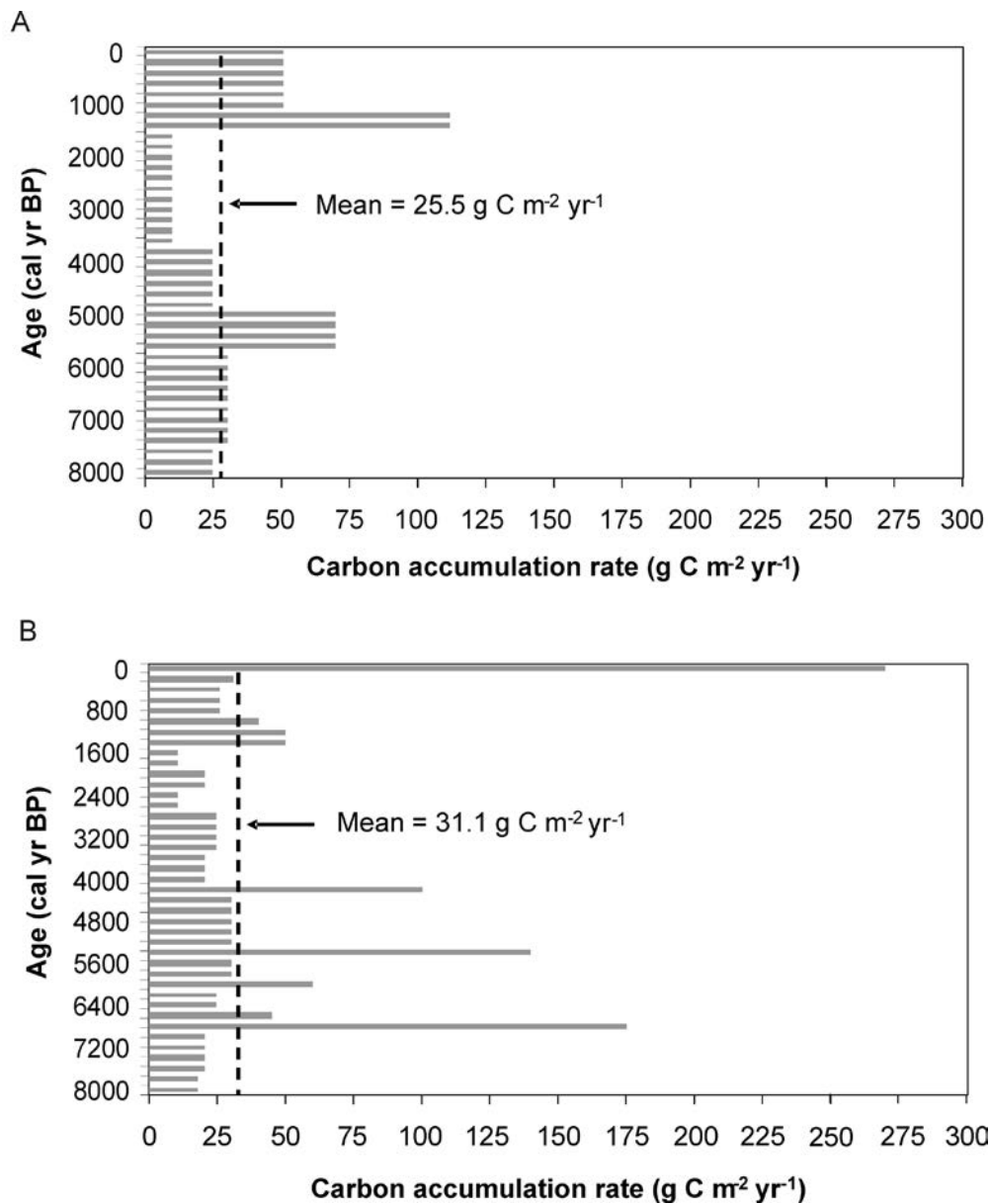


Figure 2.6. Fen peat long-term carbon accumulation rates for two fen peatlands in Alberta: (a) Yu et al. (2003) and (b) Yu (2006).

Effects of climate change on peatland succession

Bogs and fens respond differently to temperature and precipitation changes. The more compacted fen peat, which also benefits from groundwater inflow from uplands, results in adequate water table and soil moisture levels, supporting photosynthesis, root respiration, and organic matter decomposition during drought periods (Webster et al. 2013). However, bogs have a lower water table and coarser surface peat texture. Here, prolonged drought can lead to plant moisture stress and reduced photosynthesis and microbial decomposition (see section 5, Peatland Carbon Cycling) as well as increased susceptibility to fire (see section 6, Fire Regimes). Also, bog C dynamics may change in response to changing temperature (Lafleur et al. 2005) rather than water table levels as reported for fens (Aerts et al. 2006).

Climate change may affect PFTs through warmer peat that may be either dry or wet. For example, sampling over 30 to 50 years of a permafrost peatland complex in northern Sweden showed more trees, dwarf shrubs, and hummock mosses in drier areas following permafrost thaw than previously measured (Malmer et al. 2005). However, sedges expanded in wet areas at the cost of hummocks previously vegetated by dwarf shrubs. Resampling of another Swedish peatland complex showed an increase in tree cover from less than 5% of plots initially sampled to approximately 30% of plots sampled 42 years later (Gunnarsson et al. 2002). Percentage of plots containing mosses also increased whereas plots containing sedges decreased (Figure 2.7a). In Alaskan tundra, recent thermokarst had high sedge and moss biomass (Schuur et al. 2007). In old thermokarst, moss biomass remained high but sedges decreased to levels similar to a non-disturbed tussock-sedge reference site (Figure 2.7b).

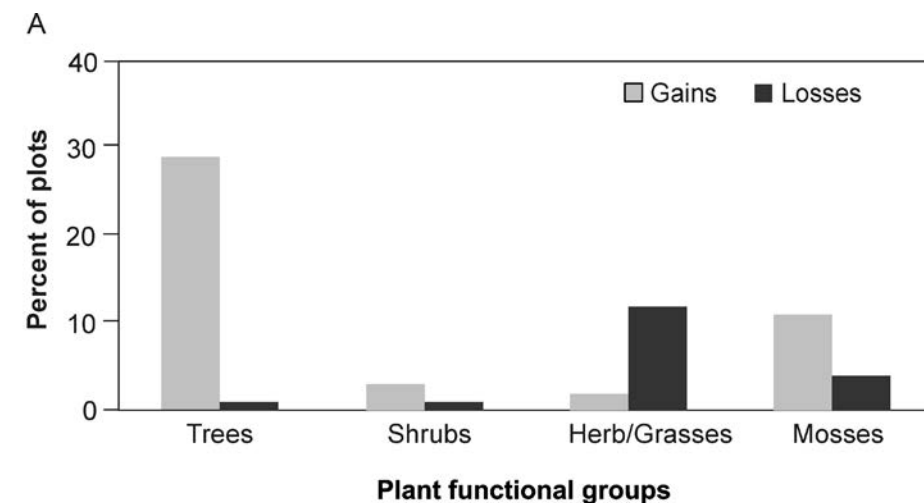
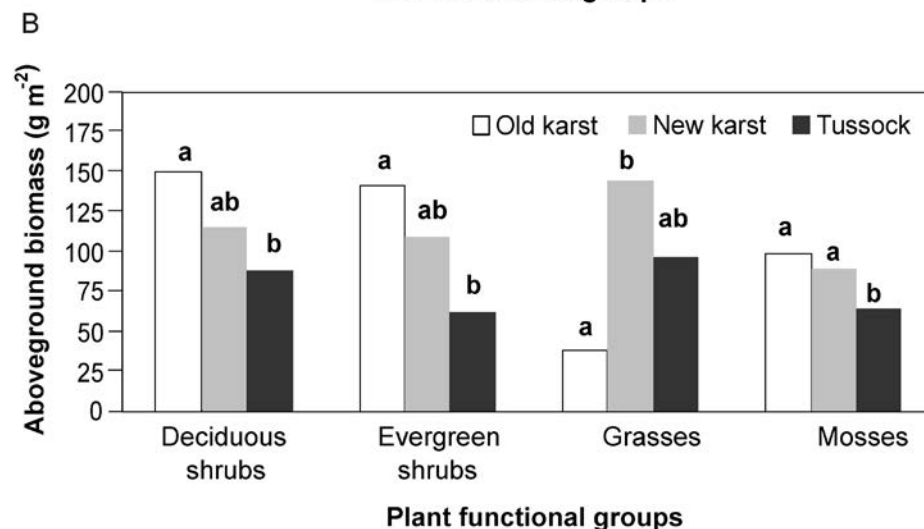


Figure 2.7. Plant functional groups in various peatland features: (a) percent of plots gained or lost for four plant functional groups after 40-year re-sampling of a Swedish peatland (adapted from Gunnarsson et al. 2002) and (b) aboveground biomass of plant functional groups at three sites with varying degrees of permafrost in Alaska (adapted from Schuur et al. 2007).



In a large-scale water table and temperature manipulation experiment in northern Minnesota (Weltzin et al. 2003), four years of treatments resulted in 50% higher shrub cover in a bog mesocosm as mean monthly soil temperature at 15 cm depth increased from 1.6 to 4.1 °C. The soil temperature treatments reduced sedge cover by 50%. Biomass allocation, however, varied with water table level: under dry conditions aboveground biomass increased 30% and belowground biomass increased 100% (Weltzin et al. 2003). Higher water table levels in a fen mesocosm resulted in increased sedge cover, especially for *C. lasiocarpa* and *C. livida*. Lower water table levels produced similar shrub cover results as those in the bog. Total sedge cover after five years of wet treatment was twice that of the intermediate and dry treatments. In contrast, shrub cover in the dry treatment was twice that of the intermediate or wet plots (Weltzin et al. 2003).

Results of the above-described field and mesocosm studies are consistent with those of studies that used remote sensing techniques (Cornelissen et al. 2001, Tape et al. 2006), which also indicated increases in tree and shrub vegetation under drier conditions versus sedges and wet-adapted *Sphagnum* mosses under wetter conditions. Remote sensing studies in permafrost regions of North America, Scandinavia, and Siberia have also provided evidence of expanding tall shrub (e.g., *Alnus* spp., *Betula* spp., and *Salix* spp.) cover in response to warming and thermokarst formation at regional assessments (Cornelissen et al. 2001, Tape et al. 2006). In addition, fire and other disturbances made possible by lower water table levels resulted in shrub expansion in small landscapes (Meyers-Smith et al. 2007). Shrub expansion may be attributed to increased temperature, N mineralization, and shade tolerance (Table 2.7) as shrubs out-compete sedges for available N, allowing only shade tolerant species to remain (Gignac et al. 2004).

In various subarctic regions across North America, Scandinavia, and Siberia, warmer temperature and soil drying have also contributed to perpetuation of trees and the advancement of tree lines (Vallée and Payette 2004, Kullman 2007). However, forest establishment on permafrost soil requires active layers to be at least one metre deep; shallower active layers (e.g., 0.5 m) inhibit tree establishment and subsequent advancement (Lloyd 2005). After the onset of warming, tree line expansion into peatlands is expected to occur, with lag times ranging from 60 to 450 years. Low water table levels and the presence of existing young trees on peatlands may support rapid tree growth and expansion (Bhatti et al. 2003). Long lag times are attributed to low seed production, slow growth, and periodic mortality from pathogens and fire (Lloyd et al. 2003, Lloyd 2005). Woody vegetation expansion may also affect permafrost thaw, with responses ultimately depending on how canopy area interacts with wind speed, snowpack thickness, and soil temperature and moisture (see section 3, Permafrost Patterns).

Table 2.7. Directional changes in plant functional types (↑ = increased numbers; ↓ = decreased numbers) in response to physical and chemical site changes associated with climate change.

Plant functional type	Temperature increase	Nitrogen increase	Water table		Shading
			Increase	Decrease	
Mosses	↓	↓	↓	↑	↓
Grasses	↑	↑	↑	↓	↓
Dwarf shrubs	↑	↑	↓	↑	↑
Tall shrubs	↑	↑	↑	↓	↑
Trees	↑	↑	↓	↑	↑

Summary and conclusions

Peatlands are divided into bogs and fens, each of which is subdivided into various non-permafrost and permafrost ecological types. In expansive peatland complexes, such as the HBL, bogs, fens, and permafrost features dominate landscape structure. The composition of peatland types and permafrost features, however, is not spatially or temporally static, suggesting that C cycling changes also occur through both space and time. Bogs are populated primarily by dwarf shrubs and trees with high leaf area. Those PFTs, along with dry-adapted mosses, also contribute litter that decomposes relatively slowly to bog surfaces. Despite its slow decomposition rate, low water table levels contribute to relatively high (compared to fens) volumes of aerobic peat, increasing the overall peat mineralization rate, which emits more CO₂ from the bog surfaces to the atmosphere. In contrast, the higher leaf area (compared to fens) of dwarf shrubs and trees generally enhances NPP, with more C sequestration allocated to aboveground (and belowground) biomass and less to peat.

In contrast to bogs, fens have higher water tables, promoting both aerobic and anaerobic organic matter decomposition along with higher CH_4 fluxes. Methane emission from fens is positively correlated with the amount of sedges present, and enhanced CH_4 emission from fens can augment GWP fluxes. Furthermore, relatively highly decomposable organic matter is stored as peat in fens, especially rich (e.g., open, sedge) fens. Therefore, lower water table levels and warmer peat temperatures may result in the release of substantial amounts of CO_2 and CH_4 from rich fen surfaces to the atmosphere. Fens also transport more DOC and GHGs to surface waters because of relatively rapid near-surface water flow, although surface water DOC and GHG cycling are poorly documented.

As peatlands warm and dry in response to expected changes in climate, fen transformations to bogs may intensify due to faster peat acidification and nutrient mineralization. Subsequent shifts from tall shrubs and sedges to dwarf shrubs and trees may increase CO_2 sequestration in aboveground biomass. Moreover, longer future growing seasons may interact with leaf area, further enhancing biomass CO_2 sequestration. In spite of accelerated CO_2 release from peat mineralization, enhanced shrub and tree NPP may result in bogs retaining their C sink function as peat warms, only shifting CO_2 sequestration from predominately peat to aboveground vegetation.

Collapse scars, thermokarst ponds, and fens may be net C sinks because rates of NPP are much greater than those of peat decomposition. However, as succession proceeds and features dry, peat respiratory CO_2 losses will increase, slowing net CO_2 sequestration rates. These changes have been linked to changes in PFTs from sedges, tall shrubs, and wet-adapted mosses to dwarf shrubs, trees, and to dry-adapted mosses. Although they are CO_2 sinks, wet features are frequently net CH_4 sources to the atmosphere, thereby potentially increasing GWP over decadal timeframes.

The complex C cycling patterns in sizeable peatland complexes requires enhanced research efforts to document PFTs and their correlations with hydrology, fire, and C accumulation patterns. Stratigraphic studies combining charcoal, radiocarbon (^{14}C), macrofossil, and pollen analyses allow correlations among plant associations, hydrology, fire, permafrost features, and C accumulation rates. These correlations have been used to identify the general sequence of peatland succession from open water to marsh (saltwater or freshwater) to fen and eventually to bog and to provide estimates for LORCA rates across northern peatlands. Coupling stratigraphic studies with those of PFTs and C sequestration on current landscapes will enhance certainty of model and scaling results of peatland C storage and sequestration to more confidently prescribe appropriate land use plans.

3. Permafrost Patterns

Background

Permafrost regulates various ecological processes and functions, including terrestrial C storage and atmospheric GHG concentrations (Schuur et al. 2009). However, permafrost occurrence is not static and its area and ice content are spatially and temporally variable within and among terrestrial landscapes. In terms of temporal variation, GCM hind-casting ('predicting' what happened during past episodes of climate change) studies (Zhang et al. 2005, Chen et al. 2003) along with paleoecological studies (Arien-Pouliot et al. 2005, Kuhry and Turunen 2006) point to permafrost formation and thawing commonly occurring during the Holocene (see section 2; Peatland Development and Plant Associations).

Despite its important role in peatland C storage and sequestration, the knowledge base to incorporate spatial and temporal permafrost dynamics into land use planning and climate change assessments is rudimentary. Therefore, in this section, we discuss permafrost dynamics and climate change interactions, including (1) aggrading and degrading permafrost features, (2) environmental controls on permafrost dynamics, (3) 20th and 21st century permafrost trends and their controlling factors, and (4) identify research needed to document permafrost thaw dynamics and their controls to assess future permafrost effects on northern peatland C storage and GHG emissions to the atmosphere.

Permafrost dynamics

Permafrost soil layers

Permafrost soils are classified as Turbic and Static (mineral soil) and Organic Cryosols. Turbic and Static Cryosols are differentiated by the degree of cryoturbation (the mixing of soil layers due to repeated freeze-thaw processes), with the former having marked evidence of cryoturbation and the latter showing little to no evidence of cryoturbation. Organic Cryosols develop primarily from organic material over either a lithic contact (10 to 160 cm of organic soil overlying consolidated bedrock), or an ice layer at least 30 cm thick (Siltanen et al. 1997).

Permafrost soils comprise three general layers: (1) active, (2) transitional, and (3) frozen, all of which expand and contract depending on internal heat production and air temperatures. The active layer is the surface-most region of soil that alternates between winter freezing and summer thawing (Hinzman et al. 1991). Active layer thickness is maximal during September to October and is the location of intense soil microbial nutrient and C mineralization (Schuur et al. 2008). Mineralized nutrients, including N and phosphorus are critical to CO₂ sequestration in vegetative biomass and, subsequently, peat (Laiho et al. 2003).

In the CPZ, active layers are cold and only a few centimetres thick (Schuur et al. 2008). This results in slow organic matter mineralization, with few nutrients available to plants and therefore low NPP. In contrast, warm and thick active layers frequently occur in the DPZ, mineralizing more nutrients that are effectively assimilated by plants; thereby supporting more NPP and organic matter mineralization (Hobbie et al. 2000). The above relationships are further discussed in section 5, Peatland Carbon Cycling. Transitional layers are ice-rich zones of a few centimetres to more than one metre thick that separate active and frozen layers (Allard et al. 1996). Transitional layers contain large amounts of soil C that, as the ice melts, may be lost as CO₂ to the atmosphere via enhanced organic matter mineralization (Turetsky et al. 2007), but these dynamics are poorly documented.

Aggrading permafrost features

General patterns: Permafrost growth results in various aggrading features that are elevated beyond the surface of the surrounding landscape (Table 3.1, Figures 3.1a and 3.2a,b). Across aggrading features, ice formation in peat during the winter causes it to lift. At this time raised, dry peat insulates the soil during summer, maintaining the ice core (Hinzman et al. 1991). Most aggrading features occur in both the CPZ and DPZ, with pingos and polygonal peatlands primarily occurring in the CPZ (Table 3.1). Palsas, lithalsas, and peat plateaus are common aggrading features in the DPZ (Beilman et al. 2001, Gurney 2001) and have been proposed as potential indicators of a changing climate (FPTGC 2010).

Table 3.1. Permafrost aggrading and degrading features common in Ontario's Far North.

Permafrost feature	Characteristics	Zone of occurrence
Aggrading to mature		
Pingo	Land elevated due to ice-wedge growth	CPZ ^a
Polygonal peatland	Land elevated due to cracks in shrinking permafrost	CPZ
Palsa	Peat elevated due to ground ice expansion; ice penetration into mineral sediment	CPZ, DPZ ^b
Peat plateau	Peat elevated due to ground ice expansion; ice core only in peat; coalesced palsas	CPZ, DPZ
Lithalsa	Mineral sediment elevated due to ground ice expansion	CPZ, DPZ
Degrading		
Floating mat	Subsiding material under peat due to ice thaw along lake shorelines	
Thermokarst pond	Surface inundated due to ice thaw	CPZ, DPZ
Thermokarst lake	Ground collapsed following thawing of ground ice in regions underlain by permafrost resulting in shallow body of water	CPZ, DPZ
Internal lawn	Area inundated outside peat plateau or palsa due to thawing of ice	DPZ
Collapse scar	Internal regions of a peat plateau collapse where ice has thawed	CPZ, DPZ
Talik	Patch of permanently unfrozen ground above permafrost surface	CPZ, DPZ

^aCPZ = continuous permafrost zone^bDPZ = discontinuous permafrost zone

Palsas and lithalsas: Palsas are permafrost mounds in peat (Figure 3.1a) that are generally less than 100 m in diameter and vary from 1 to 5 m high (Railton and Sparling 1973, Beilman et al. 2001). Lithalsas are similar types of mounds whose surface layer is composed primarily of mineral soil (Gurney 2001). Palsas and lithalsas contain perennially frozen cores of alternating layers of ice and organic or mineral material (Allard et al. 1996, Calmels et al. 2008a). Mound formation occurs through two processes: (1) meteoric water (i.e., precipitation) percolation through the active layer to the transitional layer and (2) cryosuction of groundwater from surrounding non-permafrost landscape features (Gurney 2001). Both processes contribute to ice formation and growth, with subsequent lifting of surface peat (Zhang 2005).

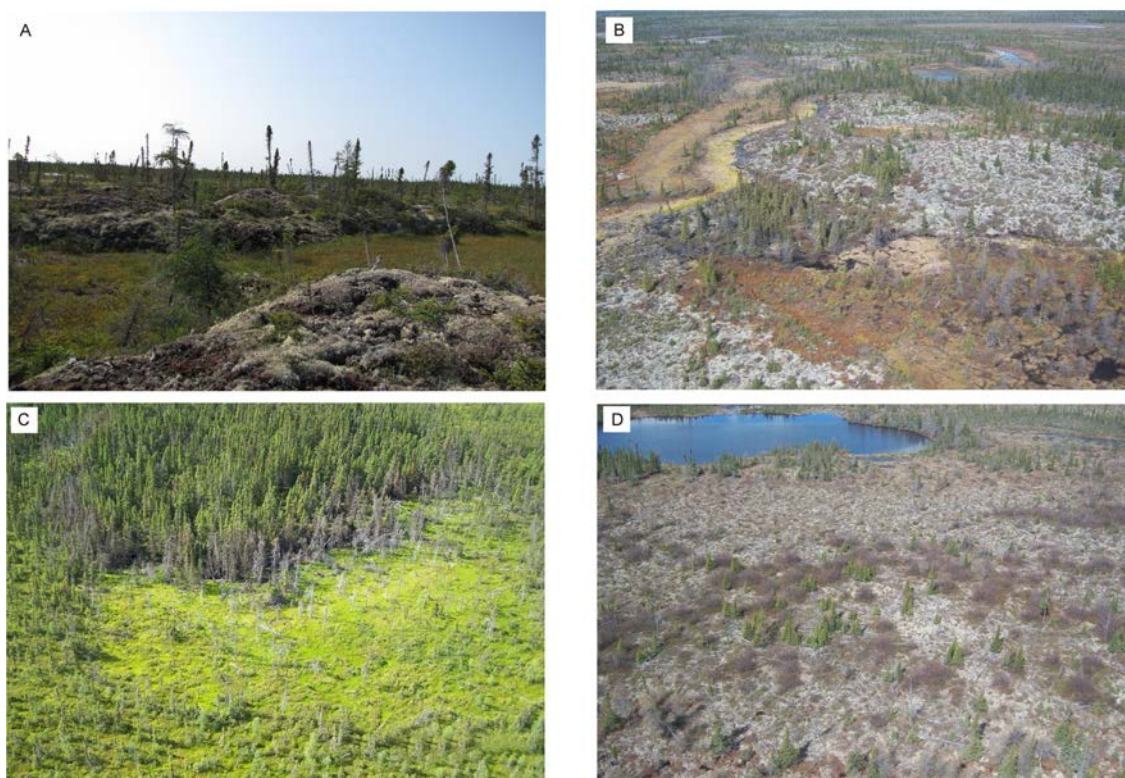
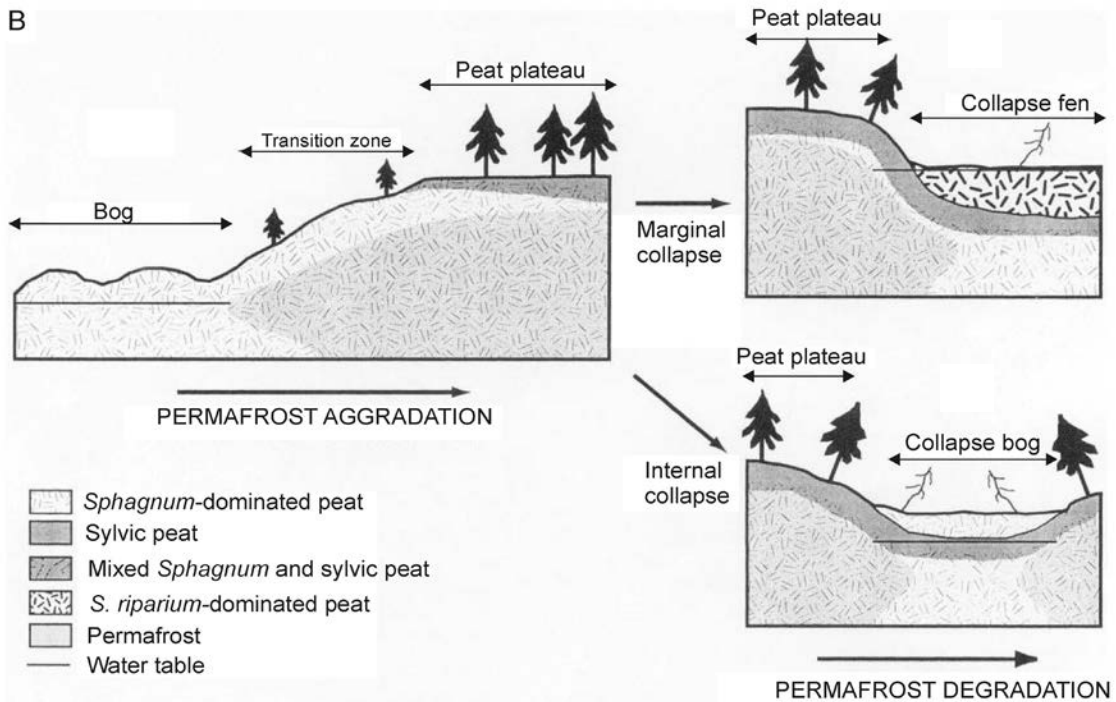
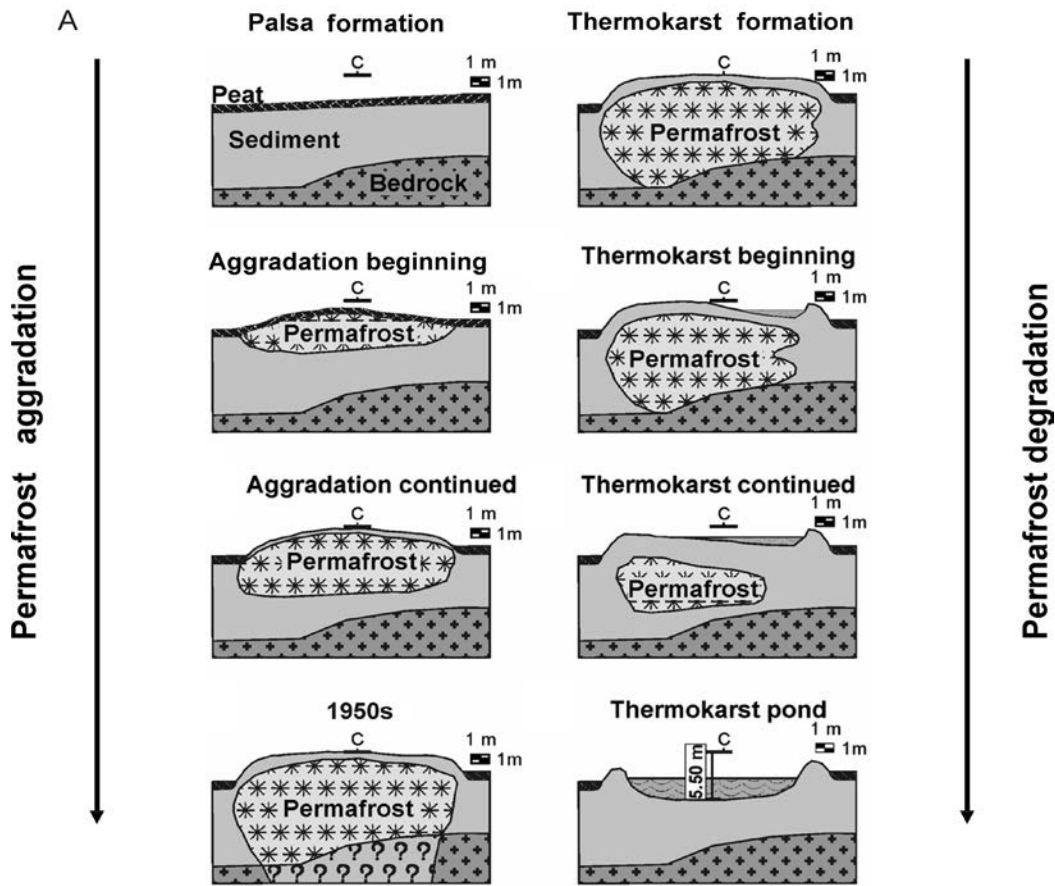


Figure 3.1 Common permafrost features: (a) peat plateau and collapse scar landscape, (b) palsa field, (c) internal lawn at edge of a peat plateau, and (d) peat plateau and thermokarst lake landscape in the Hudson Bay Lowlands of Ontario.



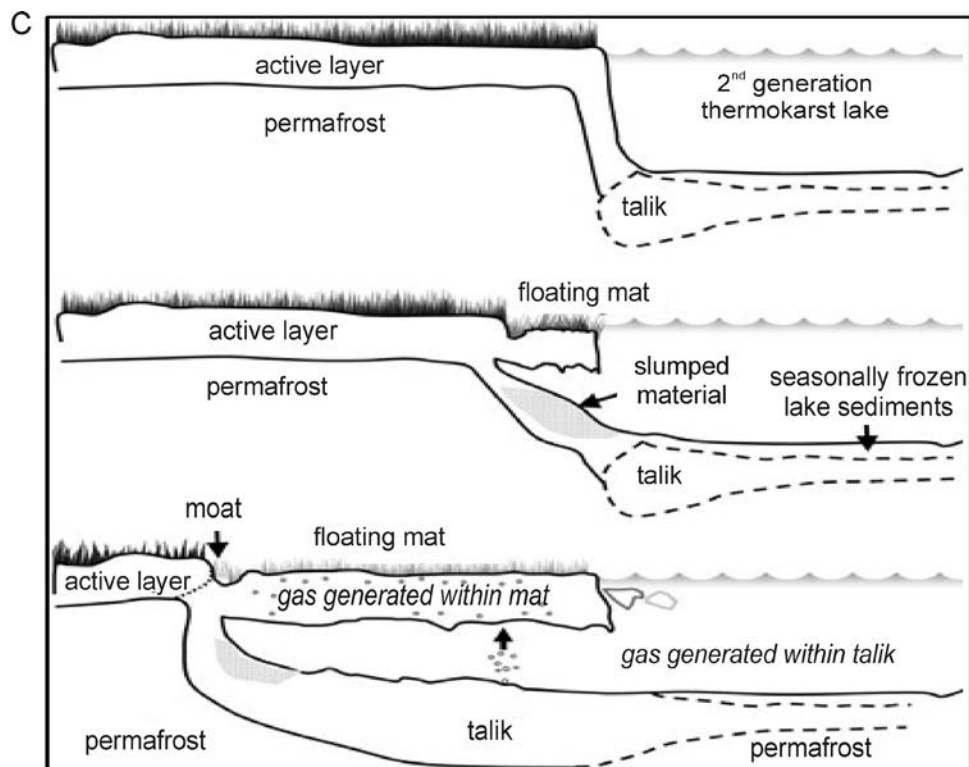


Figure 3.2. Stages of permafrost aggradation and degradation: (a) palsa formation followed by thermokarst pond formation (Calmels et al. 2008b; reprinted with permission from Elsevier), (b) collapse scar formation (Robinson and Moore 2000; reprinted with permission from Arctic, Antarctic, and Alpine Research), and (c) floating vegetation mat formation (Parsekian et al. 2011; reprinted with permission from John Wiley and Sons.).

Ice growth is regulated by soil thermal properties and peat has lower thawed and frozen thermal conductance than mineral soil (Table 3.2). As such, peat is a better insulator than mineral soil, augmenting ice formation and growth. However, thermal conductivity of thawed saturated peat ranges between 0.41 and 0.60 W m⁻¹ K⁻¹ and it is an excellent conductor of energy that melts ice. In contrast, thawed unsaturated peat has a thermal conductivity between 0.23 and 0.28 W m⁻¹ K⁻¹, which is near the thermal conductivity of dry snow making it an excellent insulator (Goodrich 1982, Moore 1987). Dried peat slows its heat loss during the summer and enhances cold air penetration throughout the peat profile during the winter (Romanovsky and Osterkamp 2000). This enables meteoric water to be converted to ice, where it accounts for 50 to 80% of the soil volume in the transitional layer (Allard et al. 1996).

Table 3.2. Range of soil and water thermal properties reported in the literature (from Halliwell and Rouse 1987, Moore 1987, Rouse et al. 1987, Hinzman et al. 1991, Boike et al. 1998, Romanovsky and Osterkamp 2000, Westin and Zuidhoff 2001, Zhang 2005, Ling and Zhang 2006, Overduin et al. 2006, Kujala et al. 2008).

Material	Thawed thermal conductivity (W m ⁻¹ K ⁻¹)	Thawed volumetric heat capacity (MJ m ⁻³ K ⁻¹)	Thawed thermal diffusivity (10 ⁻⁶ m ² s ⁻¹)	Frozen thermal conductivity (W m ⁻¹ K ⁻¹)	Frozen volumetric heat capacity (MJ m ⁻³ K ⁻¹)	Frozen thermal diffusivity (10 ⁻⁶ m ² s ⁻¹)
Snow	-	-	-	0.09 to 0.50 ^a	0.52 to 0.91 ^b	0.35
Water-ice	0.57	4.18	0.14	2.24	2.04	1.10
Mineral soil	1.13 to 2.19	2.40 to 2.87	0.49 to 0.91	2.21 to 3.01	1.86 to 1.92	1.15 to 1.62
Peat	0.23 to 0.60	2.60 to 3.89	0.05 to 0.13	0.43 to 1.50	1.50 to 2.40	0.05 to 0.52

^a frozen thermal conductivity of snow increases with increasing snow density

^b frozen volumetric heat capacity of snow increases with increasing snow density

During cryosuction, the ice core draws water from the neighbouring saturated non-permafrost peat that freezes within the palsa, promoting ice core expansion. Ice is maintained because latent heat fusion (amount of heat required to melt ice to water and vice-versa without a temperature change) stabilizes soil temperature at 0 °C for

extended periods (Halliwell and Rouse 1987, Boike et al. 1998). This is particularly important in the DPZ, where latent heat fusion maintains ice in soils at temperatures near freezing (Calmels et al. 2008a).

Peat plateaus: Peat plateaus (Figures 3.1b and 3.2b) also occur as elevated features containing a perennially frozen core. In contrast to palsas, peat plateaus are generally low, seldom exceeding one metre high, but may cover areas greater than 1 km² (Vitt et al. 1994). Peat plateaus result from prolonged cold temperature, rapid *Sphagnum* accumulation, and uplifting of ice. Once elevated, shrubs and trees colonize the plateau, further drying the peat through ET. In western Canada, palsas and peat plateaus are considered geomorphic variations of the same permafrost processes (Zoltai 1993, Vitt et al. 1994), where several palsas coalesce into a plateau. However, in the Hudson Bay region, palsas may occur as fragmented peat plateaus (Payette et al. 2004). Therefore, to adequately measure their responses to changes in climate, it is critical to understand the effects of both climate and local conditions on peat plateau and palsa distribution.

Pingos: Pingos are mounds consisting of a core of massive ice, produced primarily by injection of water (Ross et al. 2007). Most pingos have a circular or oval base and a fissured top that may be cratered. The fissures and craters result from rupturing of surface soil and vegetation cover when the ice core lifts.

Polygonal peatlands: Polygonal peatlands are closed, multi-sided features of similar dimension resulting from ice wedge formation in ground layers. Ice wedges form in thermal contraction cracks. Here, meltwater percolates through the active layer during snowmelt, creating a frost layer in the transitional soil zone (Vardy et al. 2005). Repeated annual contraction cracking followed by ice formation in the wedge gradually increases polygon width.

Degrading permafrost features

General patterns: Permafrost features have been proposed as being cyclic in nature, where each feature undergoes a natural successional process (Zoltai 1993, Vitt et al. 1994). For example, in the boreal and subarctic regions of central Canada various stages of palsa and peat plateau development have been characterized (Zoltai and Tamocai 1971) (Table 3.3). After reaching a maximum degree of development, a palsa and peat plateau may begin to decay due to changes in insulating cover (e.g., snowpack, peat layer, vegetation) (Halsey et al. 1995). Depending on the amount of ice present and its thaw rate, this decay produces various permafrost degrading features (Table 3.1, Figures 3.1b-d and 3.2a-c),

Thermokarst is the generic term describing permafrost degrading features (Table 3.1). Thermokarst origin is grouped by regional (e.g., fire, air temperature, excessive precipitation) or local (local topography, ground (soil) conditions) controls (Harris 2002, Toniolo et al. 2009). Thermokarst formation encompasses multiple stages, including ice thawing, surface subsidence and erosion (e.g., peat slumping), and ponding of meltwater (Figure 3.1a-d).

Table 3.3. Stages of peat plateau and palsa evolution in Central Canada (Zoltai and Tamocai 1971).

Relative age	Characteristics
Young (incipient)	Found under very dense (>4 trees m ⁻²) black spruce in a treeless fen or a fen with stunted tamarack. No plants grow in the dense shade, although some lichens occur. Little, if any relief; peat accumulates faster on the fen under dense tree growth.
Young	Low mounds, generally less than 20 cm high. Small in extent, generally less than 200 m ² ; may be adjacent to, but not confluent with, other structures. Open stands of stunted black spruce occur on the peat plateau, with <i>Ledum groenlandicum</i> Oeder, <i>Chamaedaphne calyculata</i> (L.) Moench in the shrub layer, and <i>Cladonia</i> (mainly <i>C. rangiferina</i> (L.) Web and <i>C. alpestris</i> (L.) Rabenh.) as ground cover.
Mature	High (about 1 m) plateau with local undulations. Large in extent, may reach several km ² . Open stands of stunted black spruce occur on the peat plateau, with <i>L. groenlandicum</i> and some <i>C. calyculata</i> . <i>Cladonia</i> usually forms nearly a continuous mat on the ground.
Overmature	High (about 1 m) plateau. Thermokarst features (water-filled depressions) and collapsing edges are prominent. May be large in extent (several km). Usually with dense stands of tall black spruce, and feathermoss cover. <i>Ledum groenlandicum</i> and lichens may occur in openings.
Palsa	Height depending on stage of development, mature or somewhat decadent palsas may be over 3 m high. Area usually small, less than 10 m in diameter. Vegetation similar to peat plateau in corresponding stage of development.

Collapse scars: Collapse scars (Figures 3.1b and 3.2c) are common circular to oval-shaped thermokarst features present in the DPZ. Collapse scars result from thaw-induced peat slumping within a peat plateau or *palsa*, forming localized topographic depressions (Vitt et al. 1994, Camill 1999a). Generally, a leading edge to the depression forms a wetting front called a bog 'moat,' while the trailing edge is relatively stable. Vegetation in collapse scars changes from trees and dwarf shrubs to tall shrubs, wet-adapted mosses, and sedges, changing C cycling processes and GHG emissions (see sections 2, Peatland Development and Plant Associations, and 5, Peatland Carbon Cycling). As succession proceeds, old collapsed scar vegetation changes to that representative of fens or bogs, depending on inundation and soil fertility, further modifying C cycling and GHG emissions (Vitt et al. 1994, Prater et al. 2007). When MAAT is less than 0 °C, ice formation and growth may restart in older collapse scars (Halsey et al. 1995).

Internal lawns: Internal lawns are areas of wet depressions derived from recent permafrost thaw (Figure 3.2c). As internal lawns form, vegetation structure changes from black spruce trees and dwarf shrubs to wet-adapted *Sphagnum* mosses, tall shrubs, and sedges (Vitt et al. 1994, Beilman et al. 2001). Those changes have frequently been correlated with elevated CH₄ emissions to the atmosphere (Prater et al. 2007, Turetsky et al. 2007), but variable CO₂ sequestration results have been reported (see section 5, Peatland Carbon Cycling).

Thermokarst ponds and lakes: Thermokarst ponds are shallow water bodies produced through ice melting and peat subsidence (Figures 3.1d and 3.2a). Thermokarst ponds can coalesce into larger thermokarst lakes. Continued permafrost thawing can lead to lake drainage by breaching the top of permafrost surface and eventual disappearance of large thermokarst lakes, forming many smaller lakes and ponds. Thermokarst ponds and lakes are relatively shallow and, therefore, may be important CH₄ emitters to the atmosphere (Blodau et al. 2008). However, lake and pond distributions and their contributions to GHG fluxes are poorly documented (see section 5, Peatland Carbon Cycling).

Taliks: Taliks are bodies of unfrozen ground occurring in permafrost that result from local changes in thermal, hydrological, or hydrochemical conditions (Muskett and Romanovsky 2011). Taliks occur in peat profiles and beneath thermokarst ponds and lakes due to the downward extension of the active layer, which inhibits it from complete freezing during winter (Zhang et al. 2008b). Extension of the ALT is also known to be a vital component of C balances in permafrost landscapes (Schuur et al. 2008).

Two classes of taliks have been defined based on temperature; noncryogenic taliks form at temperatures above 0 °C and cryogenic taliks form below 0 °C. Non-cryogenic taliks include: (1) closed taliks, which are depressions in permafrost tables below a river or lake; (2) hydrothermal taliks, where heat supplied by groundwater maintains ground temperatures above freezing; (3) thermal taliks, where the thermal regime of the ground maintains temperatures above freezing; and (4) transient taliks, which are located below small lakes and are gradually eliminated by permafrost aggradation. Hydrochemical taliks are cryogenic forms where freezing is inhibited by mineralized groundwater flowing through the soil, although temperatures are below freezing. A variety of taliks may be cryogenic or non-cryogenic, including: (1) isolated taliks, which are entirely surrounded by perennially frozen ground; (2) lateral taliks, which are overlain and underlain by perennially frozen ground; and (3) open taliks, which completely penetrate permafrost, connecting suprapermafrost (non-frozen ground above permafrost) and subpermafrost (non-frozen ground below permafrost) zones.

Environmental controls of permafrost dynamics

Temperature

Heginbottom et al. (1995) used physiographic and climate data to divide Canada into five permafrost zones (Figure 1.1) based on the amount of area underlain by permafrost:

- Continuous permafrost zone (CPZ): >90%
- Extensive discontinuous permafrost zone (DPZ): 51 to 90%
- Sporadic discontinuous permafrost zone (SPZ): 11 to 50%
- Isolated permafrost zone (IPZ): 0 to 10%
- No permafrost: 0%

The permafrost zones are broadly correlated with MAAT (Anisimov and Nelson 1996, Smith and Riseborough 2002). The CPZ occurs north of the -8°C temperature isotherm. The transition from CPZ to the northern (e.g., extensive) DPZ occurs between MAAT of -6 to -8°C , while the southern part of the DPZ occurs at approximately -1°C (French and Slaymaker 1993). Mean annual ground temperature is generally -2°C or warmer in the DPZ, but ranges between -15 and -1°C in the CPZ (Romanovsky et al. 2010).

Although permafrost distribution based on MAAT is generally well mapped, its relationships with ground temperature are complex, and only sparse data exist at regional and local landscapes that describe MAAT and MAGT associations (Smith et al. 2010, Seppälä 2011, Throop et al. 2012). Furthermore, presence of aggrading and degrading permafrost features in the same area indicates that all developmental stages occur within current temperature ranges in the various permafrost zones (Gurney 2001, Johansson et al. 2006, Hjort et al. 2007). These patterns result from local variations in vegetation, topography, snow cover, and soil conditions that play important roles in controlling MAGT and subsequent permafrost presence (Figure 3.3; Riseborough 2002, Zhang 2005). Local variations have been deemed as *n*-factors and when MAAT is within a few degrees of 0°C (i.e., southern DPZ), variations in snow cover and peatland area (and its vegetation cover) are the *n*-factors mostly responsible for permafrost occurrence (Smith and Riseborough 2002, Overduin et al. 2006). In addition to distribution, *n*-factors play critical roles in ALT of permafrost soils and subsequent biogeochemical cycles, water flow, and GHG exchange with the atmosphere (Hinkel et al. 2001, Woo and Young 2006, Boike et al. 2008).

The influence of vegetation on snow cover differs within and among permafrost zones (Romanovsky et al. 2010, Smith et al. 2010). In the CPZ and at its transition with the northern DPZ, stunted trees or shrubby vegetation reduce wind speed over a stand (e.g., Seppälä 1986, 1990). As a result, localized snow accumulation occurs, increasing soil water volume and temperature, leading to permafrost thawing and thermokarst formation. In contrast, in the DPZ trees generally stimulate permafrost aggradation as previously mentioned.

Thaw dynamics

Thermokarst formation begins within two to three years following ground temperature increases (Calmels et al. 2008a,b). Here, onset of thawing leads to ice melting and subsidence of mature palsas, peat plateaus, or lithalsas. However, palsas may occur as fragments of peat plateau degradation (Payette et al. 2004) and lithalsas may be remnant palsas whose surface peat layer has eroded (Allard et al. 1996). Without a peat layer, ice-core degradation of lithalsas commences at a MAAT of approximately -2.0°C (Kujala et al. 2008). This value is higher than the threshold MAAT of -3.0 to -3.5°C for palsa and peat plateau aggradation/degradation (Halsey et al. 1995, Dyke

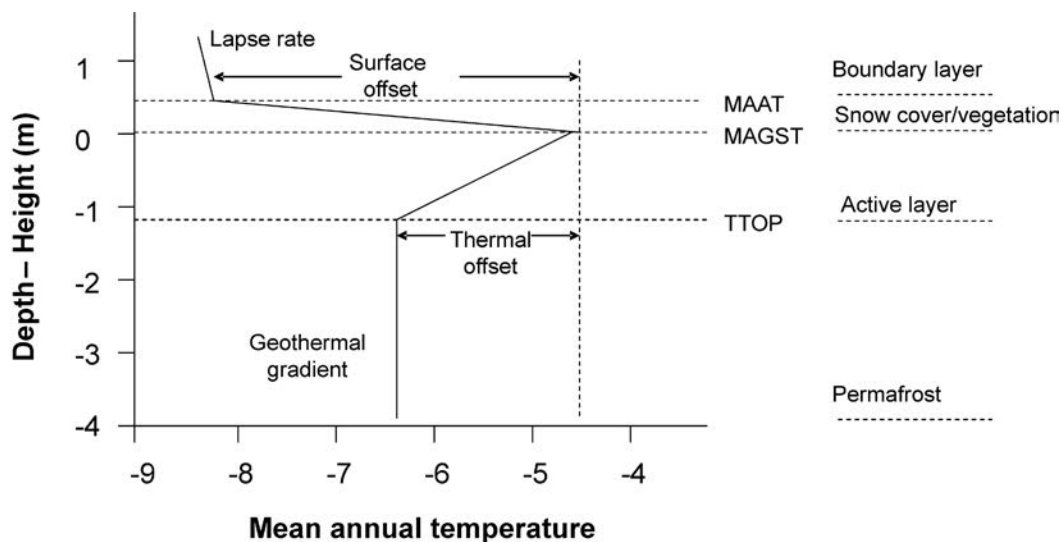


Figure 3.3. Schematic of mean annual temperature profile through the surface boundary layer of permafrost peat, showing the relationship between air temperature and permafrost; MAAT = mean annual air temperature, MAGST = mean annual ground surface temperature, and TTOP = temperature at top of permafrost (adapted from Zhang 2005).

and Sladen 2010). Thus, palsa evolution to lithalsa between -3.5 and -2.0 °C might be an important control point on permafrost thawing.

Calmels et al. (2008a,b) studied lithalsa thermal and physical properties at a site located on the eastern Hudson Bay coast in Québec (Boniface River) (Figure 3.4). Here, lithalsa warming progressed along a high to low elevational gradient. Erosion of the insulating peat layer enhanced deeper thawing at the highest lithalsa elevations in response to increased MAAT. Furthermore, the ice core was permeable to meltwater percolating through the active layer. Once it infiltrated the top of the permafrost, meltwater flowed to lower elevations in the lithalsa. Lateral heat flow from meltwater stimulated ice melting and enhanced subsidence of the lithalsa, with a thermokarst pond forming at the lower elevation. These changes also promoted snow accumulation at the lithalsa and pond interface, further enhancing lithalsa thaw rates along its edges (Calmels et al. 2008b).

Dyke and Sladen (2010) studied temperature patterns of aggrading and degrading permafrost features in the western HBL near Churchill, Manitoba (Figure 3.4). They reported ground temperatures at the edge of a peat plateau ($+0.2$ to $+1.9$ °C) and thermokarst pond (-2.7 to -1.2 °C) were higher than the plateau's centre (-6.2 to -4.7 °C). Dyke and Sladen (2010) suggested that ground temperatures at the centre of the peat plateau were indicative of its maintenance under current temperature regimes (e.g., <-3.5 to -3.0 °C). However, warmer ground temperatures of the plateau edge and thermokarst pond suggest the possibility of thawing along the fringe of the plateau, similar to the lithalsa results of Calmels et al. (2008a,b). Findings from Calmels et al. (2008a,b) and Dyke and Sladen (2010) were consistent with data from Baker Lake, Manitoba located in the CPZ along northern Hudson Bay (Figure 3.4). Here, ground temperature was above freezing in a fen containing no permafrost that bordered a peat plateau (Smith et al. 2010). In contrast, the ice core in the plateau had a MAGT below -4.0 °C.

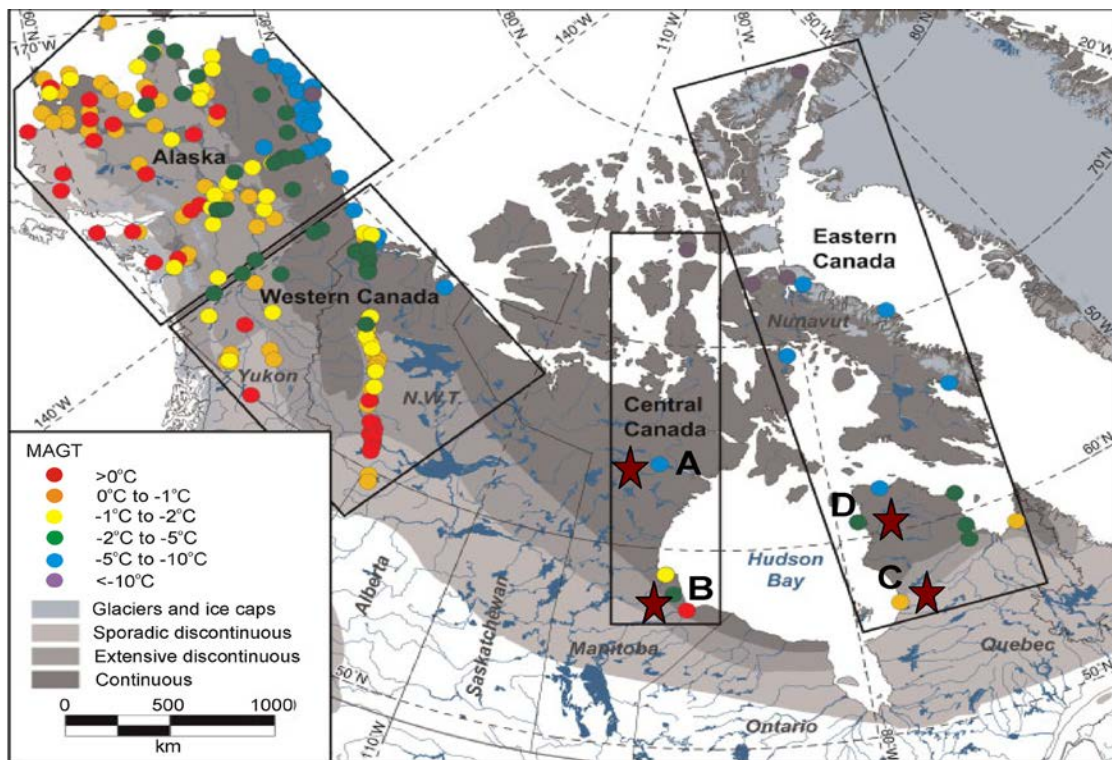


Figure 3.4. Mean annual ground temperature (MAGT) during the International Polar Year period (red stars in central and eastern Canada along Hudson Bay indicate study sites from which results were synthesized for the Hudson Bay region: (a) Baker Lake, Manitoba, (b) Churchill, Manitoba, (c) Umiujaq, Kuujjuarapik, and Boniface River, Quebec, and (d) Puvirnituk, Quebec; remainder shown as circles).

Permafrost and climate change

Twentieth-century permafrost dynamics

Understanding 20th century permafrost thaw dynamics provides a framework from which to compare future permafrost changes. Aerial photographic and remote sensing studies during this timeframe indicate permafrost landscapes in the DPZ changed more than those in the CPZ. For example, at the Boniface River site (Figure 3.4), permafrost decreased from approximately 80% of the land area in 1957 to 20% in 2003 (Payette et al. 2004). This decrease was accompanied by increases in (1) fen area from less than 5% in 1957 to approximately 50% in 2003 and (2) thermokarst pond area from 20 to 40% during the same timeframe. Furthermore, Sannel and Kuhry (2011) reported that a thermokarst lake expanded more in the DPZ relative to that in the CPZ in Europe between the 1950s and 2000s. Various studies have shown similar results in Europe (Harris et al. 2009), Asia (Zhao et al. 2010), and North America (Romanovsky et al. 2010, Smith et al. 2010).

Changes in permafrost thawing are less evident in the CPZ. For example, Sannel and Kuhry (2011) reported no differences in thermokarst lake expansion between 1954 and 2006 in the CPZ near Churchill. Jones et al. (2011) reported similar results for thermokarst lake expansion between 1950 and 2007 in the CPZ of Alaska. However, they also reported more ponds greater than 0.1 ha occurred during 2007 relative to 1950; this was attributed to lake drainage through breaching of permafrost surfaces. In contrast, Parsekian et al. (2011) reported thermokarst lake expansion rates of 1 to 2 m year⁻¹ in the CPZ of Alaska between 1951 and 2006. Here, expansion was primarily attributed to floating vegetation mat area increases from 16 to 55% along lake shorelines following thaw and slumping processes. Once thaw and slumping occurred, sediment underlying the peat subsided and the structurally interconnected peat mat floated due to buoyancy provided by gases trapped in the mat (Figure 3.2c). Greater water volume and faster flow at the shoreline likely provided energy to melt ice, enhancing active layer and talik expansions.

Twenty-first century permafrost dynamics

General patterns: In boreal and subarctic biomes, peatlands are commonly associated with permafrost, the coverage of which is expected to decrease by 16 to 63% in Canada relative to current area (Table 3.4). In addition, ALT may increase by 0.3 to 0.9 m during the 21st century (Table 3.4). Permafrost loss and deeper active layers are consistent with soil temperature warming, especially at 0.2 m depth (Figure 3.5) across Canadian permafrost zones (Zhang et al. 2008b). Variable estimates result from an assortment of causes, including (1) different modelling domains: (a) biospheric (e.g., boreal, subarctic, arctic; Koven et al. 2011, Schaefer et al., 2011), (b) national (Zhang et al. 2008b), and (c) regional (Sushama et al. 2006); (2) assumptions of equilibrium between MAAT and MAGT (Gagnon and Gough 2005); and (3) uncertainties in soil temperature projections from use of poorly calibrated coefficients to describe soil parameters (Sushama et al. 2006).

Table 3.4. Predicted change in permafrost area and active layer depth during the 21st century in Canada.

Domain	Climate change scenario ¹	Model ²	Percent permafrost loss	Active layer depth increase (cm)	Reference
Alaska	3A1B ^a	1	7	162	Marchenko et al. 2008
Alaska	A1B ^b	2	22 to 61	69 to 105	Schaefer et al. 2011
Canada	A1B ^b	2	22 to 63	55 to 90	Schaefer et al. 2011
Canada	B2, A2 ^c	3	16 to 20	30 to 70	Zhang et al. 2008b
Canada	A1B ^c	3	21 to 24	30 to 80	Zhang et al. 2008b
Northern Hemisphere	A1B ^d	4	27	-	Euskirchen et al. 2006
Northern Hemisphere	A2, B2 ^e	5	40 to 57	50 to 300	Saito et al. 2007
Northern Hemisphere	B1, A1B, A2 ^f	6	60 to 90	50 to 300	Lawrence and Slater 2005
Northern Hemisphere	A1B ^f	6	73 to 88	-	Lawrence and Slater 2010
Northern Hemisphere	A1B ^f	6	80 to 85	50 to 300	Lawrence et al. 2008
Northern Hemisphere	A1B ^b	2	20 to 39	56 to 92	Schaefer et al. 2011

¹ A1B = medium based scenario or a balance across all energy sources (where balanced is defined as not relying too heavily on one particular energy source, on the assumption that similar improvement rates apply to all energy supply and end-use technologies).

² Permafrost models: 1 – GIPL 2.0 - Spatially Distributed Model of Permafrost Dynamics in Alaska (Sazonova & Romanovsky 2003); 2 – Simple Biosphere/Carnegie-Ames-Stanford Approach Mode (Schaefer et al. 2008); 3 – Northern Ecosystem Soil Temperature (Zhang et al. 2008b); 4 – Terrestrial Ecosystem Model (Raich et al. 1991); 5 – Minimal Advanced Treatments of Surface Interaction and Runoff (Takata et al. 2003); 6 – Community Land Model (Oleson et al. 2004)

³ Climate models: ^a HADCM2; ^b CCSM3, HadCM3, and MIROC3.2; ^c CGCM, CSIROM, ECHAM, GFDL, HadCM, and NCAR; ^d NCAR; ^e MIROC3.2; ^f CCSM3 (see acronyms list for definitions).

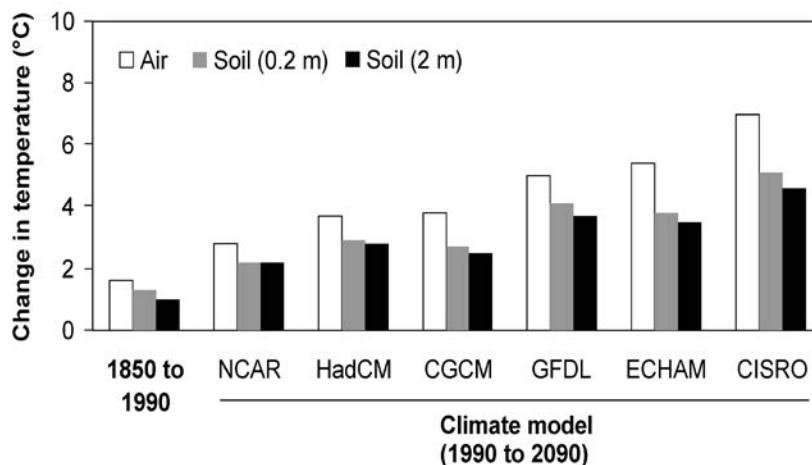


Figure 3.5. Changes in air and soil temperature across permafrost zones in Canada projected using the Northern Ecosystem Soil Temperature Model (Zhang et al. 2008b; NCAR = United States Center for Atmospheric Research; HadCM = Hadley Centre for Climate Prediction Research; CGCM = Canadian Centre for Climate Modelling and Analysis; GFDL = United States Geophysical Fluid Dynamics Laboratory Coupled Model; ECHAM = German Max-Planck-Institut für Meteorologie; CSIRO = Australian Commonwealth Scientific and Industrial Organization). Scenarios used were A2 - GFDL, ECHAM, CSIRO; B2 - NCAR, CGCM.

Biospheric models produce general patterns of MAAT and permafrost occurrence across biomes (Koven et al. 2011, Schaefer et al. 2011). National and regional model results can be obtained using equilibrium or disequilibrium assumptions of soil thermal regimes (Gagnon and Gough 2005, Sushama et al. 2006, Zhang et al. 2008b). An equilibrium between MAAT and MAGT assumption forecasts permafrost temperature regimes that directly mimic those of MAAT. In contrast, an assumption of disequilibrium between MAAT and MAGT is best tested using spatially explicit, process-based models. These models account for snow property (e.g., depth, amount, water equivalents), soil characteristic (peat versus mineral soil), and/or vegetation community controls on soil thermal regimes, and subsequent permafrost dynamics.

All models (equilibrium and disequilibrium) indicate most surface (<0.5 m depth) soil warming occurs during winter (e.g., December through March) and spring (e.g., April through May) rather than summer and fall (e.g., Gagnon and Gough 2005, Zhang et al. 2008b). Disequilibrium models, however, suggest smaller areas of permafrost loss and shallower ALT at the end of the 21st century than those based on equilibrium between MAAT and MAGT. Issues of scale are further discussed in section 7, Mapping, Monitoring, and Modelling Permafrost Peatlands.

Hudson Bay region: Permafrost thaw has been modelled for the Hudson Bay region using both equilibrium and disequilibrium assumptions. Assuming equilibrium between MAAT and MAGT, Gagnon and Gough (2005) used output from six GCMs (Table 3.5) with spatial coverage ranging from 2.8° x 2.8° to 5.6° x 5.6° (latitude x longitude). They further defined a permanently frozen grid cell as those with MAAT less than -5 °C. Based on those assumptions and depending on the model used, they projected 24 to 67% permafrost loss by 2041 to 2070 and 35 to 100% loss by 2070 to 2100 in the Hudson Bay region (Figure 3.6).

In contrast to Gagnon and Gough's (2005) results, Zhang et al. (2008b) simulated permafrost dynamics using 0.5° x 0.5° (latitude x longitude) grid cells across northern Canada. They further assumed disequilibrium between MAAT and MAGT to apply output from six GCMs (Table 3.5) in the process-based Northern Ecosystem Soil Temperature (NEST) model (Zhang et al. 2003). The NEST model accounted for differences in snow depth, vegetation communities, and soil characteristics (peat vs. mineral soil). Zhang et al. (2008b) reported only minor losses in permafrost occurrence in the HBL during the 21st century, primarily along the southern fringe of its DPZ (Figure 3.7a-c). However, frequency of taliks (Figure 3.7d-f) and depth to the permafrost table (e.g., active layer; Figure 3.7g-i) increased in the northern portion of the HBL relative to the 1990s. Higher talik frequency by the end of the 21st century resulted from gradual increases in ALT that could not completely freeze the following winter. Formation of supra-taliks (non-frozen surface soil above the top of the permafrost) significantly enhanced permafrost thaw from the top and accounted for permafrost loss along the southern fringe of the HBL.

Sushama et al. (2006) used a one-dimensional heat conductance model of solid-liquid water phase changes to simulate soil surface temperature, soil freezing and thawing indices, and snow water equivalents for northeastern Canada (Table 3.5). Their projections also accounted for variation in snow cover. The Canadian Regional Climate Model (Laprise et al. 2003) provided input data to the heat conductance model (Sushama et al. 2006). Two simulations were conducted that corresponded to current (1961 to 1990) and future (2041 to 2070) climates.

Table 3.5. Climate models used to provide input data for modelling studies in the Hudson Bay, Canada region.

Climate model	Scenario	Soil model	Significant results	Reference
Global				
Canadian Centre for Climate Modelling and Analysis (CGCM1)	IS92a, 2 x CO ₂	Air temperature < -5 °C	2041 – 2070: permafrost loss of 24 to 67%	Gagnon and Gough (2005)
Hadley Centre for Climate Prediction Research (HadCM2)	IS92a, 3 x CO ₂		2070-2100: permafrost loss of 35 to 100%	
Australian Commonwealth Scientific and Industrial Research Organization (CISRO Mk2)				
German Max-Planck-Institut für Meteorologie (ECHAM4)				
Japanese Center for Climate Research Studies (CCSR-98)				
United States Geophysical Fluid Dynamics Laboratory (GFDL-R15)				
Regional				
CGCM	B2, A2	Northern Ecosystem Soil Temperature (NEST)	1990s - 2090:	Zhang et al. (2008b)
CSIROM			Minor rates of permafrost loss	
ECHAM			Increase in talik frequency and depth to permafrost	
GFDL			Soil temperature increase smaller than air temperature	
HadCM			Hudson Bay Lowlands are relatively persistent because of large amount of peatlands	
Canada Regional Climate Model (CRCM)	IS92a, 2 x CO ₂	One-dimensional soil thermal model	1961 – 2070:	Sushama et al. (2006)
			Increase in surface temperature	
			Decrease in snow water equivalents	
			Winter warming most important	
			Increase in thawing index	
			Soil temperature increase smaller than air temperature	

Sushama et al. (2006) reported annual increases in MAAT of 0.04 to 0.05 °C year⁻¹ in the HBL between 2041 and 2070, relative to current estimates (Figure 3.8a). In addition, snow water equivalent decreased by 0.4 kg m⁻² year⁻¹ across the eastern part of the HBL, but did not change in the CPZ along the Hudson Bay coast in Ontario (Figure 3.8a).

Sushama et al. (2006) also reported soil temperature at 0.2 m depth increased in a pattern similar to MAAT (Figure 3.8b), although soil warming occurred at a slower rate. Differences between surface and soil temperatures were presumed to result from limited responses in soil temperature between January and May, timeframes of thick snowpacks and snowmelt. However, soil temperature results are uncertain because both rates and magnitude of soil temperature changes may differ depending on ET trends; ET can decrease soil temperature by drying surface peat (Robinson and Moore 2000, Sushama et al. 2006). Evapotranspiration becomes a more important soil temperature regulator when precipitation changes are less than 25% of MAP amounts (Roulet and Woo 1986). Finally, only minor changes occurred in the freezing index (days per year below 0 °C), whereas the thawing index (days above year below 0 °C) increased by five to eight days across most of the HBL (Figure 3.8c).

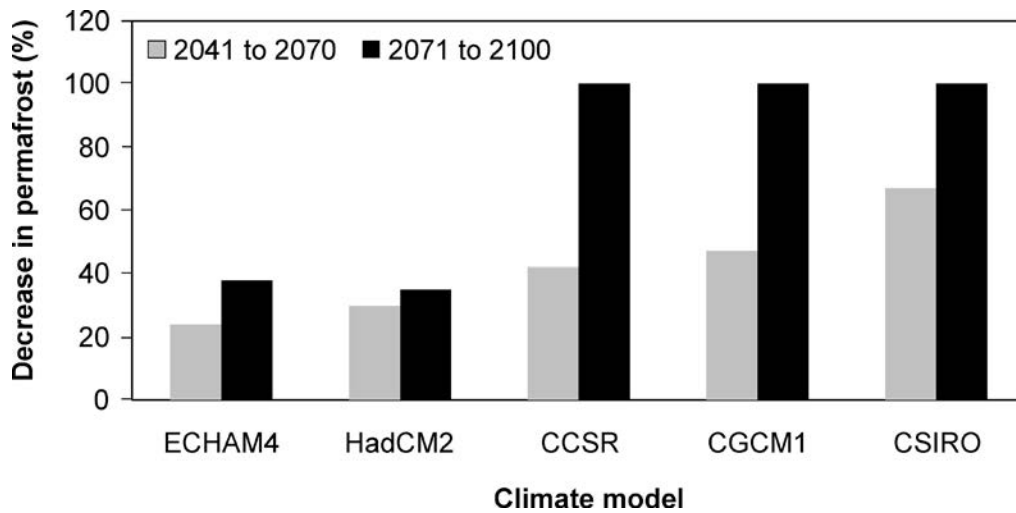


Figure 3.6. Percent losses in permafrost in the Hudson Bay region (Gagnon and Gough 2005; ECHAM4 = German Max-Planck-Institut für Meteorologie; HadCM2 = Hadley Centre for Climate Prediction Research; CCSR = Japanese Center for Climate Research Studies; CGCM1 = Canadian Centre for Climate Modelling and Analysis; CSIRO = Australian Commonwealth Scientific and Industrial Organization). Scenario used was IPCC IS92a.

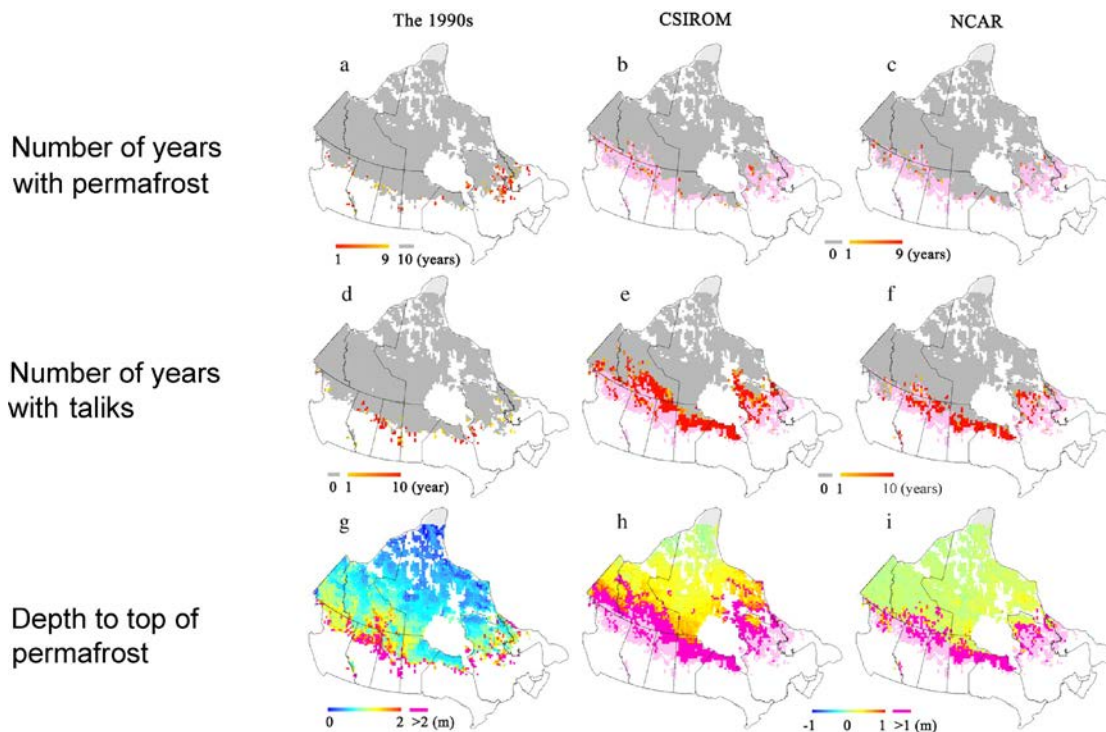


Figure 3.7. Spatial distributions of permafrost status in the 1990s (the first column panels) and the changes from the 1990s to the 2090s under scenarios simulated using models of the Australian Commonwealth Scientific and Industrial Organization (CSIRO) (A2) and United States Center for Atmospheric Research (NCAR) (B2) (second and third column panels, respectively). Panel (a) is the number of years with permafrost in the 1990s, and panels (b) and (c) are its changes from the 1990s to the 2090s (light pink means permafrost has completely disappeared, and dark grey means that permafrost exists throughout); panels (d), (e) and (f) are the number of years with taliks; panel (g) is the average depth to permafrost table in the 1990s, and panels (h) and (i) are its changes from the 1990s to the 2090s; light grey is for glacier, and white areas are water bodies or outside Canada (from Zhang et al. 2008b; reprinted with permission from Elsevier).

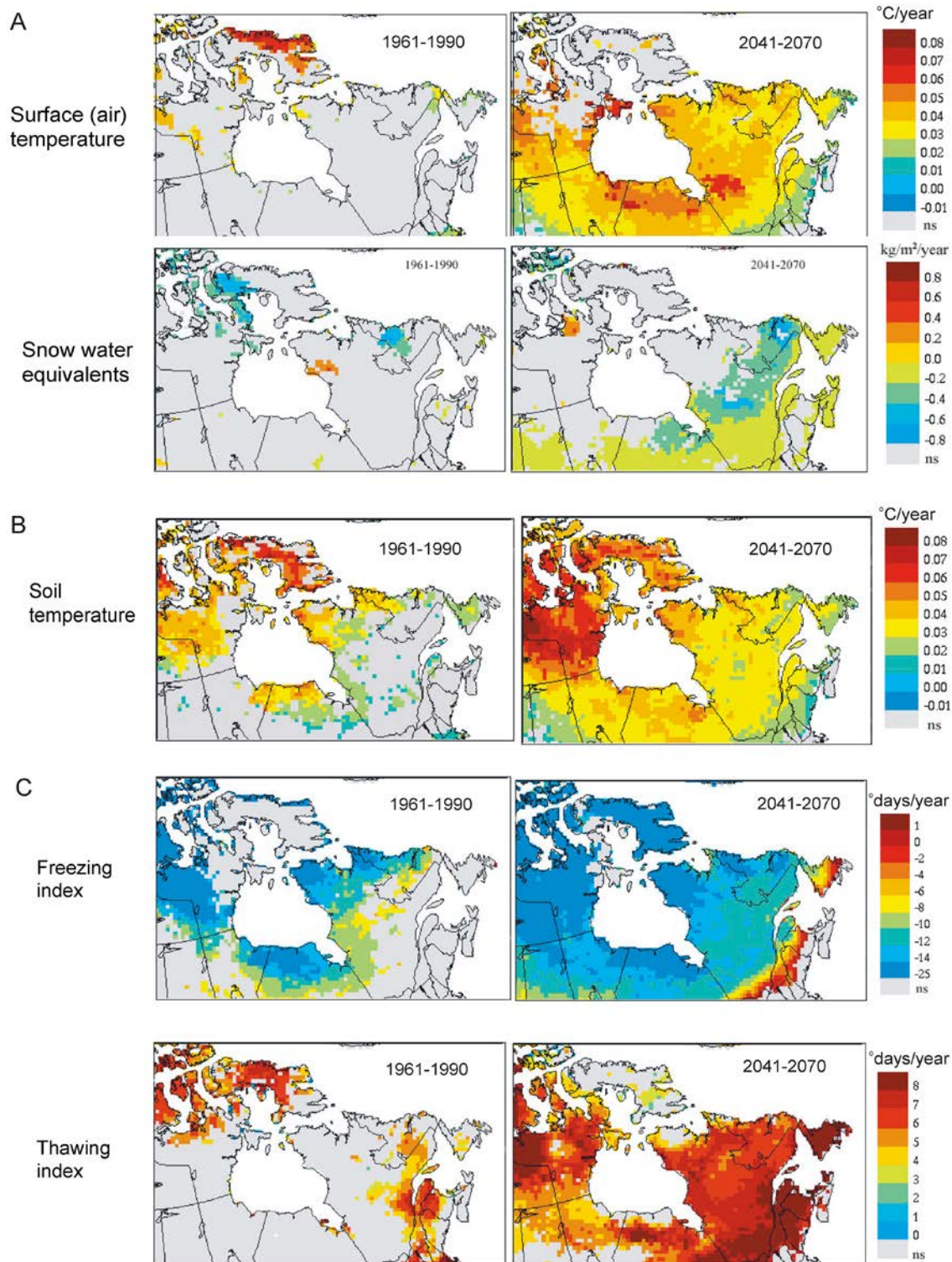


Figure 3.8. Estimated trends in (a) Canadian Regional Climate Model predictions for surface (air) temperature and snow water equivalents, (b) soil temperature at 0.2 m below surface, and (c) freezing and thawing (degree days per year); scenario used was IPCC IS92a. Regions with statistically significant trends (positive or negative) at 90% confidence level are shown in colour, while regions without significant trends are shown in grey (from Sushama et al. 2006; reprinted with permission from John Wiley and

Summary and conclusions

Permafrost occurrence is important to multiple ecological processes that affect peatland C storage and sequestration. Permafrost landscapes consist of complexes containing a variety of aggrading and degrading (e.g., thermokarst) features, along with non-permafrost peatlands. However, spatial and temporal patterns of permafrost landscape structure are variable and not well documented.

Mean annual air temperature is the major control on permafrost occurrence at biospheric scales. However, environmental conditions, such as amounts of snowfall and peatland area, along with vegetation structure are critical to permafrost occurrence at regional and local levels. In the DPZ, permafrost is commonly associated with peatlands because, relative to mineral soil, thermal properties of peat enhance ice growth, especially in treed peatlands. Thin snowpacks beneath tree canopies allow cold air to penetrate deeply into peat profiles during the winter and minimize cold air losses during summer. Both conditions enhance ice growth. Conversely, shrub and moss vegetation intercept less snow than trees, contributing to relatively thick snowpacks that overlay warmer and wetter soils resulting in conditions that stimulate permafrost thawing in the DPZ. Vegetation has the opposite effect on snowpack depths and subsequent permafrost thawing in the CPZ.

Permafrost formed primarily during the Little Ice Age; since then permafrost thawing has been common across the DPZ in North America. The vast extent of peatlands in the Hudson Bay area has contributed to it being thought of as one of the most persistent permafrost regions in Canada. However, during the 20th century losses in permafrost in parts of the Hudson Bay region were up to 80% of the permafrost formed during the Little Ice Age. The permafrost area loss was balanced by concomitant increases in areas of fen peatlands and thermokarst ponds and lakes. Furthermore, GCMs point to continued permafrost losses of 16 to 100% in the Hudson Bay region by the end of the 21st century. Although highly variable, evidence points to warmer soil temperatures and higher thawing indices in future. Coupled with higher talik frequencies and increased depths to the top of permafrost, its thawing in the Hudson Bay region is anticipated to continue during the 21st century; expected thawing rates are poorly documented. Those permafrost changes may ultimately alter peatland C storage and GHG emissions at a variety of scales. To improve model calibrations, further research is needed that documents permafrost thaw rates and their local (e.g., snow, peat, vegetation communities, ET) controls. Furthermore, knowledge of changes in permafrost aggrading and degrading features and their arrays within landscapes is needed at local to national scales. Only then will it be possible to reasonably estimate future permafrost effects on northern peatland C storage and GHG emissions to the atmosphere.

4. Peatland Hydrology

Background

Peatlands in permafrost regions have unique hydrological features. For example, frozen peat has low water storage capacity resulting in shallow water flow paths to draining streams and lakes (Hayashi et al. 2004). In contrast, thawed peat has deeper water flow paths and higher water storage capacity that supports ET. Changes in climate may affect peatland hydrology via (1) permafrost degradation (Anisimov and Nelson 1996), (2) soil warming (Rouse 1998), (3) and deeper or altered groundwater flow paths (Quinton et al. 2005). In addition, the nature and seasonal timing of precipitation is expected to change, altering peatland ET and runoff (Pohl et al. 2007).

In peatland complexes, changes in runoff rates are largely the result of changes in ET (Quinton et al. 2009, 2011). However, paucity of data on climate, geomorphology, and vegetation interactions on peatland functions inhibits reliable model projections of future hydrological cycles. Because hydrology is a primary driver of C budgets, future C storage and GHG emissions are also largely uncertain. Therefore, in this section, we provide (1) background information about how water balances are calculated and how water flow is assessed, and (2) what is known about water balances and flows to identify gaps and uncertainties that require further study to improve projections of the effects of climate change on peatland hydrology in permafrost zones.

Water balance

The three main features of the water balance equation are the input (P), changes in various storage terms (ΔS) and outputs (ET and runoff):

$$P = ET - R + \Delta S_{\text{sur}} + \Delta S_{\text{sub}} + \Delta S_{\text{vad}} + \Delta S_{\text{glac}} + \Delta S_{\text{snow/ice}} = \eta \quad (4.1)$$

where, P = precipitation (rainfall and snowfall), ET = evapotranspiration, R = runoff; ΔS_{sur} = change in surface storage (lakes, wetlands, reservoirs, channels, etc.), ΔS_{sub} = changes in subsurface storage of groundwater, ΔS_{vad} = changes in storage of unsaturated (vadose or active layer) zone, ΔS_{ice} = changes in permafrost ice storage, $\Delta S_{\text{snow/ice}}$ = changes in storage of snowpack and lake ice, η = error term on closure of water balance.

We focus this section on describing controlling factors of water output (ET and runoff) and their responses to changes in climate. We further contrast ET and runoff from stands or catchments across peatland types and permafrost features and identify important research needs for long- and short-term studies.

Evapotranspiration

General characteristics: Evaporation and transpiration are diffusive processes that follow Fick's first law, and are a function of the vapour pressures of the evaporating surface and overlying air, wind speed, and the efficiency of vertical transport of water vapour (Dingman 2002). This combined loss of water is referred to as ET and differs with site conditions, and is more difficult to measure than other components of the water budget. As such, various measures of ET have been developed for specific surface and energy exchange situations determined by the type of surface (e.g., open water, bare soil, leaf or leaf canopy), availability of water (i.e., limited or not), and stored or water-advected energy (i.e., existent or not).

Evapotranspiration (e.g., latent heat flux) is a major component of energy flux as well as water balance. The amount of water withdrawn through ET is highly variable and ranges from 20 to 80% of the water balance (or energy balance), depending on terrain unit (e.g., site type), permafrost conditions, and temperature and precipitation regimes (Rouse 1998, Eaton et al. 2001, MacKay et al. 2003). Moreover, error in calculated ET values can be as high as 200% due to land surface heterogeneity, including temperature, wetness, water vapour resistance, albedo, and roughness (Guo and Schuepp 1994).

Methods to calculate evapotranspiration: Methods for measuring/estimating ET are many, ranging from mass energy balances to simple empirical approaches (Drexler et al. 2004, Woo et al. 2008). Moreover, ET is reported as actual (ET_a) and potential (ET_p), and northern peatlands frequently evaporate water at rates lower than their

potential (Rouse 2000). Examples of selected methods used to estimate ET in wetland ecosystems are given in Table 4.1. For a more in-depth discussion of these methods, see Drexler et al. (2004).

The scale at which ET is measured also varies. Most common at the site-level are the Bowen Ratio Energy Balance (BREB; β) and empirical equations that are used to estimate ET_p (Rouse et al. 1987). For homogenous landscapes of 30 m² to 1 km², eddy covariance methods that provide ET_a estimates (Lafleur and Humphreys 2008) are common. For watersheds, semi-distributed and distributed models are frequently used, providing ET_p estimates (Kuchment et al. 2000, Engstrom et al. 2006). All methods have advantages and disadvantages (Table 4.1), with the level of uncertainty in ET estimates increasing for larger landscapes (Boudreau and Rouse 1995). This uncertainty stems from difficulties in capturing spatial and temporal variation in energy and soil moisture (Petroni et al. 2000).

Table 4.1. Advantages and disadvantages of various evapotranspiration (ET) measurement and estimation methods (from Drexler et al. 2004).

Method	Advantages	Disadvantages
Bowen ratio energy balance	<ul style="list-style-type: none"> • Is a robust measure of ET • Provides adequate results for large, relatively homogenous peatlands • Instrumentation is less costly than that for eddy covariance systems 	<ul style="list-style-type: none"> • Assumes that transfer coefficients are equal for sensible heat and latent heat
Eddy covariance	<ul style="list-style-type: none"> • Provides a direct measure of ET • Measurements can be verified 	<ul style="list-style-type: none"> • Is expensive • Equipment is complex and sensitive to damage • Requires much maintenance to ensure adequate results
Empirical equations	<ul style="list-style-type: none"> • Require parameters that can be easily collected from typical weather stations • Are convenient and inexpensive 	<ul style="list-style-type: none"> • Most provide only crude ET estimates • Application outside the original climate area for which they were developed may result in large error terms
Combination equations	<ul style="list-style-type: none"> • Require minimal data • Account for wind speed or surface resistance 	<ul style="list-style-type: none"> • Penman Monteith assumes surface is uniform and wet
LIDAR	<ul style="list-style-type: none"> • Provides weighted average of latent heat flux from variety of surfaces in variable terrain 	<ul style="list-style-type: none"> • Is complex and expensive

The major energy sink in permafrost and non-permafrost peatlands is latent heat flux (Q_e ; i.e., ET) (Rouse et al. 1987). However, in permafrost features high soil moisture contents and melting of ice limit energy appropriations to latent heat and sensible heat (Q_h). This contributes to larger ground heat flux (Q_g) relative to non-permafrost peatlands and forests (Eugster et al. 2000, Boike et al. 2003, Ohta et al. 2008).

The surface energy balance is expressed differently for terrestrial and lake ecosystems. For a homogenous terrestrial surface, the energy balance is represented as:

$$Q^* = Q_e + Q_h + Q_g \quad (4.2)$$

where Q^* (W m⁻²) is the net radiation, Q_e is the latent heat flux (i.e. ET), Q_h is the sensible heat flux, and Q_g is the ground heat flux. For a lake, the energy balance is represented as:

$$Q^* = Q_e + Q_h + Q_w + Q_b \quad (4.3)$$

where Q_w is the lake heat storage and Q_b is the heat flux through the bottom of the lake. Q_b is negligible for deep lakes and accounts for less than 4% of Q^* for shallow subarctic lakes (Marsh and Bigras 1988, Bello and Smith 1990). Therefore, Q_b is generally ignored in lake energy balance calculations (Eaton et al. 2001). Energy balance partitioning is used to compare directly among the surface energy balance characteristics (and each terrain unit) (Rouse et al. 1987, Lafleur and Rouse 1988). It distributes total available energy by calculating the ratios of each component to net radiation. These ratios indicate the relative magnitudes of latent, sensible, and ground heat fluxes in the surface energy balance.

Various empirical equations have been developed and used to estimate latent heat flux (e.g., ET_p), with varying success. The most commonly applied equations are the Penman-Monteith (P-M) (Penman 1948, Monteith 1965), Shuttleworth-Wallace (S-W) (Shuttleworth and Wallace 1985), and Priestly-Taylor (P-T) (Priestly and Taylor 1972) combination models. In addition, a modified P-M equation (W-P-M) has been used to estimate ET from different terrain units within a landscape (Wessel and Rouse 1994). These equations are detailed in Table 4.2.

Table 4.2. Energy balance calculation methods, equations, and the properties that they can be used to assess.

Method	Equation	Properties assessed	Source
Bowen energy balance	$\beta = Q_h / Q_e = \gamma (\Delta T_a / \Delta e_a)$ <p>Where γ is the psychrometric constant (65 Pa K^{-1}), T_a is the air temperature (K), and e_a is the atmospheric vapour pressure.</p>	<p>Ratio of the sensible and latent heat fluxes above a surface</p> <p>When $\beta > 1$, more energy is directed from the surface as sensible heat than latent heat; when $\beta < 1$, latent heat flux is the primary pathway for convective heat loss. Wet surfaces have a lower β than dry surfaces.</p>	Bowen 1926
Empirical equations			
Penman-Monteith	$Q_e = \frac{\Delta AE + (\rho C_p D / r_a)}{\Delta + \gamma(1 + r_c / r_a)}$ <p>$AE = Q^* - Q_g$ and is available energy, ρ is air density, C_p is specific heat, r_c and r_a are canopy and aerodynamic resistances, respectively, D is vapour pressure deficit, Δ is the slope of the saturation vapour pressure vs. temperature curve, and γ is the psychrometer constant, r_c is calculated as:</p> $r_c = r_{st} / LAI$	<p>Simulates ET from a surface covered by a closed canopy of vascular plants and assumes that the contribution from the substrate is negligible.</p>	Penman 1948, Monteith 1965
Shuttleworth-Wallace	$Q_e = Q_{ec} + Q_{es}$ $Q_{ec} = \frac{\Delta(AE - EA_{es}) + (\rho C_p D / r_a^c)}{\Delta + \gamma(1 + r_c / r_a^c)}$ $Q_{es} = \frac{\Delta(AE_{es}) + (\rho C_p D / r_a^s)}{\Delta + \gamma(1 + r_s^s / r_a^s)}$ <p>Q_{ec} and Q_{es} are the components of evaporation from the canopy and soil, respectively. These components are developed as:</p> $Q_{ec} = \frac{\Delta(AE - EA_{es}) + (\rho C_p D / r_a^c)}{\Delta + \gamma(1 + r_c / r_a^c)}$ $Q_{es} = \frac{\Delta(AE_{es}) + (\rho C_p D / r_a^s)}{\Delta + \gamma(1 + r_s^s / r_a^s)}$ <p>AE_s is available energy for bare soil, D is vapour pressure deficit and mean canopy level, r_a^c and r_c define bulk boundary-layer and bulk stomata resistances, respectively, r_s^s represents soil surface resistance, and r_a^s is the aerodynamic resistance below mean canopy.</p>	<p>Simulates the individual contributions of two sources of ET: canopy and bare soil. It uses the P-M approach for both sources and assumes that the total evaporative flux is the sum of the two layers.</p>	Shuttleworth and Wallace 1985

Table 4.2. Con't.

Method	Equation	Properties assessed	Source
Weighted Penman-Monteith	$Q_e = LAI \times Q_{ec} + S \times Q_{es} + W \times Q_{ew}$ <p>Where, S and W are the proportions of bare soil and open water, respectively, and Q_{ew} is the evaporation from open water.</p> <p>The canopy latent heat flux (Q_{ec}) is defined as:</p> $Q_{ec} = \frac{\Delta(AE_c) + (\rho C_p D / r_a)}{\Delta + \gamma(1 + r_s / r_a)}$ <p>The bare soil component (Q_{es}) becomes:</p> $Q_{es} = \frac{\Delta(AE_s) + (\rho C_p D / r_a)}{\Delta + \gamma(1 + r_s / r_a)}$ <p>AE_s is the available energy for the bare soil. The r_s term is the same soil surface resistance term defined for S-W.</p> <p>The open water latent heat flux (Q_{ew}) follows the same approach as the canopy and soil components except that the surface resistance is assumed to be zero:</p> $Q_{ew} = \frac{\Delta(AE_w) + (\rho C_p D / r_a)}{\Delta + \gamma}$	Estimates total evaporation separately for each surface type. These component evaporation calculations are then weighted for surface area of canopy, bare soil, and open water, and are summed to give the total ET from the site.	Wessel and Rouse 1994
Priestly-Taylor	$Q_e = \alpha * [S / (S + \gamma)] * (Q^* - Q_g)$ <p>Where S is the slope of the saturation vapour pressure-temperature curve (Pa K⁻¹)</p> <p>By incorporating the β, α can be calculated as:</p> $\alpha = (S + \gamma) / [S * (1 + \beta)]$ <p>α varies widely according to surface type and micrometeorological conditions. Wet surfaces have higher α than dry surfaces</p>	Used in areas of low soil moisture stress. The P-T equation provides an evaporative term (α) and eliminates the need for input data other than radiation.	Priestly and Taylor 1972

Energy balance in northern peatlands

To accurately evaluate how climate change will affect peatland hydrology, ET needs to be determined for each of the major terrain units on a landscape. Since large areas of peatlands occur as palsa-bog-fen-pool/pond complexes and small lakes (Martini 2006), ET estimates are also needed for all surface types before a scaled value can be derived for a specific peatland complex (e.g., Petrone et al. 2000, Wright et al. 2008). We compiled ET rates (Table 4.3) and energy budget data (Table 4.4) reported in the literature for dominant terrain units that occur north of 50° latitude. Although ET rates vary (Table 4.3), excluding results of Bello and Smith (1990) for large lakes, tundra ponds and lakes (2.3 to 4.8 mm d⁻¹) and fens, marshes, and tundra wetlands (2.0 to 4.5 mm d⁻¹) displayed the highest ET rates followed by spruce forests (2.2 to 3.3 mm d⁻¹) and bogs (1.5 to 2.5 mm d⁻¹). Lichen/heath, heath/shrub and tussock tundra, along with peat plateaus/polygonal tundra (1.4 to 1.7 mm d⁻¹) had the lowest ET rates. Furthermore, similar terrain types generally partition energy the same way regardless of location (Table 4.4).

Shallow lakes and sedge wetlands have the highest latent heat flux-to-net radiation (Q_e/Q^*) ratio, indicating that much of their energy budget goes to evaporating water (Table 4.4). This is because moisture is available and

surface vegetation is not resistant to ET (Rouse 2000). Tundra, bogs, conifer forests, and polygonal permafrost features have relatively similar energy partitioning, with Q_g/Q^* values lower than those of ponds and sedge wetlands (Table 4.4). Energy balance partitioning is consistent with highest ET rates (Table 4.3) reported for tundra ponds and fens, followed by the other terrain units. Lower Q_g/Q^* values result from a combination of (1) higher surface resistance, non-transpiring lichen vegetation, and (2) low water holding capacity of mineral soil relative to peat and *Sphagnum*-peat relative to sedge-peat (Boudreau and Rouse 1995, Eaton et al. 2001, Rouse et al. 2003).

Table 4.3. Evapotranspiration (ET) rates for common terrain types in High Boreal and Subarctic drainage basins north of 50° latitude.

Terrain type	Study period	Location	ET (mm d ⁻¹)	Source
Tundra lake	June – August 1985	Manitoba	6.1	Bello and Smith 1990
	June – August 1991	Manitoba	4.8	Boudreau and Rouse 1995
	June – November 1997-1999	Northwest Territories	2.3	Rouse et al. 2003
Open water	May – September 1977	Quebec	2.8	Boudreau and Rouse 1995
Tundra pond	June – September 2000	Northwest Territories	2.5	Spence et al. 2003
Flat fen	June – August 1983	Northwest Territories	4.5	Roulet and Woo 1986
	June – September 1985	Ontario	3.5	Rouse et al. 1987
	June – August 1991	Manitoba	3.5	Boudreau and Rouse 1995
Sedge fen	May – August 1990	Quebec	2.8	Moore et al. 1994
	June – September 1987-1994	Manitoba	2.7	Rouse 1998
	June – August 1989	Manitoba	2.5	Lafleur et al. 1993
Wooded fen	June – August 1996-1997	Manitoba	2.5	Petrone et al. 2000
	July – August 2004	Alberta	2.0	Humphreys et al. 2006
	July – August 2004	Saskatchewan	2.0	Humphreys et al. 2006
Open poor fen	July – August 2004	Alberta	2.5	Humphreys et al. 2006
Marsh	May – August 1984	Ontario	2.8	Price and Woo 1988
Alder-willow covered ridge	May – August 1985	Ontario	3.0	Woo and diCenzo 1989
Willow-birch wetland	June – August 1991	Manitoba	3.2	Boudreau and Rouse 1995
	May – September 1977	Quebec	2.7	Boudreau and Rouse 1995
Open spruce, tamarack	June – September 1989	Manitoba	2.1	Lafleur 1992
Shrub bog	June – September 1998-2000	Siberia	2.1	Kurbatova et al. 2002
	June – September 1998-2000	Russia	1.9	Kurbatova et al. 2002
Open bog	June – September 1996-1997	Sweden	2.0	Kellner 2001
String bog	June – July 1989	Labrador	2.5	Price et al. 1991
Blanket bog	May – July 1989	Newfoundland	1.7	Price 1991
Spruce forest	June – August 1991	Manitoba	3.3	Boudreau and Rouse 1995
	June – August 1989	Manitoba	2.2	Lafleur 1992
Lichen-heath	June – August 1991	Manitoba	2.3	Boudreau and Rouse 1995
	May – September 1977	Quebec	1.7	Boudreau and Rouse 1995
Mixed, heath and shrub tundra	May – August 2004-2006	Northwest Territories	1.4	Lafleur and Humphreys 2008
Tussock tundra	July – October 2003-2004	Siberia	1.5	Corradi et al. 2005
Coastal tundra, wet	June – August 1004	Alaska	1.3	Vourlitis and Oechel 1997
Polygonal tundra	June – August 1999, 2003	Siberia	1.6	Boike et al. 2008

Table 4.4. Energy balance partitioning, Bowen ratio [latent heat flux (Q_e)/net radiation (Q^*); sensible (Q_h)/ Q^* ; ground heat flux (Q_g)/ Q^* ; lake heat storage Q_w/Q^*], Bowen ratio energy balance (β), and Priestly-Taylor alpha (α) for various terrain units in peatlands and permafrost features north of 50° latitude.

Terrain unit	Location	Years	Q_e/Q^*	Q_h/Q^*	Q_g/Q^* (Q_w/Q^* for lakes)	β	Priestly-Taylor (α)	Source
Deep lake	Northwest Territories	1997-1998	0.34	-0.01	0.68	-0.11	1.92	Eaton et al. 2001
	Northwest Territories	1991-1995	0.75	0.23	0.03	0.34	1.31	Eaton et al. 2001
Shallow lake	Ontario	1972	0.74	0.26	0.00	0.35	1.26	Stewart and Rouse 1976
	Manitoba	1985	1.05	-0.14	0.04	-0.13	1.35	Bello and Smith 1990
Sedge wetland	Manitoba	1990-1995	0.64	0.28	0.11	0.48	1.18	Eaton et al. 2001
	Quebec	1990	0.63	0.25	0.10	0.50	0.73	Moore et al. 1994
	Ontario	1985	0.69	0.16	0.15	0.23	0.87	Rouse et al. 1987
Willow-birch wetland	Manitoba	1991	0.64	0.21	0.14	0.33	0.75	Boudreau and Rouse 1995
	Ontario	1990	0.46	0.34	0.10	0.86	0.58	den Hartog et al. 1994
Open bog	Sweden	1996-1997	0.58	0.17	0.08	0.66	0.80	Kellner 2001
	Siberia	1996	0.53	0.31	0.16	-	0.63	Eugster et al. 2000
Conifer forest	Northwest Territories	1996	0.46	0.45	0.09	0.98	0.77	Eaton et al. 2001
	Manitoba	1993-1994	0.54	0.39	0.07	0.72	0.94	Eaton et al. 2001
Shrub tundra	Northwest Territories	1996-1997	0.52	0.28	0.21	0.54	1.04	Eaton et al. 2001
	Manitoba	1990-1991	0.56	0.30	0.14	0.55	1.08	Eaton et al. 2001
Lichen-heath tundra	Manitoba	1991, 1996	0.50	0.38	0.14	0.79	0.90	Eaton et al. 2001
	Ontario		0.57	0.41	0.04	0.72	0.95	Rouse et al. 1987
Tussock tundra – wet	Alaska	1995	0.49	0.40	0.17	0.81	0.55	Harazono et al. 1998
Tussock tundra – dry	Alaska	1995	0.37	0.48	0.15	1.27	0.43	Harazono et al. 1998
Polygonal tundra – dry	Siberia	1999	0.31	0.40	0.29	1.29	0.44	Boike et al. 2008
Polygonal tundra – wet	Siberia	2003	0.61	0.22	0.17	0.36	0.73	Boike et al. 2008
Wetland tundra	Northwest Territories	1996-1997	0.64	0.28	0.06	0.44	1.08	Eaton et al. 2001

Most Q_e/Q^* values reported for peatland and permafrost exceeded 0.50 (Table 4.4), indicating that, on average, latent heat flux is the principle component of the summertime energy budget (e.g., Boudreau and Rouse 1995, Eaton et al. 2001). However, where permafrost occurs, Q_e/Q^* can be less than 0.40 and sensible and ground heat fluxes become more important in energy partitioning (Harazono et al. 1998, Boike et al. 2008). Terrain units with high Q_e/Q^* values (shallow lakes and sedge wetlands) have a relatively low β , while those with low Q_e/Q^* values have a high β (Table 4.4). High α values (calculated from the Priestly-Wallace equation) are generally associated with high Q_e/Q^* values (Table 4.4).

Based on among-study mean and standard deviation of Q_e/Q^* ratios, we grouped the data from Table 4.4 into three general landscape categories: (1) shallow lakes ($Q_e/Q^* = 0.85 \pm 0.18$), (2) sedge wetlands including open fens, marshes, and wetland tundra ($Q_e/Q^* = 0.65 \pm 0.03$), and (3) conifer forest, bog, shrub tundra, lichen/heath tundra, tussock tundra, and polygonal tundra ($Q_e/Q^* = 0.50 \pm 0.08$). Research efforts are required to further assess Q_e/Q^* for peat plateau/palsa because of the lack of data availability to confidently estimate ET rates for those permafrost features. Differences in energy partitioning among terrain units in Table 4.4 are assumed to reflect both ecosystem properties and climate (Eugster et al. 2000). Variability in ET rates across landscape categories is more likely to reflect interannual and intraseasonal variation in soil moisture and temperature. These categories can initially be used to scale the energy balance and the proportion of net energy consumed by latent heat flux (i.e., ET) and the ground heat flux (Q_g) to melt ice and warm the ground.

Climate influence on evapotranspiration

Sedge wetlands

Evapotranspiration rates in terrain units north of 50° latitude vary in sensitivity to temperature and precipitation, with sedge wetlands most sensitive (Rouse 1998, Eaton et al. 2001). Warmer temperatures and reduced precipitation decreases latent heat and increases ground heat fluxes (Rouse et al. 1987, Lafleur and Rouse 1988, Petrone et al. 2000). For example, Rouse et al. (1987) reported a Q_e/Q^* ratio of 0.57 for a sedge wetland when cold winds came from James Bay, but a higher Q_e/Q^* ratio of 0.80 when warm winds came from the interior. These differences were larger than those for a sedge wetland on Hudson Bay near Churchill, Manitoba, which were 0.40 when exposed to onshore winds and 0.56 for offshore winds (Rouse et al. 1987). The lower Q_e/Q^* ratio during onshore winds was reported to be due to rapid increases in sedge canopy resistance at temperatures lower than 16 °C. Other researchers have reported similar results for coastal sedge wetlands (Harazono et al. 1998, Boike et al. 2008). Eaton and Rouse (2001) indicated that variation in the cumulative Q_e (Q_{eCUM}) at the Churchill site accounted for 47 to 85% of the cumulative annual net radiation (Q^*_{CUM}) over a 10-year study period. They further provided evidence suggesting that changes in precipitation affect Q_e/Q^* more than changes in net radiation.

Looking at estimates of how expected changes in climate might influence ET, Rouse (1998) reported that a two times CO₂ climate warming scenario with an annual temperature increase of 4 °C and no precipitation change would result in less snow and a shorter snow cover period at the Churchill sedge wetland. A greater summer water deficit was indicated in the warming scenario, triggered mainly by greater ET during May. The water deficit could be counter-balanced by a 23% increase in summer rainfall (Rouse 1998). A warming scenario with a 10% decline in summer rainfall indicated a longer, more severe water deficit that would double during drier years. For a sedge wetland in the James Bay Lowland (JBL), Lafleur et al. (1993) reported that summer temperature increases of 4 °C would require an increase of 25% in summer precipitation to maintain contemporary soil moisture values. Roulet et al. (1992) assumed a 3.5 °C increase in temperature and 1 mm day⁻¹ increase in precipitation for several northern fens and reported an increase in the soil moisture deficit in excess of 100%, possibly due to rapid ET rates offsetting the 1 mm day⁻¹ precipitation increase. Other studies across Canadian peatlands have since shown that thresholds of about a 25% increase in precipitation are required to maintain future soil moisture levels under warmer temperatures (Woo and Guan 2006, Quinton et al. 2009, 2011).

Rouse et al. (2003) reported that changes in the energy balance components of a tundra wetland were two to four times larger in the spring compared to fall and winter. They proposed that the timing of snowmelt was important to the magnitude of spring and fall differences. They further suggested that because the spring shoulder season is potentially the most sensitive to regional warming or cooling, earlier snowmelt would increase the magnitude of latent and ground heat fluxes; a similar result was reported for wet tundra (Lafleur and Humphreys 2008).

Bogs

Energy partitioning in bogs varies more than that in sedge wetlands, making projections about the effects of climate change on bog energy partitioning more difficult (Shimoyama et al. 2003). Some commonalities corresponding to microtopography, soil moisture, and surface cover (e.g., non-vegetated vs. moss/lichens vs. vascular plants) and the presence of hummock and hollow microtopography do exist, all of which contribute to partitioning energy to latent heat (Admiral et al. 2006). For example, moss and non-vegetated surfaces are important to spring latent flux and subsequent ET, whereas vascular plants become important from mid-spring to late-summer (Kellner 2001, Kurbatova et al. 2002, Admiral and Lafleur 2007).

The phenology of vascular plants, predominantly leaf area index (LAI), controls energy partitioning in sparsely vegetated bogs (LAI <1.0) (Admiral et al. 2006). Leaf area index is minimal in spring, when peat is generally saturated (Lafleur and Humphreys 2008). This corresponds to the time of highest solar energy reaching peatland surfaces and high Q_e/Q^* values due to *Sphagnum* mosses occurring in both hummocks and hollows. *Sphagnum* mosses evaporate water passively through capillary flow and they account for 50 to 70% of the total annual ET from bogs (Kim and Verma 1996, Kellner 2001). Increasing LAI decreases the amount of radiation reaching the surface (Boike et al. 2008). At this time, ET switches from moss- to vascular plant-dominated, and subsequently dries the peat (Kellner 2001). The ground energy flux is also highest in spring and decreases throughout the year, becoming

negative by mid-August to mid-September, depending on latitude (Eugster et al. 2000). Because increasing LAI reduces the amount of energy reaching the surface of peatlands, ground heat flux in bogs decreases as vascular plants develop (Boike et al. 2008).

Understanding moss and vascular plant interactions with earlier snowmelt is critical to comprehend future ET trends of bogs. Earlier snowmelt is expected to lead to earlier onset of ET by mosses. However, few studies have documented the competition between mosses and vascular plants following snowmelt. Therefore, it is uncertain if earlier snowmelt will only shift moss ET to earlier in the year or, if soil warming during spring will enhance nutrient mineralization and subsequent vascular plant biomass and LAI values. Most models indicate vascular plant and LAI increases during the 21st century (Zhuang et al. 2006, Balshi et al. 2009), which have been positively correlated to aboveground biomass and soil C accretion (Frolking et al. 2011). However, LAI increases are also positively correlated with fire frequency and area burned (Zoltai et al. 1998), often switching peatlands from net C sinks to sources (see section 6, Fire Regimes). As such, we view (1) moss and vascular plant competition following earlier snowmelt and (2) effects of extended growing season, energy partitioning, along with peatland drying and fire interactions on C storage and GHG exchange as key research areas, where data are vital to understand and improve future bog C budget projections.

Permafrost features

Permafrost is a strong heat sink and has a larger ground heat flux value than non-permafrost peatlands, and changes in temperature and moisture may alter permafrost thaw rates (Quinton et al. 2011). However, few data are available to confidently describe and model the energy balance in permafrost features. Boike et al. (2008) reported that during a wet year in the polygonal tundra of the CPZ, energy partitioning was typical of sedge wetlands. Here, 61, 22, and 17% of the net energy occurred as latent, sensible, and ground heat fluxes, respectively. However, when peat was dry, a relatively even partitioning of energy among latent (31%), sensible (37%), and ground (29%) heat occurred; similar to that of forests and bogs. This shift in partitioning was predominantly the result of lower precipitation (manifested through lower soil moisture). Thus, dry conditions generally resulted in high ground heat fluxes compared to those in wet years (Eugster et al. 2000, Rouse 2000). In addition, during dry years, energy partitioning is not affected by differences in air temperature. However, during wet years latent heat flux increases as temperatures increase, which decreases energy partitioning to sensible and ground heat (Boike et al. 2008). Similar patterns were shown for wet and dry tussock tundra underlain by permafrost (Harazono et al. 1998) and mesic tundra and heath/shrub tundra (Lafleur and Humphreys 2008). Increases in air temperature combined with adequate water supply (e.g., precipitation and permafrost thaw) could maintain current, or increase, ET rates in permafrost-dominated landscapes, thereby maintaining current soil moisture levels.

Upland/heath and shrub tundra

Upland/heath and shrub tundra have the lowest ET rates of all terrain units (Table 4.3). Because LAI at most tundra sites is less than 1.0, a significant portion of ET flux results from soil evaporation (Lafleur and Humphreys 2008). As such, soil drying reduces energy partitioned to latent heat flux and lowers ET rates. However, as with bogs, actual ET in tundra ecosystems is often below potential values (Harazono et al. 1998, Eaton et al. 2001, Rouse et al. 2003), indicating partial vegetative control of ET rates does occur; this is primarily attributed to stomatal conductance (Boike et al. 2008, Lafleur and Humphreys 2008). Shrub and lichen/heath tundra have relatively similar energy partitioning (Table 4.4). In contrast, tussock tundra partitions more energy to sensible heat at the expense of latent heat (Harazono et al. 1998). In addition, as with polygonal tundra (Boike et al. 2008), tussock tundra partitions more energy to latent heat during wet years (Harazono et al. 1998). Also, wetland tundra (commonly dominated by sedge vegetation) partitions energy in much the same way as sedge wetlands (Eaton et al. 2001).

Runoff

Peatlands in the Far North are exposed to varied climate, with temperature and precipitation decreasing from south to north (Figure 4.1). Peatland complexes also differ along the permafrost gradient, with the proportion of bogs decreasing and the proportion of peat plateaus, palsas, and fens increasing from the southern zone

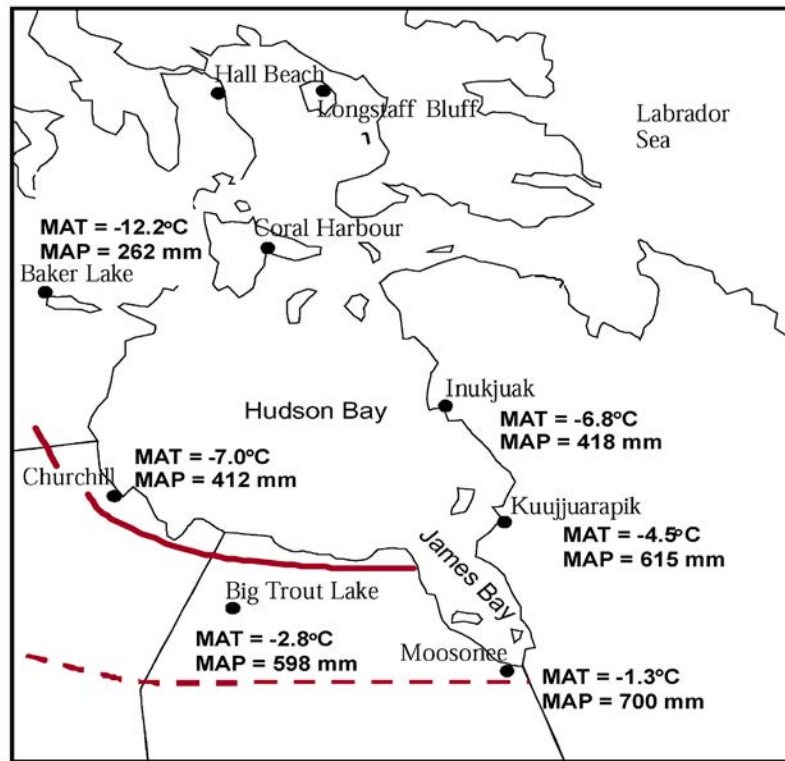


Figure 4.1. Mean annual temperature (MAT), mean annual precipitation (MAP), and southern limit of continuous (red solid line) and discontinuous (red dotted line) permafrost boundaries for the Hudson Bay region, Canada. MAT and MAP data are from Gagnon and Gough (2005) and permafrost boundaries are from Tarnocai (2006).

northward into the DPZ and CPZ (e.g., Tarnocai et al. 2000, Vitt et al. 2000a). Important features controlling runoff in permafrost regions include (1) presence and distribution of fens and bogs, which establishes hydrologic routing and water storage capacity (Hayashi et al. 2004, Wright et al. 2008); (2) aspect and vegetation, which identify areas likely to be affected by permafrost (Quinton et al. 2003) and control snow distribution and snowmelt processes (Zhang 2005); and (3) surficial geology, which controls groundwater flow and chemistry (Reeve et al. 2000, Thompson and Woo 2009).

Hydrogeological settings in large peatland complexes

Geology is the main factor affecting hydrology in large peatland complexes. For example, in the Albany River Basin of the JBL, raised bogs are limited to interfluvial divides between eroding streams and shifting river channels. Further bog growth is constrained by the width of the interfluvium (region of higher land between two rivers that are in the same drainage system) and depth of river incision (Glaser et al. 2004b). These bogs are situated on water table mounds, with mound height and location controlled by interfluvial width and stream or river water height (Glaser et al. 2006). Because the mineral sediment underlying bogs in the JBL is primarily glaciomarine clays, vertical water flow into those deposits is restricted and water drains outwards from a central crest to the bog margin and then to channel fens. These broad (50- to >100-m-wide) fens have dendritic drainage patterns and water flows over and below their surfaces (Glaser et al. 2004a). The largest channel fens arise from the flanks of mounded bogs and plateaus or at extreme down-gradient portions in local basins (Hayashi et al. 2004, St. Amour et al. 2005). Longer channel fens may be interrupted by a dense system of tributary streams, which act as discharge zones for the local recharge water mounds (Glaser et al. 2004a).

Various groundwater models have been proposed to explain groundwater/peatland interactions. Roulet and McKenzie (1998) used a two-dimensional finite-difference model based on MODFLOW (McDonald and Harbaugh

1984, Harbaugh and McDonald 1996). Model results indicated that under a zone of raised bog complexes precipitation recharges the regional groundwater system. Groundwater then flows laterally within calcareous glacial deposits and discharges to the land surface within a riparian zone of channel fens.

Reeve et al. (2000, 2001) proposed that lateral flow systems develop across low-lying plains where glaciomarine silt and clay deposits are thickest and most extensive. Under this coupled groundwater flow-transport model, inorganic solutes from the underlying calcareous glaciomarine sediments are transported upwards to the surface by transverse dispersion and dispersive mixing along lateral flow paths. Vertical flow systems (e.g., recharge or discharge zones) develop in the wide-interfluvial areas, where water is driven down and outward from the water table mound under wet conditions (Figure 4.2). Under dry conditions, however, little vertical water transport occurs. Instead, the water mixes with upwelling groundwater from deeper peat and mineral sediment below the peat (Reeve et al. 2000, 2001), potentially increasing ET rates and reducing runoff rates.

Peatland hydrological connectedness

General patterns: For large peatland complexes in the DPZ, hydrological connectedness to surface water exists for 10 to 80% of the area, with the proportion of connectedness increasing with amount of area in the basin covered by peat plateaus, palsas, and fens (Quinton et al. 2003, Stadnyk et al. 2005). However, in permafrost regions scant data are available on inter-seasonal and interannual hydrological connectedness of peatlands and the streams and rivers they drain into (Kane et al. 2008, Woo et al. 2008). Furthermore, various results have been reported about the importance of snowmelt and groundwater runoff events at local to regional landscapes. Some research indicates that snowmelt runoff accounts for more than 50% of mean annual runoff (Quinton and Roulet 1998), whereas other studies show that 60 to 95% of stream flow is attributed to groundwater inputs (Hayashi et al. 2004, St. Amour et al. 2005, Stadnyk et al. 2005). Understanding the factors that control the volume and timing of runoff is an essential first step towards developing methods to accurately assess basin runoff from peatland-dominated basins, as well as understanding the basin response to hydrological changes initiated by the thawing of permafrost peatlands (Woo et al. 2008).

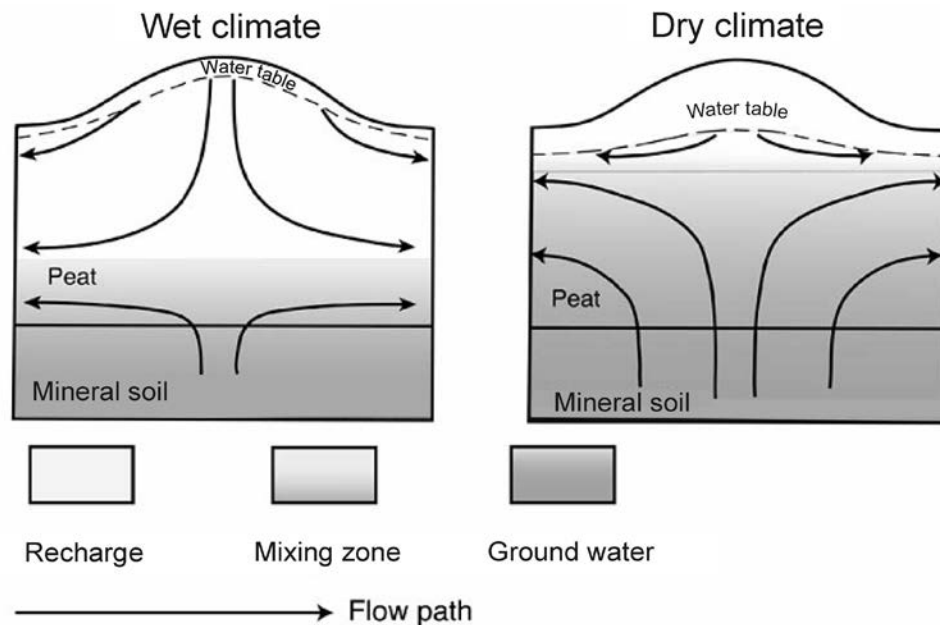


Figure 4.2. Hydraulic-head measurements from a raised bog in the Red Lake peatland in 1990 (left) and 1991 (right). All head measurements are relative to the water table (from Reeve et al. 2000; reprinted with permission from Elsevier).

Water flow paths: Water flow paths describe water routes and the time required for it to move from soil to stream (Woo et al. 2008). Water flow paths are commonly estimated using hydrometric (precipitation, soil moisture, groundwater, and stream flow) and hydrochemical (chemical and isotopic tracers) measurements to assess peatland water movement and its residence time. Water fluxes can be directly measured from surface runoff and soil moisture, and subsurface water flux can be calculated from groundwater level data (Quinton et al. 2009). However, soil moisture and groundwater levels are spatially heterogeneous and measurements are few. Groundwater levels near streams are usually highly correlated with discharge (Woo et al. 2008). Higher soil moisture leads to more catchment discharge, which increases the synchrony between soil moisture and groundwater (Frey and McClelland 2009).

Hydrochemical data are collected from solute concentration and isotope measurements that are often defined as 'tracers' for water flow paths and water residence time. Water residence time can be assessed using different approaches. The most common is based on conservative tracers that preserve temporal variations in rainwater (Hooper 2003). Stable isotopes of hydrogen ($\delta^2\text{H}$) and oxygen ($\delta^{18}\text{O}$) are ideal tracers, but other chemical constituents of soil water and groundwater can also be used (Frey and McClelland 2009).

Hydrograph (time series of discharge measurement at a catchment outlet) separations can be used to determine the contributions of different components (e.g., rainwater, soil water, groundwater, and snowmelt) to stream flow and water residence time, either as mean values for long timeframes or as temporally varying contributions during single runoff events (Hooper et al. 1990). Hydrograph separations assume that individual components differ significantly with respect to their tracer concentrations. Often, spatial and temporal heterogeneity within a single runoff component is assumed negligible (Hooper 2003). Second, stream water is assumed to contain exclusively these different components. Third, only 'conservative' tracers are investigated, that is, solutes or isotopes that are not subject to sorption to the soil matrix, chemical reactions, biological alteration, or radioactive decay at the timeframe of interest.

Once the assumptions have been met, a mass balance approach can be used, where the tracer flux is the product of its concentration and corresponding water flux, and the total tracer flux in a stream equals the sum of tracer fluxes of the contributing components (Frey et al. 2007). Studies of the $\delta^{18}\text{O}$ and $\delta^2\text{H}$ isotopes indicate relatively higher contributions of snowpack to stream flow during snowmelt periods in bog- than in fen-dominated catchments (Table 4.5). The $\delta^{18}\text{O}$ and $\delta^2\text{H}$ signatures of stream water in fen-dominated catchments, however, indicate that groundwater contributions to stream flow are important (Hayashi et al. 2004, St. Amour et al. 2005). Surface water (pools, ponds, and small lakes) appears to contribute similarly to stream flow during the post-snowmelt period in bog- and fen-dominated catchments (Table 4.6).

Table 4.5. Source water contributions to stream flow for a peat plateau-bog-fen complex in the discontinuous permafrost zone of the Northwest Territories, Canada assessed using oxygen (O) and hydrogen (H) tracing techniques (St. Amour et al. 2005).

Catchment	Freshet period		Post-freshet period					
	Maximum snowmelt contribution (%)		Maximum surface water (%)		Average surface water (%)		Average groundwater (%)	
	$\delta^{18}\text{O}^a$	$\delta^2\text{H}^b$	$\delta^{18}\text{O}$	$\delta^2\text{H}$	$\delta^{18}\text{O}$	$\delta^2\text{H}$	$\delta^{18}\text{O}$	$\delta^2\text{H}$
Bog-dominated								
Birch River	37	34	39	51	29	21	71	79
Blackstone River	40	41	48	61	36	39	64	61
Mixed-peatland-dominated								
Martin River	46	44	27	39	14	20	86	80
Fen-dominated								
Jean-Marie River	21	21	32	35	29	28	71	72
Scotty Creek	31	33	42	60	30	34	70	66
Laird River	20	24	22	24	20	20	80	80

^a $\delta^{18}\text{O}$ - isotope of oxygen.

^b $\delta^2\text{H}$ - isotope of hydrogen.

Table 4.6. Stable isotopic composition of stream flow components in peatland-dominated permafrost regions of the Northwest Territories, Canada (summarized from Gibson et al. 1993, Hayashi et al. 2004, and St. Amour et al. 2005).

Sample type	$\delta^{18}\text{O}^a$ (‰)	$\delta^2\text{H}^b$ (‰)
Rainwater	-17.8 to -19.9	-140 to -150
Surface water	-12.8 to -12.9	-126 to -129
Snow	-29.3 to -29.6	-223 to -228
Snowpack	-27.0	-203 to -206
Active layer (peat plateau)	-19.9	-150
Stream flow (freshet period)		
Bog-dominated	-20.0 to -24.0	-156 to -192
Fen-dominated	-18.2 to -21.4	-148 to -192
Stream flow (base flow period)		
Bog-dominated	-18.1 to -20.1	-148 to -164
Fen-dominated	-18.7 to -19.5	-148 to -164
Groundwater		
Bog-dominated	-18.9 to -21.5	-150 to -172
Fen-dominated	-20.4 to -16.8	-150 to -170

^a $\delta^{18}\text{O} = ^{18}\text{O}:^{16}\text{O}$ oxygen isotopes in parts per thousand (‰).

^b $\delta^2\text{H} = ^2\text{H}:^1\text{H}$ hydrogen in parts per thousand (‰).

Hydrograph separations also indicate that bog-dominated catchments have a quick-flow response attributed to moisture from active layer thawing (St. Amour et al. 2005) and reduced infiltration rates because the permafrost is relatively impermeable (Hayashi et al. 2004). In contrast, fen-dominated catchments have broader hydrographic peaks, indicating greater infiltration and longer response and recession times (Wright et al. 2008). Also, in fen-dominated catchments snowmelt mixes with and displaces more of the groundwater to stream flow.

Runoff processes: The water balance components assessed for terrain units in permafrost regions vary widely (Table 4.7). Some of this variability is attributable to differences in study methods; however, the hydrogeology and climate of the region likely also contribute. A common theme from the literature is that active layer thawing and snowmelt contribute significantly to water balances (Table 4.7).

Table 4.7. Water balance for various landscape units in permafrost zones.

Terrain unit	Location	Study period	Snowmelt	Precipitation	Active layer melt	Evapo-transpiration	Soil moisture change	Runoff	Source
Peat plateau	Northwest Territories	Snowmelt period 2004 – 2005	206 to 222	0	32 to 58	21 to 25	29 to 88	184 to 204	Wright et al. 2008
		Post-snowmelt period 2004 – 2005	0	53 to 63	105 to 130	35 to 42	97 to 114	29 to 34	Wright et al. 2008
Sedge wetland	Manitoba	June – August 1982-1983	146	34	210 to 251	223	285 to 306	332	Roulet and Woo 1986
	Ontario	April – August 1985	5 to 70	-	-	13 to 21	-36 to -24		Woo and DiCenzo 1989
Shrub tundra	Northwest Territories	June – August 2003	98 to 276	-	52 to 133	2 to 5	0 to 55	8 to 114	McCartney et al. 2006
String bog	Alaska	January – December 2001 – 2003	140 to 175	200 to 300	-	140 to 230	-10 to 40	170 to 340	Schramm et al. 2007
Arctic tundra	Siberia	May – August 1967 – 1976	203	-	108	136	-	176	Kuchment et al. 2000

Permafrost is often saturated or oversaturated with ice, and, therefore acts as a confining layer (Figure 4.3), limiting the movement and storage of groundwater to the seasonal active layer (Boike et al. 2003, 2008; Wright et al. 2008). This promotes surface ponding and runoff during snowmelt and spring rainfall events (McCartney et al. 2006). Consequently, snowmelt hydrographs for subarctic wetland basins have larger peaks than those for non-wetland basins (Roulet and Woo 1986).

The pre-freeze-up available soil moisture storage capacity in late fall and winter is a critical factor in determining dominant flow paths and amounts of runoff following snowmelt periods. Unfrozen soil water storage is estimated to range between 50 and 100 mm during winter (Hayashi et al. 2004, Carey and Quinton 2005). An additional 50 to 250 mm of water is added during active layer thaw (Table 4.5). Most of this water is transported to draining bogs and fens where it contributes to runoff during snowmelt, but most is stored or lost to ET post-snowmelt (Hayashi et al. 2004, Wright et al. 2008).

Frost (permafrost and seasonal frost) table topography affects runoff, particularly during snowmelt (Wright et al. 2008, 2009). Therefore, knowledge of the spatial and temporal variation of thaw depths is essential to understanding water flow. It is particularly important to consider variation in frost table topography when point measurements are scaled up for use in basin studies (Woo et al. 2008). Furthermore, understanding the factors that control the distribution of frost table depths is critical to modelling runoff in permafrost basins, particularly in peatland-dominated, discontinuous permafrost basins, where permafrost often exists as scattered patches (ranging from 0.2 to 2.0 m above the surrounding terrain and extending up to several km² in area) that appear as islands among otherwise unfrozen, peat-covered saturated terrain (Quinton et al. 2003). During the snowmelt period, all but the upper 5 to 10 cm of peat in plateaus are frozen. This results in more surface (peatland pools, ponds, small lakes) runoff. However, even in these situations only 17 to 56% of event water is partitioned to stream flow, with the remaining 54 to 83% partitioned to basin storage where it is eventually released through ET and drainage during the post-snowmelt period (Hayashi et al. 2004, Carey and Quinton 2005, St. Amour et al. 2005).

River discharge

Rivers integrate atmospheric and watershed processes providing a mechanism for detecting changes in climate (Welp et al. 2005). Modifications in high-latitude environments include decreasing depth and duration of snow-cover, warming and thawing of permafrost, and increasing storminess and precipitation. Such changes affect freshwater discharge in complex ways; however, given that river runoff is driven mainly by precipitation and surface

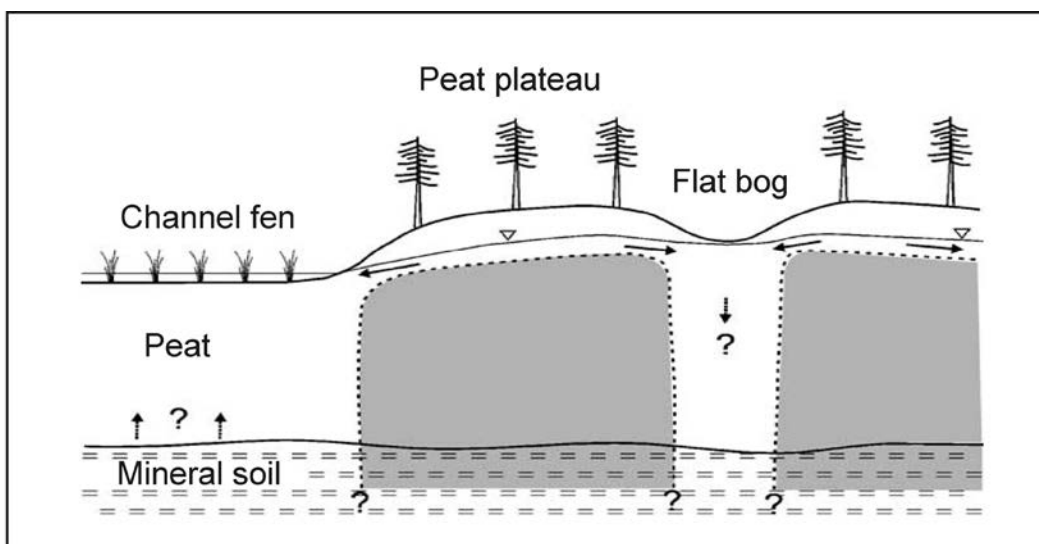


Figure 4.3. A schematic cross-section of a peat plateau and adjacent channel fen and flat bog areas, with arrows indicating subsurface flow. Shaded areas indicate frozen soil. Note that the vertical dimension is greatly exaggerated and plants are not drawn to scale (from Hayashi et al. 2004; reprinted with permission from Elsevier).

air temperature, recent observations point to an acceleration of the hydrologic cycle including higher freshwater discharge in many northern regions (Déry and Wood 2005, Smith et al. 2007).

Between 1964 and 2000, discharge from rivers draining through permafrost zones to the Arctic Ocean increased by $5.6 \text{ km}^3 \text{ yr}^{-1}$ (McClelland et al. 2006). This increase is the net result of a large increase in discharge from Eurasia moderated by a decrease in HJUB (Déry et al. 2005, McClelland et al. 2006, Smith et al. 2007) (Table 4.8). The difference between Eurasia and the HJUB may result from teleconnections (i.e., North Atlantic Oscillation, Arctic Oscillation, El Niño/Southern Oscillation, Pacific Decadal Oscillation). During a positive phase of Arctic Oscillation, Hudson Bay is subject to colder than average temperatures, whereas Eurasia has warmer than average temperatures. During a negative phase of Arctic Oscillation, this is reversed (Déry and Wood 2004).

The HJUB drains an area of $3.7 \times 10^6 \text{ km}^2$ and has a freshwater discharge of $950 \text{ km}^3 \text{ yr}^{-1}$, accounting for one-fifth of the total annual river runoff to the Arctic Ocean (Ontario accounts for one-fifth of the discharge into the HJUB) (Déry and Wood 2004, McClelland et al. 2006). Although Hudson Bay accounts for nearly 70% of the drainage area, James Bay has a higher discharge rate per contributing area (Figure 4.4a). Moreover, discharge rates per contributing area are greatest for rivers draining into eastern Hudson Bay (Figure 4.4b), where annual precipitation rates are relatively high and annual ET rates are relatively low (Déry et al. 2005). Ocean currents transport the Hudson Bay discharge to the Labrador Sea, where it affects high-latitude oceanographic, atmospheric, cryospheric, and biological processes (Saulnier-Talbot et al. 2007).

Table 4.8. Average and changes in discharge to the Arctic and Hudson, James, and Ungava bays between 1962 and 2000 (from McClelland et al. 2006).

Input	Average combined discharge ($\text{km}^3 \text{ yr}^{-1}$)	Annual change ^a ($\text{km}^3 \text{ yr}^{-1}$)	Cumulative change ($\text{km}^3 \text{ yr}^{-1}$ over 37 years)	Cumulative change (% over 37 years)
Eurasia to Arctic Ocean				
Six largest rivers	1839 (1847)	5.34 (4.57)	198 (169)	11.3 (9.6)
Ten smallest rivers	224	0.80	29	14.3
North America to Arctic Ocean	357 (359)	-0.41 (-0.57)	-15 (-21)	-4.2 (-11.6)
North America to HJUBs ^b	717	-2.49 (-2.41)	-92 (-89)	-12.1 (-11.6)

^a $\delta^2\text{H} = {}^2\text{H}:{}^1\text{H}$ hydrogen in parts per thousand (‰)³ Values in the annual change column are the slopes of Kendall Theil Robust Lines; bold font identifies statistically significant changes ($p < 0.05$) determined using the Mann-Kendall test. Values in parentheses reflect adjustments made to remove discharge deficits from years of reservoir filling.

^b HJUBs = Hudson, James, and Ungava bays.

For 35 rivers that are not directly affected by anthropogenic activities, the observed spring peak discharge rates decreased on average by $302 \text{ m}^3 \text{ s}^{-1}$. Rivers in Ontario and Québec also show declining stream flow rates (Déry et al. 2005). Between 1964 and 2000, river runoff in the Hudson Bay basin decreased 15% (Déry et al. 2005). During the same period, in Ontario's Far North, runoff in the three most northerly rivers that are monitored (Severn, Winisk, and Attawapiskat) decreased significantly. Discharge peaked in mid-June and was lowest in March. Moreover, peak discharge associated with snowmelt advanced by 8 days and diminished by $0.036 \text{ km}^3 \text{ yr}^{-1}$ (Déry et al. 2005). Ninety percent of the recent variability in Hudson Bay river discharge could be explained by the Arctic Oscillation (Déry and Wood 2004). Despite the statistical link established between the Arctic Oscillation and observed and modelled stream flow in Hudson Bay, more research into the physical mechanisms is needed.

Studies conducted in Eurasia (Smith et al. 2007), the Northwest Territories (St. Jacques and Sauchyn 2009), and Alaska (Walvoord and Striegl 2007) indicate increasing winter flow rates for large rivers draining into the Arctic Ocean. These increases have been attributed to changes in precipitation, permafrost, fire frequency, and ET. For example, St. Jacques and Sauchyn (2009) proposed that the increases in winter base flow and mean annual stream flow in the Northwest Territories were caused primarily by climate warming via permafrost thawing that increases infiltration, creating deeper flow paths. However, Adam et al. (2007) suggested that the mechanisms behind observed discharge increases may vary from region to region, with permafrost thaw dominating in some, precipitation in some, and combinations of both in others.

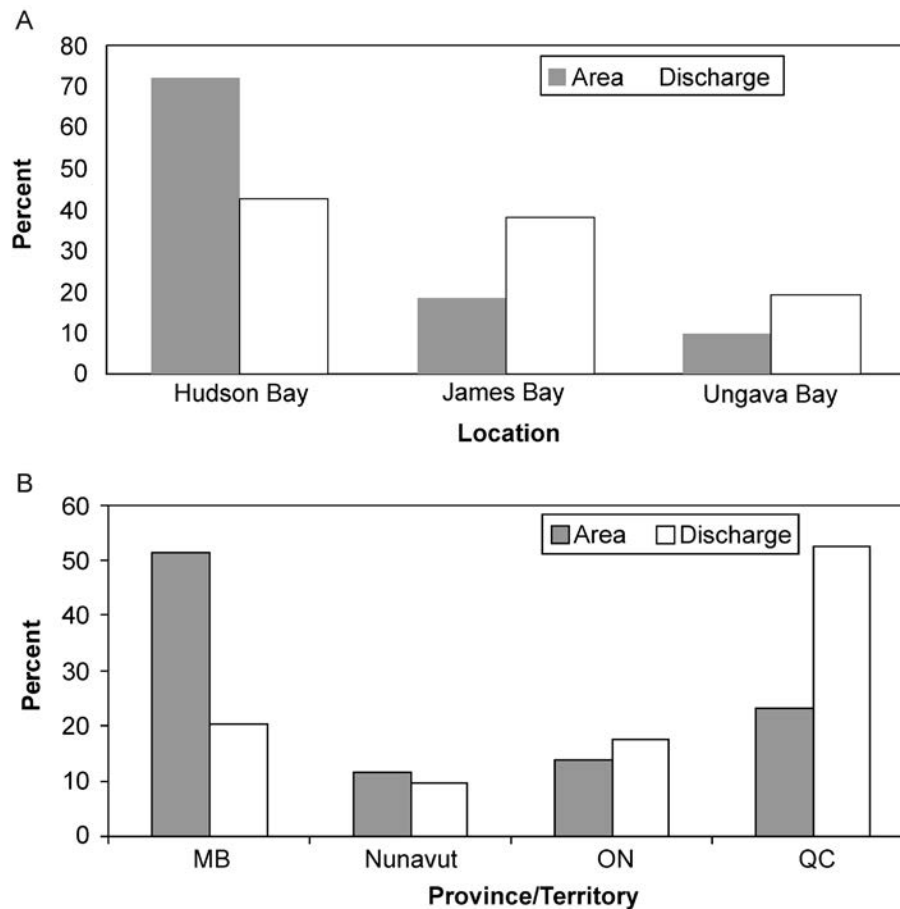


Figure 4.4. Freshwater discharge into the Hudson-James-Ungava bays from 1964 to 2000 relative to land area: (a) contribution of each bay and (b) contribution of each Canadian province/territory; MB = Manitoba, ON = Ontario, QC = Quebec (adapted from Déry et al. 2005).

Regardless of exact mechanisms in each region, the finding of increased winter, and presumably groundwater, flow throughout much of the permafrost region signifies increases in the role of groundwater processes in the high-latitude water cycle under global warming. This could mean shifts from surface to deep water storage, and increased soil infiltration, unsaturated zone storage, and groundwater movement in permafrost regions.

Climate change effects on runoff

Twenty-first century runoff patterns

Effects of climate warming are anticipated to be most noticeable during winter and spring, affecting snow accumulation, snow cover duration, and snowmelt properties in permafrost regions (Bonsal and Prowse 2003). A shorter snow cover period will lead to lower overall albedo, and this process may be further stimulated by vegetation shifts from sedge wetlands and tundra to shrub or forested communities. These vegetation shifts are also likely to affect snow accumulation and ablation patterns (Liston et al. 2002, Marsh et al. 2002). Therefore, from a hydrological perspective, critical issues related to climate change include a shortened snow cover season, changes in winter snow cover properties, and changes in the timing and volume of snowmelt runoff (Quinton et al. 2009).

The assessment of potential future climate effects on hydrology requires projections of future climate at appropriate levels (Pohl et al. 2007). At present, climate effects research relies primarily on GCMs for future

temperature and precipitation projections (Gagnon and Gough 2005, Riseborough et al. 2008). Pohl et al. (2007) used the WATFLOOD hydrological model with data from two climate models – HadCM3 and CGCM2 – and two climate scenarios. The A2 scenario is associated with a more fossil fuel-intensive world (projected mean temperature change of 2.5 to 4.5 °C by 2100) and the B2 scenario reflects lower GHG emissions (with projected mean temperature changes of 1.5 to 3.0 °C by 2100). HadCM3-A2 and -B2 model scenarios represent cool, wet scenarios while the CGCM2-A2 and -B2 projections represent warm, dry scenarios (IPCC 2001).

The largest changes in runoff timing were suggested by the CGCM2-A2 scenario, with the average day of first runoff occurring 17 (2050s) to 25 (2080s) days earlier, and average peak runoff occurring 14 (2050s) to 22 (2080s) days earlier (Table 4.9, Figure 4.5a). The least amount of change was produced by HadCM3-B2 model scenario (Figure 4.5b), in which the average date of first runoff shifted by 6 (2050s) to 11 (2080s) days and that of peak runoff by 3 (2050s) to 6 (2080s) days; values consistent with earlier snowmelt and peak runoff of 8 days calculated for river discharge (Déry et al. 2005), and the 5 to 8 days (2041-2070) increase in soil thawing suggested by Sushama et al. (2006) (see section 3, Permafrost Patterns).

The warm, dry CGCM2 scenarios pointed to large increases in ET, but only minor runoff changes (Figure 4.5a). Model projections also suggested a shift in stream freeze-up from last runoff previously occurring in late October or early November to late September and early October in recent years. This suggests that under future climate conditions the snow-free period will be longer, potentially increasing allocation of water flux to ET. Other projections indicate vegetation shifts (Pohl et al. 2007) and ALT increases will occur, both of which are likely to change snowmelt runoff and ET.

Table 4.9. Statistics for comparing baseline climatology to future climate scenarios in snowmelt runoff for a continuous permafrost basin in the Northwest Territories using WATFLOOD hydrologic model (from Pohl et al. 2007).

Model scenario	First day of runoff		Day of peak runoff		Peak daily runoff	
	Mean projected change (days)		Mean projected change (days)		Mean projected change	
	2050s	2080s	2050s	2080s	2050s	2080s
CGCM2 A2 ^a	-17	-25	-14	-22	83	76
CGCM2 B2 ^a	-14	-19	-10	-14	92	80
HadCM3 A2 ^b	-6	-15	-3	-8	109	105
HadCM3 B2 ^b	-6	-11	-3	-6	107	106

^a HadCM3 A2 and B2 general circulation models represent projections for cool, wet conditions and minimal temperature change (A2 = 1.4 °C, B2 = 1.4 °C) but increased precipitation (A2 = 23%, B2 = 16%).

^b CGCM2 A2 and B2 projections are typical of warm, dry conditions with higher temperature increases (A2 = 4.8 °C, B2 = 3.5 °C) but low to moderate precipitation changes (A2 = 13%, B2 = 5%).

Role of permafrost in future runoff patterns

Permafrost thawing is expected to alter hydrological delivery of organic matter, inorganic nutrients, and major ions to surface water. These interacting effects are highly complex, with much spatial and temporal variability associated with current permafrost condition, sensitivity of permafrost thaw, mode of permafrost degradation (overall permafrost thaw, active layer deepening, and/or thermokarst processes), and environmental characteristics of watersheds (e.g., land cover, soil type, and topography). One of the most profound consequences of permafrost thaw may be that streams and rivers in permafrost regions will transition from surface water- to groundwater-dominated systems (Janowicz 2008, St. Jacques and Sauchyn 2009).

Deepening active layers may increase interactions between surface water and soil within newly thawed portions of the active layer, as well as liberate soluble biogeochemical compounds previously sequestered within near-surface permafrost. Over the past 40 to 50 years, active layers have thickened by 20 to more than 30 cm (Zhang et al. 2005, Frauenfeld et al. 2007). Moreover, since 1980 the active layer has thickened between 0.35 and 0.81 cm yr⁻¹ in Siberia and 0.47 cm yr⁻¹ in Canada's Northwest Territories (Oelke et al. 2003). In northern Sweden permafrost thaw rates of 0.7 to 1.3 cm yr⁻¹ have been reported for the past 90 years (Åkerman and Johansson 2008, Lyon et al. 2009). Modelling studies suggest a further 30 to 140% thickening of the active layer depth in Canada by 2100 (Zhang et al. 2008b).

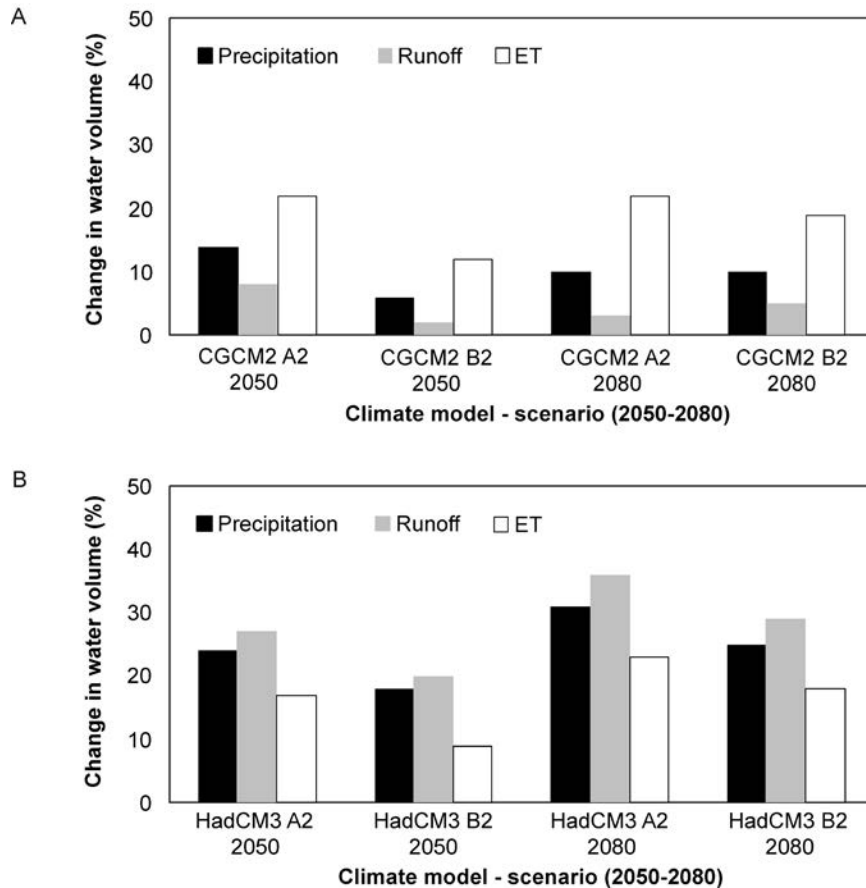


Figure 4.5. Thirty-year average water balance components for simulated future climate scenarios based on (a) CGCM global circulation model and (b) HadCM3 global circulation model compared to 1661-1990 baseline climatology for a continuous permafrost basin in the Northwest Territories (from Pohl et al. 2007; reprinted with permission from Environment Canada). ET = evapotranspiration.

Major ion concentrations may increase with permafrost degradation and lowering of water tables, due to less water interacting with shallow organic soils and more interacting with deeper soil profiles (Frey et al. 2007). In addition, thawing of permafrost and lowering of the water table will increase organic matter decomposition rates, which may in turn release and mobilize ions accumulated during peatland development. As such, meltwater can be ion rich and may contribute pulses of ions to streams and rivers following permafrost degradation (Kokelj and Burns 2005). Much more research, using combinations of hydrometric and hydrochemical hydrograph separations and incorporating these data into hydrologic models, is required to confidently identify how runoff processes will respond to changes in climate and how these changes will affect peatland C cycling and budgets in permafrost regions.

Summary and conclusions

Peatlands in permafrost zones constitute unique permafrost and non-permafrost features that are hydrologically connected for less than one third of the year, primarily during snowmelt and shortly thereafter. During this timeframe, water flow generally occurs from bogs and peat plateaus/palsas to fens. Water can continue to flow through fens to streams, ponds, and lakes or be stored as soil moisture to support ET. During snowmelt periods, low water storage capacity of frozen peat (seasonal frost and permafrost) promotes shallow water flow paths through peatland complexes. By the end of the growing season, ET dries the peat, often creating peat moisture deficits that need to be reversed before hydrological connectedness can be restored during large fall precipitation events or snowmelt the following spring.

Long-term flow records for large rivers in the HJUB—including Ontario’s Far North—show decreasing annual flow trends since the 1960s and groundwater contributions to river flow in the region appears to be increasing. Model forecasts suggest (1) shifts in last runoff of the year from late (e.g., late October or early November) to early (e.g., September and early October) fall and (2) a 10 to 30 day earlier snowmelt. Both earlier snowmelt and timing of last runoff have been implicated in lower runoff and higher ET rates in long-term (40 to 50 years) field analyses and aerial photographic studies across boreal and subarctic landscapes. Representation of ET and energy partitioning rates as input data in spatial C cycling models is one of the largest input data uncertainties in spatial C cycling models. Therefore, from hydrological and C perspectives, critical issues related to climate change requiring more research include (1) shortened snow cover seasons, (2) changes in the timing and volume of snowmelt and late-season runoff, (3) changes in vegetation structure, (4) changes in energy partitioning, and (5) their interactive controls on annual ET rates.

Although ET rates vary, they, along with energy partitioning, display common patterns within land cover types regardless of where they occur. Our ET and energy balance literature summary points to three broad land type classifications: (1) wet features, consisting of thermokarst ponds, lakes, and sedge wetlands (ET = 2.0 to 4.8 mm d⁻¹); (2) dry features, consisting of spruce forests and bogs (ET = 1.5 to 2.5 mm d⁻¹); and (3) cold features, consisting of heath, lichen, shrub, and tussock tundra, as well as peat plateaus and polygonal peatlands (ET = 1.4 to 1.7 mm d⁻¹). Wet features partition the most energy to ET, whereas dry and cold features partition relatively more energy to ground fluxes, thereby warming soils.

To calibrate spatial models, the ET and energy partitioning patterns and rates within and among wet, dry, and cold features need to be verified at research sites. For example, many uncertainties relate to ET and energy partitioning in permafrost features and across fen types (e.g., open, shrub, and treed). Therefore, further research is required to constrain energy budget projections for various fen types, peat plateaus, palsas, ponds, lakes, and collapse scars. Until the above shortcomings are rectified, the three land type designations above should provide a base for sorting ET and energy partitioning data for input to spatial models for initial peatland C storage and sequestration assessments to help guide land use planning.

5. Peatland Carbon Cycling

Background

Carbon storage and GHG emissions vary within and among peatland types (McLaughlin 2004, Godin et al. 2012). Variation within a peatland is attributed to differences in microtopographic (e.g., hummocks and hollows) and permafrost (aggrading and degrading) features. In contrast, across landscapes, peatland C dynamics depend on the amount and distribution of peatland types (e.g., bog, fen, peat plateau, palsa) and thermokarst features (e.g., ponds, collapse scars, internal lawns).

Climate change affects peatland C storage and exchange with the atmosphere via increasing air temperature and altered precipitation patterns. Subsequently, peat warms and soil moisture and water table levels increase or decrease, depending on precipitation and permafrost thaw patterns (Pohl et al. 2007). For example, changes in vegetation structure from wet- to dry-adapted plants in warming and drying peatlands (see sections 2, Peatland Development and Plant Associations and 4, Peatland Hydrology) alters CO₂ sequestration through photosynthesis and the quality of organic matter deposited to peat through above- and belowground litter inputs (Laiho 2006). However, no consensus on peatland CO₂ balance has been reported. For example, organic matter input and quality changes may alter peat decomposition rates, potentially shifting peatlands from a net C sink to a source (McLaughlin 2004). In contrast, other studies point to warm and dry peat enhancing CO₂ sequestration because photosynthesis may increase more rapidly than CO₂ loss from microbial decomposition of peat (Frolking et al. 2010), or no net changes in CO₂ sequestration may occur (Limpens et al. 2008). Therefore, in this section, we discuss the influence of permafrost and its thawing on C pools and fluxes and potential effects of climate change on C dynamics in permafrost peatlands.

Carbon accumulation and storage

Peat is composed of the remains of plant material deposited by vegetation growing on the surface of a peatland. As peat accumulation occurs, it becomes the growing medium for vegetation. The surface peat layer is aerobic and subject to decomposition (Figure 5.1), but as new material is added deeper peat becomes submerged below the water table where decomposition occurs more slowly (Tarnocai and Stolbovoy 2006). Storage of peat C is the result of long-term organic matter accumulation and thus represents higher rates of net plant photosynthesis relative to soil respiration.

Peat C accumulation rates in northern peatlands are spatially and temporally variable, ranging from weak C sources and sinks (<10 g C m⁻² yr⁻¹) to strong C sinks (>50 g C m⁻² yr⁻¹) (Table 5.1). For example, although data specific to the HBL are sparse, rates appear to be lower (-0.58 to 20 g C m⁻² yr⁻¹; Rouse 2002, Ali 2008) than those

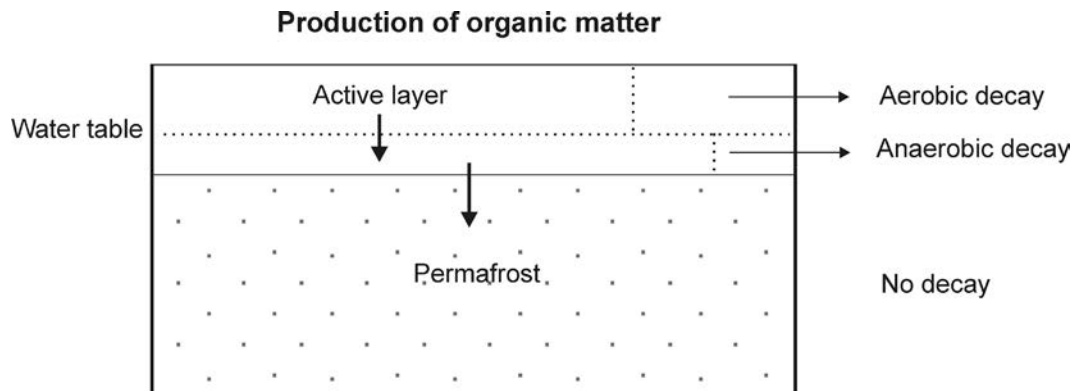


Figure 5.1. Schematic diagram of accumulation and decay of organic matter in peatlands (adapted from McLaughlin 2004).

reported for peatlands occurring in permafrost landscapes in western Canada (56 to 141 g C m⁻² yr⁻¹) but comparable to rates reported for the North American sub-arctic and West Siberian Lowlands (1.2 to 98 g C m⁻² yr⁻¹). Regional gradients in climate partially explain variability in accumulation rates. In Russia's West Siberia Lowlands, peat accumulation over the last 2,000 years is lower in the north (3.5 to 17.5 g C m⁻² yr⁻¹) than in the south (21 to 44 g C m⁻² yr⁻¹), with maximum CO₂ accumulation occurring where temperatures average between -1 and 0 °C (Beilman et al. 2009).

Table 5.1. Carbon accumulation rates for selected peatland and permafrost features.

Category	Peatland or permafrost feature	Location	Accumulation rate (g C m ⁻² yr ⁻¹)	Comments	Reference
Fen	Fen	Manitoba	-0.56	50 years	Rouse et al. 2002
	Minerotrophic peatland	Quebec	0.2 to 20		Ali et al. 2008
	Rich fen	Alberta	82	Over last 25 years	Vitt et al. 2009
Bog	Bog hummock	Northwest Territories	19.3	1200 years	Robinson and Moore 2000
	Bog hollow	Northwest Territories	22.9	1200 years	Robinson and Moore 2000
	23 bogs	Eastern Canada	77 to 178		Turunen et al. 2004
	Unfrozen bog	Western Canada	127		Turetsky et al. 2007
	Aapa mire	Siberia	84	Eddy covariance over 3 years	Schulze et al. 2002
	Bog	Alaska	114	Production over 90 days of growing season	Luken and Billings 1986
Permafrost	Six permafrost plateau sites	Manitoba	57	Surface	Camill 1999b
	Immature peat plateau	Northwest Territories	14 to 18	1200 years	Robinson and Moore 2000
	Mature peat plateau	Northwest Territories	11 to 12	1200 years	Robinson and Moore 2000
	Permafrost features	Quebec	63		Ali et al. 2008
	Peat plateau	Alaska	45	Production over 90 days of growing season	Luken and Billings 1986
Thermokarst	Peat plateau	Northwest Territories	13		Robinson and Moore 2000
	Collapse bog	Northwest Territories	13 to 14	1200 years	Robinson and Moore 2000
	Collapse fen	Northwest Territories	25	250 years,	Robinson and Moore 2000
	Collapsed scar	Manitoba	142		Camill 1999b
	Internal lawns	Quebec	131		Ali et al. 2008
	Collapsed fen	Alaska	142	Production over 90 days of growing season	Luken and Billings 1986
Other/ Compiled		Subarctic Canada	9	Since initiation	Tarnocai 1998
		Yukon	11	Since initiation	Ovenden 1990
		Arctic Alaska	1.2 to 41	Since initiation	Marion and Oechel 1993, Schell and Ziemann 1983
		North America and Eurasia	29	Long-term accumulation	Gorham 1991
			23	Recent	
		Northwest Territories	14	Since initiation	Vardy et al. 2000
			6.8	Average for late Holocene	
		Siberia	17	Last 2000 years	Beilman et al. 2009
			17	Since initiation	
		98.3	Recent		

Accumulation also varies locally due to differences among peatland and permafrost features (Table 5.1). This heterogeneity is due to variation in photosynthesis and respiration rates among features, with the highest accumulation in thaw features, moderate accumulation in non-permafrost bogs and fens, and lowest accumulation in palsas and peat plateaus with shallow active layers (Figure 5.2). For example, Robinson and Moore (2000) reported a 50% reduction in CO_2 accumulation and a 65% reduction in vertical peat accumulation when an unfrozen bog developed into a forested peat plateau. Slower accumulation rates in permafrost features are primarily due to slow vegetation growth and low organic matter inputs. Spruce canopies, which are associated with permafrost features, block radiation (Q^*) from reaching the ground surface, and thus more of the photosynthate is allocated to aboveground biomass (Wickland et al. 2006). Drier conditions in surface peat of palsas and peat plateaus (caused by peat accumulation and its uplift by ice above the local or regional water table; see section 3, Permafrost Patterns) can also stimulate soil respiration more than photosynthesis, limiting C accumulation (Turetsky et al. 2007). However, cooler temperatures moderate respiration increases (Price and Sowers 2004, Wickland et al. 2006) and even with drier conditions, C accumulation rates in palsas and peat plateaus are generally lower than those in non-permafrost peatlands (Bäckstrand et al. 2010).

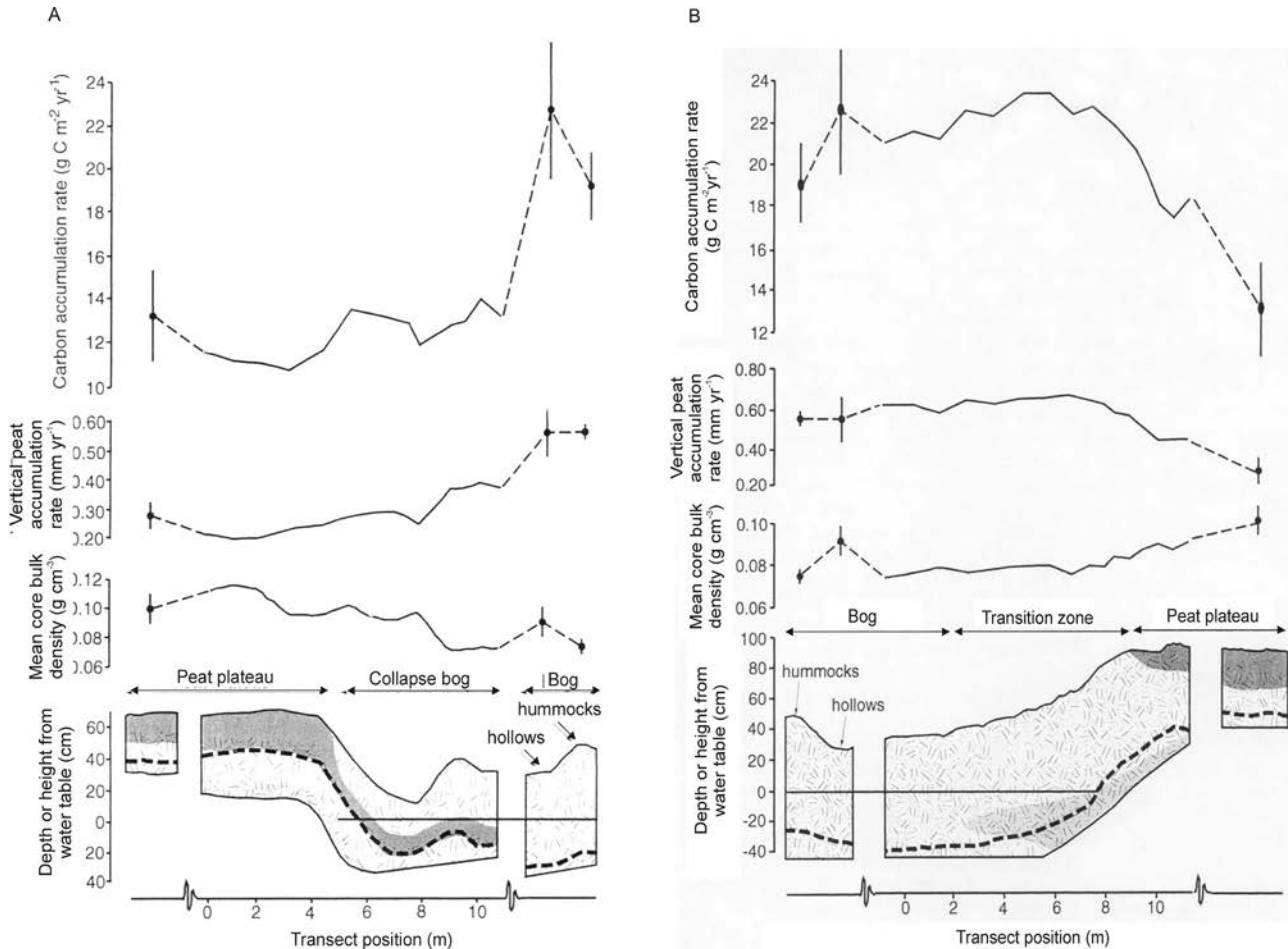


Figure 5.2. Changes in water table depth, mean core bulk density, and vertical peat and carbon accumulation rates measured over the past 1,200 yr along (a) a permafrost degradation transect from frozen peat plateau to unfrozen interior collapse bog and (b) a permafrost aggradation transect from unfrozen bog to frozen peat plateau (from Robinson and Moore 2000; reprinted with permission from Arctic, Antarctic, and Alpine Research). Dashed lines connect the landform end members, each showing the mean and standard deviation of 20 cores. The thick dashed line in the bottom figures marks the position of the White River ash.

The character of permafrost C may also affect decomposition, but evidence is conflicting as to whether permafrost C is of poor or good quality for microbial decomposition. For example, permafrost peat may be of low quality due to the higher proportion of lignin-rich sylvic (tree-derived) peat, leading to substrate limitations to decomposition (Wagner et al. 2005) or microorganisms may have decomposed peat prior to its incorporation into permafrost, with predominately recalcitrant C contained in ice (Turetsky et al. 2007). However some permafrost contains highly labile C, such as the windblown dust termed yedoma found in the East Siberian permafrost that deposited during the glacial age (Khvorostyanov et al. 2008). Carbon accumulation in permafrost features is further inhibited by increased fire frequencies on dry surfaces over longer timeframes (Zoltai et al. 1998, Vitt et al. 2000a).

Although accumulation rates in permafrost features are low, continued accumulation over long periods has resulted in storage of large amounts of C. Long-term C storage is enhanced by cryoturbation. Cryoturbation impedes decomposition by burying organic material in colder and deeper layers while enabling soil to restart C accumulation in topsoil layers (Kaiser et al. 2007). This process is more important where shallow organic layers occur over mineral soils. Bockheim (2007) determined that 55% of the soil organic C density of the active layer and near-surface permafrost in northern Alaskan mineral soils could be attributed to redistribution from cryoturbation.

When permafrost degrades, net C accumulation increases (e.g., Robinson and Moore 2000, Vardy et al. 2000, Turetsky 2004). For example, Robinson and Moore (2000) found that the transition from peat plateau to collapse bog through internal permafrost degradation resulted in a 72 and 200% increase in C and vertical peat accumulation rates, primarily due to increases in moss growth. Given that internal thaw can proceed at rates of 0.12 to 0.25 m yr⁻¹ and marginal thaw at even faster rates of 1.5 m yr⁻¹ (Camill et al. 2001), these transitions can increase the rate of CO₂ sequestration. The influence of the permafrost thaw on decomposition is unclear. Although saturated conditions typically lead to lower decomposition rates (Trettin et al. 1996), peat incubated from internal lawns produced more CO₂ than that from bogs or permafrost mounds due to more labile peat C occurring in lawns after thaw (Turetsky 2004).

Peat accumulation declines as fens succeed to bogs, which is attributed to enhanced decomposition in dry bogs relative to fens (see sections 2, Peatland Development and Plant Associations and 4, Peatland Hydrology). Theories of peat accumulation (e.g., Clymo 1984, Belyea and Baird 2006) suggest an eventual cessation of C accumulation because decomposition eventually equals the rate of fixation. However, this may not always be the case as variations in hydrology and its interaction with vegetation composition control C accumulation (Yu 2006; Vitt et al. 2009). For example, *S. fuscum* has lower C content (Trumbore and Harden 1997, Beilman et al. 2009) and *S. riparium* has lower bulk density compared to the true mosses found in fens, which can inhibit C accumulation rates where *Sphagnum* occurs (Vitt et al. 2009).

Net ecosystem exchange

General patterns

Net ecosystem exchange (NEE) is the net flux of CO₂ to the atmosphere and thus is the difference between the CO₂ released from ecosystem respiration (ER), which includes heterotrophic (i.e., organic matter decomposition) and root respiration (Moore et al. 1998), and C acquisition through gross ecosystem photosynthesis (GEP). Net ecosystem exchange is measured by the respiration and photosynthesis components using (1) ground-based chamber methods or (2) eddy covariance techniques. Permafrost peatlands vary from weak sinks (GEP > ER) to sources (GEP < ER) of CO₂ (Table 5.2), with most peatlands representing small sinks in the range of 20 to 60 g C m⁻² yr⁻¹ (Roulet et al. 2007). Variability in NEE across peatland types is due to spatial heterogeneity in plant photosynthesis and decomposition rates among peatland communities and the spatial and temporal differences in environmental conditions controlling these processes.

Table 5.2. Photosynthesis, respiration, and net ecosystem carbon dioxide exchange in selected peatlands and permafrost features in northern regions.

Category	Location	Peatland or permafrost feature	Photo-synthesis	Respiration	Net ecosystem exchange	Units	Comments	Reference	
Annual or seasonal									
<i>Fen</i>	Saskatchewan	Fen			-366		1994 (136 days)	Suyker et al. 1997	
		Sub-arctic fen			+30		1993 (27 days)	Burton et al. 1996	
					+76		1994 (75 days)	Schreader et al. 1998	
	Manitoba					-235		1996 (75 days)	Griffis et al. 2000
						-49		1997 (75 days)	
						-229		1998 (75 days)	
						-34		1999 (72 days)	
	Ontario	Coastal fen				-23		Mid-June to early October	Klinger et al. 1994
		Interior fen				77		Mid-June to early October	
	Manitoba	Rich fen				31	g CO ₂ -C m ² season ⁻¹	1994	Joiner et al. 1999
						(40)		(124 days)	
	Manitoba	Rich fen				-92		1996	Lafleur et al. 1997
						(-120)	(124 days)		
	Finland	<i>Eriophorum</i> lawns				160		Integrated over growing season late May to late October 1993	Alm et al. 1999
					108				
					115				
					154				
Greenland	High arctic fen	158	61	96		45 days 181(end June) to 235 (mid August) in 1996	Søegaard and Nordstrøm 1999		
Alberta	Moderately rich fen	713	569	-144		Annual 2004 integrated	Syed et al. 2006		
Greenland	High arctic fen	167	103	64		g CO ₂ -C m ² y ⁻¹			
Finland	Subarctic fen				-22		Mean (range) over 6 years of 1997 to 2002	Aurela et al. 2004	
					(-4 to -53)				
<i>Bog</i>	Ontario	Bog			-56		1990 (33 days)	Neumann et al. 1994	
	Ontario	Bog			34	g CO ₂ -C m ² season ⁻¹	Mid-June to early October	Klinger et al. 1994	
	Manitoba	Bog, rich fen, intermediate fen and poor fen with palsa			13 to 65			Bubier et al. 1998	
	Siberia	Permafrost-dominated bog				-396		Annual	Friborg et al. 2003
	Siberia	Aapa mire				-0.043 to -0.062	g CO ₂ -C m ² y ⁻¹	Eddy covariance	Schulze et al. 2002
	Siberia	Bog				-396			Friborg et al. 2003

Table 5.2. Cont.

Category	Location	Peatland or permafrost feature	Photo-synthesis	Respiration	Net ecosystem exchange	Units	Comments	Reference	
<i>Permafrost</i>	Alaska	Black spruce lowland- peat plateau	-119 to -199	304 to 558	315	g CO ₂ -C m ⁻² season ⁻¹		Wickland et al. 2006	
	Finland	Palsa	-174	121	-53			Nykanen et al. 2003	
	Siberia	Continuous permafrost	-168	149	-19			Nakai et al. 2008	
					-76 to -78				
<i>Thermokarst</i>	Alaska	Thermokarst edge	-130 to -228	205 to 611	193	g CO ₂ -C m ⁻² y ⁻¹		Wickland et al. 2006	
	Alaska	Thermokarst wetland	-184 to -334	231 to 612	166				
	Finland	Subarctic palsa mire	-162	80	-81			Nykanen et al. 2003	
	Finland	Subarctic palsa mire	-142	71	-71				
	Finland	Wet palsa margin	-230	136	-94				
			-212	131	-81				
			-255	101	-153				
			-193	132	-62				
<i>Tundra</i>	Alaska	Tussock tundra			53 to 286	g CO ₂ -C m ⁻² y ⁻¹		Oechel et al. 1995	
	Alaska	Wet sedge tundra			-18			Vourlitis and Oechel 1997	
					-28				
	Alaska	Moist tundra			-66				
					-48				
	Alaska	Wet sedge tundra			-101				
	Alaska	Set tundra			-69			Coyne and Kelley 1975	
	Alaska	Mixed tundra			9			Fan et al. 1992	
	Alaska	Wet sedge tundra			-70		g CO ₂ -C m ⁻² season ⁻¹		
					-46				
				-52					
				-61					
				-49					
	Alaska	Moist tussock tundra			31			Kwon et al. 2006	
					61				
					-2				
					3				
					-1				
Daily (g CO ₂ -C m ⁻² d ⁻¹)									
<i>Fen</i>	Finland	Aapa mire flarks	131	-85	52				
	Finland	Aapa mire lawn	276	-186	92				
	Finland	Aapa mire strings without birch	130	-157	-27			Heikkinen et al. 2002	
	Finland	Aapa mire strings with birch	409	-334	74				

Table 5.2. Cont.

Category	Location	Peatland or permafrost feature	Photo-synthesis	Respiration	Net ecosystem exchange	Units	Comments	Reference
<i>Bog</i>	Sweden	Subarctic wetland (ombrotrophic and minerotrophic sections) - <i>Carex rotundata</i>	-6	9.	3			Ström and Christensen 2007
	Sweden	<i>Eriophorum vaginatum</i>	-20	15	-5			
	Sweden	<i>Eriophorum angustifolium</i>	-20	13	-7			
	Alberta	Moderately rich fen				-10		Syed et al. 2006
	Ontario	Open shrub bog				-2		Neumann et al. 1994
	Russia	Boreal bog	0 to 3	1 to 2	0 to -1			Arneeth et al. 2002
			0 to 3	0 to 2	0 to -1			
	Siberia	Bog			-0			Friborg et al. 2003
					-7			
					1			
					1			
<i>Permafrost</i>	Siberia	Continuous permafrost				-2		Nakai et al. 2008
	Alaska	Black spruce lowland- peat plateau	-2	3	1			Wickland et al. 2006
	Manitoba	Bog to rich fen				1 to 3		Bellisario et al. 1999
<i>Thermokarst</i>		Thermokarst edge	-3	3	-0			Wickland et al. 2006
	Alaska	Thermokarst wetland	-4	3	-1			
		Permafrost collapse				-1		Meyers-Smith et al. 2007
<i>Tundra</i>		Moist tundra				-0		Vourlitis and Oechel 1997
						-0		
						-0		
		Wet sedge tundra				0 to 1		
		Tussock tundra				1 to 4		
	Alaska	Wet sedge tundra	-5	2	-8			Kwon et al. 2006
			-3	1	-4			
			-3	1	-4			
			-4	1	-5			
			-4	2	-6			
		Moist tussock tundra	-2	2	-4			
			-3	3	-7			
			-1	1	-2			
			-1	1	-2			
			-1	1	-3			

Carbon dioxide is absorbed from the atmosphere through photosynthesis and photosynthetic rates vary by vegetation composition, where mosses have lower photosynthetic capacity than vascular plants (Glenn et al. 2006). For example, palsa surfaces with shrub vegetation were sinks of $202 \text{ g C m}^{-2} \text{ summer}^{-1}$, whereas palsa surfaces with sparse vegetation lost $25.3 \text{ g C m}^{-2} \text{ summer}^{-1}$ to the atmosphere (Nykänen et al. 2003). Vascular and non-vascular plants are also differentially affected by moisture conditions (see section 2, Peatland Development and Plant Associations). For example, dry conditions favour increased shrub expansion and growth, although extreme drought may lead to physiological stress and subsequent slower growth rates. In contrast, sedges and bryophytes are more productive under wetter conditions (Weltzen et al. 2000). Ground vegetation growth is also affected by the presence of tree or shrub canopies, which diminish the amount of light reaching the ground. For example, groundcover photosynthesis was greater in thermokarst wetlands than at a thermokarst edge or a peat plateau partially shaded by an overstory (Wickland et al. 2006).

Carbon dioxide is released to the atmosphere through plant (leaf, stem, and root) and soil microbial respiration, which offsets C gains from photosynthesis. In boreal continental bogs an estimated 35 to 57% of total CO_2 efflux from the peat surface was from rhizosphere processes (i.e., root and associated microbes), about half of which is mineralized root exudates (Crow and Wieder 2005). Vascular plants, such as sedges, have greater biomass underground as well as higher lability of tissue compared to non-vascular plants, resulting in faster respiration where they occur (Glenn et al. 2006). Heterotrophic respiration by microbes is affected by the quality of organic matter inputs and the physical environment. Temperature modifies decomposition rates, with warmer temperatures accelerating reaction rates (Hobbie et al. 2000, Laiho 2006). Moisture conditions also affect decomposition (Christensen et al. 1998), with drier peat providing aerated conditions. The thickening of the aerobic zone enhances activity of phenol oxidase, the enzyme responsible for degrading phenolic compounds (Freeman et al. 2001). These contribute to faster respiration and enhanced CO_2 efflux to the atmosphere.

Combining the interactive controls of vegetation composition and environmental condition, maximum CO_2 uptake is generally higher in bogs than fens. In the HBL, Whitney (1994) found maximum CO_2 uptake in bogs to be $2.5 \text{ g CO}_2\text{-C g m}^{-2} \text{ d}^{-1}$ (mean of $1.7 \text{ g CO}_2\text{-C g m}^{-2} \text{ d}^{-1}$; Neumann et al. 1994) compared with interior fens at only $0.5 \text{ g CO}_2\text{-C g m}^{-2} \text{ d}^{-1}$. However, when comparing NEE from seven different bogs and fens in continental wetlands, Humphreys et al. (2006) found less variability among peatland types, with an average net sink of $1.5 \text{ g C m}^{-2} \text{ d}^{-1}$ for all peatlands (Figure 5.3). Higher C uptake rates in bogs are offset by higher respiration rates. Bubier et al. (1998) found that mid-season (July and August) NEE was lowest in a bog (5.6 to $-4.0 \text{ g CO}_2\text{-C m}^{-2} \text{ d}^{-1}$), moderate in poor and intermediate fens (6.5 to $-6.7 \text{ g CO}_2\text{-C m}^{-2} \text{ d}^{-1}$), and highest in a rich fen (10.9 to $-8.1 \text{ g CO}_2\text{-C m}^{-2} \text{ d}^{-1}$). However, this sequence changed in the spring and fall when ericaceous shrub and sedge communities occurring in the bog and in poor and intermediate fens had higher maximum CO_2 fixation than deciduous shrub-dominated (e.g., *Salix* and *Betula*) rich fens (Bubier et al. 1998).

Spatial and temporal patterns

Seasonally, NEE is influenced by the timing of snowmelt and spring hydroclimate conditions (Figure 5.4; Griffis and Rouse 2001). Frolking et al. (1996) determined that the timing of spring thaw was one of the most important factors explaining interannual variability in C balances of bogs and fens. Moreover, warm surface temperatures and wet soil conditions in the early growing season increase plant growth, which sustains C acquisition in sub-arctic sedge fens throughout the summer (Griffis and Rouse 2001). Bubier et al. (1999) showed that sedge-dominated poor fens were stronger sinks than rich fens with deciduous vegetation or ericaceous shrub bogs because of their higher photosynthesis rates relative to respiration. Also, plant species in a poor fen are strong C sinks (a sink for 4 of 6 months) because their vegetation is active earlier and later in the year than that in rich fens (a sink for 2 of 6 months) (Glenn et al. 2006). Plants in rich fens may have high photosynthetic capacity in the summer, but they have a shorter growing season compared to *Sphagnum* mosses, ericaceous plants, and trees in bogs (Bubier et al. 1998). Conditions during the fall are also important as soil respiration continues after declines in plant photosynthesis occur (Goulden et al. 1998). For example, drier peatlands can be sinks early in the growing season but become sources later, particularly in warm and dry years due to disproportionate increases in respiration during fall (Moore et al. 2002).

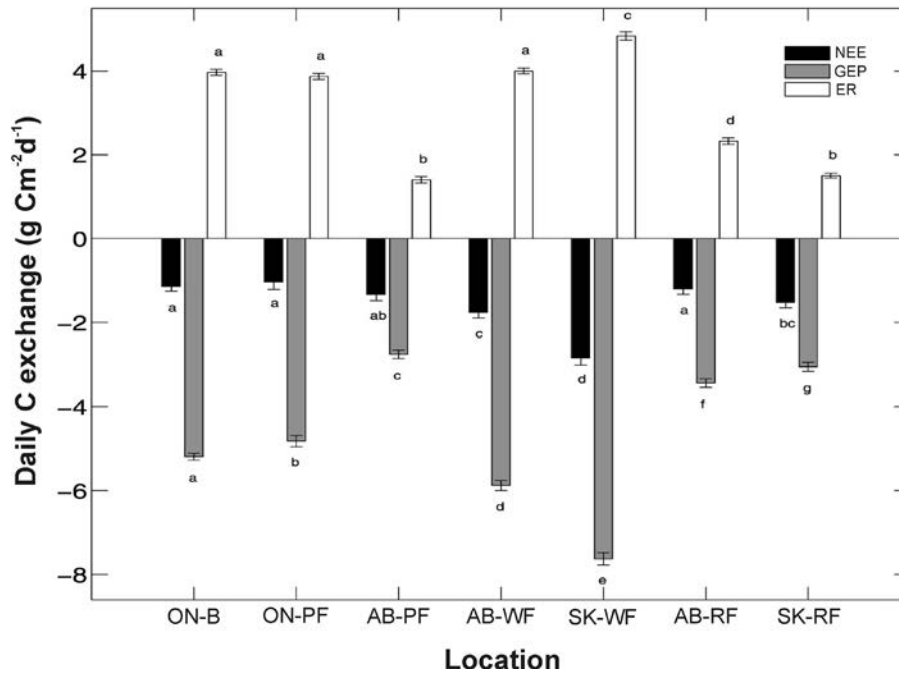


Figure 5.3. Average daily net ecosystem exchange of CO₂ (NEE), gross ecosystem production (GEP), and ecosystem respiration (ER). Error bars are ±95% confidence intervals. Like-shaded bars with different letters differ significantly ($p < 0.05$); ON = Ontario, AB = Alberta, SK = Saskatchewan, B = bog, PF = poor fen, WF = wooded intermediate fen, RF = rich fen (from Humphreys et al. 2006; reprinted with permission from John Wiley and Sons.).

Wintertime ecosystem CO₂ losses via respiration typically range from 15 to 50% of total annual respiration in the CPZ and DPZ and therefore can significantly offset summer net C gains (Grogan and Jonasson 2006). Snow depth exerts a strong influence on soil temperature and respiration rates. For example, Larsen et al. (2007) reported increases in snow depth of 20 to 30 cm during late winter increased respiration by 77 to 157%. Snow accumulation can interact with vegetation, where, in the CPZ tall vegetation enhances snow accumulation, contributing to effective thermal insulation from severe air temperatures, thereby enhancing respiration rates below tree and shrub vegetation (Grogan and Jonasson 2006).

Net ecosystem exchange also varies among years as a function of climate. Aurela et al.'s (2004) studies of a subarctic fen suggest that interannual differences in NEE are related to variation in snow-free period fluxes, even though the winter flux of CO₂ is a significant part of the annual balance (Roulet et al. 2007). However, it is unclear whether variability in growing season photosynthesis or respiration are more important in controlling interannual NEE. Griffis et al. (2000) showed that, over a six-year period, a fen in the HBL near Churchill, Manitoba, ranged from a sink of 299 g C m⁻² season⁻¹ to a source of 76 g C m⁻² season⁻¹. The increased sink strength in drier years was attributed to slower respiration relative to photosynthesis early in the growing season. However, Alm et al. (1999) reported that a bog switched from a sink to a source when respiration increased following drought. A smaller range in seasonal NEE (31 g C m⁻² season⁻¹ source to 92 g C m⁻² season⁻¹ sink) occurred in a fen near Thompson, Manitoba between 1994 and 1996 (Joiner et al. 1999). Joiner et al. (1999) speculated that warmer and drier conditions in spring and fall of 1994 contributed to heterotrophic CO₂ production at times when the vascular vegetation was not photosynthesizing. At the Mer Bleue bog complex in Ontario (a temperate bog site), drought stimulated peat respiration rates, but had varying effects on photosynthesis, whereas photosynthesis at sedge sites declined (showing signs of early senescence) over the growing season (Bubier et al. 2002). However, photosynthesis of ericaceous shrub-dominated bogs was not affected until the end of summer.

The above studies indicate that differences in NEE between wet and dry years can be attributed primarily to increases in soil respiration relative to photosynthesis. Exceptions to this occur in peatlands where soil moisture

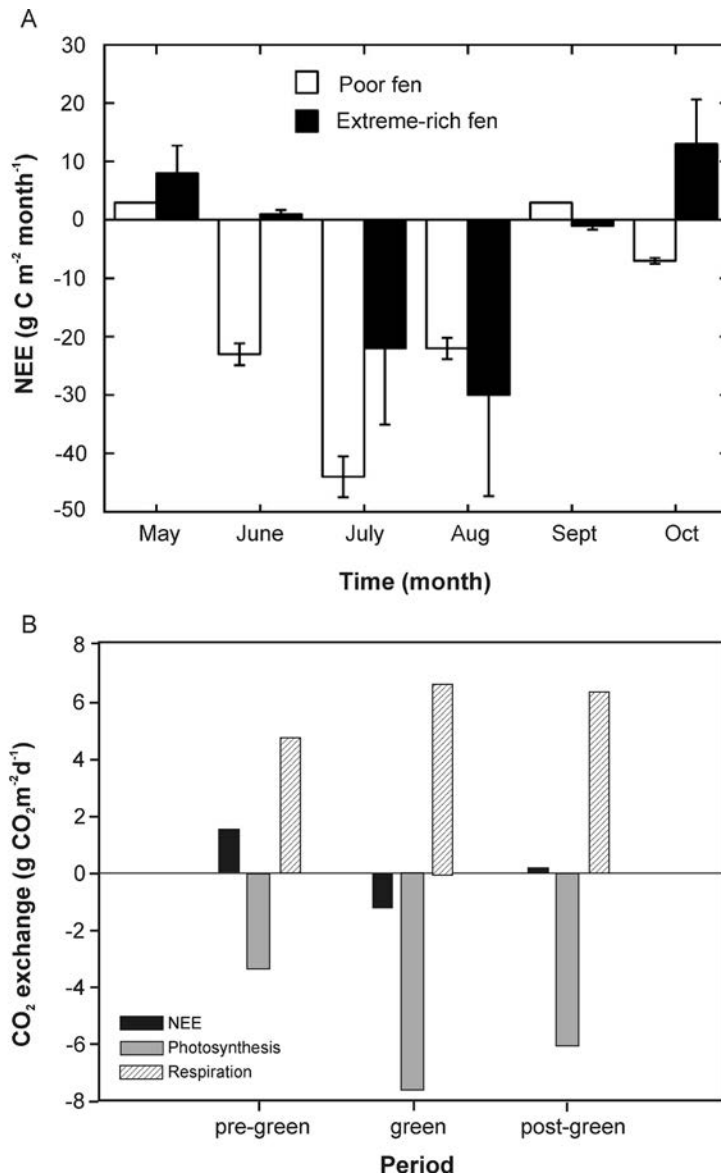


Figure 5.4. Comparison of monthly carbon ($\text{CO}_2\text{-C}$) budgets for two contrasting peatlands in northern Alberta during 2004: (a) Cumulative net CO_2 exchange for the poor fen (solid bars) and the extreme-rich fen (open bars) (from Glenn et al. 2000); and (b) mean landscape respiration, photosynthesis, and net ecosystem exchange (NEE) by phenological study period (from Griffis et al. 2000; reprinted with permission from John Wiley and Sons).

limits plant growth. For example, during a dry year, collapse scars and surrounding burned areas in interior Alaska were net sinks for CO_2 (mean daytime NEE of $-1.5 \text{ g CO}_2\text{-C m}^{-2} \text{ s}^{-1}$), with temperature reported as the dominant factor affecting CO_2 exchange (Myers-Smith et al. 2007). In a wet year, lower NEE resulted from decreased photosynthesis, which reduced CO_2 sequestration (Nykanen et al. 2003). These studies indicate that temperature is the dominant driver of peatland C sink strength. Therefore, generalizations of climate change effects of peatland NEE in permafrost regions are difficult and more studies are needed that document climate change effects on peatland NEE in permafrost regions.

Methane

In addition to CO_2 fluxes, permafrost peatlands can be sources of CH_4 , which is a more potent GHG than CO_2 in terms of radiative forcing on the atmosphere (Friborg et al. 2003). Methane transfer from the soil to the atmosphere can occur slowly by diffusion through saturated peat, or more quickly by transport through the aerenchyma of aquatic plants (ebullition) or episodic release in bubbles (ebullition) (LeMer and Roger 2001). Methane production primarily occurs through two different pathways: *acetoclastic*—fermentation of acetate by bacteria in organic matter—and CO_2 reduction.

Carbon dioxide reduction uses H_2 as the electron donor to reduce CO_2 to CH_4 . The dominant pathway in CH_4 production is debatable (McLaughlin 2004, Hornibrook and Bowes 2007) (and can vary with peatland type and depth) but CO_2 reduction appears to dominate CH_4 production in northern *Sphagnum*-dominated bogs (e.g., McLaughlin 2004). Limited acetate fermentation and acetate accumulation in bogs suggests their terminal C mineralization may differ from that in fens (Hines et al. 2001, Duddlestone et al. 2002). Acetoclastic (acetate fermentation) methanogenesis may be limited in bogs because of impeded dissociation of acetic acid at low pH (e.g., Fukuzaki et al. 1990, Lansdown et al. 1992). Equally plausible is that acidophilic (i.e., acid tolerant acetoclastic) methanogens are absent from bogs, as indicated by declines in methanogen diversity with decreasing pH of bogs (pH = 3.5 to 4.5) relative to fens (pH = 4.5 to 7.0) (Juottonen et al. 2005).

Acetate fermentation is more important in fens than bogs because sedges provide a labile energy source in terms of root exudates and higher pH values in surface peat (Bellisario et al. 1999). In permafrost features, CO_2 reduction appears to be the dominant methanogenic pathway of collapsed scars dominated by *Sphagnum*. In contrast, acetate fermentation dominates in saturated areas near moats (ponded meltwater from palsas/peat plateaus), where sedges are the most common plant species (Prater et al. 2007). Peat decomposed following thawing does not appear to stimulate acetate fermentation because fresh organic matter is required for acetogenesis (e.g., McLaughlin 2004). However, thawing provides conditions enhancing sedge colonization of moats and stimulates methanogenesis (Turetsky 2004, Yavitt and Seidmann-Zager 2006, Prater et al. 2007). Methane in deep peat can also be depleted in ^{13}C , suggesting that acetoclastic methanogenesis is more important in the upper peat layers where fresh substrates are available and CO_2 reduction dominates at greater depths (Hornibrook et al. 1997). Since CH_4 is produced under wet and anaerobic (strongly reducing) conditions, water table position is a dominant control on CH_4 emissions. Methane produced in peat anaerobic zones can be oxidized to CO_2 by methanotrophs in overlying aerobic zones. For example, 60 to 90% of CH_4 produced in anaerobic peat layers can be reoxidized to CO_2 during dry conditions when it enters overlying aerobic zones (Le Mer and Roger 2001).

Given that water table levels and vegetation play important interactive roles in CH_4 production and emission, wet permafrost thaw features, particularly those vegetated with sedges, are stronger CH_4 sources than bogs or dry permafrost features (Klinger et al. 1994, Bubier et al. 1995, Wickland et al. 2006) (Table 5.3, Figure 5.5). For example, the magnitude of CH_4 flux was low in a dry palsa site ($2.2 \text{ mg C m}^{-2} \text{ d}^{-1}$), moderate in a permafrost thaw feature with *Sphagnum* ($28 \text{ mg C m}^{-2} \text{ d}^{-1}$), and high in a wet sedge fen ($122 \text{ mg C m}^{-2} \text{ d}^{-1}$) in Sweden (Bäckstrand et al. 2008). Similarly, seasonal average CH_4 emissions from treed peatlands and palsas (0 to $20 \text{ mg CH}_4 \text{ m}^{-2} \text{ d}^{-1}$) were lower than that from open sedge bogs and fens, as well as permafrost collapse scars (92 to $320 \text{ mg CH}_4 \text{ m}^{-2} \text{ d}^{-1}$) (Bubier et al. 1995). Heikkinen et al. (2002) reported similar trends in Finland, with high CH_4 emissions from wet fens, moderate emission from moist lawns, and lowest emissions from dry hummocks.

Annual CH_4 emission ranges from a sink of 0.2 to a source of $60 \text{ g CH}_4 \text{ m}^{-2} \text{ season}^{-1}$ (Table 5.3). However, the HBL has much lower rates of CH_4 emission than those in other regions of North America and 1.31 and $2.79 \text{ g CH}_4\text{-C m}^{-2} \text{ yr}^{-1}$ were reportedly emitted from the southern and northern regions of the HBL, respectively (Roulet et al. 1994). Moreover, fens did not follow the typical pattern of high CH_4 emissions in the HBL witnessed elsewhere. McLaughlin (2004) reported that peatlands in Ontario emitted CH_4 at one of the lowest rates across northern regions. A combination of factors may cause this difference, including cold temperatures and high CH_4 oxidation rates in the surface layers, limiting its efflux (Klinger et al. 1994, Moore et al. 1994, Roulet et al. 1994), higher acidity (Valentine et al. 1994), and lower peat quality, limiting organic matter fermentation (Yavitt et al. 2000, Kuder and Krueger 2001).

Table 5.3. Seasonal, annual, and daily methane emission rates in selected peatland and permafrost features in northern regions.

Category	Location	Peatland or permafrost feature	CH ₄ flux	Units	Comments	Reference
Annual or seasonal						
<i>Bog</i>		Bog moat	50 to 60			
	Alberta	Intermediate between bog moat and mid-bog	38 to 40	g CH ₄ m ⁻² y ⁻¹	Range 2002 and 2003	Prater et al. 2007
		Mid-bog	18 to 20			
	Manitoba	Open	2.8		Mean 1990	Roulet et al. 1994
	Ontario	Open	1.3			
	Ontario		1.5 to 3.9	g CH ₄ m ⁻² season ⁻¹	June 22 to July 25, 1990	Klinger et al. 1994
<i>Fen</i>	Alberta	Open	26 to 55	g CH ₄ -C m ⁻² y ⁻¹	Annual integration for 1994, 1995, 1996	Whiting et al. 2001
		Wet surface	9.3 to 20			
		Palsa margin	15 to 25		Mean 1998 and 1999	Nykänen et al. 2003
	Finland	Rich fen	10 to 32	g CH ₄ m ⁻² season ⁻¹	June to September integrated for 1994 and 1995	Huttunen et al. 2003
		Intermediate fen	12 to 40			
		Poor fen	1 to 21			
	Sweden	Lawn	4.7		Seasonal integration May to September 1992 and 1993	Waddington and Roulet 2000
		Pool	9.2 to 10			
		Ridge	0.1			
	Greenland	Whole fen	3.7		Integrated June 1 to August 31 1997	Friberg et al. 2000
Permafrost features						
	Russia	Peat plateau	-0.2 to 0.4	g CH ₄ m ⁻² season ⁻¹	Mean June to mid September 2001 (100 days)	Heikkinen et al. 2004
		Dry	0.5			
		Wet peaty land	2.6 to 14			
		Thermokarst lake	2.4			
	Finland	Palsa	1.0 to 1.1	g CH ₄ m ⁻² y ⁻¹	Mean 1998 and 1999	Nykänen et al. 2003
Daily (mg CH ₄ -C m ⁻² d ⁻¹)						
<i>Bog</i>	Manitoba	Treed	0.2		Mean 1990	Roulet et al. 1994
		Treed	1.8			
		Open	53			
	Ontario	Pool	110		Mean June 22 to July 25, 1990	Klinger et al. 1994
		Open	47			
	Western Canada	Forested	2.4 to 273		Mean June to October 1999 to 2001	Turetsky et al. 2007
		Bog	4.8			
	Finland	Bog	5.0		Mean July and August 1988	Alm et al. 1999
	Sweden	Semi-wet	2.9 to 67		Based on compilation of published numbers for the mire	Christensen et al. 2004
		Wet	24 to 180			
Permafrost features						
	Alaska	Moat	14		Mean daytime growing season flux 2004 (unusually dry)	Myers-Smith et al. 2007

Table 5.3. *Con't.*

Category	Location	Peatland or permafrost feature	CH ₄ flux	Units	Comments	Reference
	Western Canada	Frost mound	0		Mean June to October 1999 to 2001	Turetsky et al. 2007
		Internal lawn	18			
	Saskatchewan	Frost mound	<0.1		Mean August to October 1998 and July to October 1999	Turetsky et al. 2002
	Sweden	Palsa	<0.1		Mean 2003 to 2006 (DOY ^a 173 to 235)	Bäckstrand et al. 2010
		Palsa	2.2			
		Thermokarst pond	110 to 170		Mean of August 2006	Blodau et al. 2008
	Siberia	Polygon depression	0 to 120		Range from May to September 1999, August 2000	Wagner et al. 2005
		Permafrost wetland	46		Mean for summer of 1993 and 1995	Nakano et al. 2000
<i>Fens</i>		Treed fen	2.5			
		Open fen	7.9		Mean 1990	Roulet et al. 1994
		Pool	163			
	Ontario	Coastal fen	17 to 64			
		Coastal marsh	7.5 to 101		Mean June 22 to July 25, 1990	Klinger et al. 1994
		Interior fen	-3.2 to 31			
		Open	88			
		Wetland pond	110 to 180		Mean June to October 1990	Hamilton et al. 1994
	Québec	Hummock	53		Summer 2003	Pelletier et al. 2007
		Coastal marsh	84			
	Manitoba	Shallow lake	125		Mean 1990	Roulet et al. 1994
		Open	65 to 100			
	Saskatchewan	Internal lawn	<0.1 to 0.3		Mean August to October 1998 and July to October 1999	Turetsky et al. 2002
	Alaska	Sedge tundra	15 to 426		Mean July and August 1988	Bartlett et al. 1992
		Lagg	22		Mean July and August 1988	Alm et al. 1999
		Centre	10			
		Rich fen	81 to 260		June to September integrated for 1994, 1995	Huttunen et al. 2003
		Intermediate fen	99 to 330			
		Poor fen	8.1 to 170			
	Finland	Forested	0.6			
		Lawn	68			
		Flark	78			
		String	6.0		June to mid September 2001 (100 days)	Heikkinen et al. 2002
		Open	68			
		Dry string	6.2			
		Melt feature	28		Mean 2003 to 2006 (DOY 173 to 235)	Bäckstrand et al. 2010
		Wet site	122			
	Sweden	Open	1.2 to 2.8		Mean for summer	Strom and Christensen 2007
		Minerotrophic peatland	77 to 432		Based on compilation of published numbers for the mire	Christensen et al. 2004
		Hummocky fen	17 to 372		Thaw season of 1997	Christensen et al. 2000
	Greenland	Continuous fen	67 to 304		Integrated June 1 to August 31 1997	Friberg et al. 2000
		Whole fen	0 to 120			

^aDOY = day of year.

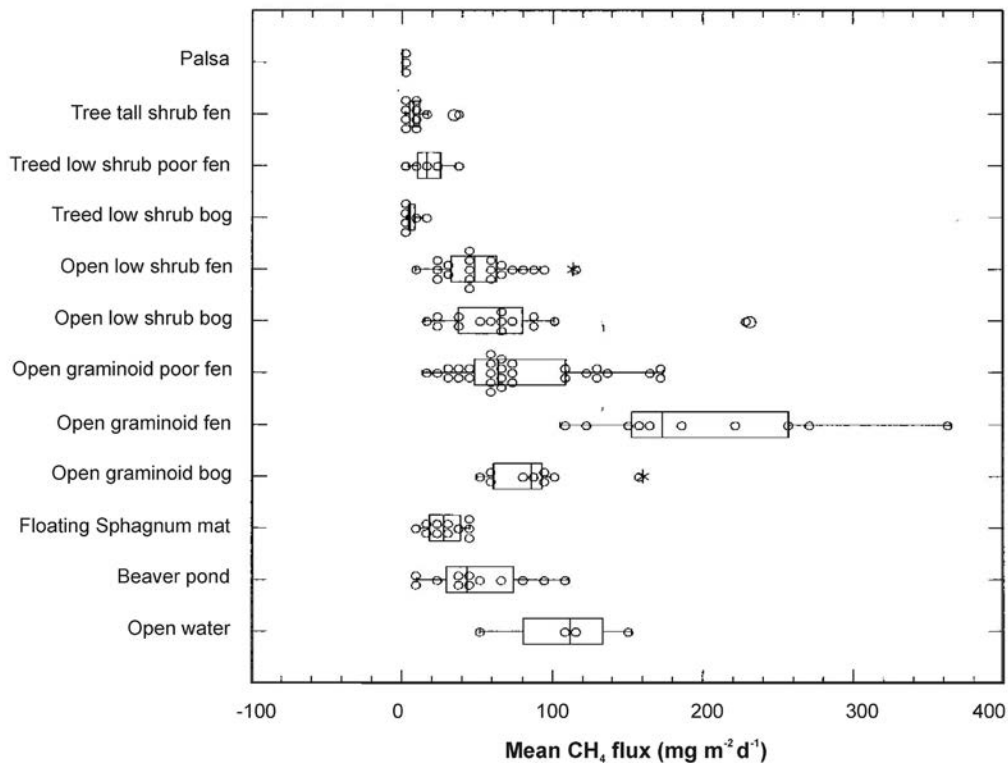


Figure 5.5. Mean methane (CH_4) flux by site classification category (from Bubier et al. 1995; reprinted with permission from John Wiley and Sons). The bars represent quartiles and class means.

Ponds

Ponds form from peat collapsing when permafrost thaws or in topographic depressions (Beilman 2001). They accumulate sediment from internal processes as well as receiving dissolved and particulate matter leached from neighbouring peatlands. Ponds contribute to the landscape C budget by accumulating C in sediments and exchanging GHG, but the amount of gases they produce and consume varies (Martini 2006). Carbon dioxide exchange in ponds in the HBL has been linked to sediment type, where ponds with organic sediments are CO_2 sinks (internal CO_2 production is insufficient to meet photosynthetic demand of algae), whereas ponds with mineral sediments are CO_2 sources (Macrae et al. 2004). Carbon dioxide and CH_4 exchange are also influenced by pond depth (Moore et al. 1994, McEnroe et al. 2009): shallow ponds emitted $0.35 \pm 0.47 \text{ g C m}^{-2} \text{ d}^{-1} \text{ CO}_2\text{-C}$ and $0.31 \pm 0.69 \text{ g C m}^{-2} \text{ d}^{-1} \text{ CH}_4\text{-C}$, both of which are approximately 15 times more than CO_2 or CH_4 emitted from large ponds (McEnroe et al. 2009). These differences may be due to shallow pools supporting faster decomposition of added organic matter to sediments (McEnroe et al. 2009).

Thermokarst ponds are among the strongest CH_4 sources (Blodau et al. 2008). For example, ponds at sites on the HBL had emissions of 0.11 to $0.18 \text{ g CH}_4 \text{ m}^{-2} \text{ d}^{-1}$, which was approximately three times that in the adjacent bogs (Hamilton et al. 1994). Similar patterns of CH_4 emissions from thermokarst ponds have been reported in Alaska (Wickland et al. 2006), Saskatchewan (Turetsky et al. 2002b), and Siberia (Walter et al. 2006). Given enhanced CH_4 emission from thermokarst ponds, they can have a disproportionate influence on landscape-level CH_4 emissions. For example, in the HBL although thermokarst ponds only cover between 8 and 12% of the landscape, they represent about 30% of the total CH_4 emission (Hamilton et al. 1994).

Dissolved carbon and nutrient export

A portion of the peatland C pool is DIC and DOC. Dissolved inorganic C contributes to fen porewater alkalinity, primarily through bicarbonate alkalinity (see section 2, Peatland Development and Plant Associations) and originates from carbonate rock weathering and organic matter decomposition (McLaughlin and Webster 2010). In bogs, alkalinity is primarily the result of organic acids produced from organic matter decomposition because of a

lack of carbonate minerals (Siegel et al. 2006). Dissolved organic C is a chemically complex entity composed of root exudates, microbial byproducts, and organic matter leached from live plants and dead organic matter at various stages of decay (Kalbitz et al. 2000). These contribute to peat porewater acidity through H^+ dissociation from organic acids (Thurman 1985).

Hydrologic export of DIC and DOC (and other dissolved nutrients) is important to aquatic and coastal productivity, C balances, and transport of metals (e.g., aluminum, mercury) (Thurman 1985, Steinberg 2003). At high latitudes, Arctic rivers make up about 10% of the global river water runoff and contain high concentrations of dissolved and particulate organic C, originating from the C rich soils and peatlands (Guo et al. 2004). Dissolved C and nutrients are influenced by hydrologic flows through peatlands. In unfrozen peatlands, surface water flow is generally vertical, resulting in deeper water flowpaths, with longer water residence times (see section 4, Peatland Hydrology).

Where permafrost exists, raised features lead to drier conditions, but ice layers function to confine water infiltration, maintaining shallow water flowpaths. This results in rapid export of DOC and nutrients to streams and lakes (Woo et al. 2008). Drier conditions and shallower flow paths may explain some seemingly conflicting patterns in DOC and nutrient export in permafrost areas. For example, Frey et al. (2007) reported higher concentrations of dissolved organic N, total dissolved N, and total dissolved P in a permafrost-free watershed (increasing as a function of watershed peatland coverage) than in a permafrost-influenced watershed in western Siberia. The dry conditions may have impeded nutrient export. However, in a central Siberian upland, the chemical and isotopic composition of stream DOC was similar to that produced in soils of colder, north-facing slopes with a shallow active layer. However, south-facing slopes with deeper active layers had low DOC export, suggesting that DOC produced in the active layer is retained and stabilized in underlying, unfrozen mineral soils or decomposed by microorganisms in the active layer (Prokushkin et al. 2007).

Raymond et al. (2007) reported enhanced DOC export with increasing discharge (approximately 60% of the annual export occurs during the 2-month period following spring ice breakup) for the five largest Arctic rivers (Yenisey, Lena, Ob', McKenzie, and Yukon). Based on ^{14}C measurements, they also estimated 50% of DOC exported during Arctic spring thaw was 1 to 5 years old, about 25% was 6 to 10 years old, and 15% was 11 to 20 years old. However, this is not always the case, for example, although snowmelt may be responsible for 50% of the annual DOC export in Alaskan rivers, it may be more aromatic and hydrophobic and less subject to decomposition.

Carbon and climate change

General patterns

Changes in global air temperature and regional precipitation cause shifts in soil temperature and moisture regimes, which influence permafrost thaw, growing season length, plant growth rates, and species composition and disturbance (see sections 2, Peatland Development and Plant Associations and 3, Permafrost Patterns). In turn this leads to changes in the cycling of C and other nutrients (Schuur et al. 2008). Changes in air temperature and snow cover across boreal North America have resulted in increases in near-surface permafrost temperatures (Osterkamp et al. 2000, Jorgenson et al. 2001, Osterkamp 2005). This has changed the surface energy balance (see section 4, Peatland Hydrology) and led to widespread permafrost degradation (see section 3, Permafrost Patterns).

The type and rate of permafrost thawing affects the fate of C cycling and fluxes; however, permafrost areas respond differently to thawing (Bäckstrand et al. 2008). Once thawed, permafrost C can enter an environment that is either relatively dry or relatively wet. Increased moisture conditions following thaw are common in subarctic and boreal peatlands in Europe and North America (Jorgenson et al. 2001, Luoto et al. 2004, Malmer et al. 2005, Johansson et al. 2006). In a wet environment, organic matter decomposition depletes oxygen (O_2) in the peat porewater, creating anoxic conditions (McLaughlin 2004). Saturation and inundation lead to higher hydrologic flow rates and POC and DOC export to aquatic ecosystems (Walter et al. 2006). In some instances the thawing may decrease soil moisture (e.g., Oechel et al. 1995, 2000). For example, permafrost thawing can remove barriers to drainage, but this is less common in peatland systems. In a drier environment, aerobic conditions dominate and vertical hydrologic flow may be more important than lateral flow (see section 4, Peatland Hydrology).

Carbon sequestration

Permafrost thawing, as discussed, can increase peatland C accumulation (Bubier et al. 1995, Robinson and Moore 2000, Vitt et al. 2000, Camill et al. 2001). Warmer and wetter conditions following thaw in northern peatlands are generally optimal for net C storage (Griffis and Rouse 2001). However, areas of stagnant water result in progressively more reducing conditions producing more CH₄ (Robinson and Moore 2000, Turetsky et al. 2000, Myers-Smith et al. 2007). Friberg et al. (1997) further reported an increase of approximately 25% in the mid-summer CH₄ release from a subarctic peatland during the thawing period. Johansson et al. (2006) also reported that an increase of 6.5 to 10% in land cover of wet sites dominated by sedge vegetation raised landscape CH₄ emissions from a subarctic peatland in northern Sweden by 22 to 66%.

Short-term effects of climate change on CO₂ sequestration are the result of immediate changes to photosynthesis and respiration. In communities characterized by mosses (e.g., open bogs), photosynthesis may be reduced under dry surface conditions. In contrast, vascular plant-dominated communities (e.g., shrub, treed, and forested bogs and fens) may continue to photosynthesize near their potential because their roots access water deeper in peat saturated zones (Griffis et al. 2000). Effects of decomposition will depend on (1) decomposition rates of 'old' organic matter located in deep peat layers and (2) input and decomposition rates of 'new' organic matter entering the system as litter (Belyea and Baird 2006, Laiho 2006).

New organic matter accumulation exceeding decomposition losses from the old peat contributes to continued C sequestration. New litter inputs primarily depend on vegetation composition and peat microorganisms may prefer easily decomposable litter over the older substrate (Myers et al. 2012) but decreasing litter quality (e.g., black spruce or ericaceous shrub litter) may have the opposite effect (Lang et al. 2009). In contrast, decomposition of C-rich soil following permafrost thaw can lead to large C emissions via decay of labile organic matter (Walter et al. 2006). This can enhance mineralization of other elements such as N and further stimulate plant growth (Rinnan et al. 2007). For example, Johnson et al. (2000) found that even during peak growing season wet sedge plots were weak sinks for C, but additions of N and P to wet sedge plots enhanced the C sink throughout the growing season.

The short- and long-term response of peatlands to climate change, as well as the relative roles of photosynthesis and respiration on the net C balance, remains uncertain (Bubier et al. 2003). Thornley and Cannell (2001) reported that most models indicate that in response to warming alone soil respiration will increase more than photosynthesis, especially in peatlands. Using a hydrologic model in boreal and subarctic regions of Canada, Waddington et al. (1998) projected a summer water table drop of 0.14 m in fens, given a 3 °C increase in summer temperature and 1 mm d⁻¹ increase in precipitation. These climatic changes contributed to a 2.3 °C increase in peat surface temperature. Waddington et al. (1998) further projected that the CO₂ sink function of fens would increase, but that of bogs would diminish to where they became a net C source.

Vegetation and succession

Acclimation of plant physiology and succession of communities adapted to the new conditions may offset the initial effects on climate. Shrubs and trees generally increase ecosystem CO₂ sequestration and storage (see section 2, Peatland Development and Plant Associations). A typical permafrost degradation trajectory to wetter conditions rapidly reduces the cover of trees (e.g., black spruce) and shifts the bryophyte community structure towards more aquatic *Sphagnum* species (i.e., *S. riparium*) (Beilman 2001, Camill et al. 2001). Internal lawns succeed relatively quickly (within 200 years) to more bog-like conditions. Thus, although initially high CH₄ production rates create a C source, over the long term the lawn becomes a net C sink (Turetsky et al. 2007). In addition, artificial drainage in an arctic wet tundra ecosystem had no effect on net C fluxes (source of 15 g C m⁻² to source of 8 g C m⁻²). Accounting for CH₄ emissions still resulted in a net GHG source to the atmosphere although after drainage it decreased from 475 to 23 g C m⁻², as CO₂ equivalents (Merbold et al. 2009).

Treeline advance may affect C storage in northern regions and it is likely that any long-term shifts from tundra to forest will be accompanied by a loss of soil C and concomitant C gain by aboveground biomass (Figure 5.6), with no net effect on the C budget. However, if deep soil C is recalcitrant, no change in peat C storage will occur, and peatlands will retain their C sink function (Wilmking et al. 2006). Conversion of tundra sites to forest have been calculated to result in a net loss of >7.8 kg C m⁻² since aboveground C gains were more than offset by belowground

C losses to decomposition. Therefore, increases in C storage in northern ecosystems due to treeline advancement are debatable.

Dissolved organic carbon

The net effects of warming on fluvial DOC export may be determined by soil characteristics, vegetation responses, permafrost dynamics, hydrology, and C quality (McClelland et al. 2007). If initial thawing is widespread, increased runoff and accelerated erosion may occur (Guo et al. 2004). However, after an initial flush of water, deeper flow paths and higher residence times will likely decrease flow rates. Annual flows in the three largest rivers flowing through Ontario's Far North have shown decreasing flow rates since the 1960s (see section 4, Peatland Hydrology). In addition, low river flow has been correlated with changes in dissolved C and N. Striegl et al. (2007) postulated that thawing of permafrost would initially result in higher DOC concentrations in meltwater and possibly increase DOC yield. However, as flow paths deepen and more DOC is consumed in soil and groundwater, DOC yield may decrease coincident with increased respiration and DIC yield. Striegl et al. (2005) showed that from 1978 to 2003 DOC export decreased significantly as a result of deeper flow paths, residence times, and microbial mineralization of DOC in active soil layers and groundwater. In the Kuparuk River, Alaska, McClelland et al. (2007) also showed that DOC export decreased from 1991 to 2001 and that annual nitrate (NO_3) export increased due to enhanced peat N mineralization and nitrification following regional warming. Significantly increased sediment and nutrient loading (ammonium, NO_3 , and phosphate) from thermokarst features to streams have also been observed (Bowden et al. 2008).

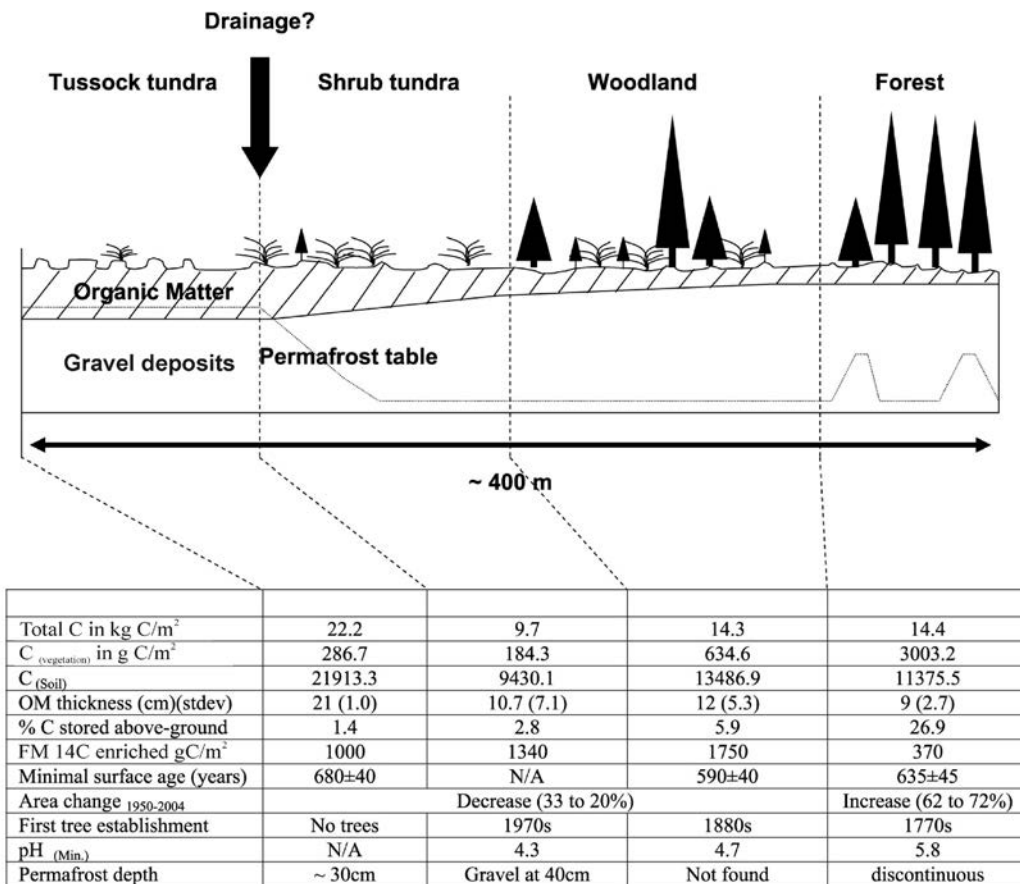


Figure 5.6. Conceptual transect of ecosystem transition from tussock tundra to forest under warming climate (from Wilkening et al. 2006; reprinted with permission from John Wiley and Sons).

Summary and conclusions

Carbon storage and GHG emissions are variable within and among peatland types. Much of this variability is explained by regional and local controls on photosynthesis and soil respiration (organic matter decomposition and roots) rates and subsequent peat accumulation. As such, peatlands vary from C sources to sinks and future C storage and sequestration responses to changes in climate are challenging to predict.

Along regional gradients, MAAT is the most correlated to peat accumulation, with rates highest for peatlands located in regions with average temperatures near 0 °C. Peat accumulation steadily decreases northward as declining MAAT reduces photosynthesis and southward as increasing MAAT stimulates peat respiration. However, variation in types and distributions of peatland and permafrost features on a landscape, along with water table levels primarily control local peat CO₂ sequestration rates. Wet features including collapse scars, ponds, and internal lawns display high CO₂ sequestration and CH₄ emission rates.

The timing of snowmelt and spring hydroclimatic conditions are the primary controls on intra-annual variability in peatland GHG balances, with warmer spring temperatures sustaining net CO₂ sequestration throughout the growing season. Net ecosystem exchange of CO₂ also varies among years, where a specific peatland can be a net C sink or source; again primarily related to spring months. In addition, wintertime CO₂ effluxes from peat surfaces (which are seldom measured) can contribute up to 50% of total annual respiratory CO₂ loss, potentially resulting in a peatland being a net CO₂ source to the atmosphere.

Methane emission from peatlands to the atmosphere is more variable than NEE. Methane emission from wet features vary intra- and inter-annually and spatially due to relationships between (1) ebullition and atmospheric pressure, where ebullition is highest at low to high atmospheric pressure changes and (2) water table level controls on sedge photosynthesis, root exudation, and CH₄ transport.

The distribution of wet features on a landscape and their longevity of occurrence are important controls on century-long GHG balances. For example, peat decomposition is limited by high water tables during the internal lawn stage of succession. However, as dwarf shrubs and trees replace sedges, water table levels become lower and peat accumulated during the internal lawn phase dries out and is decomposed. Further hummock development and lowering of the water table in bogs increases the volume of peat available for aerobic decomposition, elevating peat CO₂ losses. Therefore, proper representation of wet and dry features on a landscape and their transformation rates along successional timelines are central to calculating landscape C budgets and their future responses to temperature and precipitation changes.

Combinations of remote sensing classification of peatland and permafrost features and research on, and monitoring of, climate and site controls on CO₂ sequestration, CH₄ emissions, and C storage of various peatland and permafrost features is a powerful approach to calibrate models of peatland and permafrost C budgets. This allows more confidence in C budget projections for current and future landscapes, which can then aid in land use planning decisions for peatland complexes extending across regional climate and permafrost gradients.

6. Fire Regimes

Background

In North American boreal and subarctic biomes, fire is an important disturbance affecting regional C cycles. Here, black spruce forests growing on mineral soils currently form the site type most sensitive to fire and that releases the most combusted C to the atmosphere (Kasischke et al. 2010). As such, understanding fire effects on C dynamics in upland black spruce forests should be a near-term priority research area. However, as peatlands become drier and warmer, fire-induced C release from peatlands via a combination of increased area burned and more intense fires may increase, resulting in peatlands surpassing black spruce forests in relative research importance (Flannigan et al. 2009).

Understanding current and future effects of fire on peatland C dynamics is inhibited by lack of data related to (1) historic and current fire behaviour in permafrost and non-permafrost peatlands, (2) peatland C cycle responses to changes in fire and permafrost patterns, and (3) permafrost and fire interaction effects on landscape C dynamics. Therefore, in this section, we explore the role of fire and its interactions with permafrost and resulting effects on C dynamics in boreal and subarctic landscapes in relation to (1) boreal and subarctic biome fire patterns, including area burned, fire return intervals, and fire severity, (2) cover types and fire behaviour, including (a) fire behaviour and fuel types in black spruce forests, and (b) Holocene fire patterns, current fire patterns, and successional processes in peatlands, and (3) climate change and fire behaviour, including (a) general patterns of coupled carbon-climate change model projections for northern (>45°N) biomes and factors affecting those results and (b) uncertainties and challenges in predicting peatland C storage and sequestration.

Boreal and subarctic biome fire patterns

At present, approximately 12 million ha of boreal and subarctic landscapes burn annually (Balshi et al. 2009). Fire return intervals vary widely in this region, ranging from less than 100 to more than 3,000 years (Parisien and Sirois 2003, Jiang et al. 2009, Mansuy et al. 2010). Forests generally have shorter fire return intervals than peatlands, and forests and peatlands located in dry, continental regions have shorter intervals than those in humid regions (Arseneault and Payette 1997).

Fires in boreal and subarctic biomes directly emit 110 to 382 Mt (million tons = 1 Tg = 10¹²g) C yr⁻¹ to the atmosphere from biomass consumption, with Siberia contributing 85% to the total C released (Balshi et al. 2007). In North America, 42 to 55 Mt C yr⁻¹ are released to the atmosphere due to fire (French et al. 2000, Conrad et al. 2002, van der Werf et al. 2006), with 50 to 70% released from fires in the boreal zone of Canada (Amiro et al. 2001, Balshi et al. 2007, 2009). Across Canadian ecozones, large (>400 ha) fires burn approximately 2 million ha (range = 0.3 to 7.5 million ha for individual large fires), with burned area larger (Amiro et al. 2001) and fire return intervals shorter (Stocks et al. 2003) in western than in eastern Canada (Figure 6.1). Direct C emissions from large fires in Canada (Balshi et al. 2007) range from 0.2 Mt yr⁻¹ in the East Boreal Shield to 15.2 Mt yr⁻¹ in the West Boreal Shield ecozones (Table 6.1). Consequently, the West Boreal Shield ecozone contributes nearly one-half of all C directly released via fire in Canada (Balshi et al. 2007) and combined, western Canadian ecozones release nearly 80% of the total C emissions from fires across the country.

Different fire patterns occur in boreal and subarctic North America, with area burned in Canada increasing from the 1940s (0.82 million ha yr⁻¹) to the 1990s (3.17 million ha yr⁻¹) and decreasing (to 1.7 million ha yr⁻¹) during the 2000s (Gillett et al. 2004). In contrast, area burned in Alaska decreased from the 1950s (3.3 million ha yr⁻¹) to the 1980s (0.7 million ha yr⁻¹) and increased (to 4.3 million ha yr⁻¹) in the 2000s (Kasischke et al. 2010). In addition, fire occurred early (i.e., June and July) in the growing season from the 1950s through the 1990s, but was more common late (i.e., August and September) in the growing season during the 2000s. During this period in Alaska, fire return interval decreased from 199 to 144 years, with the most prominent decreases occurring in upland areas, although slight decreases were also evident in lowland areas (Kasischke et al. 2010).

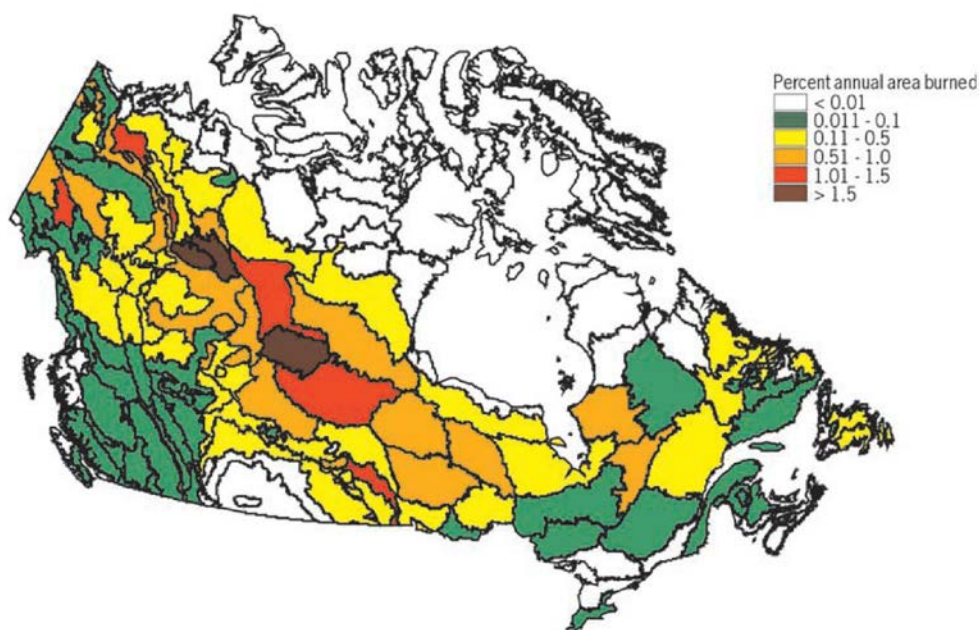


Figure 6.1. The distribution of percent annual area burned across Canada by ecoregions for the 1959 to 1997 period based on the large fire database (Stocks et al. 2003; reprinted with permission from John Wiley and Sons).

Table 6.1. Published estimates of average consumption of aboveground and ground layer carbon (C) fraction during a fire event that are used as emission estimates for various locations/site types in North America (Balshi et al. 2007).

Ecozone	Fraction of aboveground C consumed	Fraction of organic layer C consumed	Average area burned (ha)	Average emission (Tg C yr ⁻¹)	Average emission per unit of burned area (kg C m ² yr ⁻¹)
Alaska Boreal Interior	0.23	0.36	289,000	7.2	2.47
Boreal Cordillera	0.13	0.38	159,000	5.7	3.58
Taiga Plain	0.25	0.06	362,000	6.0	1.65
West Taiga Shield	0.25	0.05	369,000	3.3	0.90
East Taiga Shield	0.25	0.05	141,000	2.1	1.49
West Boreal Shield	0.26	0.06	531,000	15.2	2.86
East Boreal Shield	0.22	0.06	95,000	0.2	0.26
Boreal Plain	0.24	0.11	227,000	7.8	3.42
Hudson Plain	0.24	0.05	56,300	0.8	1.43

Cover types and fire dynamics

Black spruce forests

Site types and fire behaviour: Black spruce forests grow on a variety of site types, with occurrence based on slope and aspect (Table 6.2). Those growing on dry sites have thin soil organic layers (i.e., forest floor) that burn more frequently and severely than those on wet lowland permafrost and non-permafrost soils (Ping et al. 2005, Kane et al. 2007). Furthermore, lowland spruce forests containing permafrost often burn later in the growing season than their upland and non-permafrost lowland counterparts, due to high soil moisture constraints on fire ignition and spread early in the year. During August, however, ALT increases and the surface dries, providing more fuel for ignition and fire spread. This results in more severe burning (Table 6.2) than is the case for early season fires

(Kasischke et al. 2010, Turetsky et al. 2011b). When permafrost is present, more than 50% of the area burned and C consumed during severe fire years occurs during late season fires (Kasischke and Hoy 2012). This pattern may not hold for non-permafrost lowland black spruce forests, where fire severity differs little (Table 6.2) among seasons.

Table 6.2. Mean (and standard deviation) depth of burning and associated carbon emissions for different fire periods and landscape classes in the interior of Alaska (Turetsky et al. 2011b).

Landscape class	Sample size	Drainage type	Early season burning		Late season burning	
			Depth of burn (cm)	Carbon emitted into atmosphere (kg C m ⁻²)	Depth of burn (cm)	Carbon emitted into atmosphere (kg C m ⁻²)
Flat upland	70	Xeric	11.5 ± 0.6	2.60 ± 0.21	15.8 ± 0.6	3.50 ± 0.30
South-facing slopes	31	Xeric	11.4 ± 0.6	3.90 ± 0.29	18.0 ± 2.1	7.11 ± 1.12
East- and west-facing slopes	19	Mesic	11.5 ± 0.8	2.15 ± 0.22	31.0 ± 1.3	8.29 ± 0.84
North-facing slopes	27	Hydric	12.4 ± 0.8	3.33 ± 0.27	20.5 ± 3.2	5.56 ± 0.97
Flat lowland	31	Hydric	12.7 ± 1.0	3.26 ± 0.34	13.5 ± 1.9	3.58 ± 0.65
Weighted landscape mean	178	-	11.9 ± 1.8	2.95 ± 0.12	21.7 ± 2.8	6.15 ± 0.41

Spatial distribution of fire varies across landscapes, depending on the number of fires (Kasischke and Turetsky 2006, Kasischke and Hoy 2012). For example, in Alaska during years with many fires, 45% of all burned area was black spruce forest and 15% was non-forested wetlands (Kasischke and Hoy 2012). In the most severe fire years, black spruce forests represented up to 65% of the total burned area (Kasischke and Turetsky 2006). In contrast, when fires were few, upland black spruce forests and wetlands each accounted for about one-third of burned area (Kasischke and Hoy 2012). Furthermore, during severe fire years, nearly 80% of the C released in the Alaskan Boreal Interior ecozone was from upland black spruce forests. The remainder came from lowland black spruce and upland and lowland shrub cover types (Kasischke et al. 2010). During years with few fires, upland black spruce forests accounted for approximately 60% of C consumption, while lowland spruce and shrubs (lowland and upland) accounted for the remainder.

Between 2000 and 2009, C sequestration in Alaskan black spruce forests (approximately 55 Mt C) was similar to decadal (1950s to 1990s; averaging 49 Mt C decade⁻¹) losses due to burning (Turetsky et al. 2011b), suggesting that in black spruce forests increases in area burned or fire severity may shift the Alaskan Boreal Interior ecozone to a regional C source to the atmosphere, even without accounting for potential increases in wetland fires (Kasischke et al. 2010, Turetsky et al. 2011b).

During recent years, fire patterns have also changed in boreal and subarctic landscapes in eastern Canada, although C cycle responses to fire are understudied in this area. In central Québec, Mansuy et al. (2010) reported moraine and outwash surficial deposits had the coarsest textured soils (primarily sandy), highest burn rates (mean range of 0.58 to 0.69), and shortest fire return intervals (mean range from 144 to 173 years), followed by undifferentiated sandy-silty-clay till and organic (>40 cm thick) surficial deposits (Table 6.3). In addition, dry slopes were vulnerable to fire (Cyr et al. 2007), similar to the Alaskan Boreal Interior (Kasischke et al. 2010). In the Clay Belt region of northeastern Ontario and northwestern Québec, standing tree biomass was higher and soil organic layer (e.g., forest floor) thinner in black spruce forests exposed to high than to low severity fires along a 2,355-year chronosequence study (Lecomte et al. 2006). However, black spruce forests exposed to low fire severity accumulated 73% thicker forest floor and 50% less tree biomass since the time of last fire, with forest floor biomass increasing at a rate of 58 g organic matter m⁻² yr⁻¹ for numerous centuries after fire. This accumulation rate is similar to that of bogs and fens in the Clay Belt region (range from 55 to 62 g organic matter m⁻² yr⁻¹) (Gorham et al. 2003, McLaughlin 2004). Assuming soil organic matter to be approximately 50% C (McLaughlin and Phillips 2006), black spruce forests in the Clay Belt may accumulate nearly 30 g C m⁻² yr⁻¹ in the forest floor. The rapid C accumulation rate likely resulted from *Sphagnum* moss invasions and rapid paludification during succession (Lavoie et al. 2005, Simard et al. 2009, Paré et al. 2011).

Table 6.3. Fire return intervals for boreal forests growing on surficial deposits in central Quebec (Mansuy et al. 2010).

Surficial deposit	Texture	Thickness (metres)	Drainage	Mean fire return interval (years)	Data range
Juxtaglacial and disintegration moraine	Sand	≈10	Xeric	146	92 – 774
Juxtaglacial and disintegration moraine	Sand	≈10	Mesic	144	82 – 348
Ablation till and rogen moraine	Sandy-silt	1 – 5	Xeric	157	90 – 295
Bedrock (>50%)	Null/sandy-silt-clay	0.25	Xeric	171	85 – 683
Outwash	Sandy-silt	≈10	Xeric	173	82 – 498
Undifferentiated till	Sandy-silt-clay	0.25 – 1	Xeric	425	130 – 719
Undifferentiated till	Sandy-silt-clay	0.25 – 1	Mesic	213	83 – 818
Undifferentiated till	Sand-silt-clay	5 – 10	Mesic	178	94 – 594
Undifferentiated till	Sand-silt-clay	5 – 10	Hydric	290	97 – 1031
Organic (>40 cm)	Organic	1 – 2	Hydric	279	95 – 1173

Lecomte et al. (2006) also suggested that regardless of fire severity in the Clay Belt, in the absence of additional fires, forests in that area converge to the same biomass accumulation rates and partitioning between trees and forest floor. Other work in the Clay Belt has shown that with the exception of the first few decades of the 1900s, the fire return interval has consistently increased (i.e., fire frequency decreased) during the past 300 years (Bergeron et al. 2001, 2004), with the interval in coniferous forests increasing from an average of 101 years (range of 79 to 129) prior to 1850 to an average of 398 years (range of 302 to 527) during the 1990s. As such, fire return intervals are much longer in the Clay Belt relative to those in western Canada and Alaska, potentially resulting in more C accumulation in the former region.

In the JBL of Québec, forest cover types changed and fire return interval decreased along a transect from the James Bay coast to 90 km inland (Parsekian and Sirois 2003). Here, pure white spruce stands, with fire return intervals of 3,142 years occurred within the first 0.2 km from the James Bay coast, followed by pure black spruce stands occurring between 0.75 to 22 km inland with fire return intervals of 495 years, and black spruce–jack pine (*Pinus banksiana*) mixed stands occurring between 22 to 90 km inland with fire return intervals of 115 years. The latter is comparable to fire return intervals reported in upland black spruce forests in western Canadian and Alaskan Boreal Interior ecozones. Meanwhile, black spruce forest fire return intervals compare to the 398 years reported for the Clay Belt (Bergeron et al. 2001, 2004).

Additionally in the James Bay region, closed-canopy black spruce forests growing on mineral soil have been shown to store more C than burned (after 2 and 17 years) and open-canopy stands growing on similar soils. Burned and open-canopy stands were reported to contain similar amounts of soil C (Paré et al. 2011). Carbon storage in the forest floor and upper 20 cm of mineral soil of closed-canopy forests also increased with increasing soil wetness, suggesting that closed-canopy black spruce forests do not burn as frequently as open-canopy forests. Further evidence from vegetation regeneration and paleoecological studies in the James Bay region point to frequent black spruce regeneration failures following fire (Bouchon and Arsenault 2004, Payette et al. 2008), which may explain the predominance of open-canopy forests on the James Bay landscape. The James Bay area is also experiencing rapid permafrost thawing (Payette et al. 2004, Thibault and Payette 2009), potentially contributing to increased area burned and fire severity. This in turn may escalate tree regeneration failures, increasing the area of open-canopy stands (Payette et al. 2008) that store less C than closed-canopy black spruce forests growing on mineral soils (Paré et al. 2011).

Fuel types and contributions to carbon emissions: A large part of the boreal and subarctic C pool is stored in moss, litter, and peat layers that are partially or entirely consumed during fires (Zoltai et al. 1998). Since ground layer biomass combustion represents more than 80% of total fuel consumed during Canadian forest and peatland fires (Zoltai et al. 1998, de Groot et al. 2009), this section is focused on ground fuels. Average C consumption of

ground fuels varies from 1.32 to 7.11 kg C m⁻² per individual fire event (Table 6.4); similarly C consumption varies among fire events (de Groot et al. 2009). Fuel types have been described using various methods ranging from surveys of regional land cover class (forested, non-forested, upland, lowland) (Kasischke et al. 2010, Turetsky et al. 2011b) to inventories of site-scale ground layer (lichen, moss, and soil organic layer), crown, and woody debris cover in forests and peatlands (Harden et al. 2006).

Table 6.4. Carbon combustion rates for different site types in northern landscapes.

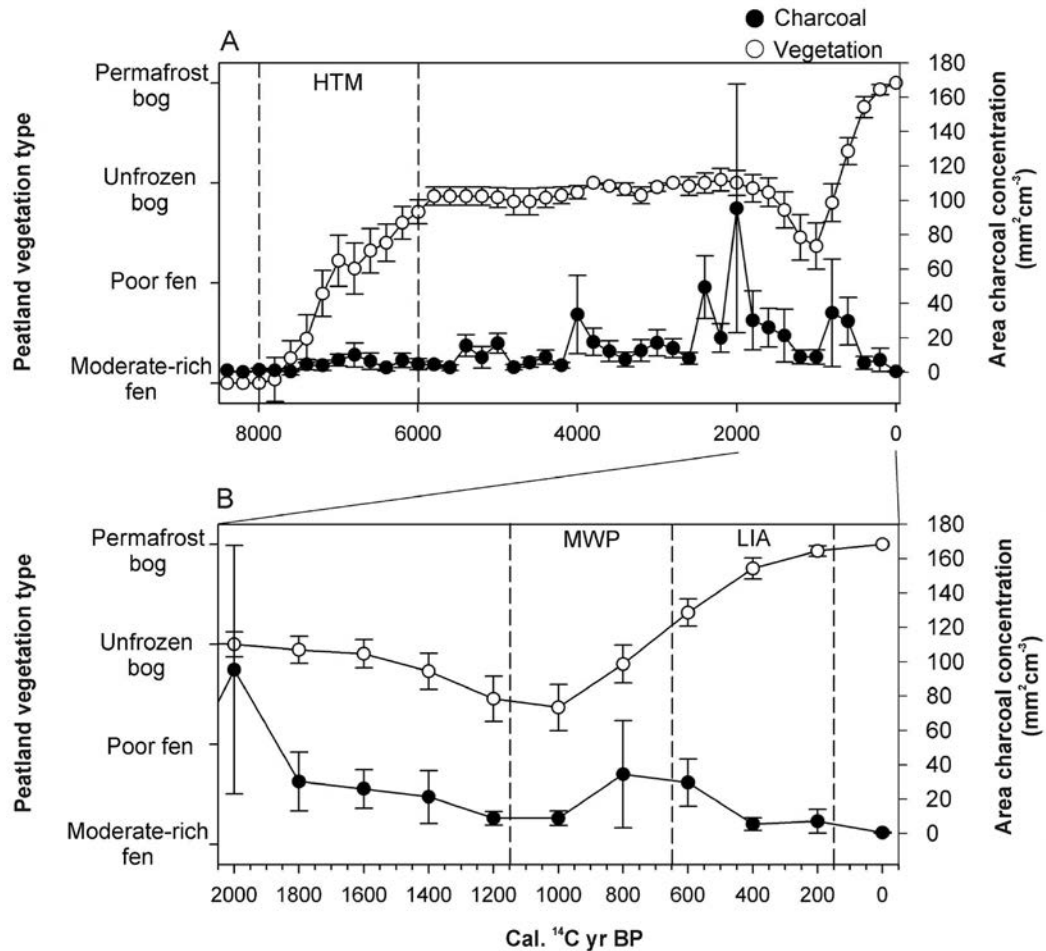
Location	Stand type/fuel type	Carbon emission (kg m ⁻² fire ⁻¹)	Reference
Alaska	Black spruce forest		Kasasichke et al. 2011
	Large fire	6.15	
	Small fire	3.28	Turetsky et al. 2011a
	Flat upland		
	Early season	2.60 ± 0.21	
	Late season	3.50 ± 0.30	
	Dry slope		
	Early season	3.90 ± 0.39	
	Late season	7.11 ± 1.12	
	Wet slope		
	Early season	3.33 ± 0.27	
	Late season	5.56 ± 0.97	
	Flat lowland		
	Early season	3.26 ± 0.34	
Late season	3.58 ± 0.65		
Saskatchewan	Black spruce		
	Non-permafrost bog	1.35 ± 0.24	
	Permafrost bog	2.98 ± 0.67	
Northwest Territories	Black spruce	3.90	de Groot et al. 2009
	Non-forested peatland		
	Large fire	2.84	
	Small fire	1.32	
Ontario	Jack pine, black spruce	3.80	de Groot et al. 2009
Alberta	Non-forested bog		Benscoter and Wieder 2003
	Hummock	1.45 ± 0.11	
	Hollow	2.76 ± 0.33	

In black spruce forests, pre- and post-fire soil organic layer depth have successfully been used as an indicator of fire severity across boreal and subarctic biomes. For example, ranking sensitivity to shifts from early to late season fires in the Alaskan Boreal Interior ecozone, Turetsky et al. (2011b) indicated that upland black spruce forests growing on mesic slopes were the most sensitive to increased fire severity later in the growing season (Table 6.2). Here, early season post-fire soil organic layers (range from 11.4 to 12.7 cm deep) and the C released in their combustion (ranging from 2.15 kg C m⁻² yr⁻¹ for stands on moderately drained soils to 3.90 kg C m⁻² yr⁻¹ for dry soils) were relatively consistent across site types (Table 6.2). Forests on moderately drained slopes were the most affected by late season burning (Turetsky et al. 2011b); soil organic layer burn depth was more than twice and C release through combustion nearly four times larger during late compared to early season fires (Table 6.2). Other research in the Alaskan Boreal Interior also showed moderately drained (e.g., mesic) soils to be most susceptible to increased fire severity (Kasischke and Johnstone 2005, Harden et al. 2006, Kasischke et al. 2010). In addition, Kasischke and Johnstone (2005) reported that acidic, dry black spruce forests growing on deep soils were more sensitive than those on shallow soils, with nearly three times deeper burning of the soil organic layer. A similar result

occurred for acidic elevational woodland black spruce forests growing on deep versus shallow soils (Kasischke and Johnstone 2005). Soil organic layer thickness of 20 cm may be a threshold controlling late season fire severity, with thicker soil organic layers experiencing more severe C losses during late than early season fires (Turetsky et al. 2011b).

Peatlands

Holocene fire patterns: Understanding Holocene peatland fire and permafrost interactions aids in projecting peatland C responses to future climate change (Camill et al. 2009, Froking et al. 2011). In peat stratigraphy, macroscopic charcoal layers per 1,000 years are used as fire frequency and severity indicators and, when used in combination with radiocarbon dating, can delineate fire and LORCA interactions (Kuhry 1994). Stratigraphic studies produced mean peatland fire return intervals between 624 and 2,930 years across Canada (Kuhry 1994, Payette et al. 2008, Camill et al. 2009). Here, and in Finland (Pitkänen et al. 1999), peatland fires were most prevalent between 9000 and 6000 cal yr BP. In Manitoba, fen transition to forested bogs between 8000 and 6000 cal yr BP corresponded to two-thirds to three-quarters lower LORCA values compared to other peatland developmental timeframes (Camill et al. 2009). Fluctuations were correlated to charcoal layers and vegetation structure, with unfrozen bogs having the highest amounts of macroscopic charcoal, followed by palsas and poor fens (Figure 6.2a). Similar patterns reported from other studies in Canada (Kuhry 1994) and Finland (Pitkänen et al. 1999) have been correlated to the Holocene Thermal Maximum (HTM) period when warmer temperatures and drier conditions prevailed (Kuhry 1994).



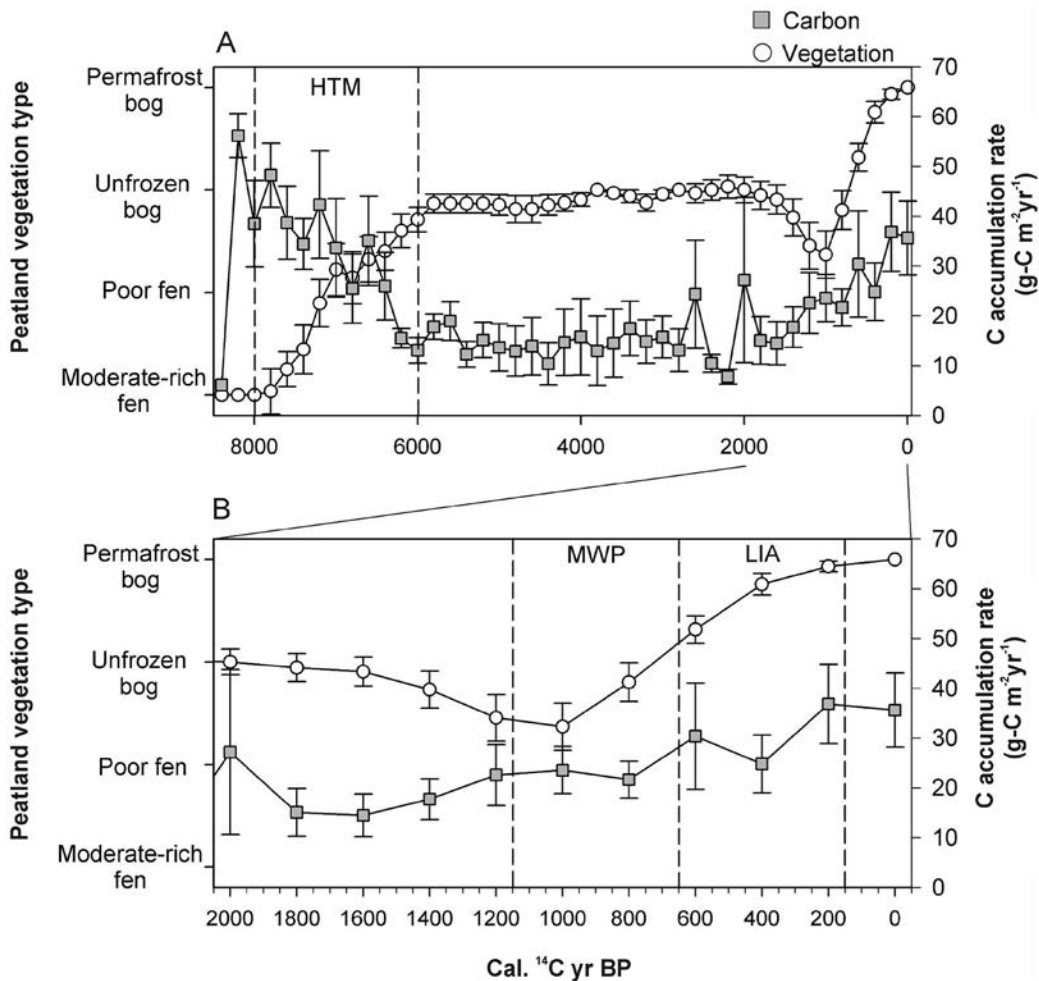


Figure 6.3. Mean changes in the plant community (open circles) and carbon accumulation rate (filled squares) for a Manitoba peatland landscape (a) during the Holocene and (b) during the last 2,000 years (Camill et al. 2009; reprinted with permission from John Wiley and Sons).

Increasing fire severity was also correlated to significant decreases in C accumulation from 6000 to 2000 cal yr BP, but at slower rates than the previous 3000 cal yr BP, and was associated with bog vegetation (Camill et al. 2009). Between 1400 and 1200 cal yr BP, however, conditions were wetter, fires were fewer, and C accumulation rates were higher (Figure 6.3a,b). Vegetative indicators (e.g., macrofossils, pollen) point to 1400 to 1200 cal yr BP being a transition stage from unfrozen bog to poor fen (Figure 6.3b). Dry conditions have prevailed from 1000 cal yr BP until recently. However, peatland fire frequencies decreased and C accumulation increased, with rates generally more than 30 g C m⁻² yr⁻¹ accumulated for the past 600 cal yr BP (Figure 6.3b; Camill et al. 2009). Higher C accumulation rates may be attributed to colder soils and permafrost formation during the Little Ice Age (Kuhry 1994, Pitkänen et al. 1999), although peatlands characterized by more area of palsas and peat plateaus would be expected to have high fire frequencies and low C accumulation rates (see section 2, Peatland Development and Plant Associations). Other work has shown recent C accumulation rates (e.g., past 150 years) to exceed 60 g C m⁻² yr⁻¹ (Pitkänen et al. 1999). As such, permafrost (through higher active layer soil moisture and cold temperatures) may currently counteract the effects of warming on increased fire and C emissions and understanding these dynamics is critical to correctly predict future peatland C balances, as well as their importance to regional C budgets.

Current fire patterns: While fire return intervals are generally longer in peatlands than in upland black spruce forests (Camill et al. 2009), based on relatively scarce data it seems that peatlands may account for 10 to 30% of the current total direct C emissions from western Canadian ecozones (Zoltai et al. 1998, Turetsky et al. 2002a, Flannigan et al. 2009). Peatlands in western Canada have shorter fire return intervals than those in eastern Canada (Kuhry 1994, Payette et al. 2008, Camill et al. 2009). Similar to black spruce forests, fire patterns within and among peatlands are primarily controlled by ground fuel moisture content (Benscoter et al. 2005). For example, peat ignition generally occurs at levels less than 30% moisture (water) content by weight but combustion can be maintained at moisture contents up to 235% (Chistjakov et al. 1983). Other researchers have identified peat burning thresholds of 140 to 310% moisture content by weight (Hawkes 1993), vertical peat combustion at moisture contents up to 200%, and lateral fire spread at moisture contents up to 400 to 500% (Sofronov and Volkitina 1986). Furthermore, Turetsky et al. (2004) reported no statistical difference in ground fuel ignition between bogs and upland black spruce forests in western Canada, although area burned in the latter was higher. As such, ground fuel moisture influences on lateral fire spread may be an important factor affecting peatland area burned.

In North America, 0.15 to 0.64 million ha of peatlands burn annually (Zoltai et al. 1998, Turetsky et al. 2004) and approximately 80% of C released from peatland fires (Table 6.5) comes from peat combustion in permafrost bogs (e.g., peat plateaus; Zoltai et al. 1998). In addition, permafrost bog fires reduced surface peat thickness, emitting C that was centuries old (Robinson and Moore 2000). This is consistent with lower LORCA values of forested and treed bogs and palsas and peat plateaus measured with radiocarbon dating (section 2, Peatland Types and Plant Associations). Another consequence of fire is palsa/plateau collapse and subsequent losses of forested area and increases in shrub- and moss-dominated wetlands (Beilman 2001, Yoshikawa et al. 2003), all of which may increase soil C sequestration rates (see section 3, Permafrost Patterns).

Table 6.5. Estimates of annual aboveground and peat biomass loss from northern bogs and swamps due to peat fires (Zoltai et al. 1998).

Peatland type	Wetland region ^a	Peatland area (km ²)	Long-term average annual burn area	Fire return interval (years)	Biomass burned (10 ³ tonnes)	
					Aboveground	Peat
Bogs	Subarctic	10,000	65	400	11	60
	Boreal, continental	63,000	420	400	147	416
	Boreal, humid	100,000	125	1,000	22	198
Permafrost bogs	Subarctic	343,000	3,340	250	1,200	12,419
	Boreal, continental	4,000	25	250	26	155
	Boreal, humid	- ^b	-	-	-	-
Fens	Subarctic	280,000	935	300	327	-
	Boreal, continental	144,000	480	300	168	-
	Boreal, humid	102,000	100	1,000	35	-
Swamps	Subarctic	-	-	-	-	-
	Boreal, continental	44,000	585	200	3,071	859
	Boreal, humid	51,000	255	400	1,339	399
Total		1,141,000	6,330	-	6,346	14,505

^a Defined as per Wetland regions of Canada (Zoltai et al. 1988).

^b Assumed to be zero.

Northern portions of the subarctic region contain thicker permafrost that extends over larger land areas (Osterkamp and Romanovsky 1999, Camels et al. 2008). These areas contain more saturated surface fuels, with low probabilities of ignition following lightning strikes (Kuhry 1994, Camill et al. 2009); this maintains C sequestered as peat (Arlen-Pouliot and Bhiry 2005, Meyers-Smith et al. 2008) as discussed for black spruce forests. However, in terms of global warming potential, enhanced CH₄ emissions from saturated peat (Prater et al. 2007, Wickland et al. 2008) and surrounding thermokarst may offset C sequestered as CO₂ (Frolking et al. 2006). In contrast, southern portions of the DPZ contain less permafrost area with thicker active layers. These conditions contribute to drier surface fuels with high probability of ignition following lightning strikes, resulting in higher C losses than in northern regions (Schafer et al. 2011).

Successional processes and carbon exchange: Fire affects peatland plant species by differentially removing vegetation and resetting succession, resulting in changes in peat accumulation rates (Benscoter et al. 2005). Bogs vary microtopographically, with hummocks and hollows separated by as much as 0.5 m of vertical change, contributing to within-bog hydrological variation (Wallén and Malmer 1992). This variability greatly influences peatland fire severity (Benscoter and Wieder 2003). Although drier than hollows, hummocks tend to burn less severely because of greater water retention capacity of hummock-*Sphagnum*, such as *S. fuscum*, which tolerates drier hummocks. Therefore, during short post-fire intervals hummocks composed of *S. fuscum* can accumulate peat earlier than hollows (Turetsky et al. 2010). As succession proceeds, hollow-*Sphagnum* (e.g., *S. angustifolium*), which has higher NPP than *S. fuscum*, establishes and NPP increases. At the same time, *S. fuscum* hummocks become water limited because of vertical peat accumulation, slowing rates of hummock peat accumulation. By 60 years after fire, peat accumulation rates in hollows and hummocks are similar, coinciding with a period of rapid peat accumulation (Benscoter and Vitt 2008).

Wieder et al. (2009) studied the same bog chronosequence as Benscoter et al. (2005) and reported a mean fire return interval of 123 years (comparable to upland black spruce forests) with 106 g C m⁻² yr⁻¹ released to the atmosphere for 10 years following fire. During this period, pioneering mosses, such as *Polytrichum strictum* dominated hollows (e.g., Turetsky et al. 2010). However by 13 years following fire, *Sphagnum* species displaced pioneer mosses in hollows, while shrubs re-established on hummocks. These vegetation changes coincided with the timeframe in which bogs switched from being a net C source to a sink (Wieder et al. 2009). The next major ground vegetation shift occurred between approximately 70 to 80 years following fire, when moss composition changed from *Sphagnum*- to feathermoss-dominated. This timeframe coincided with rapid C sequestration of approximately 200 g C m⁻² yr⁻¹, which decreased to 120 g C m⁻² yr⁻¹ by 100 years after fire (Benscoter and Vitt 2008, Wieder et al. 2009). Similar patterns occurred along a 120-year-old black spruce chronosequence in Alaska (O'Neill et al. 2003). Here, forests were a net source of 180 to 1100 g C m⁻² yr⁻¹ for the first 7 to 15 years after fire. However, they were an overall net sink of 28 to 54 g C m⁻² yr⁻¹ across the chronosequence. Changes in C accumulation generally occurred at the same time intervals reported by Wieder et al. (2009) who also reported that the changes were associated with major shifts in moss community structure. Both Wieder et al.'s (2009) and O'Neill et al.'s (2003) results indicate that under current fire regimes peatlands have retained their regional C sink function.

Climate change and fire behaviour

Coupled carbon-climate change model projections for northern (>45°N) biomes

General patterns in carbon projections: Climate change-induced warming and its effects on fire and permafrost patterns is frequently cited as a stressor that may decrease the C sink strength of northern peatlands (Frolking et al. 2011, Grosse et al. 2011). However, peatlands were excluded from biospheric coupled carbon-climate change models used in the International Panel on Climate Change's fourth annual report (IPCC 4AR; IPCC 2007). Assessing an ensemble of 11 coupled carbon-climate change model projections for the end of the 21st century, northern terrestrial ecosystems (i.e., all terrestrial cover types, combined) would accumulate approximately 30 to 40 Gt C above current values; of which more than 50% would be sequestered as soil organic matter (e.g., Qian et al. 2010).

Carbon accumulation resulted from a 10- to 30-day lengthening of the growing season, increasing NPP relative to heterotrophic respiration prior to 2060. However, C sequestered as NPP and C released as heterotrophic

respiration were similar between 2060 and 2100 as heterotrophic respiration from previous years' litterfall balanced NPP (Koven et al. 2011, Schaefer et al. 2011). Although more uncertain after 2100, most coupled carbon-climate change models indicated that northern regions would be a net C source (Balshi et al. 2009, Koven et al. 2011, Schaefer et al. 2011). However, depending on the ecological processes simulated and their assigned coefficient values, much variation existed across individual coupled carbon-climate change model outputs. Consequently, estimates varied from northern terrestrial ecosystems being a source of 52 (Zhuang et al. 2006) to a sink of 88 (Koven et al. 2011) Gt C by 2100 (Table 6.6).

In addition to variation in ecological processes and rates used as assumptions in coupled carbon-climate models, variable C storage was also attributed to an inadequate understanding of soil temperature and moisture (Sushama et al. 2007) interactions with NPP and heterotrophic respiration rates (Qian et al. 2010). Coupled carbon-climate change models do not simulate fine scale soil temperature and moisture patterns, so these are only crudely represented in biospheric C assessments (Schaefer et al. 2011). Furthermore, simulations conducted for the IPCC 4AR did not include fire or permafrost processes (IPCC 2007). Nor did any of the coupled carbon-climate change models include peatland distribution and CH₄ emissions (Koven et al. 2011). Incorporating those factors, along with CO₂ fertilization (enhancement) and climate warming may significantly change C balance results for northern ecosystems (Table 6.6).

Table 6.6. Coupled carbon-climate change model predicted changes in C storage in northern terrestrial ecosystems by 2100.

Biosphere (latitude)	Scenario	Predicted changes in terrestrial carbon storage in 2100 (Gt)	Reference
Pan-boreal ^a (>45°N)	Control (IPCC B2)	23	Balshi et al. 2009
	CO ₂ + warming + fire (IPCC A2)	17	
Pan-boreal ^b (>45°N)	Control	33 to 46	Schaefer et al. 2011
	Permafrost	-104 ± 37	
Pan-boreal ^c (>50°N)	Control	-35 to -51	Zhuang et al. 2006
	CO ₂	-5 to -33	
	Fire	-20 to -30	
	Permafrost	-7 to -17	
Pan-arctic ^d (>60°N)	CO ₂ + warming	38 ± 20	Qian et al. 2010
Pan-arctic ^e (>60°N)	Control	69 to 88	Koven et al. 2011
	CO ₂	29 (range = 0 to 66)	
	Warming	14 (range = 77 to -20)	
	Permafrost	-62 ± 6	
	Freezing	-25 ± 3	
	Heating	-85 ± 16	

^aModels: CGCM2 and TEM (Raich et al. 1991); ^bCCSM3, HadCM3, MIRCO3.2 and SiBCASA (Schaefer et al. 2008); ^cIGSM and TEM; ^dmean of 10 linked models; BERN-CC-LPJ (Haxeltine et al. 1996); CLIMBER2-LPJ; CCSM-1-LSM, CSA; HadCM3CL-TRIFFID; IPSL-CM2C-SLAVE; IPSL-CM4-LOOP-ORCHIDEE; MPI-JSBACH; FRCGC-Sim-CYCLE; UVic-TRIFFID; UMD-VEGAS;

^eSPLCM4-ORCHIDEE (Ducoudré, et al. 1993); see acronym list for definitions.

Factors affecting coupled carbon-climate change model carbon projections: Carbon dioxide fertilization is a key uncertainty and controversial area of coupled carbon-climate change model projections of future C sinks (Prentice et al. 2001). In the absence of other limiting factors, elevated atmospheric CO₂ may stimulate NPP thereby slowing increases in atmospheric CO₂ accumulation (Matthews and Keith 2007). Carbon dioxide fertilization may account for more than 50% of the predicted C accumulated by 2100, with warming primarily accounting for the remainder (Table 6.6, Figures 6.4 and 6.5). Exclusion of CO₂ fertilization, however, reduces the amount of C sequestered and, depending on the model, indicates that the boreal biome will be a net atmospheric C source (Balshi et al. 2009, Koven et al. 2011, Schaeffer et al. 2011).

Coupled carbon-climate change model studies suggest that fire may reduce the C sink strength of northern ecosystems by 20 to 30 Gt (approximately 10 g C m⁻² yr⁻¹; Zhuang et al. 2006), potentially offsetting one-half to three-quarters of the projected C sequestered during the 21st century. Without including the effects of fire, Zhuang

et al. (2006) reported the current northern landscape is a 276 Mt C yr⁻¹ source and that value may approximately double by 2100 due to increased numbers of fires and their intensity, and permafrost thawing. They further reported that when area burned was low to moderate but CO₂ fertilization was considered, 5 to 33 Gt C were predicted to be released to the atmosphere by northern terrestrial ecosystems. Without CO₂ fertilization, this amount increased to 34 to 54 Gt C. Furthermore, fire emissions were not linearly correlated with area burned or years with fewer fires. In these studies, vegetation and soil C accumulation were associated with the most C released per fire event.

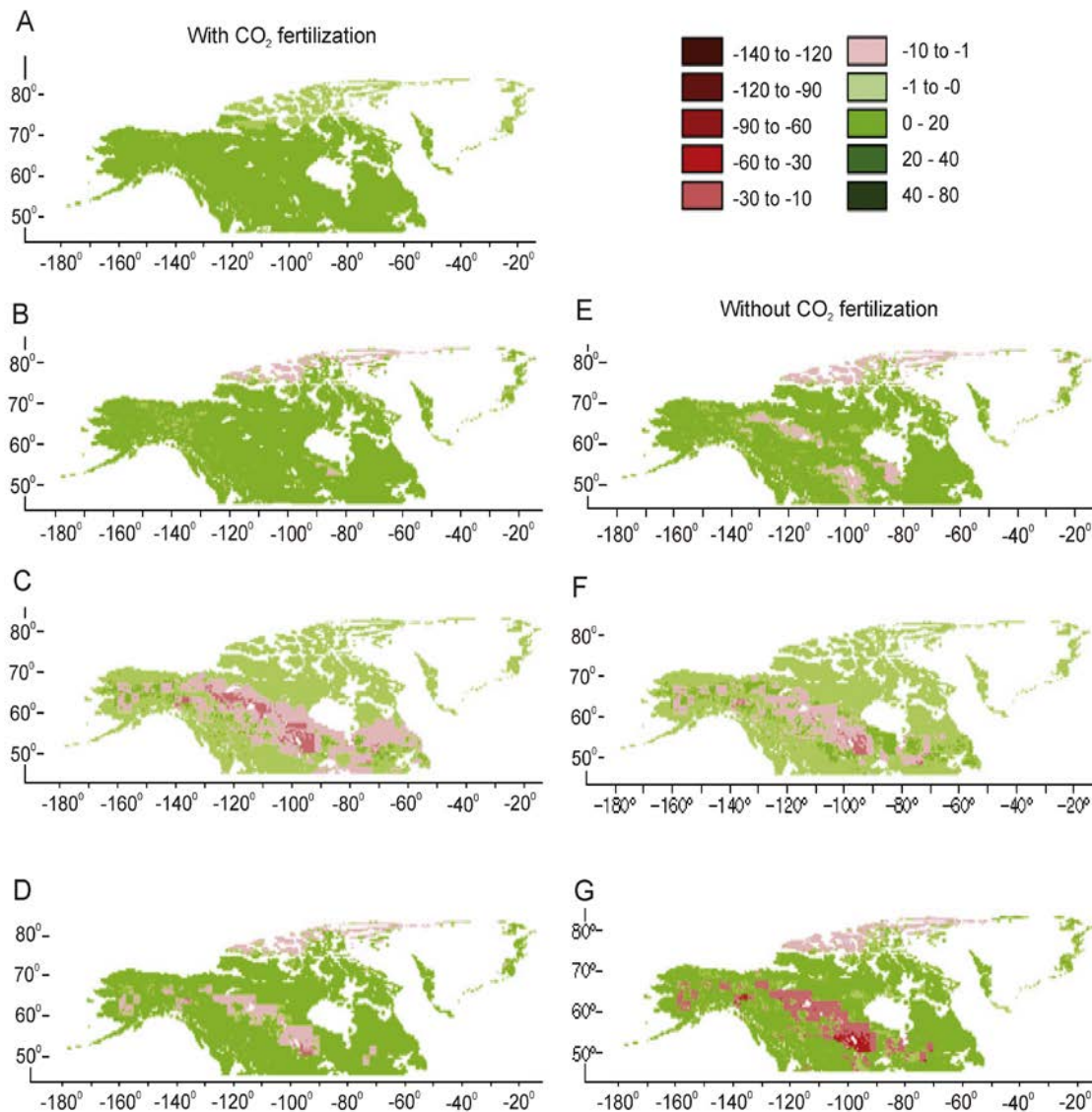


Figure 6.4. Simulated mean annual net ecosystem carbon balance (g C m⁻² yr⁻¹) for boreal North America estimated using CACM2 under the A2 scenario from 2003 to 2100 in response to (a) CO₂ fertilization, (b, e) climate, (c, f) fire, and (d, g) the combination of CO₂, climate, and fire. Results are presented with and without a CO₂ fertilization effect on photosynthesis. Positive values represent C sequestration while negative values represent C release from land to the atmosphere (Balshi et al. 2009; reprinted with permission from John Wiley and Sons).

In contrast to Zhuang et al. (2006), Balshi et al. (2009) reported that CO₂ fertilization contributed to northern terrestrial ecosystems being a net C sink of 20 to 40 Gt or 178 to 235 Mt C yr⁻¹ (14.8 to 19.6 g C m⁻² yr⁻¹). Without CO₂ fertilization, approximately 30% less C was sequestered. Including fire in the model resulted in parts of boreal and subarctic Canada remaining a net sink of 20 to 40 g C m⁻² yr⁻¹ while other parts, coinciding with dense peatland and permafrost regions (including the Far North of Ontario), became sources of 1 to 60 g C m⁻² yr⁻¹ (Figure 6.5; Balshi et al. 2009). Including fire but not CO₂ fertilization provided similar results, although the proportion of North America with high C fluxes decreased (Figure 6.5). Here, scenarios of lower (B2) and higher (A2) warming, excluding CO₂ fertilization, resulted in smaller increases in fire-caused emissions of C across all decades until

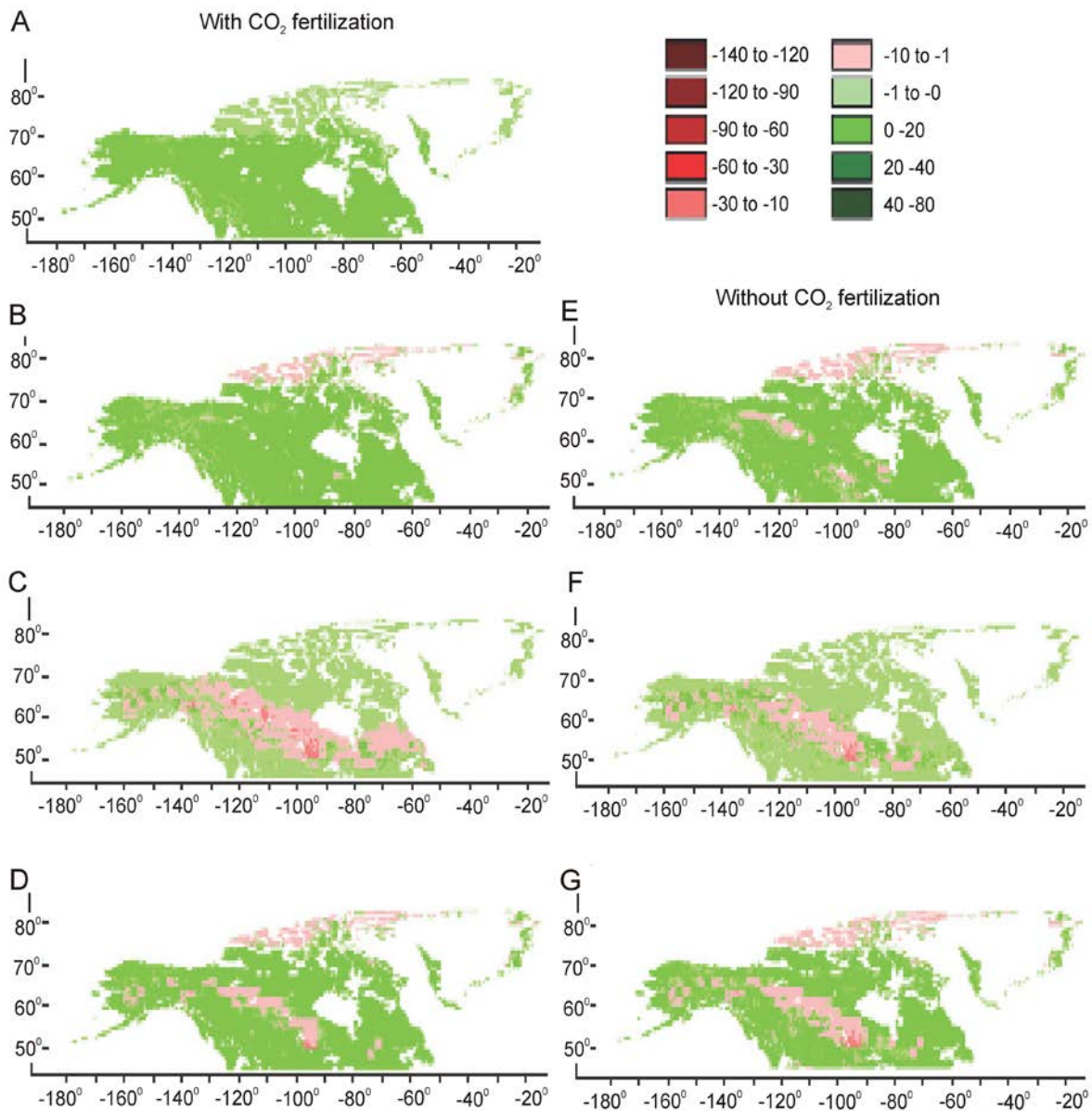


Figure 6.5. Simulated mean annual net ecosystem carbon balance (g C m⁻² yr⁻¹) for boreal North America estimated using CACM2 under the B2 scenario from 2003 to 2100 in response to (a) CO₂ fertilization, (b, e) climate, (c, f) fire, and (d, g) the combination of CO₂, climate, and fire. Results are presented with and without a CO₂ fertilization effect on photosynthesis. Positive values represent C sequestration while negative values represent C release from the land to the atmosphere (Balshi et al. 2009; reprinted with permission of John Wiley and Sons).

2100, whereas CO₂ fertilization increased C sequestration until about 2050. This in turn resulted in more biomass for burning during the latter half of the 21st century, at which time C emissions due to fire were predicted to increase between 300 and 400% (Balshi et al. 2009).

Permafrost thawing may increase C emissions by an additional 7 to 104 Gt C by 2100 (Table 6.6), depending on the model used and the regions included in the simulations (Zhuang et al. 2006, Koven et al. 2011, Schaefer et al. 2011). It should be reiterated that coupled carbon-climate change models do not include the complex interactions among thermokarst, fire, and hydrologic dynamics, and that such interactions may exacerbate CH₄ emissions (Grosse et al. 2011).

Forecasts from coupled carbon-climate change models indicate that permafrost will begin thawing by the mid-2020s, with the HBL and other regions having possibly surpassed their critical thresholds for net permafrost thawing in the early 2000s (Koven et al. 2011). Applying a slow warming rate in the AIB scenario using the CCSM3 model resulted in estimates of 54% of initial permafrost C stock thawed by 2200, with 61 ± 20% of the original 313 Gt C initially stored in permafrost released to the atmosphere. Carbon liberated from permafrost thawing and its release as CO₂ to the atmosphere may balance the approximately 160 Gt C accumulated globally by 2100 (Schaefer et al. 2011). An approximately a 70-year lag time is expected between exposure of thawed permafrost C to soil microorganisms and its atmospheric release via decomposition.

Uncertainties and challenges in predicting peatland carbon

Using the Canadian Global Climate Model version 1 (CGCM1), Amiro et al. (2009) predicted fire frequency and area burned across Canada would double to approximately 4 million ha by 2100. The larger area burned was accompanied by 161 to 310 Mt CO₂-equivalent yr⁻¹ directly released from biomass combustion. This was primarily attributed to a five-fold increase in burned area during May and a smaller increase during June, resulting from earlier snowmelt and lower soil moisture. Their results were not entirely consistent with those from an empirical study in the Alaskan boreal region where evidence points to increased area burned during August in future years (Turetsky et al. 2011b). If Amiro et al.'s (2009) projections of burned area increases occurring primarily in May are correct, then effects on peatland area burned and fire severity may be minimal (e.g., Frolking et al. 2011) and most of the excess CO₂ release will likely be from upland black spruce forests (e.g., Kasischke et al. 2010). Earlier snowmelt is also predicted to extend the growing season by 10 to 30 days; in combination with enhanced ET, this extension could lead to drier peat during August and September, elevating late season fires and C combustion, particularly from palsas and peat plateaus (e.g., Zoltai et al. 1998).

As discussed in the coupled carbon-climate change modelling section, evidence is contradictory as to the effects of permafrost thawing on C balances and CH₄ emissions. By 2100, both C accumulation and losses from terrestrial ecosystems are predicted (Zhuang et al. 2006, Koven et al. 2011). Results from field-based studies suggest that permafrost thaw alone will likely enhance C sequestration rates and CH₄ emissions. Frolking et al. (2011) provided a basic calculation, suggesting that by 2100, 30 to 100 Mt yr⁻¹ C may be sequestered and up to 50 Mt CH₄ yr⁻¹ released from permafrost regions (beyond current values). This is consistent with coupled carbon-climate-change biospheric model assessments (e.g., Koven et al. 2011, Schaefer et al. 2011).

Complicating projections is that both current and future peatland GHG emissions may be underestimated due to the relatively unknown effects of (1) multiple perturbations (e.g., permafrost thaw, fire, hydrology, and temperature) that may destabilize peatland C cycling, (2) rates of both climate change and peatland adaptation, and (3) occurrence of new climate states outside the range of Holocene climate variation. At present, the only approach available to address these issues is limited process-based modelling and the results from those models are inconsistent with respect to peatland C responses to projected climate change. For example, warming may increase peatland C losses by 40 to 85% in coming centuries (Ise et al. 2008), or peatland C stocks may stabilize in response to drying (Frolking et al. 2010). However, none of the available models fully represent the complexity of peatland responses to climate forcing or fire, nor do they incorporate responses of various peatland types following exposure to changing climate. Furthermore, because permafrost thaw may enhance or inhibit peatland

sensitivity to fire, priorities for field-based research and monitoring as well as further model development include the destabilization of peatland C cycling by multiple perturbations, the rate of climate change and subsequent peatland adaptation to the changes, and the effects of potential new climate states outside the range of Holocene climate variation.

From the boreal to northern subarctic zone, permafrost coverage increases from 10 to 90% of the land base (see section 3, Permafrost Patterns). Spatial configurations of landscape features (Figure 3.1a-d) depend on a variety of internal (e.g., peat accumulation and acidification) and external (e.g., climate and fire behaviour) factors. At the most northern regions of the subarctic biome, palsas/peat plateaus (occurring in various stages of maturity) and thermokarst features dominate landscape patterns, along with non-permafrost bogs and fens (Camill 1999a, Beilman 2001). In contrast, in southern regions of the boreal zone mostly non-permafrost bog and fen complexes (dominated by bogs) occur, with forested bog, which is susceptible to burning, as a dominant peatland type (Zoltai et al. 1998).

The spatial distribution of permafrost extent implies that, during the 21st century, southern and northern portions of the DPZ may respond differently to climate change. For example, the boreal zone is projected to warm and dry, increasing the probability that remaining palsas, peat plateaus, as well as non-permafrost forested bogs, will burn more frequently and severely than they do now (Zoltai et al. 1998, Flannigan et al. 2009). These changes may switch the boreal region from a C sink to a source (Turetsky et al. 2002a, 2004). In contrast, permafrost thawing in the northern portion of the DPZ may lead to soil saturation and lower probability of lightning-caused biomass ignition (Schaefer et al. 2011). Under these conditions, organic matter breakdown is dominated by slowly decomposing anaerobic processes, resulting in faster rates and longer periods of C accumulation as peat (Hobbie et al. 2000). Saturation also stimulates CH₄ production and higher emissions of this gas may increase the GWP of the atmosphere (Roulet 2000, Malmer et al. 2005). However, successful modelling of peatland C responses to climate change requires data from long-term field studies to parameterize the models.

Landscape climate change and peatland modelling also need to adequately represent local heterogeneity (e.g., microtopography, fire intensity, ALT, collapse features), which affect peatland C cycling and GHG emissions and successional trajectories (i.e., transitions in vegetation composition). The cumulative effects of multiple factors adds to the complexity of peatland C dynamics and few studies have addressed the combined effects of climate change, fire, and permafrost interactions across landscapes. Typical uncertainties in quantifying peatland C responses to climate change range from ± 20 to $\pm 100\%$ and can span a factor of two or more orders of magnitude (Lund et al. 2010, Frohking et al. 2011).

Modelling peat accumulation and post-fire peatland C budgets requires consideration of vegetation succession because inundation and drying promote different successional trajectories affecting plant species presence and their growth rates, quantity and quality of litter inputs to soils and its subsequent decomposition, and GHG exchange between the atmosphere and peat surface. Therefore, it is critical to properly account for landscape fire patterns and how they interact with hydrology, permafrost, and subsequent vegetation recovery and succession. Because peatlands are generally wetter than the surrounding landscape after a fire, increased CH₄ emissions from burned—relative to unburned—sites have been reported (Nakano et al. 2006). Furthermore, should bogs burn more frequently in future, resulting water movement to surrounding fens may increase their CH₄ emissions (Frohking et al. 2011).

In large peatland complexes, such as the HBL, water flow is an important factor in C dynamics (see section 4, Peatland Hydrology) and accurate specification of peat properties requires that models are constructed to factor in the dynamic representation of peat accumulation during succession. Other challenges with respect to regional assessments of peat responses to fire include modelling peat combustion across the landscape under a changing climate, particularly with respect to combustion and active layer interactions. Furthermore, thermokarst affects C storage, but efforts to model this phenomenon are few.

Summary and conclusions

In North American boreal and subarctic biomes, 42 to 55 Mt C yr⁻¹ is released to the atmosphere from fire in natural ecosystems, mostly from black spruce forests growing on mineral soils. However, wetlands in western North America, including non-peatlands and peatlands, may account for as much as one-third of total fire emissions from natural sources.

Approximately 80% of C released from peatland fires comes from peat combustion in permafrost bogs. Furthermore, as peatlands become drier and warmer in future years, fire-induced C release is expected to increase as larger fires burn deeper into peat. In fact, peatlands may surpass black spruce forests in relative fire research importance. Understanding current and future effects of fire on peatland C dynamics is limited by lack of data related to (1) historic and current fire behaviour in permafrost and non-permafrost peatlands, (2) peatland C cycle responses to changes in fire and permafrost patterns, and (3) permafrost and fire interaction effects on landscape C dynamics. Thus, in boreal and subarctic regions, current and future C peatland budgets are uncertain.

Results from the few chronosequence studies reported indicate that a bog will retain its net C sink function for at least a century following fire. In the first decade after a fire, bogs may release up to 100 g C m⁻² yr⁻¹ to the atmosphere. By the end of the second decade after fire, however, bogs are C neutral, and by 75 years post-fire they sequester approximately 200 g C m⁻² yr⁻¹ from the atmosphere. Net C sequestration continues for at least 100 years, with bogs sequestering a net of 100 g C m⁻² yr⁻¹ from the atmosphere. However, increases in peat drying can lead to bogs being more vulnerable to deep soil consumption because burning is more likely to occur during the period of maximum water table drawdown and fuel exposure.

Current and future peatland GHG emissions from fire may be underestimated. This may partially explain contrasting process-model results in terms of C stabilization and losses in future years. Furthermore, because permafrost thaw may enhance or inhibit peatland sensitivity to fire, priorities for field-based research and monitoring as well as further model development are the destabilization of peatland C cycling by multiple perturbations, the rate of climate change and subsequent peatland adaptation to the changes, and the effects of potential new climate states outside the range of Holocene climate variation.

7. Mapping, Monitoring, and Modelling Permafrost Peatlands

Background

Quantifying peatland C pools at regional scales and understanding how C pools are affected by climate change requires knowledge of peatland (1) extent and peat depth, (2) species composition, biomass, and productivity, and (3) environmental drivers (e.g., climate, water table, soil temperature, and active layer depth), all of which control C storage and release. Collecting data to develop this knowledge can be achieved through direct field measurements or indirect measurements by airborne or satellite remote sensors (Aplin 2005). Direct measurements provide accurate local characterization but logistical constraints and cost limit temporal and spatial intensity of sampling at larger extents. Furthermore, extrapolating highly detailed fine-scale point-based measurements across vast expanses of peatland complexes will not capture regional heterogeneity, thereby biasing estimates of peatland properties.

Observations from remote sensing provide detailed, non-invasive and spatially explicit data over large areas, reducing the need to extrapolate site-level point data (Aplin 2005). However, accuracy of remote sensing for characterizing peatlands depends on the type of sensor, its resolution, and how well it represents the property of interest. High resolution remote sensing data are practical at local landscapes, but at regional to global scales, high resolution data becomes prohibitive in both cost and required computing power (Aplin 2005). Where conditions are heterogeneous, coarse resolution satellite sensors (e.g., 1° by 1° grid square) provide information for larger areas but may bias estimates of peatland properties (Harris and Bryant 2009a). In this section, we explore possible approaches to mapping permafrost peatlands and discuss the importance of mapping to monitor and predict changes in the biophysical properties of peatlands.

Mapping permafrost peatlands and their properties

No consistent, spatially explicit national wetland distribution map is available for Canada at this time (Li and Chen 2005). Existing databases, such as the Canadian peatlands database (Tarnocai et al. 2000) and the national wetland database (Zoltai et al. 2000) are compilations of mostly ground-based surveys carried out in different time periods, for different purposes, and often using different methods (Cihlar and Tarnocai 2000, Milton and Helie 2003). The accuracy of maps derived from these data sets, which represent the best available information at the time, has not been rigorously assessed. Furthermore, since peatlands change over time these maps will likely become even less accurate in future (Pflugmacher et al. 2007). Confounding the problems with mapping peatlands is the difficulty in mapping permafrost distribution. The Geological Survey of Canada produces permafrost and ground temperature maps, but data in certain regions, particularly the Hudson Bay Lowlands, are noticeably sparse (Smith and Burgess 2000). An initiative is underway to map Canada's wetlands (Canadian Wetland Inventory) using remote sensing, including optical, radar, and digital elevation approaches (Fournier et al. 2007). The following discussion highlights some of the methods and approaches used for and issues to consider when mapping permafrost peatlands.

Remote sensing of peatlands

Satellite remote sensing is an important tool in regional mapping of biophysical variables needed for peatland research, and provides information at spatial and temporal scales that are generally inaccessible or impractical for field observations (Sitch et al. 2007). Remote sensing works on the principle of detecting reflected radiation energy (incident from the sun or a source provided by the sensor) from a target (Figure 7.1). Depending on the energy reflected and the type of sensor, information can be collected to (1) classify vegetation greenness and phenology, (2) detect saturated and inundated water, and (3) measure permafrost and other environmental parameters (e.g., surface temperature, snow cover, topography) (Pietroniro and Leconte 2005). These properties can be extracted from remotely sensed data using two different approaches (Sitch et al. 2007). The simplest application of remote sensing imagery is to identify and delineate simple surface features, such as snow-covered areas or surface water extent. A second application involves retrieving information such as land cover, geological features, or other hydrologic parameters by classifying remotely sensed images based on calibration with field data.

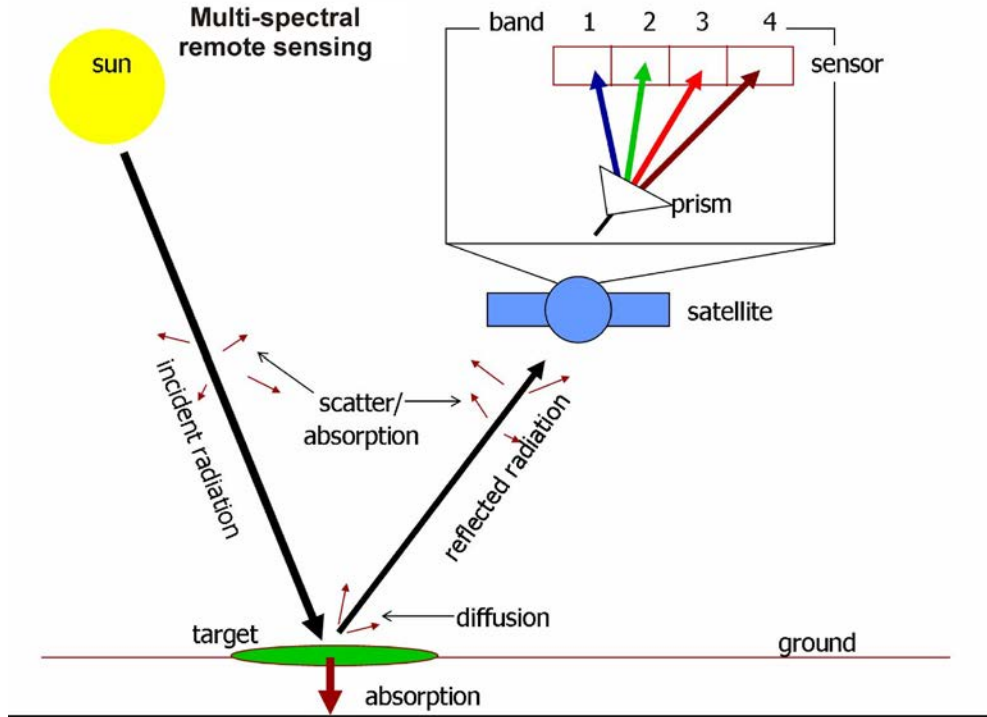


Figure 7.1. Principles of remote sensing. (image from <http://auracle.ca/news/>).

Sensors differ in their spectral bandwidth, spatial resolution, and temporal coverage (Pietroniro and Leconte 2000; Table 7.1). Remote sensing of peatlands can be done using optical and near infrared (NIR) sensors (400 to 2500 nm) that measure reflectance of surface vegetation and ground, as well as microwave sensors that measure peat dielectric properties (Krankina et al. 2008). The most extensively used optical and NIR sensors for high latitude research (Pietroniro and Leconte 2000) include NOAA's (National Oceanic and Atmospheric Administration) Advanced Very High Resolution Radiometer (AVHRR, 8 km), moderate resolution imaging spectroradiometer (MODIS) onboard NASA (National Aeronautics and Space Administration) Terra and Aqua satellites (250 m to 1 km), and Landsat's Thematic Mapper (TM 15 to 30 m). These provide broad landscape coverage at low resolution. Other satellites that must be aimed at the location of interest provide less coverage but at higher resolution (e.g., System pour observation de la terre [SPOT], 5 to 20 m; IKONOS, 1 to 4 m; QuickBird, 0.6 to 2.4 m). These satellites acquire images in broad, sometimes non-contiguous bands. Satellites that simultaneously acquire images in many, narrow, contiguous, spectral bands (e.g., Hyperion and CHRIS satellites, 18 to 36 m resolution) are referred to as *hyperspectral*. Hyperspectral remote sensing data offers a more detailed view of the spectral properties of a scene than the more conventional broadband data (Harris and Bryant 2009b).

Despite recent advances in data processing and sensor technology, optical/NIR remote sensing is limited by frequent cloud cover, atmospheric aerosols, shadowing, and reduced solar illumination common to high-latitude environments (Sitch et al. 2007). In contrast, microwave wavelengths are largely independent of solar illumination, cloud cover, and other atmospheric attenuations. Current microwave satellite sensors can potentially be used to resolve trends at better temporal (i.e., daily) accuracy than existing optical and NIR-based satellite records, but whether they can accurately resolve these trends at finer (<25 km) spatial scales is less certain, resulting in a trade off between spatial and temporal fidelity (Pietroniro et al. 2005). For example, SeaWinds and European Remote Sensing (ERS) scatterometers and the Special Sensor Microwave/Imager (SSM/I) radiometer provide high-repeat (≈daily) observations at high latitudes, but for coarse (25 to 50 km) scales. Synthetic aperture radars (SARs), such as Radarsat (Figure 7.2) and ERS-1/2, provide finer (3 to 200 m) spatial resolutions, but with reduced (10 to 168 day) temporal fidelity.

Table 7.1. Common satellite sensors used for land cover mapping and their associated spectral and spatial resolutions.

Satellite sensor	Launch date	Spectral bandwidths ^a	Spatial resolution
Multi-spectral			
AVHRR	1981		8 km (10-15 days)
MODIS	2001	Red Near infrared Blue Green Infrared Shortwave-IR Shortwave-IR	1 km (8 – 16 days) 250 m 250 m 500 m 500 m 500 m 500 m
Landsat ETM+	1999	Blue: 450-515 nm Green: 525-605 nm Red: 630-690 nm NIR: 750-900 nm MIR: 1550-1750 nm TIR: 10400-12500 nm SWIR: 2090-2350 nm PAN: 520-900 nm	30 30 30 30 30 60 30 15
ASTER		Visible and NIR (3 bands) SWIR (6 bands) TIR (5 bands)	15 30 90
SPOT-5 (4)	2002	Blue: 500-590 nm Green: 610-680 nm Red: 790-890 nm SWIR: 1580-1750 nm PAN: 510-730 nm	10 (20) 10 (20) 10 (20) 20 5 (10)
IKONOS	1999	Blue: 445-516 nm Green: 506-595 nm Red: 632-698 nm NIR: 757-853 nm PAN: 450-900 nm	4 4 4 4 1
QUICKBIRD		PAN (1 band) Multi-spectral (4 bands)	0.6 2.4
Hyperion ^b	1999	Hyperspectral: 400-2500 nm; 220 bands in 10 nm resolution	30
CHRIS ^b	2001	Hyperspectral: 400- 1050 nm; 19-63 bands 1.3-12 nm resolution	18-36
Radar			
SeaWinds and European Remote Sensing (ERS)	Scatterometer		25-50 km (≈daily)
Nimbus 7	Scanning Multi-channel Microwave Radiometer (SMMR)	18, 37 GHz	30 km (0.5 days)
DMSP	Special Sensor Microwave/Imager (SSM/I) radiometer	19, 37, 85 GHz	25-50 km (≈daily)
MOS-1	Microwave Scanning Radiometer (MRS)	23, 31 GHz	23-32 km (0.5 days)
Aqua	Advanced Microwave Scanning Radiometer (AMSR)	6.9 10.7 GHz	36-58 km (daily)
Radarsat	Synthetic Aperture Radar (SAR)	C band 5.3 GHz HH ^c	3-200 m (10-168 days)
ERS-1/2	Synthetic Aperture Radar (SAR)	C band 5.3 GHz VV ^d	
Envisat	Advanced SAR	C band 5.3 GHz HH, VV, HV ^e , VH ^f	

^a NIR, near infrared; MIR, mid infrared; TIR, thermal infrared; SWIR, shortwave infrared; PAN, panchromatic.

^b Experimental prototype sensors.

^c HH = transmitted waves are polarized in the horizontal direction, and the antenna only received horizontally polarized radiation.

^d VV = both transmit and receive, vertically polarized waves.

^e HV = transmitted waves are polarized in the horizontal direction, and the antenna only received vertically polarized radiation.

^f VH = transmitted waves are polarized in the vertical direction, while the received waves are restricted to those waves horizontally polarized.

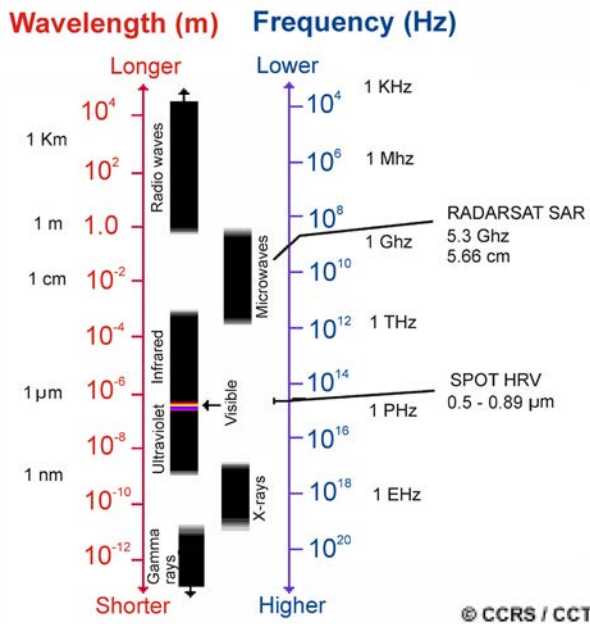


Figure 7.2. The electromagnetic spectrum showing the wavelengths covered by Radarsat (visible radiation) and Spot (microwave radiation); image from <http://www.nrcan.gc.ca/earth-sciences/geography-boundary/remote-sensing/fundamentals/1639>.

Remote sensing of vegetation using optical and near-infrared sensors

The spectral characteristics of objects in the visible (Figure 7.3) and shortwave infrared (SWIR; Figure 7.4) regions depend on their chemical and biophysical properties, and on viewing and illumination geometry (Ulrich et al. 2009). Differences in reflectance spectra, and particularly in specific absorption features, can be used to differentiate a variety of surfaces. Three major spectral groups can be distinguished: vegetation, bare soil, and surface water (Figure 7.5). The spectral surface signatures are usually complexes of mixed signals influenced by type and state of vegetation, soil surface features, and moisture content of soils and vegetation.

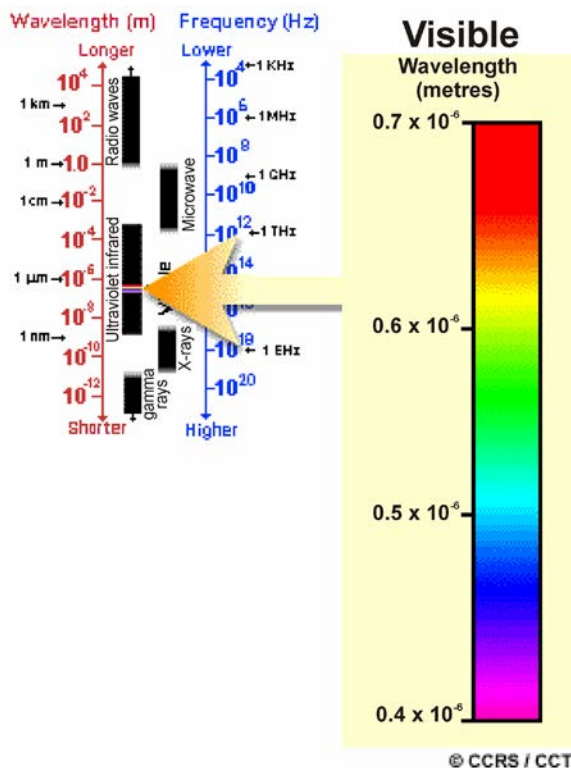


Figure 7.3. The visible range of the electromagnetic spectrum; image from <http://www.nrcan.gc.ca/earth-sciences/geography-boundary/remote-sensing/fundamentals/1639>.

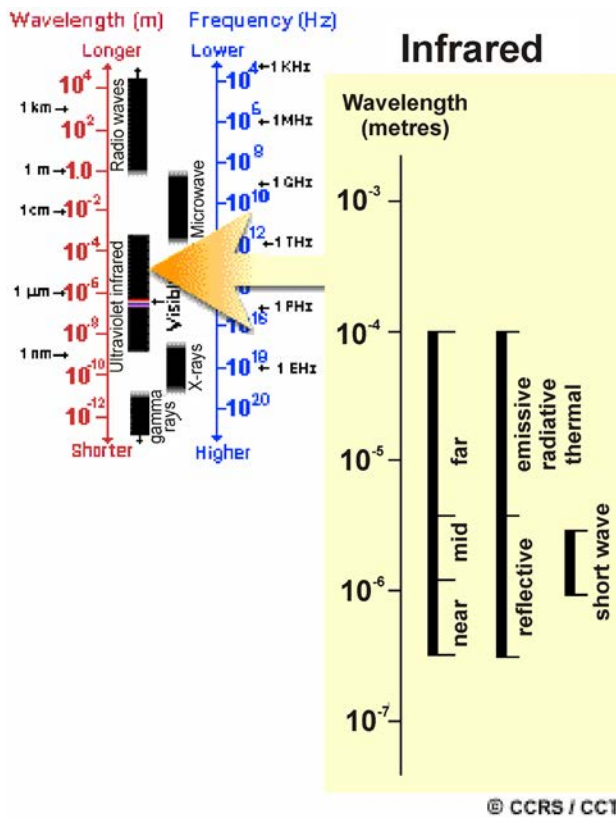


Figure 7.4. The infrared range of the electromagnetic spectrum; image from <http://www.nrcan.gc.ca/earth-sciences/geography-boundary/remote-sensing/fundamentals/1639>.

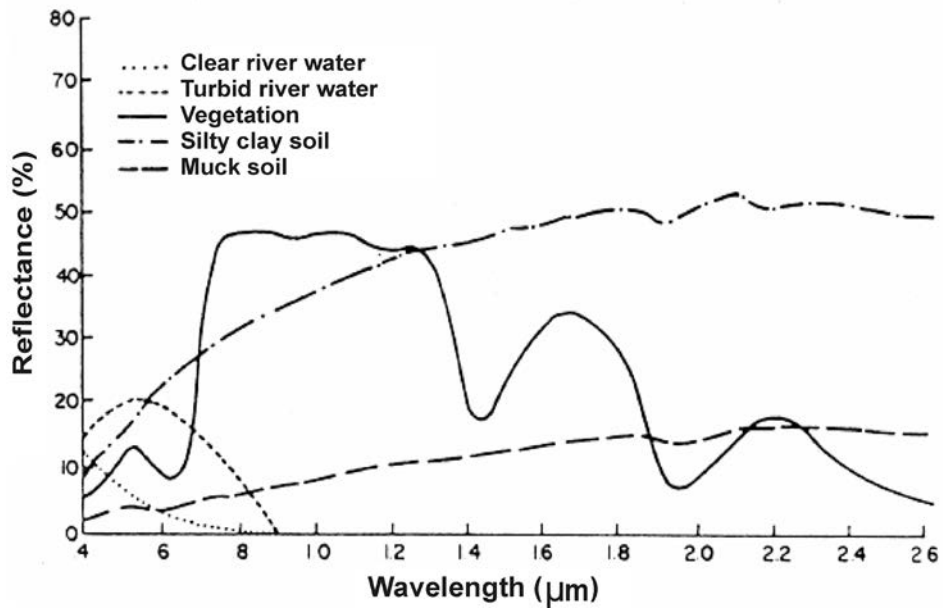


Figure 7.5. The spectral signatures of soil, water, and vegetation; image from <http://www.fao.org/docrep/003/W0615E/W0615E02.HTM>.

Detecting surface water bodies is one of the most straightforward optical remote sensing procedures (Pietroniro and Leconte 2005). The reflectance of water is low in all spectral ranges, because water absorbs most energy in the near- and middle-infrared wavelengths (0.8 to 2 μm), whereas vegetation and soil have higher reflectance in these wavelengths. Complications can arise when lakes or wetlands are surrounded by significant amounts of submerged vegetation, are covered with floating and emergent vegetation, or have high suspended sediment loads.

The spectral signature of bare soil typically increases with wavelength in the visible range and stays relatively constant in the NIR and SWIR range. It is affected by soil moisture, texture, mineral content, and organic matter (Ulrich et al. 2009). For example, a coarse grained, wet soil has lower reflectance than a fine grained, dry soil. Generally, reflectance decreases when soil moisture increases. However, estimating soil moisture using distinct water absorption features is difficult when the soil is covered by vegetation. Radar remote sensing is a better approach than optical remote sensing for measuring soil properties such as moisture content (Pietroniro et al. 2005).

Much of the use of optical remote sensing has been confined to identifying and monitoring patterns of vascular vegetation (Sitch et al. 2007). The spectral reflectance of vegetation is influenced by leaf pigments (mainly chlorophyll), cellulose and lignin in dry vegetation, cell structure, water content, and canopy structure, all of which may vary with a plant's phenological stage (Ulrich et al. 2009). In peatlands, the three main plant functional types (mosses, sedges, and shrubs) differ in structure and biochemistry. This includes differences in leaf construction (vascular vs. non-vascular), water and pigment content, and architecture (Schaepman-Strub et al. 2009) that result in distinct spectral characteristics at both the leaf and canopy level. Bubier et al. (1997) found distinctly different spectral characteristics among *Sphagnum*, feathermosses, and brown mosses, and vascular plants and lichens in the visible, NIR, and SWIR ranges of the spectrum (Figure 7.6). In the visible portion of the spectrum, mosses exhibit typical plant absorption in the blue and red regions, but differ from vascular plants in having a 'green' peak reflective of the colour (red, brown, or green) of the individual species. The overall reflectance of mosses in the SWIR is lower than that of vascular plants because of the high water content in moss tissue, whereas lichen has higher reflectance in SWIR than mosses and vascular plants due to drier tissues (Bubier et al. 1997). Ericoid species can also be spectrally differentiated based on low NIR reflectance (Schaepman-Strub et al. 2009). The differences between species and functional groups are based on narrowband spectral reflectance characteristics in the visible and NIR regions, highlighting the utility of hyperspectral over broadband approaches. Libraries of spectral signatures have been developed to catalogue common species and peatland landcover types (e.g., Peltoniemi et al. 2008). These extensive data sets serve as a unique reference for interpreting plant community types from imagery (Figure 7.7).

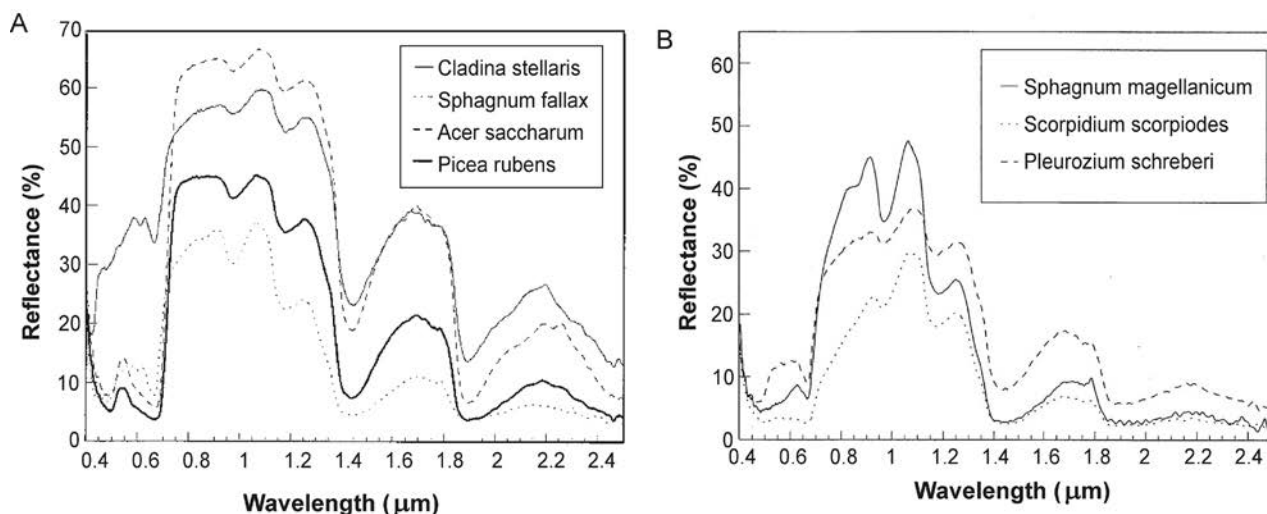


Figure 7.6. Differences in spectral characteristics for selected examples of (a) conifer, broadleaf, moss, and lichen plant groups, and (b) three species of moss (Bubier et al. 1997; reprinted with permission from John Wiley and Sons).

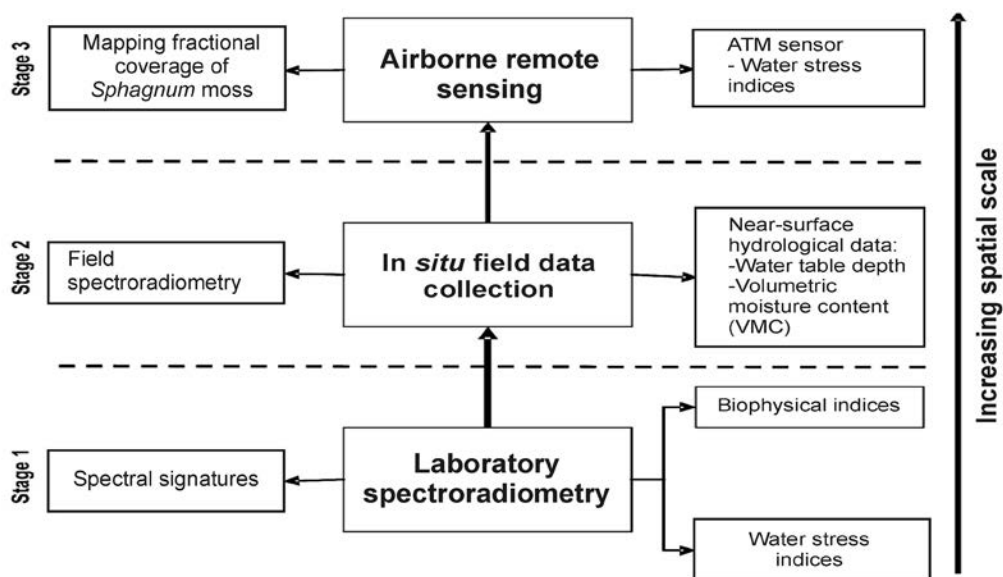


Figure 7.7. Methods used to collect and interpret spectral signatures at different spatial scales (Harris and Bryant 2009a; reprinted with permission from Elsevier).

Optical remote sensing has recently been applied to assess near-surface peatland hydrology using the spectral reflectance signature of *Sphagnum* mosses, a key species in many northern peatland environments (Harris et al. 2005, 2006). *Sphagnum* mosses are extremely sensitive to changes in hydrology, and individual species are adapted to grow at different heights above the water table (Bubier et al. 1997). Because of vast numbers of hyaline cells contained within the plant, its water holding capacity is large. Due to a lack of internal water-conducting tissue, water can only be supplied to the moss capitula by precipitation or capillary rise from the water table (Harris et al. 2005, 2006). Thus, when water availability is low, moisture is readily lost from the hyaline cells, accompanied by an apparent loss of canopy pigmentation, resulting in a whitish appearance (Figure 7.8; van Breemen 1995). Since electromagnetic radiation is readily absorbed by plant pigments and water in specific parts of the electromagnetic spectrum, Harris et al. (2005, 2006) were able to relate the spectral reflectance signature of *Sphagnum* mosses to near-surface hydrological conditions.

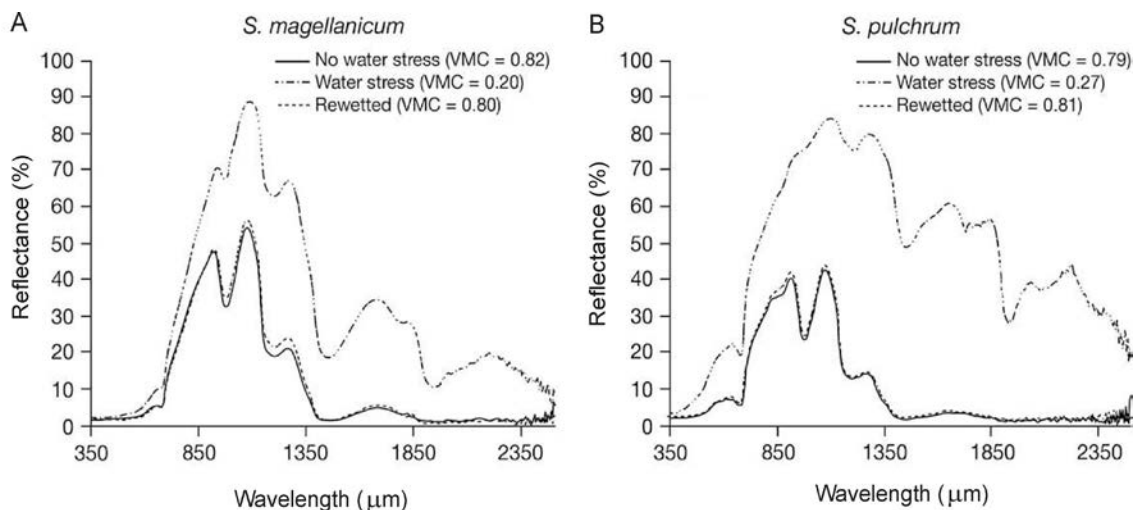


Figure 7.8. Changes in spectral signatures under different soil moisture regimes for the mosses (a) *Sphagnum magellanicum* and (b) *S. pulchrum* (Harris et al. 2005; reprinted with permission from Elsevier).

Remote sensing in the visible and NIR wavelengths is sensitive to the energy absorbed by leaf chlorophyll, which is the ratio of NIR minus red reflectance to NIR plus red reflectance (Table 7.2). This measure, known as the Normalized Difference Vegetation Index (NDVI), is a well established index of land surface 'greenness' (Rouse et al. 1974). The NDVI is well correlated with leaf area index (LAI), leaf biomass, and potential photosynthesis, and is useful for biosphere studies of the spatial distribution of plants and their seasonal functioning (Sitch et al. 2007). The simple ratio (NIR/red) and the reduced simple ratio $(\text{NIR/red} * (1 - (\text{SWIR} - \text{SWIR}_{\min}) / (\text{SWIR}_{\max} - \text{SWIR}_{\min})))$ are similar 'greenness' indices (Sonnentag et al. 2007). Other spectral indices in the SWIR (2020 to 2200 nm) range have been developed to express the depth of cellulose, lignin, and water absorption as an indicator of peat humification (e.g., the cellulose absorption index, CAI; McMorroo et al. 2004). Other indices in the NIR and SWIR have shown promise for tracking changes in foliar moisture (e.g., floating water band index, Peñuelas et al. 1993, 1997; moisture stress index, Rock et al. 1986), and chlorophyll content (chlorophyll index). Harris and Bryant (2009a) reported that these indices correlated with measures of near-surface moisture in the laboratory, in the field, and from airborne imagery, although the strength of correlations diminished as landscape area increased.

Table 7.2. Examples of spectral indices that have been used to collect information about peatlands.

Spectral index	Formula	Reference
fWBI ₉₈₀	$R_{920} / \min(R_{960} - 1000)$	Peñuelas et al. 1997
fWBI ₁₂₀₀	$R_{920} / \min(R_{1150} - 1220)$	Peñuelas et al. 1997
MSI	$(R_{1150} - 1220) / (R_{760} - 800)$	Vogelmann and Rock 1986
CI	$(R_{750} - 800) / (R_{695} - 700)$	Gitelson et al. 2003

Mapping regions of peatlands using optical and SWIR methods has been achieved at various resolutions. Dissanska et al. (2009) used a semi-automatic object-based method for QuickBird panchromatic image classification of a wetland, obtaining accuracy of 81%. Grenier et al. (2008) used SPOT-4 images to identify five classes of wetlands (bog, fen, marsh, swamp, shallow water) in northern Québec and describe their components (e.g., pool complexes and vegetation structures). Thomas et al. (2002) used airborne Compact Airborne Spectrographic Imager (CASI) to identify peat features within a fen complex near Thompson, Manitoba. Remote sensing at fine resolutions in much of the north is impractical because of the lack of cloud-free imagery for many areas, plus logistical difficulties with handling the enormous volume of data. For frequent observations of large areas, Pflugmacher et al. (2007) found that MODIS provided a good option for extensive coverage at low cost. However, depending on the intended application the low resolution can limit its usefulness. Moderate resolutions, such as those available from Landsat TM and ETM+, provide a reasonable compromise. Roulet et al. (1994) created 16 classes of peatlands for a 4800 km² area north of Moosonee, Ontario, and a 900 km² area near Churchill, Manitoba, in the Hudson Plain, which they used to scale CH₄ measurements. Krankina et al. (2008) used Landsat TM to differentiate peatlands in the St. Petersburg area of Russia. Sonnentag et al. (2007) used Landsat TM to classify the Mer Bleue bog near Ottawa, Ontario.

Mapping peatland hydrology using active and passive microwave sensors

Microwave remote sensing detects longer wavelengths of radiation (1 mm to 1 m; Figure 7.9). Microwave satellite sensors are either active (i.e., produce own microwave source) or passive (i.e., detect naturally reflected microwave sources). The sensor is sensitive to landscape and vegetation structure, orientation, and dielectric properties associated with variable moisture content in plant biomass, soils, and snow cover (Pietroniro et al. 2005). The ability of microwave sensors to detect changes in the structure and moisture status of various landscape components depends on sensor wavelength, polarization, and spatial resolution, as well as landscape topography, vegetation structure, soil type, and the presence/absence and structure of snow cover. Under similar conditions, longer wavelengths (e.g., L-band) are generally sensitive to a greater volume of surface vegetation and soil media relative to shorter (Ku-C-band) wavelengths (Pietroniro et al. 2005).

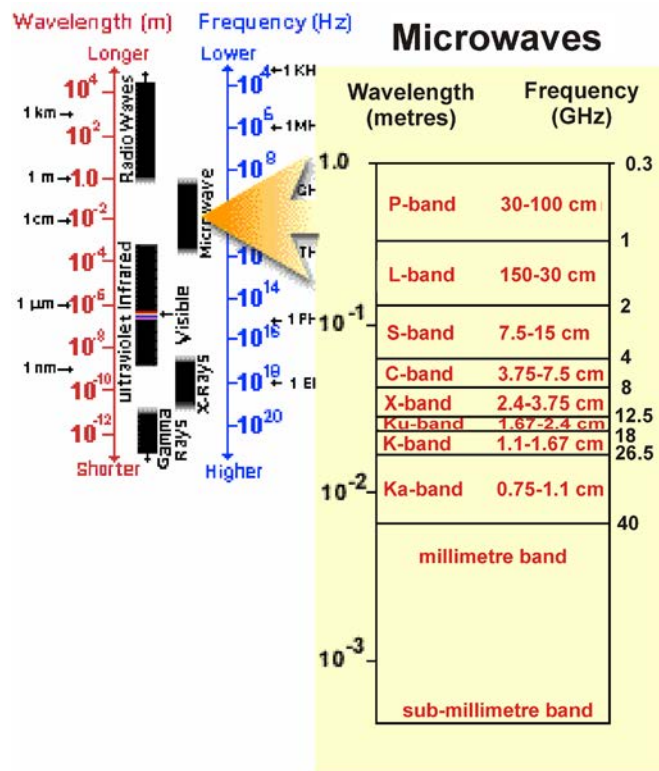


Figure 7.9. The microwave range of the electromagnetic spectrum; image from <http://www.nrcan.gc.ca/earth-sciences/geography-boundary/remote-sensing/fundamentals/1639>.

Delineating open water bodies is most easily done using near- and middle-infrared wavelengths (0.8 to 2 μm) because water absorbs most of the energy in these wavelengths and little remains to be reflected (Pietroniro and Leconte 2005). However, as previously discussed, complications can arise when lakes or wetlands are surrounded by significant amounts of submerged vegetation, are covered with floating and emergent vegetation, or have high suspended sediment loads. Microwave sensors can help to compensate for these problems. However, particularly under windy conditions, ripples and waves can complicate the identification of open water bodies.

Over the last few decades, significant research has been focused on developing remote sensing algorithms for soil moisture (Pietroniro and Leconte 2005) in the ranges of reflected visible and infrared (0.3 to 3 μm), thermal infrared (10 to 12 μm), and active (1 to 50 cm) and passive microwave (1 to 50 cm) wavelengths. Statistical models, such as linear regression between observed radar backscatter and measured soil moisture, are still the most widely used approach. Using multi-temporal fine-mode RADARSAT-1 images in the La Grande River watershed, near James Bay, Québec, Racine et al. (2005) showed that changes in hydrological conditions influenced radar backscatter coefficients. The major difficulty in extracting soil moisture from SAR data is due to the complex interactions among the radar signal and sensor and target characteristics, such as radar incidence angle, vegetation cover, topography, and soil surface roughness.

Despite some of these limitations, Bartsch et al. (2007) used Advanced Synthetic Aperture Radar (ASAR, 150 m x 150 m) to identify peatland types based on seasonal changes in backscatter that were related to differences in the intensity and duration of soil moisture conditions. Baghdadi et al. (2001) demonstrated some of the capabilities of SAR C band for mapping wetlands, showing that cross polarization provided the best separation. The Canadian Wetland Inventory is supplementing the Landsat images with RADARSAT-1 images for mapping wetlands. RADARSAT-2 has the potential to provide greater opportunities for mapping hydrologic conditions in peatlands. With high resolution (3 m) data and multi-polarization, RADARSAT-2 will allow for enhanced soil moisture measurement (Touzi et al. 2007).

Challenges and future work in mapping peatlands using remote sensing

Under-representation of wetland area

Coarse resolution maps can underestimate peatland area, particularly in regions where peatlands are small or hidden by an overstory. Resolutions of 1 km for AVHRR, 250 m for MODIS, and 30 m for Landsat ETM images are limited in their use for identifying peatlands. Rapalee et al. (2001) found that although moss cover maps produced by Landsat TM and AVHRR for a study site near Thompson, Manitoba, were comparable, finer resolution was necessary for detecting smaller wetland features. As spatial resolution continues to improve (e.g., IKONOS-1 1 m; QuickBird 0.6 m panchromatic and 2.4 m multiband images) heterogeneity will be better resolved. Very high resolution images such as IKONOS and QuickBird have shown their usefulness for defining wetland components such as vegetation and watercourses (Grenier et al. 2008), but low spatial coverage limits their application to large areas. Similarly, light detection and ranging (LIDAR) airborne images were successfully used to identify vegetation structures in wetlands, but rarely for large areas, and are limited to capture by airplane. SPOT images with a resolution of 10 m may constitute a good compromise between Landsat ETM and very high resolution images for mapping wetlands.

Mixed spectral signals

Peatland vegetation is often spatially heterogeneous, and separating spatial signatures can be challenging. *Mixed* pixels often occur if the spatial variation in the land cover is smaller than the size of the image pixel (Harris and Bryant 2009a). The multi-layer structure of peatlands, comprising shrubs and open, discontinuous tree canopies underlain by a continuous ground cover of different moss species, reduces the greenness contrast between the canopy and the background, and creates mixed pixels. Development of spectral separation techniques to unmix pixels is an active area of research (Harris and Bryant 2009b). Linear unmixing algorithms do not account for factors such as secondary reflections or multiple scattering effects within the vegetation canopy, necessitating non-linear mixture models (Harris and Bryant 2009a). For example, Harris and Bryant (2009a) used a soft classification technique known as mixed tuned match filtering (mTMF) to unmix each pixel to derive sub-pixel fractional coverage of *Sphagnum* from image data. It does not require spectral identification of all cover types, and only identifies the abundance of *Sphagnum* in each pixel. Sonnentag et al. (2007) mapped tree and shrub LAI in peatlands based on multiple endmember spectral mixing analysis. They found that traditional linear spectral mixture analysis with three endmembers was insufficient to capture the unique and widely varying spectral characteristics of *Sphagnum* mosses without accounting for shadow effects. Pflugmacher et al. (2007) used canonical correlation analysis on the MODIS reflectance bands and the peatland cover fractions to create a multi-spectral peatland cover index (PCI) to differentiate peatlands in the St. Petersburg area of Russia.

Another approach to unmixing pixels is to use a combination of sensors with different and complementary spectral responses (Figure 7.10; Pietroniro and Leconte 2005). For example, Grenier et al. (2007) showed that mapping using the Landsat ETM and RADARSAT-1 images with an object-based classification supported an ecological definition of wetland complexes. Others have demonstrated the usefulness of RADARSAT-1 images combined with optical imagery for wetland mapping, but the contribution of radar images to the definition of wetlands depends on ground conditions when data are acquired. The Canadian Wetland Inventory uses a rule-based method for mapping wetlands with optical, radar, and digital elevation approaches (Figure 7.11; Li and Chen 2005). Landsat TM (30 m resolution) are used as the basis for classifying bog, fen, marsh, swamp, and shallow water at a resolution of 1 ha (Fournier et al. 2007). The inventory will serve as an important baseline data source for Canadian wetland monitoring programs, either by repeating the mapping at specified intervals or monitoring targeted areas (Fournier et al. 2007). In Siberia, a multi-stage approach in which regional wetland typology maps (1:2.5 million scale) were refined by satellite image classifications (Landsat, SPOT, and RESURS 1:200,000 scale), and aerial photography (1:25,000 scale) was applied within wetland complexes.

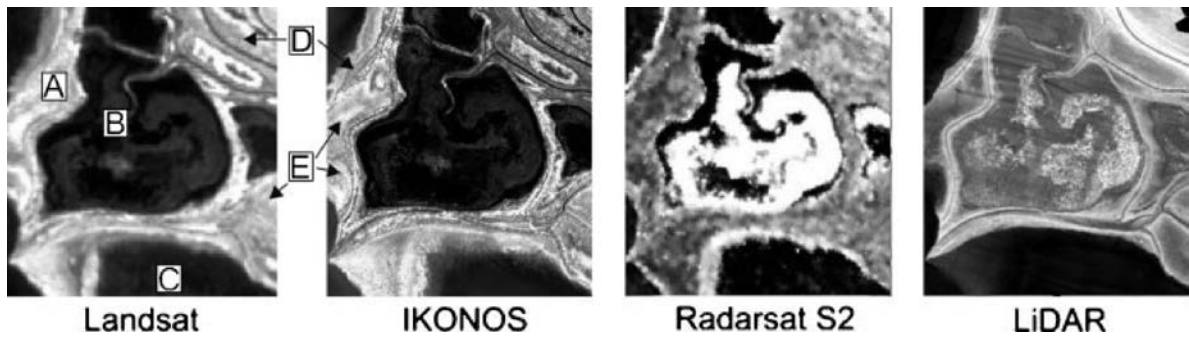


Figure 7.10. A wetland viewed through the lenses of different sensors (Pietroniro et al. 2005; reprinted with permission from John Wiley and Sons).

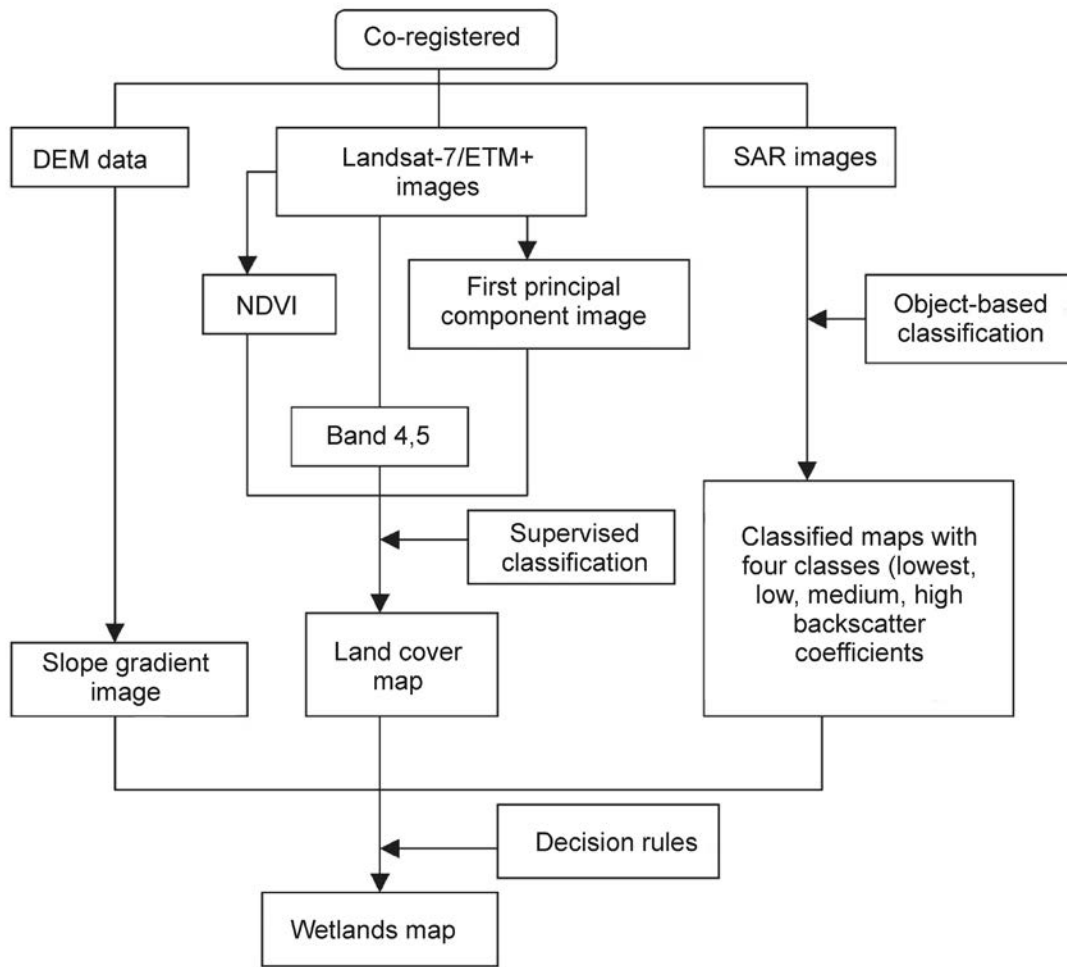


Figure 7.11. The Canadian Wetland Inventory approach for combining digital elevation mapping (DEM), Landsat, and synthetic aperture radar (SAR) data in an object-oriented approach (Li and Chen 2005; reprinted with permission from Taylor and Francis). (NDVI = normalized difference vegetation index, ETM = enhanced thematic mapper)

Narrow or out-of-range spectral bands

Many plants may have unique narrowband absorption and reflectance features occurring in the visible and NIR spectral regions. These characteristics may only be detected and discriminated using hyperspectral reflectance data and not via broadband remote sensing systems (e.g., Landsat TM) (Bubier et al. 1997). Furthermore, many of the operational and higher resolution satellites (e.g., Landsat ETM+ and TM) do not cover the spectral range of the well-defined water absorption bands shown by the *Sphagnum* endmember (Schaeppman-Strub et al. 2009). Thus, narrow or out-of-range spectral bands may be of limited use in peatland systems.

Changing spectral signals

Cover type reflectance varies. For example, even among the same cover types, reflectance varies diurnally and seasonally, which has implications for interpreting satellite and airborne images (Peltoniemi et al. 2008). For example, Ulrich et al. (2009) found that field spectra have low reflectance despite high vegetation vitality due to the very moist surface conditions and minimal vegetation cover. They suggested that to provide a basis for detecting and evaluating environmental changes in the periglacial landscapes of the Arctic, investigators should consider seasonal and long-term variations in spectral signatures.

Mapping permafrost

General patterns

The extent, timing, duration, and depth of the near-surface soil freeze and thaw affect plant growth, energy, water, and trace gas exchanges between the atmosphere and soil in cold seasons/cold regions (Zhang et al. 2004). The presence of seasonally frozen ground influences land surface energy and moisture balance due to the substantial difference in thermal and hydraulic properties of frozen and unfrozen soils. Changes in thermal and hydraulic properties of permafrost peatlands will affect energy and moisture exchange between the atmosphere and the land surface. The presence of frozen ground also influences land surface hydrological processes primarily due to the inhibition of ground water recharge and movement and increased runoff.

Conventionally, the extent of permafrost zones has been represented in terms of the continental-scale pattern of air temperature isotherms. For example in Canada, permafrost zones correspond to -8, -6, and -1 °C isotherms for continuous, discontinuous, and sporadic permafrost (French and Slaymaker 1993; also see section 1, Introduction). However, approaches for delineating permafrost at finer resolution (Zhang et al. 2004) include (1) traditional methods, which involve interpretation of various kinds of data from boreholes and wells, (2) geophysical methods, (3) remote sensing methods, and (4) numerical modelling methods.

Traditional methods

Three methods are commonly used to determine the thickness of the peat active layer: direct measurement of ground temperature by multiple sensors, ground probing, and less commonly, thaw of a water column in a thaw tube (Harris et al. 2009). Ground temperature profiles are compiled by careful interpolation between adjacent sensors and the base of the active layer is determined from the position of the 0 °C isotherm. Ground probing is done with a thin rigid rod containing a temperature sensor at its tip, an approach that is suitable for both wide-ranging reconnaissance field surveys and for long-term investigations at an undisturbed site. The location of the probe tip at refusal depends on the unfrozen water content of the soil. Timing of measurements is important. Measurements taken at the end of the thaw season may be affected by freezing in lower soil profiles resulting in an underestimate of the depth of the active layer. Measurement of the 0 °C isotherm provides the only reliable method of monitoring ALT in a manner that is both repeatable from year to year and informative regardless of site location and investigator.

Hinkel and Nelson (2003) determined thaw depth in northern Alaska through replicated measurement at 121 nodes on seven 1 km² grids, each consisting of precisely surveyed stakes anchored in ice-rich permafrost at 100 m horizontal intervals. Thaw depth was determined using the ground probing method. Probing was carried out in mid- to late August, when thaw depth was near its seasonal maximum. They found significant intra-site variation in

thaw depth and near-surface soil moisture content within each 1 km² grid, reflecting local influence of vegetation, substrate properties, snow cover, and terrain. Due to spatial and temporal variability resulting from microtopography and temporal variations in soil moisture, this method is ineffective for mapping of thaw depth for large landscapes.

Geophysical methods

Several geophysical approaches have been used to detect permafrost (Harris et al. 2009a,b). Three commonly used parameters for differentiating between frozen and unfrozen material include electrical resistivity, dielectric permittivity, and seismic compressional- and shear-wave velocities.

Electrical resistivity in moist porous rocks and soils increases markedly at the freezing point and in fine-grained soils increases exponentially until most of the pore water is frozen. Resistivity methods that take advantage of these properties include electrical resistivity tomography (ERT), electromagnetic induction mapping (EM), and ground penetrating radar (GPR). A good method for determining ice content, which was used by Ross et al. (2007) to study the internal structure of pingos, is ERT. Maurer and Hauck (2007) used EM as one of the techniques to study the internal structures of rock glaciers in the Alps. The most commonly used resistivity approach is GPR, which is particularly good for determining ALT. It is best suited to investigating the unfrozen active layer in summer and ice-rich permafrost. The popularity of GPR has increased in recent years as instrumentation has become less expensive, but the heavy and cumbersome equipment limits its wider usage. This method has been more frequently applied to study permafrost in mineral soils and sediments (e.g., Stevens et al. 2009; Jorgensen and Andreasen 2007; Munroe et al. 2007; Wu et al. 2009) than in organic soils (e.g., Bradford et al. 2005).

Dielectric permittivity, which governs the propagation speed of georadar waves, also changes significantly between frozen and unfrozen material, with the dielectric constant having values of 3 to 4 for ice, around 6 for frozen sediment, 25 for unfrozen sediment, and 80 for fresh water. Microwave remote sensing is an example of a method that uses this property and is discussed in greater detail below.

In most moist porous materials, seismic compressional- and shear-wave velocities increase sharply on freezing, with the increase being more pronounced as porosity increases. Refraction seismic techniques and crosshole methods are examples based on this property and have a long tradition in permafrost studies (e.g., Zimmerman and King 1986).

Often more than one geophysical method is used in a given study to improve interpretation in terms of permafrost delineation, ice content, or stratigraphy (Harris et al. 2009). Common complementary methods include ERT (which distinguishes between ice and air) and refraction seismics (which distinguish between ice and water) and ERT and GPR (which provide structural information).

Remote sensing methods

Remote sensing of surface freeze/thaw cycles typically uses radiometers (e.g., Advanced Microwave Scanning Radiometer on Earth Observing System, AVHRR, and MODIS) and scatterometers from passive and active microwave sensing (e.g., SAR) (Zhang et al. 2004, Jones et al. 2007). These sensors provide information on the timing, duration, and regional progression of the near-surface soil freeze/thaw cycle.

Data from passive microwave sensors, such as SMMR (1978 to 1987) and SSM/I (1987 to present) can be used to detect surface soil freeze or thaw based on the spectral sensitivity of brightness temperatures to the state of water in the near-surface soil (Figure 7.12). Separation of surface temperature and emissivity from the measured brightness temperature at 19 and 37 GHz is achieved after atmospheric correction using empirical relationships with surface emissivity at horizontal and vertical polarizations over snow- and ice-free land surfaces (Mialon et al. 2005). Their advantages are continuity, global coverage, and frequent repeat time, ensuring that temporal and spatial variations of surface soil freeze and thaw can be detected. The disadvantage is low resolution (30 to 100 km) (Duguay et al. 2005). The Advanced Microwave Scanning Radiometer-Earth Observing System (AMSR-E), launched in 2002, has lower-frequency channels and higher resolution, which may be superior for detecting soil freeze/thaw cycles. Synthetic Aperture Radar imaging also provides information on the timing, duration, and regional progression of the near-surface soil freeze/thaw status with a relatively high spatial resolution, but repeat

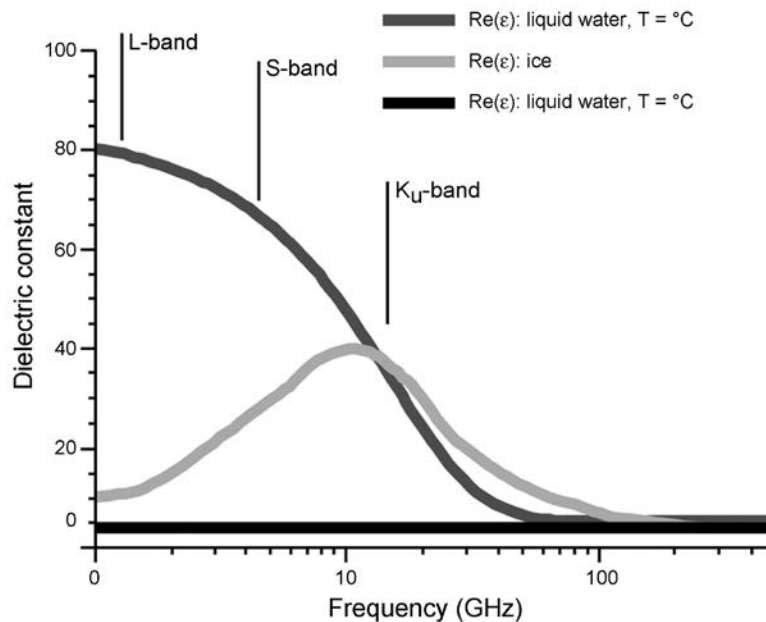


Figure 7.12. Dielectric and frequency relationships for L-, S-, and Ku-bands for phases of water remotely sensed with radar (Zhang et al. 2004; reprinted with permission from Taylor and Francis).

times are long compared to the rate of change of soil freeze/thaw cycles in autumn and spring (Zhang et al. 2004). Scatterometer data from various platforms such as ERS-1, NSCAT, and QuikScan can also be used to detect near-surface soil freeze/thaw status, similar to analysis from passive microwave sensors but with relatively coarse resolution.

Overall, microwave remote sensing is a promising technique for detecting near-surface soil freeze/thaw cycles over snow-free land. Land surface temperatures from these sensors can be used to drive numerical models that simulate the development of the active layer or to estimate thawing index and ALT. The disadvantages of these sensors are related to the effects of clouds, which can interfere with time series sampling, and inconsistent validation standards among regions (Zhang et al. 2004). Results of surface soil freeze and thaw detected from microwave sensors (both active and passive) require validation against empirical (ground) measurements, especially when snow is present at the time of image acquisition.

Terrain analysis

Given the unique geomorphic characteristics of permafrost features such as palsas, analyses using digitally derived terrain attributes have been used to map their distribution. For example, Luoto and Seppälä (2003) classified the distribution of palsas in Lapland with 97.7% accuracy using a multiple logistic regression that included the area of wetland, the proportion of flat topography, water cover, and elevation of the lowest point. Similarly Hjort et al. (2007) could accurately predict palsa distribution in subarctic Finland using mean slope angle, peat cover, and water cover. The use of terrain analyses in combination with other remotely sensed data sources for mapping the distribution of permafrost features is likely to be well researched in coming years (Hjort and Luoto 2009).

Numerical modelling

Modelling permafrost depth is a challenge in part because ALT is more heterogeneous than aboveground climate variables. This is because ground conditions (e.g., organic layers, soil moisture, soil texture, and snow cover) modify the response of ground temperature to atmospheric climate. Approaches for modelling permafrost have been empirical or semi-empirical as well as process-based.

Empirical and semi-empirical models

Anisimov and Nelson (1997) produced a map of permafrost distribution based on calculating a 'surface frost index', as described by Nelson and Outcalt (1987). The index is a dimensionless number related to the zonal arrangement of permafrost, assuming that permafrost is in equilibrium with the climate used to derive it. The premise is that the occurrence of permafrost depends on the ratio of potential depths of seasonal freezing and thawing (Equation 7.1).

$$F_+ = \frac{DDF_+^{1/2}}{DDT^{1/2} + DDF_+^{1/2}} \quad (7.1)$$

where DDF_+ represents the annual degree days of freezing, adjusted for the effects of snow cover, and DDT is the annual degree days of thawing, with degree day sums calculated from monthly air temperature. When the ratio exceeds 1.0 for two or more consecutive years, permafrost is present. Conversely, where the ratio is less than 1.0, only seasonal frost is expected, unless relic permafrost is present.

A thermal adjustment is made for snow-cover effects based on a negative exponential expression using computed values of winter snow depth, density, and thermal diffusivity, with snow falling early in the winter assigned a greater effect than that in midwinter or spring (Anisimov and Nelson 1997). The surface frost index used to represent the threshold boundaries of continuous, discontinuous, and sporadic permafrost were 0.67, 0.60, and 0.50, respectively, based on calculations involving a variety of soils (Nelson and Outcalt 1987). Maps produced using the frost index were found to be most effective to depict large (continental or hemispheric) areas of potential permafrost distribution (Anisimov and Nelson 1997), and corresponded with empirical maps. Christensen and Kuhry (2000) applied this index to a high-resolution present-day climate simulation over the Arctic part of European Russia and found that the index was useful in delineating permafrost zones.

A climate index approach was also used by Fronzek et al. (2006). They predicted palsa distributions in subarctic Fennoscandia based on annual precipitation, a continentality index (maximum – minimum of monthly mean temperatures), thawing degree days, and freezing degree days using five different modelling frameworks: generalized linear modelling, generalized additive modelling, classification tree analysis, artificial neural networks, and multiple adaptive regression splines (Fronzek et al. 2006). All of the model results have generally agreed with the observed palsa distribution, suggesting a strong dependence on climate.

Smith and Riseborough (1996, 2002) proposed a semi-empirical functional model of the permafrost-climate relationship that accounted for geographic variations of climatic, surface, and soil factors that control ground thermal regime. They argued that process-based models founded on surface energy exchange, while useful in understanding the detailed physics of the permafrost-climate relationship, are impractical beyond the site-level because of the lack of data characterizing the microclimates of a broad range of vegetation and terrain conditions. Based on work by Lachenbruch and Sass (1988), Smith and Riseborough (1996) represented the permafrost-climate relationship based on the temperatures at three levels: MAAT, MAGT, and top of permafrost (TTOP) (Figure 3.3). This functional model links air, surface, and permafrost temperature through seasonal surface transfer functions and subsurface thermal properties. The TTOP results from the interplay between the air temperature, the nival (snow) offset, and the thermal offset (Equation 7.2). These offset values vary systematically and geographically with freezing and thawing indices, snow cover conditions, and ground thermal properties.

$$TTOP = MAAT + Surface_offset + Thermal_offset \quad (7.2)$$

Explicitly, TTOP is formulated as:

$$TTOP = \frac{(rk * nt * It) - (nf * If)}{P} \quad (7.3)$$

Where rk is the thermal conductivity ratio of thawed to frozen ground, nt is the scaling factor between summer air and ground surface temperatures (i.e., the plant vegetation effect), nf is a scaling factor between winter air and ground surface temperatures (i.e., the snow cover effect), lt is the thawing index for air temperature in degree days, lf is a freezing index for air temperature in absolute degree days, and P is the annual period (365 days).

Henry and Smith (2001) used TTOP to map ground temperature in the permafrost regions of Canada and predicted ground temperatures to within one temperature class covering nearly the entire area of Heginbottom et al.'s. (1995) published permafrost map. Regionally, Wright et al. (2001) reported that the presence or absence of permafrost was correctly predicted at 134 and 154 geotechnical boreholes (87%) in the Mackenzie Valley using the TTOP model. Smith and Riseborough (2002) show that while permafrost is ultimately a climatic phenomenon, the ground thermal conductivity ratio, via the thermal offset, is the critical factor determining the southernmost extent of discontinuous permafrost, while snow cover, via the nival offset is the critical factor determining the northern limit of discontinuous permafrost. This results in a diffuse transition in the disappearance of permafrost in the south, but a more abrupt transition to continuous permafrost in the north. Similar formulations of the TTOP model that rely on a simplified version of heat transfer in a solid medium (Stefan's solution) have been used with success by others investigating permafrost conditions (e.g., Shiklomanov and Nelson 2002; Stendel and Christensen 2002). For example, Shiklomanov and Nelson (2002) found a simple, spatially distributed active layer model provided reasonable representation of thaw depth for each landcover category and physiographic province within north-central Alaska and provided estimates of the total regional volume of thawed soils (Shiklomanov and Nelson 2002).

Physical models

In contrast to the index-based approaches, physical-based one-dimensional conduction models provide a more sophisticated analysis of the energy components, without the restrictive assumption of stationarity or equilibrium conditions (Zhang et al. 2003). Soil temperatures are simulated by solving the heat conduction equation with a finite element method subject to prescribed upper and lower boundary conditions (Goodrich 1982). This method of soil temperature simulation factors in nonlinear material properties, solid-liquid phase, and latent heat changes. It includes the thermal effect of snow cover but does not include capillary moisture transport or convective flows in the ground (Sushama et al. 2006). The two inputs to the model are daily surface temperature and daily snow depth. Sushama et al. (2006) used this model, linked with the Canadian Regional Climate Model to examine trends in near-surface temperatures in northeastern Canada (Figure 7.13). Oelke et al. (2004) used this model over the entire Arctic drainage basin with results indicating high variability in daily thaw depth over permafrost and seasonally frozen ground.

A paradigm shift in modelling occurred when Zhang et al. (2003) combined a permafrost model with a land surface process model. The Northern Ecosystem Soil Temperature (NEST) model simulates soil temperature by

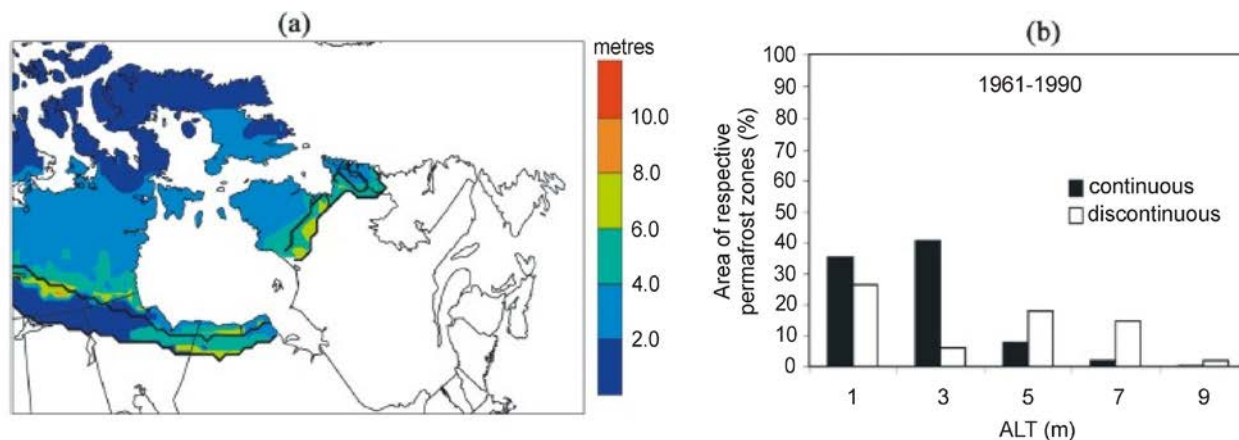


Figure 7.13. (a) Average active layer thickness (ALT, in m) (simulated using SM_CRCM2 model) for the continuous and discontinuous permafrost zones in north central Canada and (b) their distributions for present (1961-1990); average ALT is given for 2 m intervals (Sushama et al. 2006; reprinted with permission from John Wiley and Sons).

solving the heat conduction equation, with the upper boundary conditions on the ground surface (or snow surface during winter) being determined on the basis of energy balance and the lower boundary set at a depth of 35 m as defined by the geothermal flux (Figure 7.14). The effects of climate, vegetation, organic layers, soil texture, snowpack, and soil moisture on ground thermal dynamics are quantified on the basis of energy and water transfer in soil-vegetation-atmosphere systems (Chen et al. 2003). Inputs to the model include information about vegetation (landcover types, leaf area index), ground conditions (thickness of organic layers, texture of the mineral soils, SOC content in mineral soils, ground ice content, and the geothermal flux), and atmospheric climate (air temperature, precipitation, solar radiation, vapour pressure, and wind speed).

Zhang et al. (2005) found that winter soil temperatures were warmer than air temperature, while summer temperatures were cooler. The difference between annual soil and air temperatures varied depending on the combined effects of snow cover, precipitation, organic layers, and vegetation. Organic layers lowered soil temperature because of high porosity, water content, and insulation. Higher precipitation also inhibited soil warming due to higher ET and heat capacity. They determined that ALT ranged from several centimetres in the north to about 3 m in the south, related to the distribution of air temperature, especially in the summer. However, ALT was shallower in the Mackenzie basin and in the southwest of the Hudson Bay Lowlands, because of the high moisture content and low thermal conductivities of the peatlands in these regions (Zhang et al. 2006).

Results from numerical modelling show promise for its application, but the current spatial resolution (e.g., $0.5^\circ \times 0.5^\circ$ for TTOP and NEST) is too coarse to capture the regional heterogeneity of the discontinuous permafrost zone. While vegetation differences may be of secondary importance at coarser scales, they remain an important consideration in permafrost distribution at finer scales (Camill 2000) and new hierarchical approaches are needed that incorporate fine-scale processes and landscape heterogeneity.

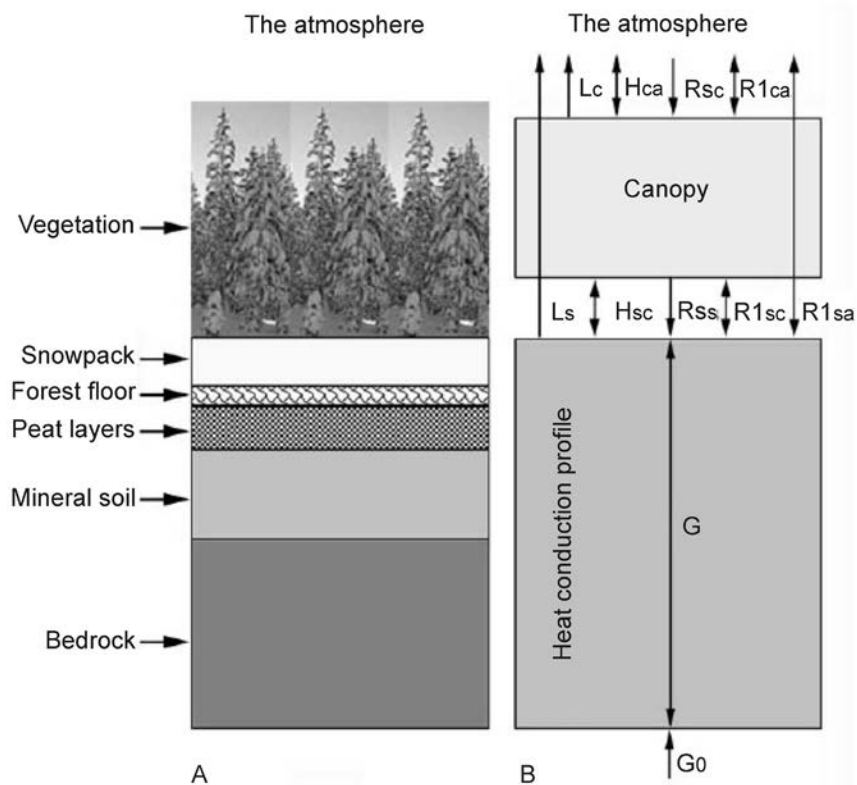


Figure 7.14. (a) Components of the system considered in the Northern Ecosystem Soil Temperature model and (b) energy fluxes between soil, vegetation, and the atmosphere (Zhang et al. 2003; reprinted with permission from John Wiley and Sons). L , H , R_s , R_l , and G are the latent heat flux, sensible heat flux, solar radiation, long-wave radiation, and conductive heat flux, respectively. Subscripts identify fluxes between different components (s , c , and a for ground surface, canopy and the atmosphere, respectively; G_0 is the geothermal flux).

Monitoring permafrost peatlands

Monitoring of permafrost peatlands requires repeated measurements of biophysical variables to detect the magnitude and direction of change over time. Monitoring changes in vegetation, hydrology, and permafrost, requires a suite of techniques.

Vegetation

On the whole, the biomass and the PFT fractional cover of bryophytes, sedges, and ericoid shrubs give a fair indication of the current state of the peatland, which as discussed previously can be assessed by optical remote sensing. Therefore, changes in the PFT fractional cover and other vegetation indices may serve as an early warning system for ensuing changes in peatland structure and C sequestration potential over the longer term (Schaeppman-Strub et al. 2009). Areas affected by disturbance (fire, insect, land clearing) and subsequent regrowth can also be detected and monitored this way.

A common application of remote sensing has been to monitor changes in ecosystem productivity. For example, based on remote sensing approaches that use a 20-year data record of satellite-derived NDVI data, Sitch et al. (2007) showed that the arctic is greening, suggesting increased photosynthetic activity and NPP. Several studies have shown evidence of an increasing trend in vegetation photosynthetic activity and NPP for the northern terrestrial latitudes during the 1980s and 1990s. While the general trend in these observations indicates greening and higher productivity for the region, they also show considerable inter-annual and spatial variability, with many areas of North American boreal forests showing decreased greenness and lower productivity since the late 1990s, which reflects the occurrence of widespread drought (Zhang et al. 2008a). While these satellite observations can provide information about changes in aboveground vegetation and snow cover, they provide little information on belowground processes affecting soil C and N dynamics (Sitch et al. 2007).

Hydrology

Wetland seasonal dynamics and inter-annual variability over northern high latitudes can be relatively easily derived from microwave satellite data (Mialon et al. 2005). Spatial and temporal variation of northern wetland area during the snow-free period is retrieved from the 19 and 27 GHz passive microwave data. For example, this approach was used to determine the total fraction of water surface area for Canada and Alaska as $10.10 \pm 0.21 \times 10^5$ km², representing an 8% increase in water surface area since 1988, attributed to a decrease in the snow cover extent (Mialon et al. 2005). Others have used time series of optical images to detect changes in hydrology. For example, Dissanka et al. (2009) compared old aerial photos to recent QuickBird panchromatic images to assess whether hydroelectric dams were causing increased aquatic area in peatlands. Radar and optical approaches could similarly be used to examine rates of permafrost melt, as palsas and peat plateaus transform to thermokarst ponds (Bartsch et al. 2007).

Permafrost

Degradation of permafrost is a slow process. Ground temperature change in deep soil layers is a delayed and attenuated response to changes in upper layers. For example, in Canada during the 20th century, soil temperature at 20 cm depth increased on average by 0.6 °C, while air temperature increased by 1 °C (Zhang et al. 2005). As discussed previously, the relationship between air temperature and ground temperature is complex, and is influenced by many local factors including surface buffer factors that act to attenuate changes in air temperature (i.e., snow thickness, vegetation type and density, and organic ground cover) and thermal properties of the soil (Smith and Burgess 2004).

Evidence of permafrost changes can be deduced from time series of air photographs or other images, field measurements, or retrospective modelling analyses (Table 7.3). All of these methods of evaluation have shown that permafrost is degrading both in extent and thickness. Field measurements over extended periods yield information about the patterns and processes associated with permafrost thawing (Payette et al. 2004). In Canada, the Circumpolar Active Layer Monitoring (CALM) program has reported on ALT at 15 sites since the early 1990s (Brown et al. 2000). At most of these sites thaw penetration has deepened, reflecting the cumulative effects of ground surface warming and ground ice melting. In general, ALT has increased, but differences among sites can be large; an exception is northern Québec where a cooling trend has been measured by Allard et al. (1995). Increases in ALT have been less in areas with thick organic layers (usually associated with peatlands) than in other areas, as more energy is used for ET in wet areas (Lawrence and Slater 2005).

Table 7.3. Summary of results from retrospective and forecasting analyses of trends in permafrost degradation.

Location	Method	Results	Reference
Retrospective modelling			
Central Manitoba/ discontinuous	Aerial photography	25% of once occurring permafrost still present (period 1947-67)	Thie 1974
Alberta, Saskatchewan, Manitoba	Aerial photography	9% decline in permafrost-affected peatlands since 1850	Halsey et al 1995, Vitt et al. 2000a
Canada	NEST* model	From 1850s to 1990s area underlain by permafrost decreased by 5.4% and mean ALT* increased by 21 cm (34%)	Zhang et al. 2006
Northern Quebec	Field monitoring	Area occupied by palsa decreased 23% in 44 years (1957-2001); 76% of present day thermokarst area formed since 1957	Vallée and Payette 2007
Western Canada	NEST and historic climate records	Over the 20 th century, ALT increased by 124 cm (79%) in isolated and sporadic zones, 59 cm (37%) in discontinuous, and 20 cm (21%) in continuous zone	Chen et al. 2003
Eastern coast of Hudson Bay, northern Quebec, discontinuous permafrost zone	Field survey	Permafrost melted rapidly over the last 50 years (1957-2003) due to increased snow precipitation	Payette et al. 2004
Arctic Alaska	Field survey	Since 1982, abrupt, large increase in the extent of permafrost degradation in northern Alaska associated with record warm temperatures during 1989-1998 due to degradation of massive ice wedges	Jorgensen et al. 2006
Forecast modelling			
Northeastern Canada	Heat conduction model with regional climate simulation using IS92a (1% CO ₂ increase) for period 2041-2070	ALT increased non-uniformly and by more than 50% over most of the continuous permafrost region and by the end of 2070 most of the discontinuous and a small patch of continuous permafrost expected to disappear south of Hudson Bay	Sushama et al. 2006
Northern Hemisphere	Semi-empirical model (Stefan's equation) and coupled atmosphere-ocean GCM* (ECHAM4/OPYC3) using A2 scenario for period 2071-2100	20-40% increase in ALT	Stendel and Christensen 2002
Hudson Bay Lowland	CCCMA GCM and air temperature thresholds for permafrost	Using -5 and -10°C thresholds for continuous permafrost, by 2100 permafrost will be reduced by at least 50%	Gough and Leung 2002
East Siberia	Six GCMs, process model	By 2099, active layer thickness could increase by 0.5 to 2.0 m and ground temperatures by 2 to 6°C	Sazonova et al. 2004
Arctic drainage	Process model	Soil warming is expected to be most pronounced at the surface of continuous permafrost region; ALT may increase significantly for parts of Alaska, northern Canada, and south and east Siberia	Oelke et al. 2004
Northern Hemisphere	Empirical model with 2°C global temperature increase	A 25 to 44% reduction in the total area occupied by equilibrium permafrost; continuous permafrost most severely affected with reductions from 29 to 67%	Anisimov and Nelson 1996
Northern Hemisphere	Empirical model using different GCMs (GFDL89, ECHAM1-A, UKTR) with 2.5°C increase to 2100	All models predict a significant decline in the area of each of the three permafrost zones	Anisimov and Nelson 1997

* NEST – northern ecosystem soil temperature, ALT – active layer thickness, GCM – general circulation model (global climate model).

Using the NEST model and data from climate records, remote sensing, vegetation, and soil features, Chen et al. (2003) simulated soil temperature and ALT for a region of western Canada during the 20th century. Based on the current permafrost map, from the 1900s to the 1986 to 1995 period, ALT increased 124 cm (79%) in the isolated and sporadic discontinuous permafrost zones, 59 cm (37%) in the extensive discontinuous permafrost zone, and 20 cm (21%) in the continuous permafrost zone. The simulated results also indicated that 17% of the permafrost in the discontinuous permafrost zone disappeared between the 1900s and 1940s and another 22% disappeared between the 1940s and 1995. In areas where soil temperatures were within a few degrees of zero and permafrost was more sensitive to climate warming, ALT increased.

The causes of permafrost decline are linked primarily to changes in climate. Ground temperatures are warming due to increased air temperatures, greater snow accumulation, and, for permafrost in riparian areas, changes in water level (Vallée and Payette 2007). Vegetation changes during succession also affect the rate of permafrost degradation. For example, Walker et al. (2003) suggested that increased warming associated with climate change will not necessarily lead to a uniform deepening of ALT, because an air temperature increase could cause the development of a thicker moss layer and denser plant cover, which may reduce ALT. Changes in fire frequency and intensity also affect ALT by decreasing albedo and changing moisture status by removing the overlying canopy (see sections 3, Permafrost Patterns and 7, Fire Regimes).

Forecast modelling indicates that the decline in permafrost extent and thickness Zhang et al. 2008 will continue (Table 7.2). Although a diversity of modelling approaches were used in these studies, the results all indicated that ALT is likely to increase by more than 50% in the permafrost regions, including much of Siberia, northeast Asia, the North Slope of Alaska, and northern Canada (Sushama et al. 2006). Fronzek et al. (2006) suggested the total disappearance of suitable areas for palsa development in some regions by the end of the 21st century. In Canada, about half of the permafrost now occurs in regions with temperatures greater than -2 °C and models suggest that most of this could ultimately disappear in response to climate warming (Smith and Burgess 2004).

Smith and Burgess (2004) mapped the sensitivity of permafrost in Canada to climate warming. Sensitivity was characterized by considering the present ground temperature regime, the thermal response to warming (i.e., the relative rate and magnitude of ground temperature change), and the physical response to warming (i.e., the relative effect of permafrost thaw) (Smith and Burgess 2004). They determined that about 90% of the present permafrost region would have a moderate to high thermal response to increases in air temperature. The northern portions are most sensitive to thermal responses because of limited vegetation and/or snow cover; however, because southern regions have ground temperatures that are greater than -2 °C, the potential for permafrost thaw is greater. The physical response to warming is high in about 13% of the permafrost region, most of which is in the southern portion where the potential for thaw is the greatest. However, extensive areas in the north have massive ice for which the effect of permafrost thaw would be high (Smith and Burgess 2004). This type of analysis helps to identify areas that may be sensitive to thawing and why they are sensitive. Such work provides a good foundation to identify key areas for research and protection, as well as providing the framework for analyzing other risks associated with permafrost thaw, such as GHG production.

Modelling permafrost peatland carbon dynamics

To predict C storage and fluxes in permafrost peatlands, models are required that integrate the biogeochemical controls. Regionally calibrated empirical-statistical models, and physically based process-oriented models are two approaches to achieve this. Empirical-statistical models use correlation and regression analysis to estimate C pools and fluxes for sub-units and then are scaled up using the area of the sub-units. To characterize regional variability, these models require data from sufficient numbers of plots but need only limited input parameters and are quite reliable. However, they assume steady-state conditions and require calibration for each region. These models generally assimilate satellite-based estimates of land surface variables (e.g., land cover type, leaf area index, absorbed photosynthetically active radiation) as major drivers of relatively simple models describing C dynamics in space and time (e.g., net photosynthesis, NPP) (Sitch et al. 2007).

Process-oriented approaches are more complex than empirical-statistical models as they account for more detailed, interacting processes to simulate C dynamics. They are also more data and computationally intensive

(Sitch et al. 2007). This modelling approach cannot occur independently of monitoring and experimentation. Data are required for parameterization, initialization, calibration, and corroboration, and observations of system behaviour are required to improve understanding of how the system works and to refine model algorithms. The use of models allows researchers to examine the natural range of variability of the system as well as the potential effects on and responses of these systems to environmental change.

While process-based models are a useful approach for studying C dynamics, several key uncertainties (Sitch et al. 2007) associated with their use include (1) the accuracy of critical processes in the models (e.g., hydrology, permafrost) and their controls, (2) the accuracy of regional climatic drivers, and (3) changes in the extent and distribution of peatland and permafrost.

Representation of processes

Process representation in models varies in sophistication. Sitch et al. (2007) reviewed different models to assess CO₂ exchange in arctic tundra systems, finding many similarities among the models, but also substantial diversity in representation of critical processes. Models with many parameters may better represent a process, but may be more difficult to calibrate. In addition, processes may be spatially heterogeneous in small landscapes and thus require 'effective' parameters that integrate the process over larger landscapes (e.g., hydraulic conductivity).

Two key processes that continue to challenge those trying to model what is happening in northern peatlands are hydrology and permafrost. Issues with and approaches to modelling permafrost processes were previously discussed. Heterogeneity in surface hydrology that affects C dynamics occurs at resolutions on the order of metres. Scaling this variability to resolutions required for regional models represents a major challenge (Sitch et al. 2007). Furthermore, in low gradient terrain such as the Hudson Bay Lowlands, hydrology is dominated by vertical processes (Woo et al. 2008), leaving precipitation, evaporation, infiltration, and percolation, and their interaction with permafrost and seasonal frost layer, as the mechanisms that affect storage in a soil column (see section 4, Peatland Hydrology). These extensive peatlands consist of wet patches that may or may not be connected, resulting in complicated water flow pathways (Hayashi et al. 2004). Models for peatlands have recently been improved through parameterization, addition of nonvascular plant representation, and accounting for the effect of microtopography on water table heights (Sitch et al. 2007). In addition, some approaches now include presence/absence of permafrost in modelling water table depth and soil thermal dynamics (Zhuang et al. 2001, 2003) but the coupling of these dynamics to hydrological processes is still rudimentary (Sitch et al. 2007).

The McGill Wetland Model (MWM) is a peatland C simulator being developed for global assessments (St. Hilaire et al. 2010). The MWM accounts for the dependence of wetland C dynamics, particularly decomposition, on the position of the water table, which separates the wetland into acrotelm (oxic zone) and catotelm (anoxic zone). Therefore, the model provides an adequate description of the hydrology of these layers, particularly the daily and seasonal variability (St. Hilaire et al. 2006). It also captures differences in the rates of decomposition caused by differences in anaerobic conditions through the peat profile and the progressively more recalcitrant residual material at depth. Furthermore, the uniqueness of the plants that inhabit peatlands is considered, particularly for ericaceous shrubs and mosses, which have unique physiochemical properties (St. Hilaire et al. 2010). Initial testing of the MWM at the Mer Bleue bog in southern Ontario showed that the model captured the primary C cycling processes and simulated the C exchanges to the atmosphere within acceptable error levels when compared to tower measurements, but it needs to be tested in other peatland types (St. Hilaire et al. 2010).

Accuracy of regional climate drivers

Using models to project future responses to climate requires projected climate scenarios. Spatially explicit climate data sets for the Arctic and Boreal biomes that are derived from atmospheric GCM simulations have relatively coarse spatial resolutions and differ substantially among GCMs (McKenney et al. 2010, Sitch et al. 2007). Methods are required to downscale these estimates to regional levels (Stendel et al. 2007). Stendel et al. (2007) found that better simulation results were achieved using finer resolution (50 km grid compared to 300 km grid). The finer spatial resolution allows simulation of greater topographic complexity and finer-scale atmospheric dynamics (Sushama et al. 2006). Specifically, topographic features were better represented, which improved the altitudinal temperature

dependencies, as was the geographical distribution of precipitation (Stendel et al. 2007). Furthermore, when interpreting model outputs, uncertainties in the assumptions associated with the applied GCM need to be considered.

Changes in the extent of peatlands and permafrost

Northern latitudes are becoming warmer and potentially drier (at least during the growing season). These climate shifts are leading to changes in the vegetation composition of permafrost peatlands as well as their extent. In the lower latitudes, peatlands are becoming drier and more shrub rich (Sitch et al. 2007). Furthermore, increasing rates of fire in these areas may convert peatland to forests. In the north, the overall pattern of change in peatland extent is not geographically uniform but appears dependent on the regional extent of current and predicted future permafrost. To better understand potential interactions, permafrost forecasting models need to account for the shifts in vegetation via succession and migration.

Summary and conclusions

Satellite remote sensing is a powerful tool in regional mapping of biophysical variables needed for peatland C research, and provides data for large landscapes and long timelines that are generally not feasible or impractical for field observations. Remote sensing information can be collected to (1) classify plant functional types and their 'greenness' and phenology, (2) detect saturated and inundated soils and open water, and (3) measure permafrost features and other environmental parameters (e.g., surface temperature, snow cover, topography). The most extensively used optical and NIR sensors include AVHRR, MODIS, and Landsat TM. Because these sensors measure at coarse resolution, other satellites (e.g., SPOT, IKONOS, and QuickBird) must be used to collect finer resolution data for smaller landscapes to assess peatland C and its sequestration.

Remote sensing techniques can be used to detect changes in PFTs that may serve as an early warning index for future changes in peatland structure and C sequestration potential in response to disturbance (e.g., climate, fire, insect, industrial development). Remote sensing techniques are also acceptable to measure decadal changes in ecosystem productivity. For example, satellite-derived NDVI indices have frequently provided indications of increased photosynthesis and NPP of boreal and arctic biomes.

Near-surface peatland hydrology can also be delineated using combinations of optical and microwave sensors. Depending on frequency of data collection, microwave sensors can further estimate temporal changes in water surface area that can be correlated to other parameters, such as changes in snow cover extent. In addition, old aerial photographs can be compared to recent QuickBird images to detect increased water surface areas in peatlands created by hydroelectric reservoirs. Microwave imagery, such as SAR (e.g., Radarsat 2), also allows permafrost features to be delineated so that their presence and distribution can be accurately mapped. Furthermore, combining radar and optical imagery can help to assess permafrost thaw rates as indicated by palsa and peat plateau transformations into thermokarst ponds. Microwave imagery is also a promising technique to detect near-surface soil freeze/thaw cycles during snow-free periods. In this instance, land surface temperatures derived from remote sensing can be used as input into numerical models to simulate thawing indices and ALT.

Permafrost features can be predicted using (1) empirical or semi-empirical and (2) physical models. Empirical models based on indices, such as a frost or climate are dimensionless numbers related to the zonal arrangement of permafrost. The premise is that permafrost occurrence depends on the ratio of potential depths of seasonal freezing and thawing. Semi-empirical models account for geographic variations in climatic, surface, and soil factors that control ground thermal regime. For example, the TTOP model describes permafrost-climate relationships based on three levels of temperature: MAAT, MAGT, and TTOP.

In contrast to the index-based approaches, physical-based models provide sophisticated analyses of energy budgets. One such model, NEST, simulates MAGT, from which ALT and permafrost presence or absence can be determined. Inputs to the model include vegetation (land cover types, leaf area index) data collected using satellite remote sensing techniques, ground conditions (thickness of organic layers, texture of the mineral soils, SOC content in mineral soils, ground ice content, and the geothermal flux), and atmospheric climate (air temperature, precipitation, solar radiation, vapour pressure, and wind speed).

Results from numerical modelling show promise for predicting temperature regimes and permafrost presence and distribution. However, the current spatial resolution for semi-empirical and physical models (e.g., $0.5^\circ \times 0.5^\circ$ for TTOP and NEST) is too coarse to capture landscape heterogeneity in the DPZ. While vegetation structure may be of secondary importance in broader landscapes, it remains an important consideration in permafrost distribution and C storage and sequestration at local landscapes. Therefore, new hierarchical approaches are needed that incorporate fine-scale processes and landscape heterogeneity. In addition, further research is required to calibrate spatial and temporal models that use remote sensing imagery as driving variables to constrain peatland water balances, permafrost thaw rates, and C storage and sequestration projections to facilitate land use planning.

8. Climate Change and Peatland Carbon in the Hudson Bay Lowlands

Background

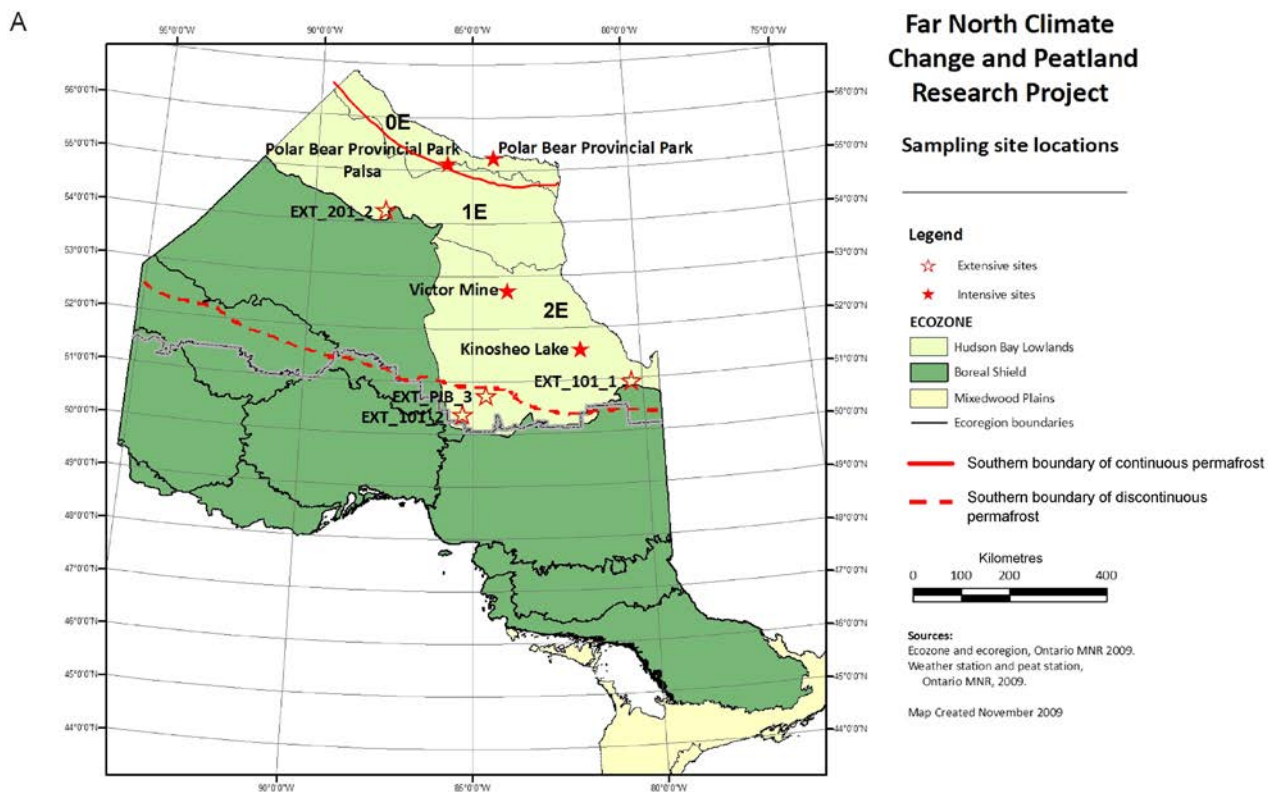
Because of the importance of the HBL to national and provincial C pools, the Federal, Provincial, and Territorial Governments of Canada (FPTGC) identified several uncertainties requiring enhanced research and monitoring data to assess land use and climate change interactions in the HBL (i.e., Hudson Plain Ecozone; FPTGC 2010). Uncertainties (Table 8.1) that inhibit delivery of Ontario's Far North climate change and C storage portion of the planning objective and policy statement have been described at length in previous sections of this report. Therefore, in this section we focus on HBL climate change and peatland C interactions. Here, we synthesize information from previous sections and discuss data from our research projects. We present two hypotheses to estimate current and future peatland C storage and sequestration in the HBL: (1) accelerated permafrost thawing and wetter peat enhances methane emissions in northern ecoregions and (2) increased evapotranspiration and drier peat accelerates carbon dioxide losses through peat decomposition (and possible fire) in southern ecoregions.

Table 8.1. Knowledge gaps and research/monitoring needs associated with Hudson Bay Lowland peatland carbon dynamics (adapted from FPTGC 2010).

Topic	Knowledge gap	Research/monitoring need(s)
<i>Climate</i>	Temperature and precipitation trends	Expand number of full-service weather stations to provide representative geographic coverage
	Soil temperature and moisture	
<i>Permafrost</i>	Active layer depth	Establish and maintain a network of permanent permafrost monitoring sites
	Temperature profiles	
<i>Natural disturbances</i>	Number, intensity, and extent of fires are unknown	Monitor fires at local levels
<i>Peatland succession</i>	Successional trajectories	Post-fire succession Permafrost thaw-induced succession
<i>Hydrology</i>	Flow paths	Water table depth, groundwater flow, and stream and river flow monitoring stations
	Water table depth	
	Stream and river discharge	
<i>Carbon cycling</i>		Monitor C storage and fluxes within an experimental design that lends itself to scaling-up using remote sensing
	Carbon storage	Controls on the fate of peatland carbon Modelling to predict interactions of climate change and management activities on HBL carbon dynamics
	Trends in carbon sink and source function	

To test our hypotheses and develop spatial modelling tools at a range of scales to support Far North land use planning in Ontario, we established various research and monitoring partnerships and collaborations with universities and governmental agencies. Our research and monitoring design includes intensive and extensive study sites along a temperature and permafrost gradient in the HBL (Figure 8.1a). Intensive sites are located at Kinoje (Kinosheo) Lake (51°30'N, 81°28'W; isolated permafrost zone), near Attawapiskat at the Victor Mine (52°49'N, 83°53'W; DPZ), and in Polar Bear Provincial Park (54°98'N, 85°44'W; CPZ). The Victor Mine site is the most studied location because multiple other research and monitoring projects are ongoing at this location. Here, we installed (1) peat stations to monitor peat temperature and moisture at depths from 0.2 to 1.0 m below the peat surface and water table depth in three bogs and three fens and (2) permafrost boreholes in three palsas to measure their active, transient, and frozen layer temperatures. We also estimated watershed peatland types and their C storage and area burned by fire between the 1980s and 2010.

Other studies being conducted at Victor Mine include: (1) CO₂ and CH₄ flux measurements using eddy covariance towers (Mr. Chris Charron, Ontario Ministry of Environment); (2) recent (Dr. Nathan Basiliko, University of Toronto) and long-term (Dr. Sarah Finkelstein, University of Toronto) peatland C dynamics; (3) peatland hydrology, DOC, and mercury cycling and fluxes (Drs. Brian Branfireun, University of Western Ontario and Murray Richardson, Carleton University); (4) peatland C modelling (Drs. Nigel Roulet and Tim Moore, McGill University; Elyn Humphreys, Carlton University and Peter Lafleur, Trent University); (5) peat temperature modelling (Dr. Yu Zhang, Natural Resources Canada, Remote Sensing Centre); and (6) permafrost mapping (Drs. Kara Webster, Natural Resources Canada, Great Lakes Forestry Centre, and Brigitte Leblon, University of New Brunswick). For research areas (3) and (4) above, we are also collaborating with MNR's Inventory Monitoring and Assessment Section (Mr. Adam Hogg) and Water Resources Information Program (Mr. Kent Todd and Frank Kenny). Our ultimate goals are to spatially and temporally measure climate change effects on peatland C storage and sequestration and provide modelling tools for land use planning decisions in the HBL.



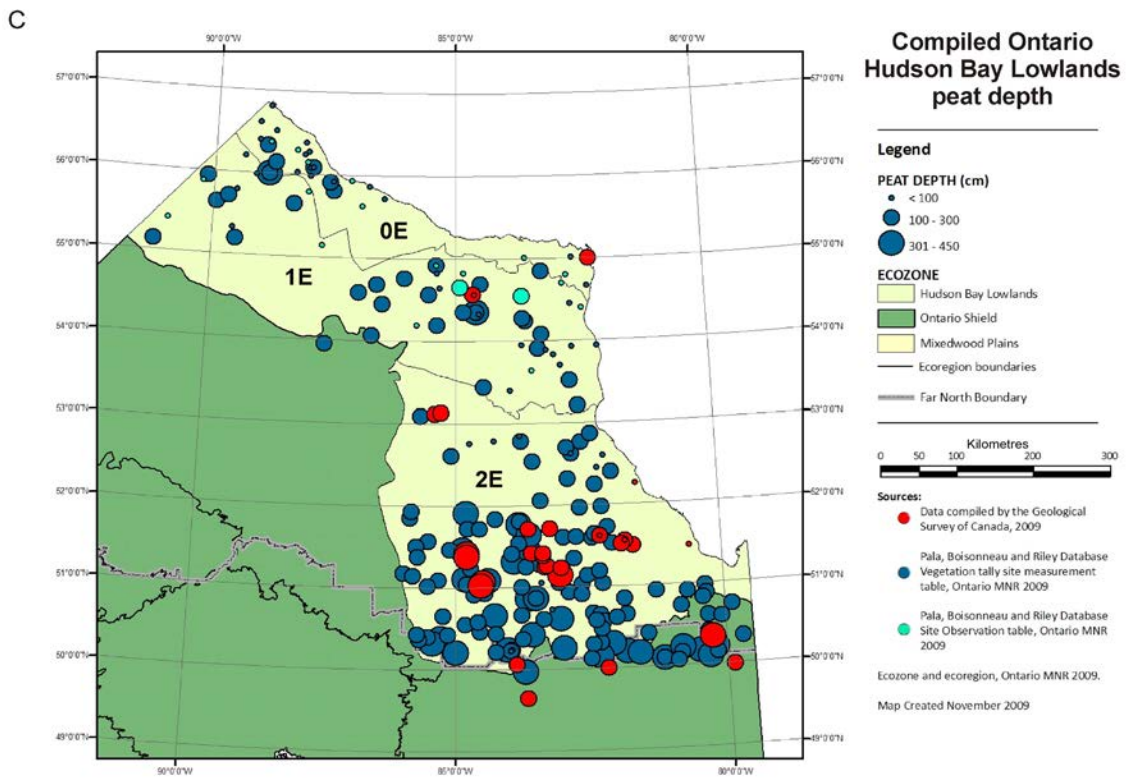
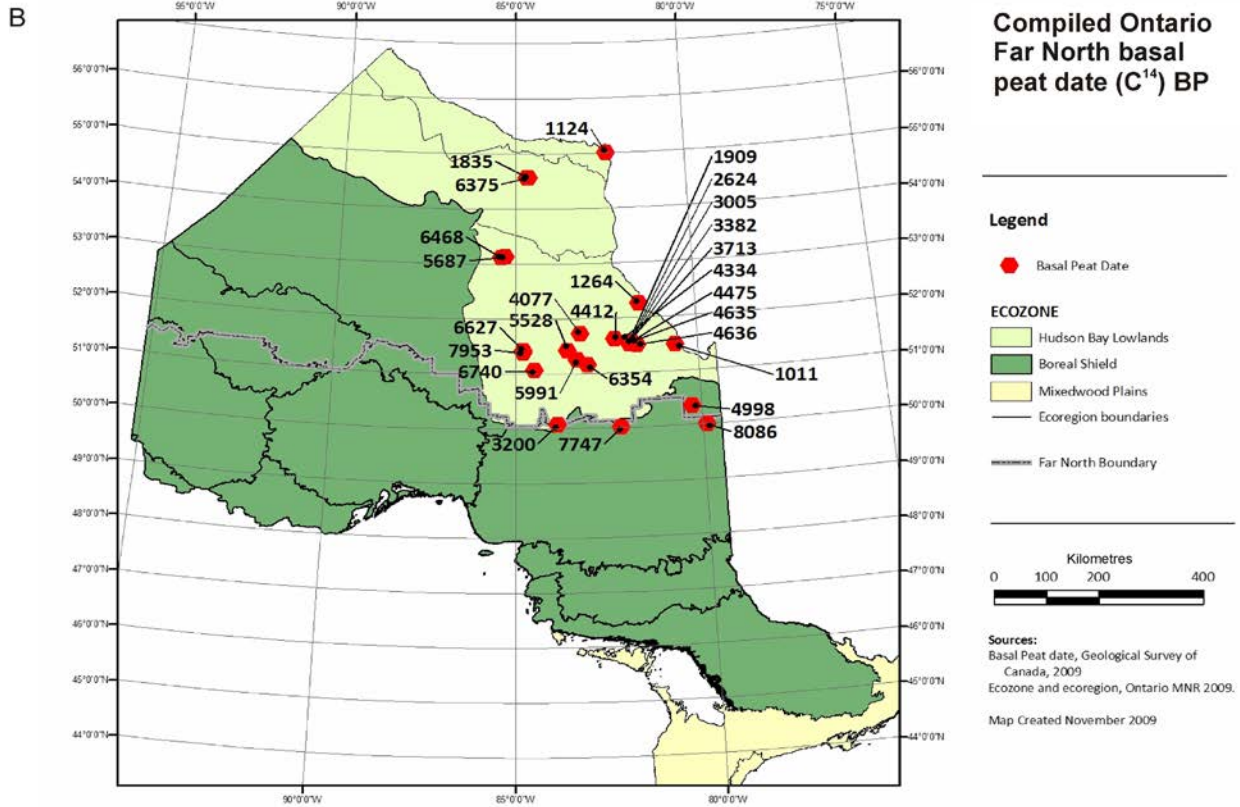


Figure 8.1. (a) Study site locations, (b) basal peat radiocarbon dates, and (c) spatial distributions of peat depth used to calculate Hudson Bay Lowland peatland carbon storage.

Hudson Bay Lowlands climate

Climate change is considered the most important threat to HBL peatlands (Far North Science Advisory Panel 2010), with responses differing depending on peatland type (e.g., Bäckstrand et al. 2010, Webster et al. 2013) and their location (Frolking et al. 2010, Lund et al. 2010). Across the HBL, MAAT and MAP range from -1.3 °C and 700 mm, respectively, at Moosonee to -7.0 °C and 412 mm at Churchill, Manitoba (see section 4, Peatland Hydrology; Figure 4.1). However, only a few active climate monitoring stations are maintained in this region (Far North Science Advisory Panel 2010, FPTGC 2010). Therefore, climate trends cannot accurately be analyzed across the HBL. The limited data indicate that MAAT may have increased, but no precipitation trend occurred between 1950 and 2007 (FPTGC 2010).

It is generally accepted that the main effect of climate will be a shorter ice season in Hudson and James bays, which is expected to alter air temperature and precipitation amounts (Gagnon and Gough 2005). Global circulation models indicate MAAT in the Hudson Bay region may increase by 2.5 to 8.0 °C, with the largest increases occurring during winter (Table 8.2, Figure 8.2). Although MAP was increased by 3.2 to 11.3 mm per month (Table 8.2), these changes are below the 25% threshold of higher MAP to sustain current soil moisture levels. Furthermore, permafrost area is predicted to decrease by 16 (Zhang et al. 2008b) to 100% (Gagnon and Gough 2005) depending on the scale of the modelling study and assumption of equilibrium and non-equilibrium conditions between the atmosphere and soil (see section 3, Permafrost Patterns).

The thawing index across the DPZ in the HBL may increase by four to eight days assuming a two times atmospheric CO₂ scenario (see section 3, Permafrost Patterns; Figure 3.7, Sushama et al. 2006). In the eastern HBL, peatlands are expected to dry and this may increase both NPP and decomposition, for which the net effect commonly is increased CO₂ sequestration (Balshi et al. 2009). The sequestered CO₂ in drier peatlands is mostly stored as aboveground biomass, with sequestration increasing as vegetation changes from sedges-to-shrubs-to-trees (Laiho et al. 2003).

In the western HBL, no significant changes are expected for soil moisture levels, although temperature may increase by approximately 0.04 °C per year. Similar soil moisture levels in the western HBL may result from a combination of more precipitation or ice meltwater due to permafrost thawing (see sections 3, Permafrost Patterns, and 4, Peatland Hydrology). Increased water input may balance increases in ET, thereby maintaining future soil moisture comparable to current levels. Although a minimum threshold of 25% more water input than current values is required to balance ET-induced water loss and peat drying under warmer temperatures (see section 4, Peatland Hydrology), lack of data for HBL peatlands limits the testing of this hypothesis. This has led to low confidence in future ET trends and other components of the water balance. Furthermore, the western HBL is already wet (Martini 2006). Thus, higher MAAT may also enhance CH₄ emissions due to more microbial CH₄ production occurring at warmer temperatures when conditions are wet (Godin et al. 2012, Preston et al. 2012). However, this concept has rarely been tested in the HBL and surrounding ecozones.

Table 8.2. General circulation model (GCM)-based temperature predictions for 2071 to 2100 for the Far North of Ontario.

Reference	Mean annual		Mean summer		Mean winter	
	B2	A2	B2	A2	B2	A2
	Temperature (°C)					
Gagnon and Gough (2005) ¹	2.5 to 4.5	4.8 to 8.0	1.9 to 3.7	2.7 to 6.4	3.4 to 7.5	5.0 to 13.3
McKenney et al. (2010) ²	3.4 to 3.9	4.9 to 5.7	2.4 to 5.7	4.4 to 6.2	3.9 to 5.8	6.7 to 9.6
	Precipitation (mm month ⁻¹)					
Gagnon and Gough (2005) ¹	3.2 to 7.1	5.2 to 11.3	2.7 to 6.3	4.2 to 9.3	0.9 to 9.3	3.3 to 14.4
McKenney et al. (2010) ²	2.3 to 7.3	2.9 to 6.3	0.3 to 2.3	-0.7 to 1.6	0.1 to 1.9	0.6 to 2.8

¹ Range of projections from six GCMs.

² Range of mean temperature and precipitation projections from four GCMs.

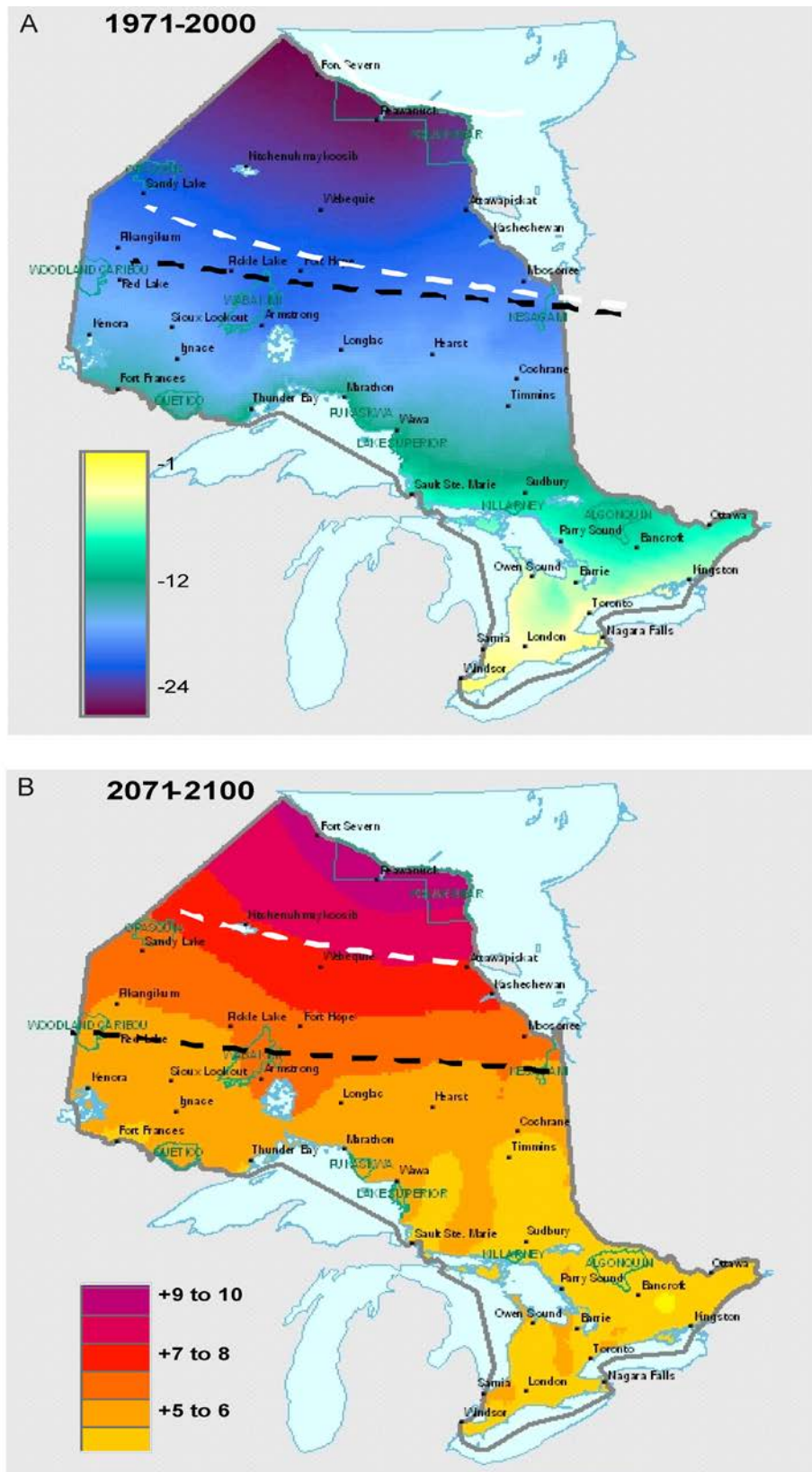


Figure 8.2. Projected changes in (a) temperature and (b) precipitation for Hudson Bay Lowlands for the period 2040 to 2069 (McKenney et al. 2010).

Peatland succession

Peatland development in the HBL is primarily controlled by recession of the Tyrell Sea and subsequent isostatic rebound of the land (Glaser et al. 2004a,b). Here, peatlands emerged more than 7000 cal yr BP, although ^{14}C dating of basal peat produced ages ranging from approximately 1000 to nearly 8000 cal yr BP (Figure 8.1b; section 2, Peatland Development and Plant Associations; Table 2.5). During these timeframes, salt marshes frequently emerged first, then transformed to fens because glacio-marine silt and clay deposits impeded water infiltration and promoted peat accumulation (Klinger and Short 1996). Some areas of the HBL were exposed to repeated glaciations, with glacial till containing silt and sand deposited over the glacio-marine material (Glaser et al. 2004a,b). Under these conditions, coarser textured mineral deposits underlying the peat enhanced water drainage and treed fens and forested peat plateaus were the first peatlands to emerge (see section 2, Peatland Development and Plant Associations; Tables 2.4 and 2.6). Continued isostatic rebound of land has led to peatlands spreading laterally through paludification that was interrupted only by river channels. Variable surficial geology and peat accumulation rates contributed to formation of complex drainage patterns in the HBL, with bogs and peat plateaus functioning primarily as groundwater recharge zones that discharged their water to fens and ponds (Glaser et al. 2006). From fens and ponds some water is transferred to lakes and rivers, eventually draining into the Hudson and James bays. Most water is stored in bogs, fens, and ponds and supports ET (see section 4, Peatland Hydrology).

Because of variable peatland types and water drainage patterns, significantly different C accumulation rates occurred during Holocene peatland development (van Bellen et al. 2011, Bunbury et al. 2012). Generally, rapid peat accumulation rates were associated with fens during periods of high water table levels and collapsed scars due to saturated peat inhibition of organic matter decomposition (see section 2, Peatland Development and Plant Associations; Tables 2.4 and 2.6). Common vegetation occurring during these periods included (1) brown mosses, sedges, and *Sphagnum* species adapted to wet conditions or (2) wet-adapted tall shrubs and larch trees.

Even though geology is the main control on peatland succession in the HBL (Glaser et al. 2004a,b), bogs and fens respond differently to temperature and precipitation changes. More compacted fen peat is wet and inflowing water from upland, bog, or peat plateaus maintains relatively high water tables and soil moisture levels. This generally supports peat C accumulation and CH_4 emissions, the proportions of which are poorly documented (see section 5, Peatland Carbon Cycling). Climate change can also affect peatland succession by accelerating permafrost thawing, leading to warmer peat that may be either dry or wet. Shrub and tree expansion occurs when soils are warm and dry—conditions that stimulate peat N mineralization rates (McLaughlin et al. 2000). Shrubs and trees are more efficient than sedges and mosses in assimilating N, and as shrubs and trees age, their higher leaf area limits the amount of radiation reaching the peat surface. At this time, sedge cover is reduced and those remaining are shade tolerant species adapted to relatively dry conditions, and moss composition changes from *Sphagnum*- to feathermoss-dominated communities (section 2, Peatland Development and Plant Associations; Table 2.7).

Limited data have been collected in the HBL on processes controlling peatland succession (Klinger and Short 1996; Glaser et al. 2004a,b; Riley 2011), either from field sampling or remote sensing studies. At our White River site (48°21'N, 85°21'W), peat acidification in response to drying was an important control on succession from an intermediate (open/shrub) to a poor (treed) fen (McLaughlin and Webster 2010). McLaughlin and Webster (2010) estimated intermediate fens may succeed to poor fens in approximately 125 years, which may be shortened to less than 50 years with climate-induced peat drying (see section 2, Peatland Development and Plant Associations).

In addition to higher leaf area, shrub and treed bogs may be exposed to longer growing seasons; leaf area index and growing season length increases may play critical roles in future aboveground peatland NPP (Lund et al. 2010). Remote sensing tools are available that map (1) biological characteristics, such as PFTs (e.g., mosses, sedges, shrubs, and trees), NPP, leaf area index, and foliar N content and (2) site physical characteristics, including surface peat moisture and permafrost extent (see section 7, Mapping, Monitoring, and Modelling Permafrost Peatlands). Therefore, efforts to calibrate these measurements at research sites need to be pursued to support local to regional scaling of peatland succession and C sequestration.

Permafrost

Warmer air temperatures and more precipitation may interactively decrease permafrost area in the HBL by 16 to 100% at the end of the 21st century (Gough and Leung 2002, Gagnon and Gough 2005, Zhang et al. 2008b). Most losses are expected to occur along the southern fringe of the DPZ (section 3, Permafrost Patterns; Figure 3.6, Zhang et al. 2008b), although talik formation may increase in the CPZ (Zhang et al. 2008a). These changes are expected to alter hydrology and biogeochemistry, vegetation composition, and subsequent peatland C storage and sequestration, the interactions of which are poorly documented. As such, resolving the controls on permafrost variability is critical to confidently project future trends. However, no permafrost monitoring networks exist in the Ontario portion of the HBL to support this effort.

In the HBL, permafrost is primarily associated with peatlands because peat thermal properties favour ice formation at temperatures near 0 °C (Moore 1987). As discussed in section 3, Permafrost Patterns, evidence is convincing that permafrost thawing is occurring in the Hudson Bay region (Arlen-Pouliot and Bhiry 2005, Payette et al. 2004), and this region may have already exceeded its temperature threshold for permafrost maintenance. Here, thawing likely occurred through sequential increases in annual ALT, forming taliks (Zhang et al. 2008b). Initial talik formation occurs at the highest palsa or peat plateau elevation. The underlying ice layer impedes meltwater infiltration and it flows laterally to points of lowest elevation, subsequently melting ice and forming a thermokarst pond or internal lawn (Calmels et al. 2008a). Pond and lawn formations enhance snow accumulation at the fringe of the palsa or plateau, further intensifying thaw rates. Should thawing continue, ponds may coalesce into lakes (Sannel and Kuhry 2011), with the latter eventually draining by overtopping palsa and peat plateau surfaces (Jones et al. 2011).

Peat plateaus degrade into many palsas (Payette et al. 2004), both of which are embedded in landscapes containing internal lawns, thermokarst ponds, and non-permafrost peatlands and forests. Because aggrading and degrading permafrost features cycle C differently (see section 5, Peatland Carbon Cycling), mapping their spatial distributions is vital to successfully assess C storage and sequestration for land use planning. The lack of a permafrost monitoring network, however, hinders projections of permafrost thaw and subsequent landscape changes. Coupled with a poor understanding of equilibrium and non-equilibrium processes between air and ground temperature in model results (see section 3, Permafrost Patterns), current peatland C storage and sequestration projections are of limited value. For example, soil and temperature are some of the most poorly calibrated model coefficients (Sushama et al. 2006). Furthermore, decomposition rates for C released from melting ice are relatively unknown, but have been indicated to have a vital role in future CO₂ and CH₄ balances between peat surfaces and the atmosphere (Turetsky et al. 2007, Schaefer et al. 2011).

At Victor Mine, we are using a combination of high resolution optical images, polarimetric SAR images (Radarsat 2), and digital elevation models to map distributions of peatland types and permafrost features (as well as other land cover types). Satellite data will provide input to the NEST model (Zhang et al. 2003) that is being calibrated from our climate, peat, and permafrost stations at Victor Mine. As mentioned above, the permafrost mapping and modelling project is being conducted in partnership with Dr. Brigitte Leblon, University of New Brunswick and Drs. Kara Webster and Yu Zhang of Natural Resources Canada.

Carbon

Carbon accumulation

Understanding peat C cycling is essential to estimate future C storage and sequestration; however, few measurements exist for the HBL. In terms of C accumulation rates, LORCA ranges between 14.4 and 18.9 g C m⁻² yr⁻¹ (Van Bellen et al. 2011, Bunbury et al. 2012) are documented, which are on the low end of those reported for Canadian peatlands (Table 5.1). Additionally, contradictory evidence has been reported for LORCA patterns during peatland development in the HBL. For example, low peat and C accumulation rates were reported during bog and poor fen successional stages near Attawapiskat, Ontario (Bunbury et al. 2012). Here, the fastest accumulation rates occurred after 1400 cal yr BP, primarily due to wetter peat. In contrast, at the southernmost portion of the HBL (Eastmain region of Québec), high C accumulation rates occurred in bogs during dry conditions because of high bulk density and C concentration in buried wood (Loisel and Garneau 2010). Carbon accumulation rates have also decreased in the Eastmain region during the past 2000 cal yr BP and rapid accumulation rates during wet conditions depended on the presence of hummock-*Sphagnum* mosses because of their slow decomposition rates (van Bellen et al. 2011).

Rates of RECA were between 42 and 184 g C m² yr⁻¹ and consistent with those reported for other regions in Canada (Lavoie et al. 2005). This wide range of values is due to a variety of causes, including (1) higher RECA in fens than bogs, (2) higher RECA occurring in wet (e.g., lawns, collapse scars) than dry (e.g., hummock, palsa) features, (3) decreasing RECA rates with increasing surface peat depth, and (4) difficulty in RECA interpretation in wet features because of groundwater influences. Controls on LORCA and RECA require further documentation because they have seldom been reported in the HBL (Loisel and Garneau 2010, van Bellen et al. 2011, Bunbury et al. 2012) and available information stems from few locations.

Climate, environmental, and microbiological controls on carbon cycling

Peat decomposition is an important CO₂ output parameter in calculating the C budget, where decomposition contributes approximately 30 to 60% of the total soil respiration (see section 5, Peatland Carbon Cycling). Although warmer and drier soils have repeatedly been shown to stimulate decomposition under laboratory conditions, this pattern has not been consistent in field experiments and no threshold level of peat drying is known that inhibits decomposition rates (e.g., Hobbie et al. 2000, Laiho 2006).

We characterized peat chemistry, microbiology, and decomposition processes from a peat core from Victor Mine and Kinoje Lake bogs and a core from a Victor Mine fen (Preston et al. 2012). Results showed that microbial community composition did not correlate with CO₂ production, but pH was positively correlated to CO₂ production across all sites and depths. Increased peat temperature and aeration enhanced CO₂ production but this did not correlate with a change in microbial communities or soil enzyme activities (Preston et al. 2012). Potential CO₂ production in the HBL appears to be influenced by peat acidity, temperature, and aeration status, along with the quality of the peat substrate. Across landscapes, acidity may be an important indicator of peat nutrient and quality status, with decomposition occurring faster at lower acidity levels (McLaughlin and Webster 2010). This concept is important because of the near 0 °C mean permafrost temperature in the HBL (Figure 8.3), which is within the temperature range of fastest peat C accumulation rates in northern peatlands; rates decrease northwards because of low NPP and southwards because of elevated peat decomposition (Yu 2012). As such, knowledge of peat quality and its association with acidity, temperature, and wetness requires documentation before permafrost thaw effects on decomposition rates and CH₄ emissions can be estimated within acceptable levels of uncertainty.

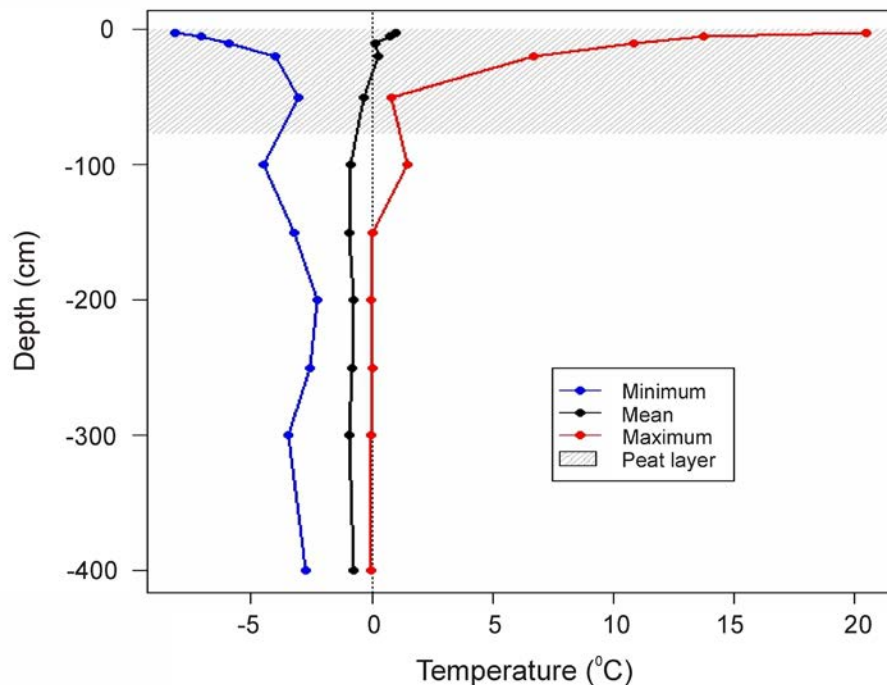


Figure 8.3. Palsa temperature profile from September 2009 to July 2010 at Polar Bear Provincial Park (McLaughlin, unpublished data).

At our White River site, Myers et al. (2012) showed bacterial activity in peat dominated over fungal activity across a range of rich (e.g., open, sedge) to poor (e.g., treed) fens, although fungal activity was more important in the poor fen peat. However, total microbial CO₂ production rate was similar across fen types. These results indicate the proportion of bacteria and fungi may not matter to broader C cycling in peat soils and GHG emissions to the atmosphere, partially corroborating our Kinoje Lake and Victor Mine peat results (Preston et al. 2012).

We also reported that at White River, CH₄ flux was highest and CO₂ flux lowest from rich and intermediate fens than from a poor fen (Godin et al. 2012). Model (Wetland-DNDC; Zhang et al. 2002) results at White River also indicated fen types responded differently to increasing temperature, wetting, and drying (Webster et al. 2013). Here, in a black spruce-tamarack-dominated poor fen, the CO₂ sink strength was projected to weaken by approximately 20% over a 30-year period, which resulted from elevated organic matter decomposition. In contrast, the CO₂ sink strength was relatively unchanged over the same timeframe in the rich and intermediate fens. All fens displayed significant increases in CH₄ sink strength when peat dried, with the poor and intermediate fens displaying the largest increases. For warm and wet peat CO₂ sequestration increased by 40 to 75%, while CH₄ emissions increased by 121 to 333% across fen types. Fluxes of GHGs were strongly dependent on sedge biomass. Webster et al. (2013) also reported annual C exchange was correlated with several annual meteorological variables that can serve as useful metrics to predict C responses of fens to changing conditions. In general, rich and intermediate fens responded similarly with annual C cycles linked to internal drivers (e.g., water table depth and ET_p), whereas external drivers (e.g., temperature) were important to poor fen GHG exchange. Because of the wide variation in results, further studies of PFT, especially sedge biomass and ET rates (as well as total water balance) are needed to (1) improve Wetland-DNDC model calibrations for HBL peatlands and (2) scale fen types and their vegetation structure and biomass to evaluate climate change effects on peatland C dynamics within and outside the Far North boundaries.

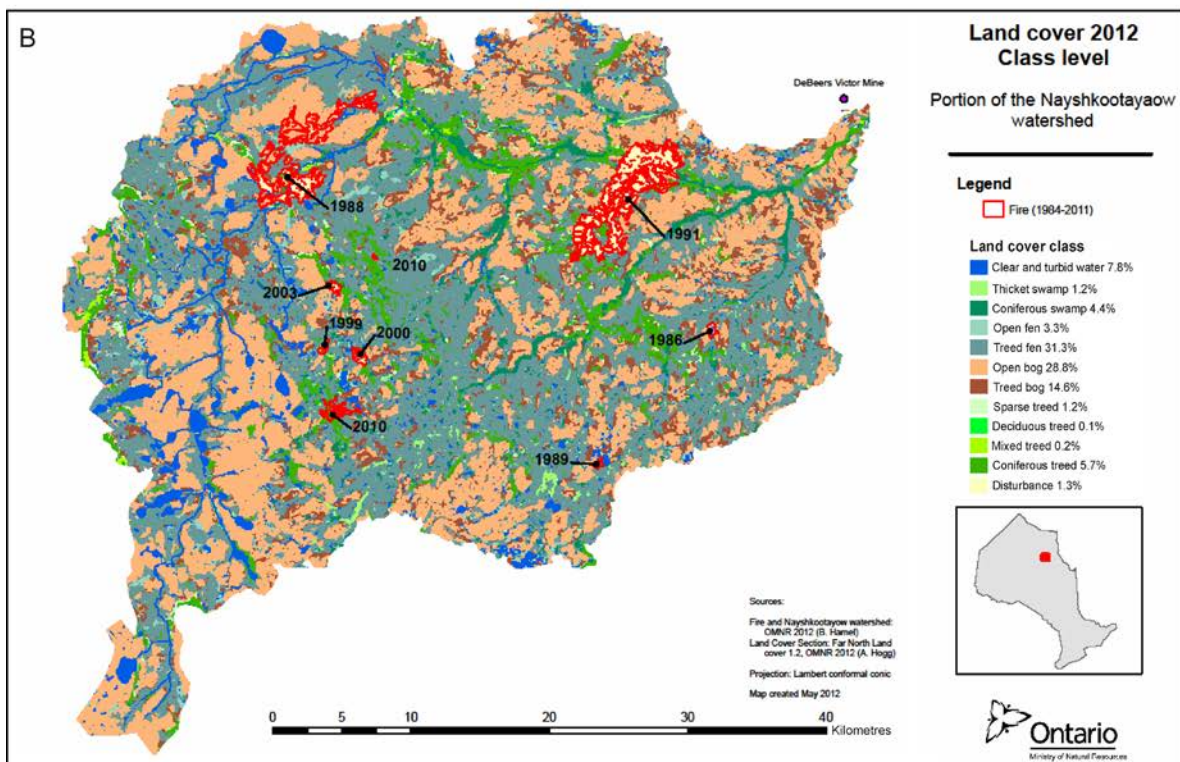
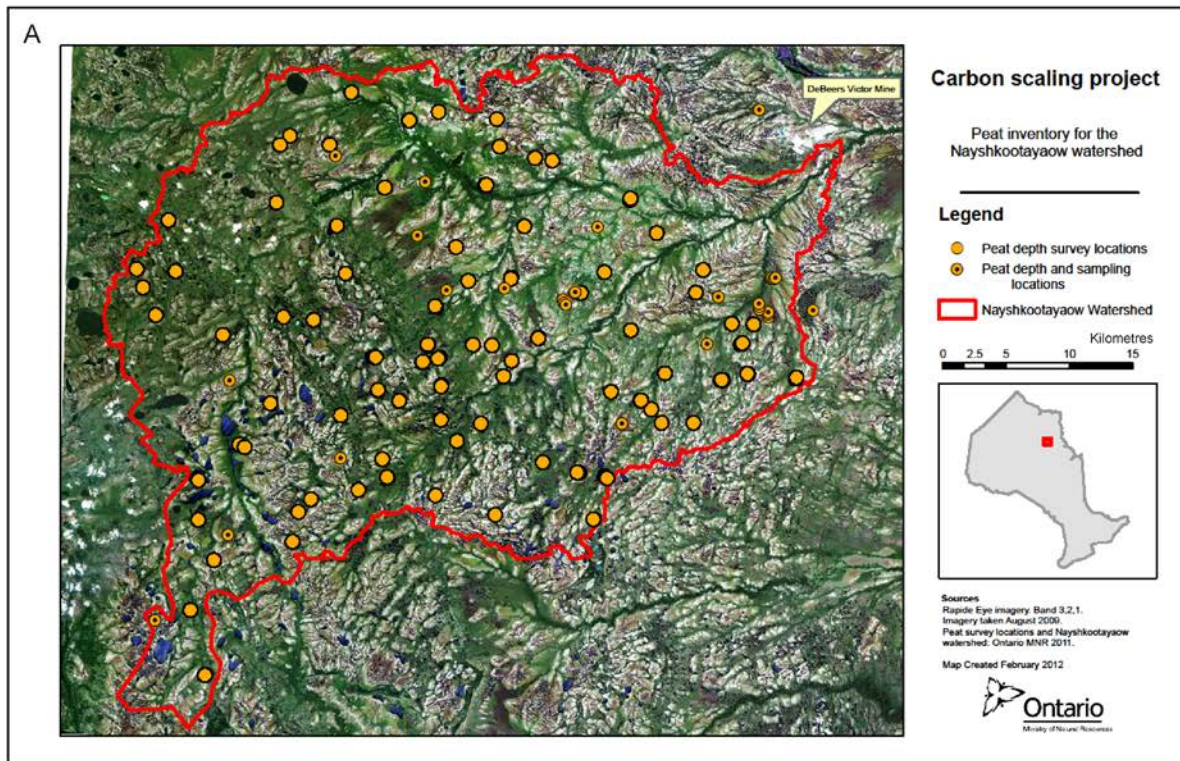
Remote sensing and carbon scaling

Previous work using the northeastern Ontario peatland survey data (Riley 1994) showed that peat C storage was highly sensitive to changes in peat depth and bulk density (McLaughlin 2004). Therefore, at Victor Mine, we characterized peatland types in an approximately 1,700 km² watershed and collected 113 peat depth measurements, with peat cores (for C and bulk density analysis) and vegetation characteristics collected at 18 sub-locations in the watershed (Figure 8.4a). We further classified peatland types using Rapid Eye, SPOT, and Landsat TM satellite images. Results indicated that smaller open and larger treed bog areas were classified more accurately at finer (i.e., Rapid Eye) compared to coarser resolution (i.e., SPOT and Landsat TM). These differences, however, were not represented in watershed total C storage estimate of approximately 128 Mt across remote sensing methods (Akumu and McLaughlin, unpublished data). Shallow peat was generally associated with higher densities of conifer trees, while no differences in C density occurred among peatland types (Figure 8.4b,c).

The C modelling research is still developing and will link to the remote sensing and C scaling work through inclusion of the McGill Wetland Model (St-Hilaire et al. 2010) and Wetland DNDC model (Zhang et al. 2002). These models are being calibrated to evaluate the effects of climate change and resource development on peatland C storage and sequestration. As mentioned above, the project is undertaken via a partnership with Drs. Nigel Roulet and Tim Moore of McGill University and Drs. Peter Lafleur and Elyn Humphries of Trent and Carleton universities. The McGill Wetland Model is being considered as the national peatland C budget assessment tool and its calibration at Victor Mine will help identify the importance of the HBL in current and future states of national peatland C budgets in response to climate change. The Wetland-DNDC model is being calibrated to assess current and future peatland carbon budgets in response to climate change and land use activities for local and regional landscapes in the HBL.

Fire

Fire regimes are projected to change with climate warming, which may also affect peatland C storage and sequestration (see section 6, Fire Regimes). At Victor Mine, only about 1% of our reference watershed burned between 1986 and 2010, resulting in a fire return interval of about 600 years (Figure 8.4b). Furthermore, considering data from the Ontario fire database between 1980 and 2007, annual area burned by large fires (≥200 ha) in the HBL has been highly variable (Figure 8.5a) and no consistent patterns in area burned have been reported for the region (FPTGC 2010). On average, approximately 150,000 ha burn annually in the Far North, with only 16% of



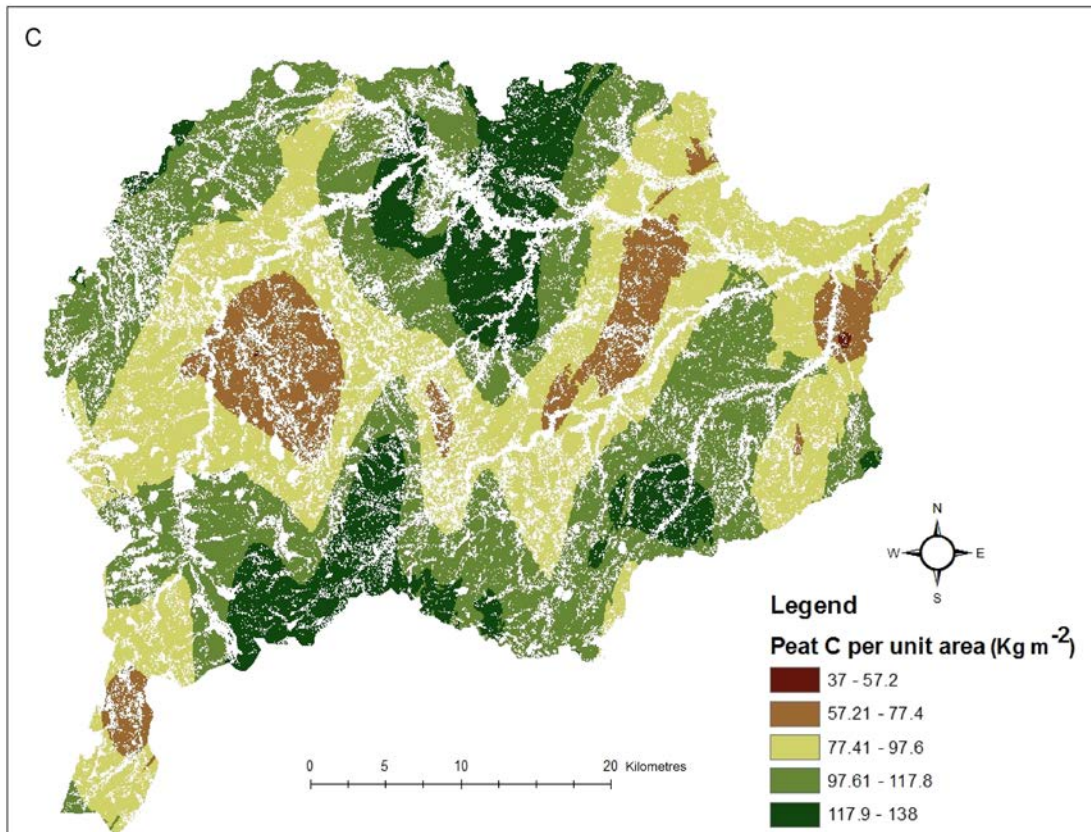


Figure 8.4. Area being used for peatland classification and carbon storage study in a reference watershed located near Victor Diamond Mine (a) sample point locations, (b) land classification and recent area burned, and (c) peat carbon density.

the area burned occurring in the HBL (Table 1.1). Fire distribution is most dense in the James Bay region and the Boreal Shield/HBL interface (Figure 8.5b), where soils tend to be drier and more forest cover occurs. As such, fire likely plays a minimal role in current peatland C dynamics in the HBL. Furthermore, stratigraphic studies based on charcoal measurements showed fire was a minor contributor to peatland C accumulation rates throughout the Holocene (Camill et al. 2009, Magnan et al. 2012, van Bellen et al. 2012). However, this region may experience two to three fold increases in area burned in future years under a three times CO_2 scenario (Flannigan et al. 2005).

A concern for the HBL is that extending fires later into the growing season in future years may render bogs and peat plateaus more vulnerable to deep soil consumption (increased depth of burning), given that burning is more likely to occur during the period of maximum water table drawdown and fuel exposure (Zoltai et al. 1998, Turetsky et al. 2011a). Another concern is that ‘holdover’ fires (those that continue to smoulder under snow cover during the winter and reappear the following spring) may become more common (Flannigan et al. 2009). However, as discussed in section 6, Fire Regimes, data are few and inconsistent for peatland area burned and fire severity (i.e., depth of burn). As such, assessing the amount of C released from fires in general, as well as by severity class, in the HBL involves a high degree of uncertainty. These data gaps should be reconciled because changes in the fire regime in the C-rich HBL may affect future atmospheric C concentration (e.g., Flannigan et al. 2005).

Summary and conclusions

Climate change poses the most important threat to Far North peatland ecosystems. However, current data limitations significantly hinder the understanding and therefore ability to predict peatland C storage and sequestration. To successfully apply C storage and sequestration to Far North land use planning, more knowledge is required in two broad areas. First, increased understanding of spatial and temporal patterns in air temperature and precipitation trends is needed at intra-annual to decadal timeframes. Temperature and precipitation interactions

with permafrost thawing, successional processes, and subsequent control on ET must be understood before confident estimates of future GHG exchange between peat surfaces and the atmosphere are possible. Secondly, intensified peatland and permafrost C inventories are needed. Few inventories exist and though we have collated data from published reports and our field sites, small sample sizes result in significant variation in C storage calculations. Because of these data deficiencies, confidence in calculated current and future C storage and sequestration is low, hindering its application to Far North land use planning. Therefore, the ultimate goal of our peatland C research and monitoring efforts is to reduce uncertainty in knowledge of C storage and sequestration, and their associated controls, to calibrate spatial and site-specific models that estimate C storage and sequestration for a variety of landscape areas and timeframes for Far North land use planning.

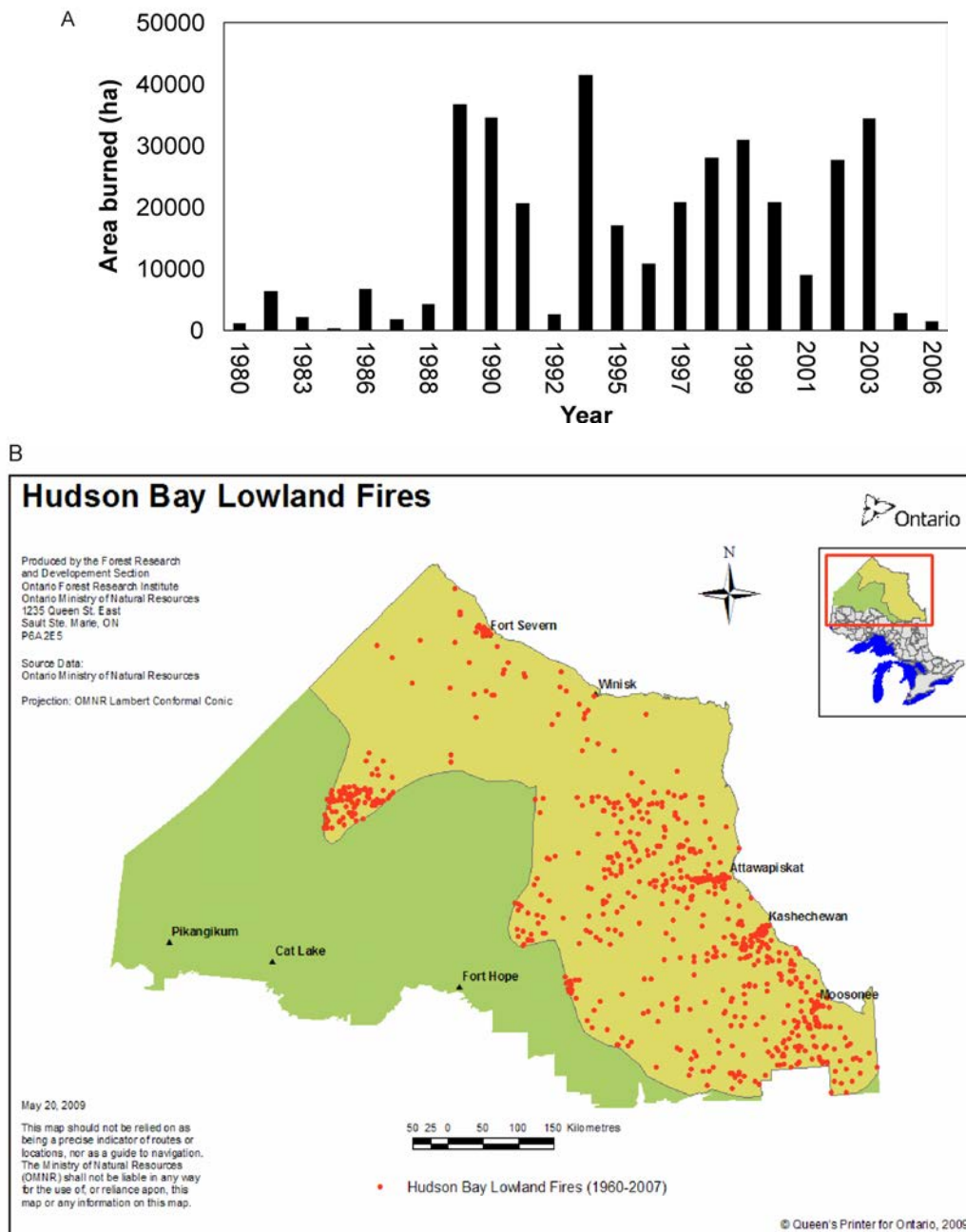


Figure 8.5 (a) Area burned by fires >200 ha in the Hudson Bay Lowlands of Ontario 1980 to 2006 and (b) spatial distribution of those fires (based on information from Ontario's Large Fire Database (AFFFM, 2012, pers. comm.).

9. Uncertainties, Challenges, and Science Priorities to Assess Peatland Carbon Storage and Sequestration

Achieving the Far North Act's planning objective of maintaining ecosystem processes and C storage and sequestration and developing the required policy statement for land use planning requires an understanding of how climate change affects peatland C storage and sequestration at landscape scale. These evaluations need to be conducted within a climate change vulnerability and adaptation assessment framework for HBL peatlands. Therefore, we conclude this report by synthesizing the collated information into a climate change vulnerability and adaptation assessment framework and presenting the major uncertainties and challenges related to the HBL.

Although scant, evidence is convincing that permafrost, ET and peat wetness, and PFTs are changing in the HBL and they show promise as scalable climate change indicators. However, rates and direction of peatland changes are complicated, poorly documented, and depend on whether peat becomes drier or wetter as it warms (Figure 9.1). Some changes, such as thermokarst formation (Arlen-Pouliot and Bhiry 2005) and transformations within fen types as they convert to bogs (McLaughlin and Webster 2010), occur rapidly (e.g., decade-to-century). We also know that thermokarst formation and fen to bog transitions have opposing effects on peatland C budgets (Table 2.6, Figure 9.1). However, successional trajectories in the HBL are poorly documented (although recent summaries of data collected from the 1980s and early 1990s are available; Riley 2011), and the remoteness of the region hinders large-scale sampling endeavours and makes them very costly.

Remote sensing using various platforms and sensors have been combined with modelling techniques to assess climate change indicators (i.e., PFTs, ET and peat wetness, and permafrost thawing) at landscape scale (Dorrepaal 2007). Furthermore, the climate indicators proposed here have consistently been correlated with various components of C budgets and successfully scaled across landscapes (Beilman et al. 2008). Given these

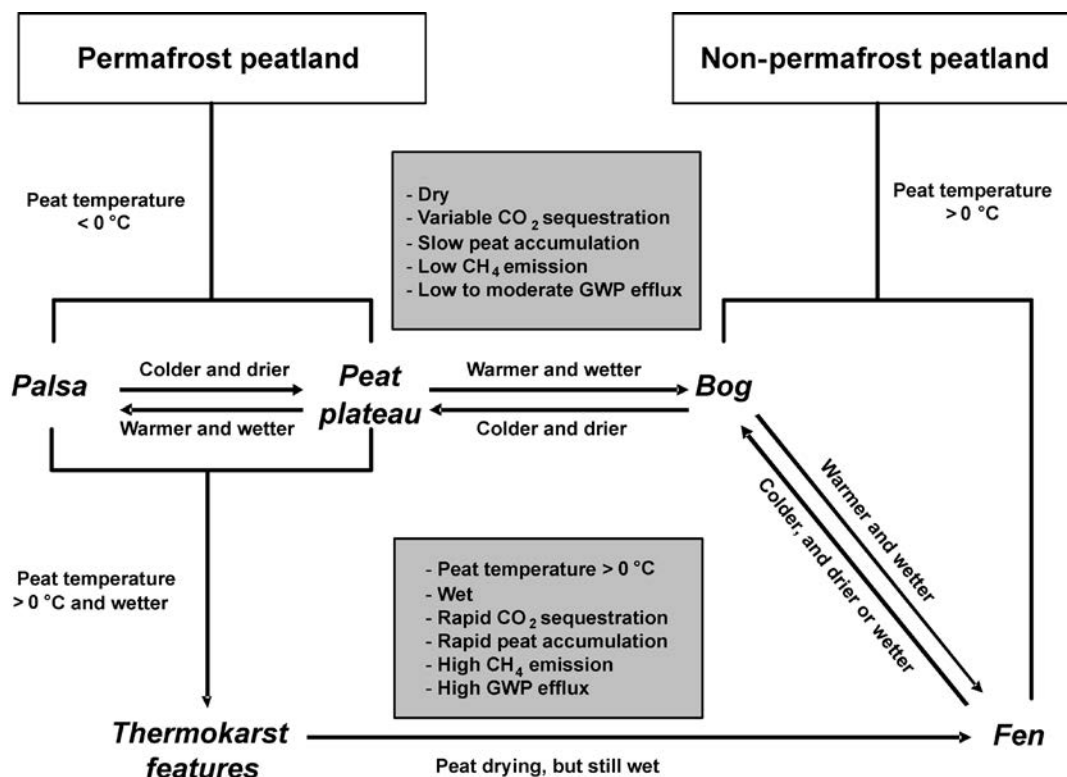


Figure 9.1. Conceptual model of permafrost and non-permafrost peatland succession (arrows) in response to changing peat conditions (grey boxes) in the Hudson Bay Lowlands of Ontario. C = carbon, CO₂ = carbon dioxide, CH₄ = methane, GWP = global warming potential.

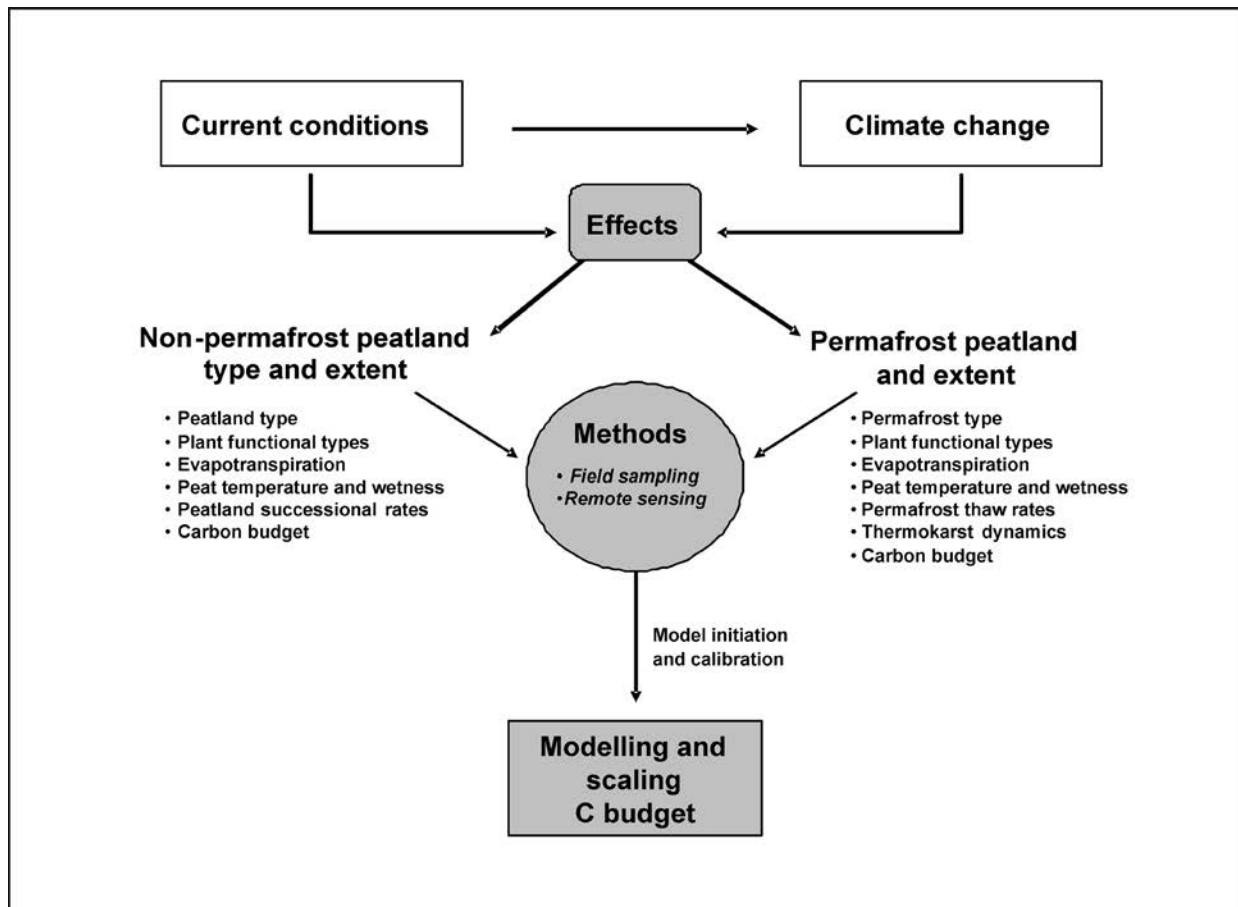


Figure 9.2. Conceptual framework of research and monitoring needed to provide information to calibrate remote sensing and modeling approaches to scale up peatland carbon budgets in the Hudson Bay Lowlands of Ontario.

associations, we propose combinations of field sampling and remote sensing of non-permafrost and permafrost peatland characteristics as central to projecting climate change effects on C budgets (Figure 9.2). However, few researchers have attempted to develop correlations between climate change and peatland C indicators for the HBL. Significant efforts are required to sample peat; calibrate satellite and aerial photographs for permafrost coverage, peatland types, PFTs, and ET and wetness; and calibrate permafrost and peatland C models. As part of these sampling, remote sensing, and modelling activities, seasonal (e.g., snowmelt, winter freezing) changes and their effects on C budgets also need to be considered.

Other uncertainties and challenges also impede the use of climate and C indicators in climate change vulnerability and adaptation assessments. For climate change, lack of weather and permafrost monitoring networks in the HBL significantly limits understanding of past and current temperature, precipitation, and permafrost regimes, contributing to highly variable projections in future conditions. For example, mean monthly precipitation projections reported for summer and winter months differed by more than 200% (Gagnon and Gough 2005; McKenney et al. 2010). Precipitation amounts are important to landscape permafrost coverage within the same temperature zone (Rouse 2000). Interactions between air temperature and precipitation with peat temperature and moisture dynamics are also some of the most poorly calibrated coefficients used to project permafrost and peatland C dynamics (Sushama et al. 2006).

Few valid estimates of permafrost amount and its thaw rate exist for the HBL. Payette et al. (2004) reported that, between 1957 and 2003, percent annual permafrost loss increased from 2.5 to 5.3%, which are much higher than model projections of 0.1 to 0.7% lost per year. These patterns between small and large scale studies need to be redefined (Gagnon and Gough 2005, Zhang et al. 2008b), as well as permafrost losses reported in Canada

(Table 3.4). Projections may differ due to variability in spatial domains simulated and assumptions of equilibrium versus non-equilibrium air and ground temperatures. Current models, such as NEST (Zhang et al. 2003), may constrain variability by accounting for plant structure, snow depth, and soil organic layer thickness effects on energy and water transfer in soil-vegetation-atmosphere systems, and subsequent ground thermal dynamics. However, all models fail to address changes in landscape pattern, which is a critical modelling gap. For example, assuming a 50% increase in fen and 20% increase in pond areas in the northern HBL (Payette et al. 2004) during the 21st century may increase landscape-level CO₂ and CH₄ emissions to the atmosphere that may not be detected in coarse scale projections. Such changes have been shown to significantly weaken C and GWP sinks, even though peat C accumulation rates may increase (Malmer et al. 2005, Johansson et al. 2006).

From a C perspective, current and future peatland content and GHG emissions in northern peatlands may be underestimated due to the relatively unknown effects of (1) multiple perturbations (e.g., permafrost thaw, ET and peat wetting or drying that may destabilize peatland C cycling, (2) rates of both climate change and peatland adaptation, and (3) occurrence of new climate states outside the range of Holocene climate variation (Frolking et al. 2011). As indicated by Frolking et al. (2011), the only approach available to address climate change and C budgets is rudimentary process-based modelling, the results of which are often inconsistent from one model to another and do not match field data. For example, warming may increase peatland C losses by 40 to 85% in coming centuries (Ise et al. 2008), or peatland C stocks may stabilize in response to drying (Frolking et al. 2010). Furthermore, none of the available permafrost (e.g., NEST) and C (e.g., McGill Wetland Model and Wetland-DNDC) models allow plant communities or spatial patterns in permafrost and peatland structure to vary during simulations, significantly limiting their applicability to functional landscapes.

Information about the quality (decomposability) of peat exposed to aerated or flooded conditions with warming temperatures is also lacking. Deeply buried peat is primarily 'recalcitrant' material due to prior decomposition in aerobic surface peat layers (Laiho 2006). However, the effects of warmer and drier (or wetter) conditions on decomposition rates of recalcitrant peat are conflicting, with some studies reporting faster decomposition under warmer temperatures (Dorrepaal 2007) and others showing no change (Davidson and Janssens, 2006). Furthermore, permafrost-enclosed peat C tends to be less decomposable than that of enclosed mineral soil organic matter (Webster and McLaughlin 2011). Data on short- and long-term decomposition of C released through ice melting in permafrost regions is also scarce. Finally, DOC may be an important regulator of microbial decomposition in peatlands (Laiho 2006). The quality of DOC to support decomposition is known to differ among peatland types and dry versus wet conditions (Webster and McLaughlin 2010). How those changes are manifested in future organic matter decomposition in peatlands, however, is virtually unknown. We propose (1) data limitations related to air temperature and precipitation effects on permafrost thaw, successional processes, ET, and subsequent C accumulation and GHG exchange between peat surfaces and the atmosphere must be overcome, and (2) intensified peatland and permafrost C inventories conducted before confident projections of long-term peatland C sink strengths are possible, and peatland climate change vulnerability and adaptation assessment can be completed with acceptable levels of uncertainty.

Literature Cited

- Adam, J.C., F. S. Haddeland and D. P. Lattermaier. 2007. Simulation of reservoir influences on annual and seasonal streamflow changes for Lena, Yenisei and Ob' rivers. *J. Geophys. Res.* 112: D24114, doi:10.2929/2007JD008525.
- Admiral, S.W. and P.M. Lafleur. 2007. Modelling of latent heat partitioning at a bog peatland. *Agric. For. Meteorol.* 144: 213-229.
- Admiral, S.W., P.M. Lafleur and N.T. Roulet. 2006. Controls on latent heat flux and energy partitioning at a peat bog in eastern Canada. *Agric. For. Meteorol.* 140: 308-321.
- Aerts, R. 2006. The freezer defrosting: Global warming and litter decomposition in cold biomes. *J. Ecol.* 94: 713-724.
- Åkerman, H.J. and M. Johansson. 2008. Thawing permafrost and thicker active layers in sub-arctic Sweden. *Permafrost Periglac.* 19: 279-292.
- Ali, A.A., B. Ghaleb, M. Garneau, H. Asnong and J. Loisel. 2008. Recent peat accumulation rates in minerotrophic peatlands of the Bay James region, eastern Canada, inferred by Pb-210 and Cs-137 radiometric techniques. *Appl. Radiat. Isotopes* 66: 1350-1358.
- Allard, M., S. Caron and Y. Begin. 1996. Climatic and ecological controls on ice segregation and thermokarst: the case history of a permafrost plateau in Northern Québec. *Permafrost Periglac.* 7: 207-227.
- Allard, M., B.L. Wang and J.A. Pilon. 1995. Recent cooling along the southern shore of Hudson Strait, Québec, Canada, documented from permafrost temperature measurements. *Arctic Alpine Res.* 27: 157-166.
- Alm, J., K. Schulman, L. Walden, H. Nykanen, P. J. Martikainen and J. Silvola. 1999. Carbon balance of a boreal bog during a year with an exceptionally dry summer. *Ecology* 80: 161-174.
- Amiro, B. D., A. Cantin, M.D. Flannigan and W.J. de Groot. 2009. Future emissions from Canadian boreal forest fires. *Can. J. For. Res.* 39: 383-395.
- Amiro, B. D., J.B. Todd, B.M. Wotton, K.A. Logan, M.D. Flannigan, B.J. Stocks, J.A. Mason, W.R. Skinner, D.L. Martell and K.G. Hirsch. 2001. Direct carbon emissions from Canadian forest fires, 1959 to 1999. *Can. J. For. Res.* 31: 512-525.
- Anderson, D.S., R.B. Davis, S. C. Rooney and C.S. Campbell. 1996. The ecology of sedges (Cyperaceae) in Maine peatlands. *Bull. Tor. Bot. Club* 123: 100-110.
- Anisimov, O.A. and F.E. Nelson. 1996. Permafrost distribution in the Northern Hemisphere under scenarios of climatic change. *Global Planet. Change* 14: 59-72.
- Anisimov, O.A. and F.E. Nelson. 1997. Permafrost zonation and climate change in the northern hemisphere: Results from transient general circulation models. *Clim. Change* 35: 241-258.
- Aplin, P. 2005. Remote sensing: ecology. *Prog. Phys. Geogr.* 29: 104-113.
- Arlen-Pouliot, Y. and N. Bhiri. 2005. Paleocology of a peatland and a filled thermokarst pond in a permafrost peatland, subarctic Québec, Canada. *Holocene* 15: 408-419.
- Arnett, A., J. Kurbatova, O. Kolle, O. Shibistova, J. Lloyd, N. Vygodskaya and E.D. Schulze. 2002. Comparative ecosystem atmosphere exchange of energy and mass in a European Russian and a central Siberian bog. II. Interseasonal and interannual variability of CO₂ fluxes. *Tellus B* 54: 514-530.
- Arseneault, D. and S. Payette. 1997. Landscape change following deforestation at the arctic tree line in Québec, Canada. *Ecology* 78: 693-706.
- Aurela, M., T. Laurila and J.P. Tuovinen. 2004. The timing of snow melt controls the annual CO₂ balance in a subarctic fen. *Geophys. Res. Lett.* 31: L16119, doi:10.1029/2004GL020315.
- Bäckstrand, K., P.M. Crill, M. Jackowicz-Korczynski, M. Mastepanov, T.R. Christensen and D. Bastviken. 2010. Annual carbon gas budget for a subarctic peatland, Northern Sweden. *Biogeosciences* 7: 95-108.
- Bäckstrand, K., P.M. Crill, M. Mastepanov, T.R. Christensen and D. Bastviken. 2008. Total hydrocarbon flux dynamics at a subarctic mire in northern Sweden. *J. Geophys. Res. – Biogeosciences* 113: G03026, doi:10.1029/2008JG000703.
- Baghdadi, N., M. Bernier, R. Gauthier and I. Neeson. 2001. Evaluation of C-band SAR data for wetlands mapping. *Int. J. Remote Sens.* 22: 71-88.
- Balshi, M.S., A.D. McGuire, P. Duffy, M. Flannigan, D.W. Kicklighter and J. Melillo. 2009. Vulnerability of carbon storage in North American boreal forests to wildfires during the 21st century. *Global Change Biol.* 15: 1491-1510.
- Balshi, M.S., A.D. McGuire, Q. Zhuang, J. Melillo, D.W. Kicklighter, E. Kasischke, C. Wirth, M. Flannigan, J. Harden, J.S. Clein, T.J. Burnside, J. McAllister, W. A. Kurz, M. Apps and A. Shvidenko. 2007. The role of historical fire in the carbon dynamics of the pan-boreal region: A process-based analysis. *J. Geophys. Res.* 112: G02029, doi:10.1029/2006JG000380.
- Bartlett, B.B., P.M. Crill, R.L. Sass, R.C. Harris and N.B. Dise. 1992. Methane emissions from tundra environments in the Yukon-Kuskokwim delta, Alaska. *J. Geophys. Res.* 97: 16645-16660.
- Bartsch, I. and T.R. Moore. 1985. A preliminary investigation of primary production and decomposition in four peatlands near Schefferville, Québec. *Can. J. Bot.* 27: 1241-1248.
- Bartsch, A., R.A. Kidd, C. Pathe, K. Scipal and W. Wagner. 2007. Satellite radar imagery for monitoring inland wetlands in boreal and sub-arctic environments. *Aquatic Conserv. Mar. Freshw. Ecosyst.* 17:305-317.
- Bartsch, A., C. Pathe, K. Scipal and W. Wagner. 2008. Detection of permanent open water surfaces in central Siberia with ENVISAT ASAR wide swath data with special emphasis on the estimation of methane fluxes from tundra wetlands. *Hydrol. Res.* 39: 89-100.
- Beilman, D.W. 2001. Plant community and diversity change due to localized permafrost dynamics in bogs of western Canada. *Can. J. Bot.* 79:983-993.
- Beilman, D.W., G.M. MacDonald, L.C. Smith and P.J. Reimer. 2009. Carbon accumulation on peatlands of West Siberia over the last 2000 years. *Global Biogeochem. Cycles* 23: GB1012, doi:10.1029/2007GB003112.
- Beilman, D.W., D.H. Vitt and L.A. Halsey. 2001. Localized permafrost peatlands in western Canada: definition, distributions, and degradation. *Arct. Antarct. Alp. Res.* 33: 70-77.
- Beilman, D.W., D.H. Vitt, J.S. Bhatti and S. Forest. 2008. Peat carbon stocks in the southern Mackenzie River Basin: Uncertainties revealed in a high-resolution case study. *Global Change Biol.* 14: 1-12.

- Bellisario, L.M., J.L. Bubier, T.R. Moore and J.P. Chanton. 1999. Controls on CH₄ emissions from a northern peatland. *Global Biogeochem. Cycles* 13: 81-91.
- Bello, R. and I.D. Smith. 1990. The effect of weather variability on the energy balance of a lake in the Hudson Bay Lowlands, Canada. *Arctic Alpine Res.* 22: 98-107.
- Belyea, L.R. and A.J. Baird. 2006. Beyond "The limits to peat bog growth": Cross-scale feedback in peatland development. *Ecol. Monogr.* 76: 299-322.
- Belyea, L.R. and N. Malmer. 2004. Carbon sequestration in peatland: Patterns and mechanisms of response to climate change. *Global Change Biol.* 10: 1043-1052.
- Benscofer, B. W. and D.H. Vitt. 2008. Spatial patterns and temporal trajectories of the bog ground layer along a post-fire chronosequence. *Ecosystems* 11: 1054-1064.
- Benscofer, B.W. and R.K. Wieder. 2003. Variability in organic matter lost by combustion in a boreal bog during the 2001 Chisholm fire. *Can. J. For. Res.* 33: 2509-2513.
- Benscofer, B.W., D.H. Vitt, and R.K. Wieder. 2005. Association of postfire peat accumulation and microtopography in boreal bogs. *Can. J. For. Res.* 35: 2188-2193.
- Bergeron, Y., S. Gauthier, M. Flannigan and V. Kafka. 2004. Fire regimes at the transition between mixedwood and coniferous boreal forest in northwestern Québec. *Ecology* 85: 1916-1932.
- Bergeron, Y., S. Gauthier, V. Kafka, P. Lefort and D. Lesieur. 2001. Natural fire frequency for the eastern Canadian boreal forest: consequences for sustainable forestry. *Can. J. For. Res.* 31: 384-391.
- Bhatti, J.S., G.C. van Kooten, M.J. Apps, L.D. Laird, I.D. Campbell, C. Campbell, M.R. Turetsky, S. Yu and E. Banfield. 2003. Carbon balance and climate change in boreal forests. Pp. 799-855 in Burton, P.J., Messier, C., Smith, D.W., and Adamowicz, W.L. (eds.). *Towards Sustainable Management of the Boreal Forest*. NRC Research Press, Ottawa, ON. 1,039 p.
- Bhry, N. and E.C. Robert. 2006. Reconstruction of changes in vegetation and trophic conditions of a tundra in a permafrost peatland, subarctic Québec, Canada. *Écoscience* 13: 56-65.
- Bhry, N., S. Payette and E.C. Robert. 2007. Peatland development at the arctic tree line (Québec, Canada) influenced by flooding and permafrost. *Quatern. Res.* 67: 426-437.
- Billett, M.F. and T.R. Moore. 2007. Supersaturation and evasion of CO₂ and CH₄ in surface waters at Mer Bleue peatland, Canada. *Hydrol. Process.* 22: 2044-2054.
- Blodau, C., R. Rees, H. Flessa, A. Rodionov, G. Guggenberger, K.-H. Knorr, O. Shibistova, G. Zrazheveskaya, N. Mikheeva and O.A. Kasansky. 2008. A snapshot of CO₂ and CH₄ evolution in a thermokarst pond near Igarka, northern Siberia. *J. Geophys. Res.* 113: G03023, doi:10.1029/JG000652.
- Bockheim, J.G. 2007. Importance of cryoturbation in redistributing organic carbon in permafrost-affected soils. *Soil Sci. Soc. Am. J.* 71: 1335-1342.
- Boike, J., K. Roth and O. Ippisch. 2003. Seasonal snow cover on frozen ground: Energy balance calculations of a permafrost site near Ny-Ålesund, Spitsbergen. *J. Geophys. Res.* 108: 8163, doi:10.1029/2001JD000939.
- Boike, J., K. Roth and P.P. Overduin. 1998. Thermal and hydrologic dynamics of the active layer at continuous permafrost site (Taymyr Peninsula, Siberia). *Water Resour. Res.* 34: 355-363.
- Boike, J., C. Wille and A. Abnizova. 2008. Climatology and summer energy and water balance of polygonal tundra in the Lena River Delta, Siberia. *J. Geophys. Res.* 113: G03025, doi:10.1029/JG000540.
- Bonsal, B.R. and T.D. Prowse. 2003. Trends and variability in spring and autumn 0 °C-isotherm dates over Canada. *Clim. Change* 57: 341-358.
- Borren, W., W. Bleuten and E.D. Lapshina. 2004. Holocene peat and carbon accumulation rates in the southern taiga of western Siberia. *Quatern. Res.* 61: 42-51.
- Bouchon, E. and D. Arseneault. 2004. Fire disturbance during climate change: failure of postfire forest recovery on a boreal floodplain. *Can. J. For. Res.* 34: 2294-2305.
- Boudreau, L.D. and W.R. Rouse. 1995. The role of individual terrain units in the water balance of wetland tundra. *Clim. Res.* 5: 31-47.
- Bowden, W.B., M.N. Gooseff, A. Balsler, A. Green, B.J. Peterson and J. Bradford. 2008. Sediment and nutrient delivery from thermokarst features in the foothills of the North Slope, Alaska: Potential impacts on headwater stream ecosystems. *J. Geophys. Res. – Biogeosciences* 113: G02026, doi:10.1029/2007JG000470.
- Bowen, I.S. 1926. The ratio of heat losses by conduction and by evaporation from any water surface. *Phys. Rev.* 2: 779-787.
- Bradford, J.H., J.P. McNamara, W. Bowden and M.N. Gooseff. 2005. Measuring thaw depth beneath peat-lined arctic streams using ground-penetrating radar. *Hydrol. Process.* 19: 2689-2699.
- Brown, R.J.E. 1967. Permafrost in Canada. Geological Survey of Canada Map 1246a and Division of Building Research Map NRC-9769. Nat. Res. Counc. Can., Ottawa, ON.
- Bubier, J. L., P. Crill and A. Mosedale. 2002. Net ecosystem CO₂ exchange measured by autochambers during the snow-covered season at a temperate peatland. *Hydrol. Process.* 16: 3667-3682.
- Bubier, J.L., B.N. Rock and P.M. Crill. 1997. Spectral reflectance measurements of boreal wetland and forest mosses. *J. Geophys. Res.* 102: 29,483-29,494.
- Bubier, J., G. Bhatia, T.R. Moore, N.T. Roulet and P.M. Lafleur. 2003. Spatial and temporal variability in growing-season net ecosystem carbon dioxide exchange at a large peatland in Ontario, Canada. *Ecosystems* 6: 353-367.
- Bubier, J.L., P.M. Crill, T.R. Moore, K. Savage and R.K. Varner. 1998. Seasonal patterns and controls on net ecosystem CO₂ exchange in a boreal peatland complex. *Global Biogeochem. Cycles* 12: 703-714.
- Bubier, J.L., S. Frohking, P.M. Crill and E. Linder. 1999. Net ecosystem productivity and its uncertainty in a diverse boreal peatland. *J. Geophys. Res.* 104: 27683-27692.
- Bubier, J.L., T.R. Moore, L. Bellisario, N.T. Comer and P.M. Crill. 1995. Ecological controls on methane emissions from a northern peatland complex in the zone of discontinuous permafrost, Manitoba, Canada. *Global Biogeochem. Cycles.* 9: 455-470.

- Bunbury, J., S.A. Finkelstein, and J. Bollman. 2012. Holocene hydro-climate and effects on carbon accumulation inferred for a peat bog in the Attawapiskat River watershed, Hudson Bay Lowlands, Canada. *Quatern. Res.* 78: 275-284.
- Burton, K.L., A.R. Rouse, and L.D. Boudreau, 1996. Factors affecting the summer carbon dioxide budget of subarctic wetland tundra. *Climate Res.* 6: 203-213.
- Calmels, F., M. Allard and G. Delisle. 2008a. Development and decay of a lithalsa in northern Québec: a geomorphological history. *Geomorphology* 97: 287-299.
- Calmels, F., G. Delisle and M. Allard. 2008b. Internal structure and the thermal and hydrological regime of a typical lithalsa: significance for permafrost growth and decay. *Can. J. Earth Sci.* 45: 31-43.
- Camill, P. 1999a. Patterns of boreal permafrost peatland vegetation across environmental gradients sensitive to climate warming. *Can. J. Bot.* 77: 721-733.
- Camill, P. 1999b. Peat accumulation and succession following permafrost thaw in the boreal peatlands of Manitoba, Canada. *Écoscience* 6: 592-602.
- Camill, P. 2000. How much do local factors matter for predicting transient ecosystem dynamics? Suggestions from permafrost formation in boreal peatlands. *Global Change Biol.* 6: 169-182.
- Camill, P., A. Barry, E. Williams, C. Andreassi, J. Limmer and D. Solick. 2009. Climate-vegetation-fire interactions and their impact on long-term carbon dynamics in a boreal peatland landscape in northern Manitoba, Canada. *J. Geophys. Res.* 114: G04017, doi:10.1029/2009JG001071.
- Camill, P., J.A. Lynch, J.S. Clark, J.B. Adams and B. Jordan. 2001. Changes in biomass, aboveground net primary production, and peat accumulation following permafrost thaw in the boreal peatlands of Manitoba, Canada. *Ecosystems* 4: 461-478.
- Campbell, C., D.H. Vitt, L.A. Halsey, I.D. Campbell, M.N. Thornton and S.E. Bayley. 2000. Net primary production and standing biomass in northern continental wetlands. *Can. For. Serv., North. For. Cent., Edmonton, AB. Info. Rep. NOR-X-369.* 57p.
- Carey, S.K. and W.L. Quinton. 2005. Evaluating runoff generation during summer using hydrometric, stable isotope, and hydrochemical methods in a discontinuous permafrost alpine catchment. *Hydrol. Process.* 19: 95-114.
- Chanton, J.P. 2005. The effect of gas transport on the isotope signature of methane in wetlands. *Organic Geochem.* 36: 753-768.
- Chen, W., Y. Zhang, J. Cihlar, S.L. Smith and D.W. Riseborough. 2003. Changes in soil temperature and active layer thickness during the twentieth century in a region in western Canada. *J. Geophys. Res.* 108: 4696, doi:10.1029/2002JD0033555.
- Chistjakov, V. I., A. I. Kuprijanov, V. V. Gorshkov and E. S. Artsybashe. 1983. Measures for fire prevention on peat deposits. 1983. Pp. 259–271 in Wein, R. W. and MacLean, D.A. (eds.). *The Role of Fire in Northern Circumpolar Ecosystems*, John Wiley, New York, NY.
- Christensen, J.H. and P. Kuhry. 2000. High-resolution regional climate model validation and permafrost simulation for the East European Russian Arctic, J. *Geophys. Res.* 105: 29,647–29,658.
- Christensen, T.R., S. Jonasson, A. Michelsen, T.V. Callaghan and M. Havström. 1998. Environmental controls on soil respiration in the Eurasian and Greenlandic Arctic. *J. Geophys. Res.* 103: 29,015-29,021.
- Christensen, T.R., T. Johansson, J. Åkerman and M. Mastepanov. 2004. Thawing sub-arctic permafrost: Effects on vegetation and methane. *Geophys. Res. Lett.* 31: L04501, doi:10.1029/2003GL018680.
- Cihlar, J. and C. Tamocai. 2000. Wetlands of Canada and climate change: Observation strategy and baseline data. Report of a Workshop 24-25 January 2000. *Nat. Resour. Can., Ottawa, ON.*
- Cirno, C.P., C.T. Driscoll and K. Bowes. 2000. Chemical fluxes from sediments in two Adirondack Wetlands: Effects of an acid-neutralization experiment. *Soil Sci. Soc. Am. J.* 64: 790-799.
- Clymo, R.S. 1984. The limits to peat bog growth. *Philos. Trans. R. Soc. Lond. Biol. Sci.* 303: 605-654.
- Collins, W.D., C.M. Bitz, M.M. Blackmon, G.B. Bonan, C.S. Bretherton, J.A. Carton, P. Chang, S.C. Doney, J.J.Hack, T.B. Henderson, J.T. Kiehl, W.G. Large, D.S. McKenna, D.B. Santer, and R.D. Smith, R.D., 2006: The community climate model version 3 (CCSM3). *J. Climate* 10: 2122-2143.
- Conrad, S. G., E.P. Davidenko, G.A. Ivanova, A.I. Sukhinin, B.J. Stocks and D.R. Cahoon. 2002. Determining effects of area burned and fire severity on carbon cycling and emissions in Siberia. *Clim. Change* 55: 197–211.
- Cornelissen, J.H.C., T.V. Callaghan, J.M. Alatalo, A. Michelsen, E. Graglia, A.E. Hartley, D.S. Hik, S.E. Hobbie, M.C. Press, H. Robinson, G.H.R. Henry, G.R. Shaver, G.K. Phoenix, D.G. Jones, S. Jonasson, F.S. Chapin III, U. Molau, C. Neill, J.A. Lee, J.M. Melillo, B. Sveinbjörnsson and R. Aerts. 2001. Global change and arctic ecosystems: Is lichen decline a function of increases in vascular plant biomass? *J. Ecol.* 89: 984-994.
- Corradi, C., O. Kolle, K. Walter, S.A. Zimov and E.D. Schultze. 2005. Carbon dioxide and methane exchange of a north-east Siberian tussock tundra. *Global Change Biol.* 2005: 1910-1925.
- Coyne, P.I. and J.J. Kelley. 1975. CO₂ exchange over the Alaskan arctic tundra: Meteorological assessments by an aerodynamic method. *J. Appl. Ecol.* 12: 5887-611.
- Crow, S.E. and R.K. Wieder. 2005. Sources of CO₂ emission from a northern peatland: Root respiration, exudation, and decomposition. *Ecology* 86: 1825-1834.
- Cyr, D., S. Gauthier and Y. Bergeron. 2007. Scale-dependent determinants of heterogeneity in fire frequency in a coniferous boreal forest of eastern Canada. *Landscape Ecol.* 22: 1325-1339.
- deGroot, W.J. J. Pritchard and T.J. Lynham. 2009. Forest fuel consumption and carbon emissions in Canadian boreal forest fires. *Can. J. For. Res.* 39: 367-382.
- den Hartog, G., H.H. Newmann, K.M. King and A.C. Chipanshi. 1994. Energy budget measurements using eddy correlation and Bowen ratio techniques at the Kinoshoo Lake tower site during the Northern Wetlands Study. *J. Geophys. Res.* 99: 1539-1549.
- Déry, S.J. and E.F. Wood. 2004. Teleconnection between the Arctic Oscillation and Hudson Bay river discharge. *Geophys. Res. Lett.* 31: L18205, doi:10.1029/2004GL020729.
- Déry, S.J. and E.F. Wood. 2005. Decreasing river discharge in northern Canada. *Geophys. Res. Lett.* 31: L10401, doi:10.1029/2005GL022845.
- Déry, S.J., M. Stieglitz, E.C. McKenna and E.F. Wood. 2005. Characteristics and trends of river discharge into Hudson, James and Ungava Bays, 1964-2000. *J. Climate* 18: 2540-2557.
- Dingman, S.L. 2002. *Physical Hydrology*, 2nd Ed. Prentice Hall. Upper Saddle River, NJ.

- Dissanska, M., M. Bernier and S. Payette. 2009. Object-based classification of very high resolution panchromatic images for evaluating recent change in the structure of patterned peatlands. *Can. J. Remote Sens.* 35: 189-215.
- Dodds, W.K. 2002. *Freshwater Ecology: Concepts and Environmental Application*. Academic Press, San Diego, CA, 569p.
- Dorrepaal, E. 2007. Are plant growth-form-based classifications useful in predicting northern ecosystem carbon cycling feedbacks to climate change? *J. Ecol.* 95: 1167-1180.
- Dorrepaal, E., S. Toet, R.S.P. van Logtestijn, E. Swart, M.J. van de Weg, T.V. Callahan and R. Aerts. 2009. Carbon respiration from subsurface peat accelerated by climate warming in the subarctic. *Nature* 460: 616-620.
- Drexler, J.Z., R.L. Snyder, D. Spano and K.T. Paw U. 2004. A review of models and micrometeorological methods used to estimate wetland evapotranspiration. *Hydrol. Process.* 18: 2071-2101.
- Ducoudré, N., Laval, K. and Perrier, A. 1993. SECHIBA, a new set of parametrizations of the hydrologic exchanges at the land/atmosphere interface within the LMD atmospheric general circulation model. *J. Clim.* 2: 248-273.
- Duddleston, K.N., M.A. Kinney, R.P. Kiene and M.E. Hines. 2002. Anaerobic microbial biogeochemistry in a northern bog: Acetate as a dominant metabolic end product. *Global Biogeochem. Cycles* 16: 1063, doi:10.1029/2001GB001402.
- Duguay, C.R., T. Zhang, D.W. Leverington and V.E. Romanovsky. 2005. Satellite remote sensing of permafrost and seasonally frozen ground. Pp. 91-118 *in* Duguay, C.R and Pietroniro A. (eds.). *Remote Sensing in Northern Hydrology: Measuring Environmental Change*, Geophys. Monogr. Ser., vol. 163, Am. Geophys. Union, Washington, DC. 160 p.
- Dutta, K., E.A.G. Schuur, J.C. Neff and S.A. Zimov. 2006. Potential carbon release from permafrost soils of northeastern Siberia. *Global Change Biol.* 12: 2336-2351.
- Dyke, L.D. and W.E. Sladen. 2010. Permafrost and peatland evolution in the northern Hudson Bay Lowland, Manitoba. *Arctic* 63: 429-441.
- Eaton, A.K. and W.R. Rouse. 2001. Controls of evapotranspiration at a subarctic sedge. *Hydrol. Process.* 15: 3423-3431.
- Eaton, A.K., W.R. Rouse, P.M. Lafleur, P. Marsh and P.D. Blanken. 2001. Surface energy balance of the western and central Canadian Subarctic: Variations in the energy balance among five major terrain types. *J. Clim.* 14: 3692-3703.
- Engstrom, R., A. Hope, H. Kwon, Y. Harazono, M. Mano and W. Oechel. 2006. Modeling evapotranspiration in Arctic coastal plain ecosystems using a modified BIOME-BGC model. *J. Geophys. Res.* 111: G02021, doi:10.1029/2005JG000102.
- Eugster, W., W.R. Rouse, R.A. Pielke, J.P. McFadden, D.D. Baldocchi, T.G.F. Kittel, F.S. Chapin, G.E. Liston, P.L. Vidale, E. Vaganov and S. Chambers. 2000. Land-atmosphere energy exchange in Arctic tundra and boreal forest: Available data and feedbacks to climate. *Global Change Biol.* (Suppl 1): 84-115.
- Euskirchen, E.S., A.D. McGuire, D.W. Kicklighter, Q. Zhuang, J.S. Clein, R.J. Dargaville, D.G. Dye, J.S. Kimball, K.C. McDonald, J.M. Meillo, V.E. Romanovsky and N.V. Smith. 2006. Importance of recent shifts in soil thermal dynamics on growing season length, productivity, and carbon sequestration in terrestrial high latitude ecosystems. *Global Change Biol.* 12: 731-750.
- Fan, S.M., S.C. Wolfsy, P.S. Bakwin and D.J. Jacob. 1992. Micrometeorological measurements of CH₄ and CO₂ exchange between the atmosphere and subarctic tundra. *J. Geophys. Res.* 102: 29,053-29,064.
- Far North Science Advisory Panel, 2010: Science for a changing Far North. The Report of the Far North Science Advisory Panel. A report submitted to the Ontario Ministry of Natural Resources. www.ontario.ca/farnorth.
- [FPTGC] Federal, Provincial, and Territorial Governments of Canada. 2010. Canadian biodiversity: ecosystem status and trends 2010. Canadian Council of Resource and Environmental Ministers. Ottawa, ON. vi+142p.
- Flannigan, M., B. Stocks, M. Turetsky and M. Wotton. 2009. Impacts of climate change on fire activity and fire management in the circumboreal forest. *Global Change Biol.* 15: 549-560.
- Flannigan, M.D., K.A. Logan, B.D. Amiro, W.R. Skinner and B.J. Stocks. 2005. Future area burned in Canada. *Clim. Change* 72: 1-16.
- Fournier, R.A., M. Grenier, A. Lavoie and R. Hélie. 2007. Towards a strategy to implement the Canadian Wetland Inventory using satellite remote sensing. *Can. J. Remote Sens.* 33 (Suppl. 1): S1-S16.
- Frauenfeld, O. W., T. Zhang and J.L. McCreight. 2007. Northern Hemisphere freezing/thawing index variations over the twentieth century. *Int. J. Climatol.* 27: 47-63.
- Freeman, C., N. Ostle and H. Kang. 2001. An enzymic 'latch' on a global carbon store - A shortage of oxygen locks up carbon in peatlands by restraining a single enzyme. *Nature* 409: 149.
- French, H.M. and O. Slaymaker. 1993. Canada's cold land mass. Pp. 3-28 *in* French, H.M. and Slaymaker, O. (eds.). *Canada's Cold Environments*. McGill-Queen's University Press, Montreal, QC.
- French, N. H. F., E. S. Kasischke, B. J. Stocks, J. P. Mudd, D. L. Martell and B. S. Lee. 2000. Carbon release from fires in the North American boreal forest. Pp. 377-388 *in* Kasischke, E.S. and Stocks B.J. (eds.). *Fire, Climate Change, and Carbon Cycling in the Boreal Forest*. Springer, New York, NY. 461 p.
- Frey, K.E. and J.W. McClelland. 2009. Impacts of permafrost degradation on arctic river biogeochemistry. *Hydrol. Process.* 23: 169-182.
- Frey, K.E. and L.C. Smith. 2005. Amplified carbon release from vast West Siberian peatlands by 2100. *Geophys. Res. Lett.* 32: L09401, doi:10.1029/2004GL022025.
- Frey, K.E., D.I. Siegel and L.C. Smith. 2007. Geochemistry of west Siberian streams and their potential response to permafrost degradation. *Water Resour. Res.* 43: W03406, doi:10.1029/2006WR004902.
- Friborg, T., T.R. Christensen and H. Sørengaard. 1997. Rapid response of greenhouse gas emission to early spring thaw in a subarctic mire as shown by micrometeorological techniques. *Geophys. Res. Lett.* 24: 3061-3064.
- Friborg, T., T.R. Christensen, B.U. Hanson, C. Nordstroem and H. Sørengaard. 2000. Trace gas exchange in a high-arctic valley. 2. Landscape CH₄ fluxes measured and modeled using eddy correlation data. *Global Biogeochem. Cycles* 14: 715-723.
- Friborg, T., H. Sørengaard, T.R. Christensen, C.R. Lloyd and N.S. Panikov. 2003. Siberian wetlands: Where a sink is a source. *Geophys. Res. Lett.* 30: 2129, doi:10.1029/2003GL017797.

- Friel, C. 2011. Diatom records of Holocene climatic and hydrological changes in the western Hudson Bay region, Canada. MSc. Dept. Geography, University of Toronto, Toronto, ON.
- Frolking, S. and N.T. Roulet. 2007. Holocene radiative forcing impact of northern peatland carbon accumulation and methane emissions. *Global Change Biol.* 13: 1079-1088.
- Frolking, S., N. Roulet and J. Fuglestedt. 2006. How northern peatlands influence the Earth's radiative budget: Sustained methane emission versus sustained carbon sequestration. *J. Geophys. Res.* 111: G01008, doi:10.1029/2005JG000091.
- Frolking, S., N. Roulet and D. Lawrence. 2009. Issues related to incorporating northern peatlands into global climate models. Pp. 19-35 in Baird, A.J., Beleyea, L.R., Comas, X., Reeve, A.S. and Slater, L.D. (eds.). *Carbon Cycling in Northern Peatlands*, Geophysical Monograph Series, 184. Am. Geophys. Union, Washington, DC.
- Frolking, S., M.L. Goulden, S.C. Wofsy, S.M. Fan, D.J. Sutton, J.W. Munger, A.M. Bazzaz, B.C. Daube, P.M. Crill, J.D. Aber, L.E. Band, X. Wang, K. Savage, T. Moore and R.C. Harriss. 1996. Modelling temporal variability in the carbon balance of a spruce/moss boreal forest. *Global Change Biol.* 2: 343-366.
- Frolking, S., N.T. Roulet, E. Tuittila, J.L. Bubier and A. Quillet. 2010. A new model of Holocene peatland net primary production, decomposition, water balance and peat accumulation. *Earth Syst. Dynam.* 1: 115-167.
- Frolking, S., J. Talbot, N. Roulet, M. Jones, C. Treat, B. Boone Kauffman and E. Tuittila. 2011. Peatlands in the Earth's 21st century coupled climate-carbon system. *Environ. Rev.* 19: 371-396.
- Fronzek, S., M. Luoto and T.R. Carter. 2006. Potential effect of climate change on the distribution of palusa mires in subarctic Fennoscandia. *Clim. Res.* 32: 1-12.
- Fuchs, H., P. Magdon, C. Kleinn and J. Flessa. 2009. Estimating aboveground carbon in a catchment of the Siberian forest tundra: Combining satellite imagery and field inventory. *Remote Sens. Environ.* 113: 518-531.
- Fukuzaki, S., N. Nishio and S. Nagai. 1990. Kinetics of the methanogenic fermentation of acetate. *Appl. Environ. Microbiol.* 56: 3158-3163.
- Gagnon, A.S. and W.A. Gough. 2005. Climate change scenarios for the Hudson Bay region: An intermodel comparison. *Clim. Change* 69: 269-297.
- Gibson, J.J., T.W.D. Edwards and T.D. Prowse. 1993. Run off generation in a high boreal wetland in northern Canada. *Nordic Hydrol.* 24: 213-224.
- Gignac, L.D., R. Gauthier, L. Rochefort and J. Bubier. 2004. Distribution and habitat niches of 37 peatland Cyperaceae species across a broad geographic range in Canada. *Can. J. Bot.* 82: 1292-1313.
- Gillet, N. P., A.J. Weaver, F.W. Zwiers and M.D. Flannigan. 2004. Detecting the effect of climate change on Canadian forest fires. *Geophys. Res. Lett.* 31: L18211, doi:10.1029/2004GL020876.
- Gitelson, A.A., Y. Gritz and M.N. Merzlyak. 2003. Relationships between leaf chlorophyll content and spectral reflectance and algorithms for non-destructive chlorophyll assessment in higher leaves. *J. Plant Physiol.* 160: 271-282.
- Glaser, P.H., J.A. Janssens and D.I. Siegel. 1990. The response of vegetation to chemical and hydrological gradients in the Lost River Peatland, northern Minnesota. *J. Ecol.* 78: 1021-1048.
- Glaser, P.H., B.S.C. Hansen, D.I. Siegel, A.S. Reeve and P.J. Morin. 2004a. Rates, pathways and drivers for peatland development in the Hudson Bay Lowlands, northern Ontario, Canada. *J. Ecol.* 92: 1036-1053.
- Glaser, P.H., D.I. Siegel, A.S. Reeve and J.P. Chanton. 2006. Hydrogeology of major peat basins in North America. Pp. 347-376 in Martini, I.P., Cortizas A.M. and Chesworth, W. (eds.). *Peatland Evolution and Records of Environmental and Climate Changes*. Elsevier, Amsterdam, NL.
- Glaser, P.H., D.I. Siegel, E.A. Romanowicz, and Y.P. Shen. 1997. Regional linkages between raised bogs and the climate, groundwater, and landscape of north-western Minnesota. *J. Ecol.* 85: 3-16.
- Glaser, P.H., D.I. Siegel, A.S. Reeve, J.A. Janssens and D.R. Janecky. 2004b. Tectonic drivers for vegetation patterning and landscape evolution in the Albany River region of the Hudson Bay Lowlands. *J. Ecol.* 92: 1054-1071.
- Glaser, P.H., G.A. Wheeler, E. Gorham and H.E. Wright Jr. 1981. The patterned mires of the Red Lake Peatland, northern Minnesota: Vegetation, water chemistry, and landforms. *J. Ecol.* 69: 575-599.
- Glenn, A.J., L.B. Flanagan, K.H. Syed and P.J. Carlson. 2006. Comparison of net ecosystem CO₂ exchange in two peatlands in western Canada with contrasting dominant vegetation, *Sphagnum* and *Carex*. *Agric. For. Meteorol.* 140: 115-135.
- Godin, A., J.W. McLaughlin, K. Webster, M. Packalen and N. Basiliko. 2012. Methane and methanogen community dynamics across a boreal peatland nutrient gradient. *Soil Biol. Biochem.* 48: 96-105.
- Goodrich, L.E. 1982. The influence of snow cover on the ground thermal regime. *Can. Geotech. J.* 19: 421-432.
- Gorham, E. 1991. Northern peatlands: Role in the climate cycle and probable responses to climatic warming. *Ecol. Appl.* 1: 182-195.
- Gorham, E., S.E. Bayley and D.W. Schindler. 1984. Ecological effects of acid deposition upon peatlands: a neglected field in "acid-rain" research. *Can. J. Fish. Aquat. Sci.* 41:1256-1268.
- Gorham, E., J.A. Janssens and P.H. Glaser. 2003. Rates of peat accumulation during the postglacial period in 32 sites from Alaska to Newfoundland, with special emphasis on northern Minnesota. *Can. J. Bot.* 81: 429-438.
- Gough, W.A. and A. Leung. 2002. Nature and fate of Hudson Bay permafrost. *Reg. Environ. Change* 2: 177-184.
- Goulden, M.L., S.C. Wofsy, J.W. Harden, S.E. Trumbore, P.M. Crill, S.T. Gower, T. Fries, B.C. Daube, S.M. Fan, D.J. Sutton, A. Bazzaz and J.W. Munger. 1998. Sensitivity of boreal forest carbon balance to soil thaw. *Science* 279: 214-217.
- Grenier, M., A.M. Demers, S. Labrecque, M. Benoit, R.A. Fournier and B. Drolet. 2007. An object-based method to map wetland using RADARSAT-1 and Landsat ETM images: test case on two sites in Québec, Canada. *Can. J. Remote Sens.* 33: S28-S45.
- Grenier, M., S. Labrecque, M. Gameau and A. Tremblay. 2008. Object-based classification of a SPOT-4 image for mapping wetlands in the context of greenhouse gasses emissions: the case of the Eastmain region, Québec, Canada. *Can. J. Remote Sens.* 34 (Suppl. 2): S398-S413.
- Griffis, T.J. and W.R. Rouse. 2001. Modelling the interannual variability of net ecosystem CO₂ exchange at a subarctic sedge fen. *Global Change Biol.* 7: 511-530.

- Griffis, T.J., W.R. Rouse and J.M. Waddington. 2000. Interannual variability of net ecosystem CO₂ exchange at a subarctic fen. *Global Biogeochem. Cycles* 14: 1109-1121.
- Grogan, P. and S. Jonasson. 2006. Ecosystem CO₂ production during winter in a Swedish subarctic region: the relative importance of climate and vegetation type. *Global Change Biol.* 12: 1479-1475.
- Grosse, G., J. Harden, M. Turetsky, A.D. McGuire, P. Camill, C. Tarnocai, S. Frolking, E.A.G. Schuur, T. Jorgenson, S. Marchenko, V. Romanovsky, K.P. Wickland, N. French, M. Waldrop, L. Bourgeau-Chavez and R.G. Striegl. 2011. Vulnerability of high-latitude soil organic carbon in North America to disturbance. *J. Geophys. Res.* 116: G00K06, doi:10.1029/2010JG001507.
- Gunnarsson, U., N. Malmer and H. Rydin. 2002. Dynamics or constancy in *Sphagnum* dominated mire ecosystems? A 40-year study. *Ecography* 25: 685-704.
- Gunnarsson, U., H. Rydin and H. Sjörs. 2000. Diversity and pH changes after 50 years on the boreal mire Skattlosbergs Storemosse, central Sweden. *J. Veg. Sci.* 11: 277-286.
- Guo, Y. and P.H. Schuepp. 1994. On surface energy balance over the northern wetlands, the effects of small-scale temperature and wetness heterogeneity. *J. Geophys. Res.* 99: 1601-1612.
- Guo, L.D., I. Semiletov, O. Gustafsson, J. Ingri, P. Andersson, O. Dudarev and D. White. 2004. Characterization of Siberian Arctic coastal sediments: Implications for terrestrial organic carbon export. *Global Biogeochem. Cycles* 18: GB1036, doi:10.1029/2003GB002087.
- Gurney, S.D. 2001. Aspects of the genesis, geomorphology and terminology of palsas: perennial cryogenic mounds. *Prog. Phys. Geogr.* 25: 249-260.
- Hagedorn, F., P.A.W. van Hees, T. Handa and S. Hattenschwiler. 2008. Elevated atmospheric CO₂ fuels leaching of old dissolved organic matter at the alpine treeline. *Global Biogeochem. Cycles* 22: GB2004, doi:10.1029/2007GB003026.
- Halliwel, D.H. and W.R. Rouse. 1987. Soil heat flux in permafrost: characteristics and accuracy of measurement. *J. Climatol.* 7: 571-584.
- Halsey, L.A., D.H. Vitt and S.C. Zoltai. 1995. Disequilibrium response of permafrost in boreal continental western Canada to climate change. *Clim. Change* 30: 57-73.
- Hamilton, J.D., C.A. Kelly, J.W.M. Rudd, R.H. Hesslein and N.T. Roulet. 1994. Flux to the atmosphere of CH₄ and CO₂ from wetlands ponds on the Hudson Bay Lowlands (HBLs). *J. Geophys. Res.* 99: 1495-1510.
- Harazono, Y., M. Yoshimoto, M. Mano, G.L. Vourlitis and W.C. Oechel. 1998. Characteristics of energy and water budgets over wet sedge and tussock tundra ecosystems at North Slope in Alaska. *Hydrol. Process.* 12: 2163-2183.
- Harbaugh, A.W. and M.G. McDonald. 1996. User's documentation for Modflow-96. An update to the U.S. Geological Survey Modular Finite-Difference Groundwater Groundwater Flow Model. U.S. Geol. Surv., Open File Rep. 96-486. 222 p.
- Harden, J.W., K.L. Manies, J.C. Neff and M.R. Turetsky. 2006. Effects of wildfire and permafrost on soil organic matter and soil climate in interior Alaska. *Global Change Biol.* 12: 1-13.
- Harris, S.A. 2002. Causes and consequences of rapid thermokarst development in permafrost or glacial terrain. *Permafrost Periglac.* 13: 237-242.
- Harris, A. and R.G. Bryant. 2009a. A multi-scale remote sensing approach for monitoring northern peatland hydrology: Present possibilities and future challenges. *J. Environ. Manage.* 90: 2178-2188.
- Harris, A. and R.G. Bryant. 2009b. Northern peatland vegetation and the carbon cycle: A remote sensing approach. Pp. 79-98 in Baird, A.J., Belyea, L.R., Comas, X., Reeve, A.S., and Slater, L.D. (eds.). *Carbon Cycling in Northern Peatlands*. Geophys. Monogr. Series 184. Am. Geophys. Union. Washington, DC. 299 p.
- Harris, A., R.G. Bryant and A.J. Baird. 2005. Detecting near-surface moisture stress in *Sphagnum* spp. *Remote Sens. Environ.* 97: 371-381.
- Harris, A., R.G. Bryant and A.J. Baird. 2006. Mapping the effects of water stress on *Sphagnum*: Preliminary observations using airborne remote sensing. *Remote Sens. Environ.* 100: 363-378.
- Harris, C., L.U. Arensen, H.H. Christiansen, B. Etzelmuller, R. Frauenfelder, S. Gruber, W. Haeberli, C. Hauck, M. Holzle, O. Humlum, K. Isaksen, A. Kaab, M. Lehning, M.A. Lutschg, M. Phillips, N. Ross, M. Seppälä, S. Springman and D. Vonderr Muhill. 2009. Permafrost and climate in Europe: monitoring and modelling thermal, geomorphological and geotechnical responses. *Earth Sci. Rev.* 92: 117-171.
- Hawkes, B.C. 1993. Factors that influence peat consumption under dependent burning conditions: A laboratory study. PhD dissertation, University of Montana, Missoula, MT.
- Hazeline, A., I.C. Prentice and D.I. Creswell. 1996. A coupled carbon and water flux model to predict vegetation structure. *J. Veg. Sci.* 7: 651-666.
- Hayashi, M., W.L. Quinton, A. Pietroniro and J.J. Gibson. 2004. Hydrologic functions of wetlands in a discontinuous permafrost basin indicated by isotopic and chemical signatures. *J. Hydrol.* 296: 81-97.
- Heginbottom, J.A., M.A. Dubreuil and P.A. Harker. 1995. Canada—Permafrost. In *National Atlas of Canada*, 5th Edition. Nat. Resour. Can., National Atlas Info. Serv., Ottawa, ON. MCR 4177.
- Heikkinen, J.E.P., M. Majanen, M. Aurela, K.J. Hargreaves and P.J. Martikainen. 2002. Carbon dioxide and methane dynamics in a sub-Arctic peatland in northern Finland. *Polar Res.* 21: 49-62.
- Heikkinen, J.E.P., T. Virtanen, J.T. Huttunen, V. Elsakov and P.J. Martikainen. 2004. Carbon balance in East European tundra. *Global Biogeochem. Cycles* 18: GB1023, doi:10.1029/2003GB002054.
- Hemond, H.F. 1980. Biogeochemistry of Thoreau's Bog, Concord, Massachusetts. *Ecol. Monogr.* 50: 507-526.
- Henry, K. and M. Smith. 2001. A model-based map of ground temperatures for permafrost regions of Canada. *Permafrost Periglac.* 12: 389-398.
- Hines, M.E., K.N. Duddlestone and R.P. Kiene. 2001. Carbon flow to acetate and C-1 compounds in northern wetlands. *Geophys. Res. Lett.* 28: 4251-4254.
- Hinkel, K.M. and F.E. Nelson. 2003. Spatial and temporal patterns of active layer thickness at Circumpolar Active Layer Monitoring (CALM) sites in northern Alaska 1995-2000. *J. Geophys. Res.* 108: 8168, doi:10.1029/2001JD000927.
- Hinkel, K.M., F. Paetzold, F.E. Nelson and J.G. Bockheim. 2001. Patterns of soil temperature and moisture in the active layer and upper permafrost at Barrow, Alaska: 1993-1999. *Global Planet. Change* 29: 293-309.

- Hinzman, L.D., D.L. Kane, R.E. Gieck and K.R. Everett. 1991. Hydrologic and thermal properties of the active layer in the Alaskan Arctic. *Cold Reg. Sci. Technol.* 19: 95-110.
- Hjort, J. and M. Luoto. 2009. Interaction of geomorphic and ecologic features across altitudinal zones in a subarctic landscape. *Geomorphology* 112: 324-333.
- Hjort, J., M. Luoto and M. Seppälä. 2007. Landscape scale determinants of periglacial features in subarctic Finland: A grid-based modelling approach. *Permafrost Periglac.* 18: 115-127.
- Hobbie, S.E., J.P. Schimel, S.E. Turmbore and J.R. Randerson. 2000. Controls over carbon storage and turnover in high-latitude soils. *Global Change Biol.* 6 (Suppl. 1): 196-210.
- Hogg, A. 2010. Far North Land Cover – 2005 to 2009. Data Specifications Version 1.1. Ont. Min. Nat. Resour., Sci. Info. Br., Peterborough, ON. Far North Info. Knowl. Mgmt. Int. Rep. (Available from IMA section, paul.sampson@ontario.ca)
- Hooper, R.P.N. 2003. Diagnostic tools for mixing models of stream water chemistry. *Water Resour. Res.* 39: 3 1055, doi:10.1029/2002WR001528.
- Hooper, R. P., N. Christophersen and N.E. Peters. 1990. Modelling streamwater chemistry as a mixture of soil-water end members—An application to the Panola Mountain watershed, GA, USA. *J. Hydrol.* 116: 321-343.
- Hornibrook, E.R.C. and H.L. Bowes. 2007. Trophic status impacts both the magnitude and stable carbon isotope composition of methane flux from peatlands. *Geophys. Res. Lett.* 34: L21401, doi:10.1029/2007GL031231.
- Hornibrook, E.R.C., F.J. Longstaffe and W.S. Fyfe. 1997. Spatial distribution of microbial methane production pathways in temperate zone wetland soils: stable carbon and hydrogen biotope evidence. *Geochem. Cosmochim. Acta* 61: 745-753.
- Humphreys, E.R., P.M. Lafleur, L.B. Flanagan, N. Hedstrom, K.H. Syed, A.J. Glenn and R. Granger. 2006. Summer carbon dioxide and water vapor fluxes across a range of northern peatlands. *J. Geophys. Res. – Biogeosciences* 111: G04011, doi:10.1029/2005JG000111.
- Huttunen, J.T., T.S. Vaisanen, M. Heikkinen, S. Hellsten, H. Nykanen, O. Nenonen and P.H. Martikainen. 2002. Exchange of CO₂, CH₄, and N₂O between the atmosphere and two northern boreal ponds with catchments dominated by peatlands or forests. *Plant Soil* 124: 137-146.
- Huttunen, J.T., H. Nykänen, J. Turunen and P.J. Martikainen. 2003. Methane emissions from natural peatlands in the northern boreal zone in Finland, Fennoscandia. *Atmos. Environ.* 37: 147-151.
- [IPCC] International Panel on Climate Change. 2007. Contribution of Working Group I to the Fourth Assessment Report of the Intergovernmental Panel on Climate Change, 2007. *The Physical Science Basis*. Solomon, S., Qin, D., Manning, M., Chen, Z., Marquis, M., Averyt, K.B., Tignor, M., and Miller, H.L. (eds.). Cambridge Univ. Press, Cambridge, UK.
- Ise, T., A.L. Dunn, S.C. Wofsy and P.R. Moorcroft. 2008. High sensitivity of peat decomposition to climate change through water-table feedback. *Nat. Geosci.* 1: 763-766.
- Janowicz, I.R. 2008. Apparent recent trends in hydrologic response in permafrost regions of northwest Canada. *Hydrol. Res.* 39: 267-275.
- Jiang, Y., Q. Zhuang, M.D. Flannigan and J.M. Little. 2009. Characterization of wildfire regimes in Canadian boreal terrestrial ecosystems. *Int. J. Wildl. Fire* 18: 992-1002.
- Johansson, T., N. Malmer, P.M. Crill, T. Friborg, J.H. Åkerman, M. Mastepanov and T.R. Christensen. 2006. Decadal vegetation changes in a northern peatland, greenhouse gas fluxes and net radiative forcing. *Global Change Biol.* 12: 2352-2369.
- Johnson, L.C., G.R. Shaver, D.H. Cades, E. Rastetter, K. Nadelhoffer, A. Giblin, J. Laundre and A. Stanley. 2000. Plant carbon-nutrient interactions control CO₂ exchange in Alaskan wet sedge tundra ecosystems. *Ecology* 81: 453-469.
- Joiner, D.W., P.M. Lafleur, J.H. McCaughy and P.A. Bartlett. 1999. Interannual variability in carbon dioxide exchanges at a boreal wetland in the BOREAS northern study area. *J. Geophys. Res.* 104: 663-672.
- Jones, B.M., G. Grosse, C.D. Arp, K.M. Walter Anthony and V.E. Romanovsky. 2011. Modern thermokarst lake dynamics in the continuous permafrost zone, northern Seaward Peninsula, Alaska. *J. Geophys. Res.* 116: G00M03, doi:10.1029/2011JG001666.
- Jones, L.A., J.S. Kimbal, K.C. McDonal, S.T.K. Chan, E.G. Njoku and W.C. Oechel. 2007. Satellite microwave remote sensing of boreal and arctic soil temperatures from AMSR-E. *IEEE Trans. Geosci. Remote Sens.* 45: doi:10.1109/TGRS.2007.898436.
- Jorgensen, A.S. and F. Andreassen. 2007. Mapping of permafrost surface using ground-penetrating radar at Kangerlussuaq Airport, western Greenland. *Cold Reg. Sci. Technol.* 48: 64-72.
- Jorgenson, M., Y. Shur and E. Pullman. 2006. Abrupt increase in permafrost degradation in Arctic Alaska. *Geophys. Res. Lett.* 33: L02503, doi:10.1029/2005GL024960.
- Jorgenson, M.T., C.H. Racine, J.C. Walters and T.E. Osterkamp. 2001. Permafrost degradation and ecological changes associated with a warming climate in central Alaska. *Clim. Change* 48: 551-579.
- Jorgenson, M.T., V. Romanovsky, J. Harden, Y. Shur, J. O'Donnell, E.A.G. Schuur, M. Kanewskiy and S. Marchenko. 2010. Resilience and vulnerability of permafrost to climate change. *Can. J. For. Res.* 40: 1219-1236.
- Juottonen, H., P.E. Galand, E.S. Tuittila, J. Laine, H. Fritze and K. Yrjala. 2005. Methanogen communities and bacteria along an ecohydrological gradient in a northern raised bog complex. *Environ. Microbiol.* 7: 1547-1557.
- Kaiser, C., H. Meyer, C. Biasi, O. Rusalimova, P. Baruskov and A. Richter. 2007. Conservation of soil organic matter through cryoturbation in arctic soils in Siberia. *J. Geophys. Res.* 112: G02017, doi:10.1029/2006JG000258.
- Kalbitz, K., S. Solinger, J.H. Park, B. Michalzik and E. Matzner. 2000. Controls on the dynamics of dissolved organic matter in soils: a review. *Soil Sci.* 165: 277-304.
- Kane, D.L., L.D. Hinzman, R.E. Gieck, J.P. McNamara, E.K. Youcha and J.A. Oatley. 2008. Contrasting extreme runoff events in areas of continuous permafrost, Arctic Alaska. *Hydrol Res.* 39: 267-298.
- Kane, E.S., E.S. Kasischke, D.W. Valentine, M.R. Turetsky and A.D. McGuire. 2007. Topographic influences on wildfire consumption of soil organic carbon in interior Alaska: Implications for black carbon accumulation. *J. Geophys. Res.* 112: G03017, doi:10.1029/2007JG000458.
- Kasischke, E. S. and E.E. Hoy. 2012. Controls on carbon consumption during Alaskan wildland fires. *Global Change Biol.* 18: 685-699.

- Kasischke, E. S. and J.F. Johnstone. 2005. Variation in postfire organic layer thickness in a black spruce forest complex in interior Alaska and its effects on soil temperature and moisture. *Can. J. For. Res.* 35: 2164-2177.
- Kasischke, E. S. and M.R. Turetsky. 2006. Recent changes in the fire regime across the North American boreal region-spatial and temporal patterns of burning across Canada and Alaska. *Geophys. Res. Lett.* 33: L09703, doi:10.1029/2006GL025677.
- Kasischke, E.S., M.A. Tanase, L.L. Bourgeau-Chavez and M. Borr. 2011. Soil moisture limitations on monitoring boreal forest regrowth using space borne L-based SAR data. *Remote Sens. Environ.* 115: 227-232.
- Kasischke ES, D.L. Verbyla, T.S. Rupp, A.D. McGuire, K.A. Murphy, R. Jandt, J.R. Barnes, E.E. Hoy, P.A. Duffy, M. Calef and M.R. Turetsky. 2010. Alaska's changing fire regime –implications for the vulnerability of its boreal forests. *Can. J. For. Res.* 40: 1313-1324.
- Kawahigashi, M., K. Kaiser, K. Kalbitz, A. Rodionov and G. Guggenberger. 2004. Dissolved organic matter in small streams along a gradient from discontinuous to continuous permafrost. *Global Change Biol.* 10: 1576-1586.
- Kellner, E. 2001. Surface energy fluxes and control of evapotranspiration from a Swedish *Sphagnum* mire. *Agric. For. Meteorol.* 110: 101-123.
- Kettles, L.M., M. Gameau and H. Jette. 2000. Macrofossil, pollen, and geochemical records of peatlands in the Kinosheo Lake and Detour Lake areas, northern Ontario. *Geol. Surv. Can. Bull.* 545, Ottawa, ON. 24p.
- Khvorostyanov, D.V., P. Ciais, G. Krinner and S.A. Zimov. 2008. Vulnerability of east Siberia's frozen carbon stores to future warming. *Geophys. Res. Lett.* 35: L10703, doi:10.1029/2008GL033639.
- Kim, J. and S.H. Verma. 1996. Surface exchange of water vapour between an open *Sphagnum* fen and the atmosphere. *Bound.-Lay. Meteorol.* 76: 243-264.
- Klinger, L.E. and S.K. Short. 1996. Succession in the Hudson Bay Lowland, northern Ontario, Canada. *Arctic Alpine Res.* 28: 172-193.
- Klinger, L.F., P.R. Zimmerman, J.P. Greenberg, L.E. Heidt and A.B. Guenther. 1994. Carbon trace gas fluxes along a successional gradient in the Hudson Bay lowland. *J. Geophys. Res.* 99: 1469-1494.
- Kokelj, S.V. and C.R. Burns. 2005. Geochemistry of the active layer and near-surface permafrost, Mackenzie delta region, Northwest Territories, Canada. *Can. J. Earth Sci.* 42: 37-48.
- Koven, C. D., B. Ringeval, P. Friedlingstein, P. Ciais, P. Cadule, D. Khvorostyanov, G. Krinner and C. Tarnocai. 2011. Permafrost carbon-climate feedbacks accelerate global warming. *Proc. Nat. Acad. Sci.* 108: 14769-14774.
- Krankina, O.N., D. Pflugmacher, M. Friedl, W.B. Cohen, P. Nelson and A. Baccini. 2008. Meeting the challenge of mapping peatlands with remotely sensed data. *Biogeosciences Discuss.* 5: 2075-2101.
- Kuchment, L.S., A.N. Gelfan and V.N. Demidov. 2000. A distributed model of runoff generation in the permafrost regions. *J. Hydrol.* 240: 1-22.
- Kuder, T. and M.A. Kruege. 2001. Carbon dynamics in peat bogs: insights from substrate macromolecular chemistry. *Global Biogeochem. Cycles* 15: 721-727.
- Kuhry, P. 1994. The role of fire in the development of Sphagnum-dominated peatlands in western boreal Canada. *J. Ecol.* 82: 899-910.
- Kuhry, P. 2008. Palsa and peat plateau development in the Hudson Bay Lowlands, Canada: Timing, pathways and causes. *Boreas* 37: 316-327.
- Kuhry, P. and J. Turunen. 2006. The postglacial development of boreal and subarctic peatlands. Pp. 25-46 in Wieder, R.K., Vitt, D.H. (eds.) *Boreal Peatland Ecosystems*. Springer, New York, NY.
- Kujala, K., M. Seppälä and T. Holappa. 2008. Physical properties of peat and palsa formation. *Cold Reg. Sci. Technol.* 52: 408-414.
- Kullman, L. 2007. Tree line population monitoring of *Pinus sylvestris* in the Swedish Scandes, 1973-2005: Implications for tree line theory and climate change ecology. *J. Ecol.* 95: 41-52.
- Kurbatova, J., A. Arneth, N.N. Vygodskaya, O. Kolle, I.M. Milyukova, N.M. Tchebakova, E.-D. Schulze and J. Lloyd. 2002. Comparative ecosystem-atmosphere exchange of energy and mass in a European Russian and central Siberian bog I. Interseasonal and interannual variability of energy and latent heat fluxes during the snowfree period. *Tellus B* 54: 497-513.
- Kwon, H.K., W.C. Oechel, R.C. Zulueta, S.J. Hastings. 2006. Effects of climate variability on carbon sequestration among adjacent wet sedge tundra and moist tussock tundra ecosystems. *J. Geophys. Res. – Biogeosciences* 111: GO3014 doi:10.1029/2005000036.
- Lachenbruch, A.H. and J.H. Sass. 1988. The stress heat-flow paradox and thermal results from Cajon Pass. *Geophys. Res. Lett.* 15: 981-984.
- Lafleur, P.M. 1992. Energy balance and evapotranspiration from a subarctic forest. *Agric. For. Meteorol.* 58: 163-175.
- Lafleur, P.M. and E.R. Humphreys. 2008. Spring warming and carbon dioxide exchange over low Arctic tundra in central Canada. *Global Change Biol.* 14: 1-17.
- Lafleur, P.M. and W.R. Rouse. 1988. The influence of surface cover and climate on energy partitioning and evaporation in a subarctic wetland. *Bound.-Lay. Meteorol.* 44: 327-347.
- Lafleur, P.M., A.V. Renzetti and B. Bello. 1993. Seasonal changes in the radiation balance of subarctic forest and tundra. *Arctic Alpine Res.* 25: 33-36.
- Lafleur, P.M., J.H. McCaughey, D.W. Joiner, P.A. Bartlett and D.E. Jelinski. 1997. Seasonal trends in energy, water, and carbon dioxide fluxes at a northern boreal wetland. *J. Geophys. Res.* 102: 29,009-29,020.
- Lafleur, P. M., T.R. Moore, N.T. Roulet and S. Frohling. 2005. Ecosystem respiration in a cool temperate bog depends on peat temperature but not hot water table. *Ecosystems* 8: 619-629.
- Laiho, R. 2006. Decomposition in peatlands: Reconciling seemingly contrasting results on the impacts of lowered water levels. *Soil Biol. Biochem.* 38: 2011-2024.
- Laiho, R., H. Vasander, T. Penttil and J. Laine. 2003. Dynamics of plant-mediated organic matter and nutrient cycling following water-level drawdown in boreal peatlands. *Global Biogeochem. Cycles* 17: 1053, doi:10.1029/2002GB002015.
- Lang, S.I., J.H.C. Cornelissen, T. Klahn, R.S.P. Van Logtestijn, R. Broekman, W. Schweikert and R. Aerts. 2009. An experimental comparison of chemical traits and litter decomposition rates in a diverse range of subarctic bryophyte, lichen and vascular plant species. *J. Ecol.* 97:886-900.
- Lansdown, J.M., P.D. Quay and S.L. King. 1992. CH₄ production via CO₂ reduction in a temperate bog – a source of C13 depleted CH₄. *Geochim. Cosmochim. Acta* 56: 3493-3503.
- Laprise, R., D. Caya, A. Frigon and D. Paquin. 2003. Current and perturbed climate as simulated by the second generation Canadian regional climate model (CRCM-II) over northwestern North America. *Clim. Dynam.* 21: 405-421.

- Larsen, K.S., P. Grogan, S. Jonasson and A. Michelsen. 2007. Dynamics and microbial dynamics in two subarctic ecosystems during winter and spring thaw: Effects of increased snow depth. *Arctic Antarct. Alpine Res.* 39: 268-276.
- Latter, P.M., G. Howson, D.M., Howard and W.A. Scott. 1998. Long-term study of litter decomposition on a Pennine peat bog: which regression? *Oecologia* 113: 94-103.
- Lavoie, C. and S. Payette. 1997. Late-Holocene light-ring chronologies from subfossil black spruce stems in mires of subarctic Québec. *Holocene* 7: 129-137.
- Lavoie, M., D. Paré, N. Fenton, A. Groot and K. Taylor. 2005. Paludification and management of forested peatlands in Canada: a literature review. *Environ. Rev.* 13: 21-50.
- Lawrence, D.M. and A.G. Slater. 2005. A projection of severe near-surface permafrost degradation during the 21st century. *Geophys. Res. Lett.* 32: L24401, doi:10.1029/2005GL025080.
- Lawrence, D.M. and A.G. Slater. 2010. The contribution of snow conditions trends to future ground climate. *Clim. Dynam.* 34: 969-981.
- Lawrence, D.M., A.G. Slater, R.A. Thomas, M.M. Holland and C. Deser. 2008. Accelerated Arctic land warming and permafrost degradation during rapid sea ice loss. *Geophys. Res. Lett.* 35: L11506, doi:10.1029/2008GL033985.
- Lazerte, B.D. 1993. The impact of drought and acidification on the chemical exports from a minerotrophic conifer swamp. *Biogeochemistry* 18: 153-175.
- Lecomte, N., M. Simard, N. Fenton and Y. Bergeron. 2006. Fire severity and longterm ecosystem biomass dynamics in coniferous boreal forests of eastern Canada. *Ecosystems* 9: 1215-1230.
- Le Mer, J. and P. Roger. 2001. Production, oxidation, emission and consumption of methane by soils: a review. *Eur. J. Soil Biol.* 37: 25-50.
- Li, J. and W. Chen. 2005. A rule-based method for mapping Canada's wetlands using optical, radar and DEM data. *Int. J. Remote Sens.* 26: 5051-5069.
- Limpens, J., F. Berendse, C. Blodau, J.G. Canadell, C. Freeman, J. Holden, N. Roulet, H. Rydin and G. Schaepman-Strub. 2008. Peatlands and the carbon cycle: from local processes to global implications - a synthesis. *Biogeosciences* 5: 1475-1491.
- Ling, F. and T. Zhang. 2006. Sensitivity of ground thermal regime and surface energy fluxes to tundra snow density in northern Alaska. *Cold Reg. Sci. Technol.* 44: 121-130.
- Liston, G.E., J.P. McFadden, M. Strum and R.A. Pielke. 2002. Modelled changes in Arctic tundra snow, energy and moisture fluxes due to increased shrubs. *Global Change Biol.* 8: 17-32.
- Lloyd, A.H. 2005. Ecological histories from Alaskan tree lines provide insight into future change. *Ecology* 86: 1687-1695.
- Lloyd, A.H., K. Yoshikawa, C.L. Fartie, L. Hinzman and M. Fraver. 2003. Effects of permafrost degradation on woody vegetation at arctic treeline on the Seward Peninsula, Alaska. *Permafrost. Periglac.* 14: 93-101.
- Luken, J.O. and W.D. Billings. 1986. Hummock-dwelling ants and the cycling of microtopography in an Alaskan peatland. *Can. Field Nat.* 100: 69-73.
- Lund, M., P.M. Lafleur, N.T. Roulet, A. Lindroth, T.R. Christensen, M. Aurela, B.H. Chrojnicky, L.B. Flanagan, E.R. Humphreys, T. Laurila, W.C. Oechel, J. Olejnik, J. Rinne, P. Schubert and M.B. Nilsson. 2010. Variability of exchange of CO₂ across 12 northern peatland and tundra sites. *Global Change Biol.* 16:2436-2448.
- Luoto, M. and M. Seppälä. 2003. Thermokarst ponds as indicators of the former distribution of palsas in Finnish Lapland. *Permafrost Periglac.* 14:19-27.
- Luoto, M., R.K. Heikkinen and T.R. Carter. 2004. Loss of palsa mires in Europe and biological consequences. *Environ. Conserv.* 31: 30-37.
- Lyon, S.W., D.R. Giesler, C. Humborg, M. Morth, J. Seibert, J. Karlsson and P.A. Troch. 2009. Estimation of permafrost thawing rates in a sub-arctic catchment using recession flow analysis. *Hydrol. Earth Syst. Sci.* 13: 595-604.
- Mackay, M.D., F. Seglenieks, D. Versegny, E.D. Soulis, K.R. Snelgrove, A. Walker and K. Szeto. 2003. Modeling Mackenzie Basin Surface Water Balance during CAGES with the Canadian Regional Climate Model. *J. Hydrometeorol.* 4 748-767.
- Macrae, M.L., R.L. Bello and L.A. Molot. 2004. Long-term carbon storage and hydrological control of CO₂ exchange in tundra ponds in the Hudson Bay Lowland. *Hydrol. Process.* 18: 2051-2069.
- Magnan, G., M. Lavoie, and S. Payette. 2012. Impact of fire on long-term vegetation dynamics of ombrotrophic peatlands in northwestern Québec, Canada. *Quatern. Res.* 77: 110-121.
- Malmer, N., T. Johansson, M. Olsrud and T.R. Christensen. 2005. Vegetation, climatic changes and net carbon sequestration in a North-Scandinavian subarctic mire over 30 years. *Global Change Biol.* 11: 1895-1909.
- Mansuy, N., S. Gauthier, A. Robitaille and Y. Bergeron. 2010. The effects of surficial deposit–drainage combinations on spatial variations of fire cycles in the boreal forest of eastern Canada. *Int. J. Wildl. Fire* 19: 1083-1098.
- Marchenko, S., V. Romanovsky and G. Tipenko. 2008. Numerical modeling of spatial permafrost dynamics in Alaska. Pp. 1125-1130 in M. Philips, Springman, S.M., Arenson, L.U. (eds.). *Proc. 8th Inter. Conf. on Permafrost.* Taylor and Francis Publ., Boca Raton, Florida. 1,380 p.
- Martini, I.P. 2006. The cold climate peatlands of the Hudson Bay Lowland, Canada: brief overview of recent work. Pp. 53-84 in Martini I.P., Cortizas, A.M., Chesworth, W. (eds.). *Peatlands: Evolution and Records of Environmental and Climate Changes.* Elsevier. Amsterdam, NL. 606 p.
- Matthews, H. D. and D.W. Keith. 2007. Carbon-cycle feedbacks increase the likelihood of a warmer future. *Geophys. Res. Lett.* 34: L09702, doi:10.1029/2006GL028685.
- Maurer, H. and C. Hauck. 2007. Geophysical imaging of alpine rock glaciers. *J. Glaciol.* 53: 110-120.
- Marion, G.M. and W.C. Oechel. 1993. Mid-to-late-Holocene carbon balance in arctic Alaska and its implications for future global warming. *Holocene* 3: 193-200.
- Marsh, P. and S.C. Bigras. 1988. Evaporation from Mackenzie Delta Lakes, N.W.T., Canada. *Arctic Alpine Res.* 20: 220-229.
- Marsh, P., C. Onclin and N.N. Neumann. 2002. Water and energy fluxes in the lower Mackenzie valley. *Atmos. Ocean* 40: 245- 256.
- McCartney, S.E., S.K. Carey and J.W. Pomeroy. 2006. Intra-basin variability of snowmelt water balance calculations in a subarctic catchment. *Hydrol. Process.* 20:1001-1016.
- McClelland, J.W., S.J. Déry, B.J. Peterson, R.M. Holmes and E.F. Wood. 2006. A pan-arctic evaluation of changes in river discharge during the latter half of the 20th century. *Geophys. Res. Lett.* 33: L06715, doi:10.1029/2006GL025753.

- McClelland, J.W., M. Stieglitz, F. Pan, R.M. Holmes and B.J. Peterson. 2007. Recent changes in nitrate and dissolved organic carbon export from the upper Kuparuk River, North Slope, Alaska. *J. Geophys. Res. – Biogeosciences* 112: G04S60, doi:10.1029/2006JG000371.
- McDonald, J.M. and A.W. Harbaugh. 1984. A modular three-dimensional finite difference groundwater flow model. U.S. Geol. Surv. Open File Rep. 83-875. 528 pp.
- McEnroe, N.A., N.T. Roulet, T.R. Moore and M. Gameau. 2009. Do pool surface area and depth control CO₂ and CH₄ fluxes from an ombrotrophic raised bog, James Bay, Canada? *J. Geophys. Res.* 114: G01001, doi:10.1029/2007JG000639.
- McGuire, A.D., S. Storch, J.S. Clein, R. Dargaville, G. Esser, J. Foley, M. Heimann, F. Joos, J. Kaplan, D.W. Kicklighter, R.A. Meier, J.M. Melillo, B. Moore III, I.C. Prentice, N. Ramankutty, T. Reichenau, A. Schloss, H. Tian, L.J. Williams, and U. Wittenberg. 2001. Carbon balance of the terrestrial biosphere in the twentieth century: Analyses of CO₂, climate and land use effects with four process-based ecosystem models. *Global Biogeochem. Cycles* 15: 183-206.
- McKenney, D.W., J.H. Pedlar, K. Lawrence, P.A. Gray, S.J. Colombo, and W.J. Crins, 2010. Current and projected future climatic conditions for ecoregions and selected Natural Heritage Areas in Ontario. *Ont. Min. Nat. Res., Sault Ste. Marie, Ont., Clim. Change Res. Rep. CCRR-16*, 42 pp.
- McKnight, D., M. Thurman and R.L. Wershaw. 1985. Biogeochemistry of aquatic humic substances in Thoreau's Bog, Concord, Massachusetts. *Ecology* 66: 1339-1352.
- McLaughlin, J.W. 2004. Carbon assessment in boreal wetlands of Ontario. *Ont. Min. Nat. Resour., Ont. For. Res. Inst., Sault Ste. Marie, ON. For. Res. Inf. Pap. No. 158*. 79p.
- McLaughlin, J. and S.A. Phillips. 2006. Soil carbon, nitrogen, and base cation cycling 17 years after whole-tree harvesting in a low-elevation red spruce *Picea rubens*-balsam fir *Abies balsamea* forested watershed in central Maine, USA. *For. Ecol. Manage.* 222: 234-253.
- McLaughlin, J.W. and K.L. Webster. 2010. Alkalinity and acidity cycling and fluxes in an intermediate fen peatland in northern Ontario. *Biogeochemistry* 99: 143-155.
- McLaughlin, J.W., E.B.W. Calhoun, M.R. Gale, M.F. Jurgensen, C.C. Trettin. 2011. Biogeochemical cycling and chemical fluxes in a managed northern forested wetland, Michigan, USA. *For. Ecol. Manage.* 261: 649-661.
- McLaughlin, J.W., M.R. Gale, M.F. Jurgensen and C.C. Trettin. 2000. Soil organic matter and nitrogen cycling in response to harvesting, mechanical site preparation, and fertilization in a wetland with a mineral substrate. *For. Ecol. Manage.* 12:7-23.
- McMorrow, J.M., M.E.J. Cutler, M.G. Evans and A. Al-Roichdi. 2004. Hyperspectral indices for characterizing upland peat composition. *Int. J. Remote Sens.* 25: 313-325.
- Merbold, L., W.L. Kutsch, C. Corradi, O. Kolle, C. Rebmann, P.C. Stoy, S.A. Zimov and E.D. Schulze. 2009. Artificial drainage and associated carbon fluxes (CO₂/CH₄) in a tundra ecosystem. *Global Change Biol.* 15: 2599-2614.
- Meyers-Smith, I.H., J.W. Harden, W. Wilking, C.C. Fuller, A.D. McGuire and F.S. Chapin III. 2008. Wetland succession in a permafrost collapse: Interactions between fire and thermokarst. *Biogeosciences* 5: 1273-1286.
- Meyers-Smith, I.H., A.D. McGuire, J.W. Harden and R.C. Chapin III. 2007. Influence of disturbance on carbon exchange in a permafrost collapse and adjacent burned forest. *J. Geophys. Res.* 112: G04017, doi:10.1029/2007JG000423.
- Mialon, A., A. Royer and M. Fily. 2005. Wetland seasonal dynamics and interannual variability over northern high latitudes, derived from microwave satellite data. *J. Geophys. Res.* 110(D17102), doi:10.1029/2004JD005697.
- Milton, G.R. and R. Helie. 2003. Wetland inventory and monitoring: partnering to provide a national coverage. Pp. 21-30 *in* Rube, C.D.A. (ed.). *Wetland Stewardship in Canada: Contributed Papers from the Conference on Canadian Wetlands Stewardship, 3-5 February 2003, Ottawa, Ontario*. North Am. Wetlands Conserv. Council (Canada), Rep. 03-2. Ottawa, ON. 145 p.
- Monteith, J.L. 1965. Evaporation and environment, *Symp. Soc. Exp. Biol.*, XIX, Cambridge Univ. Press, London, UK. pp. 205-234.
- Moore, K.E., D.R. Fitzjarrald, S.C. Wofsy, B.C. Daube, J.W. Munger and P.S. Bakwin. 1994. A season of heat, water vapour, total hydrocarbon and ozone fluxes at a subarctic fen. *J. Geophys. Res.* 99: 1937-1952.
- Moore, T.R. 1987. Thermal regime of peatlands in subarctic eastern Canada. *Can. J. Earth Sci.* 24: 1352-1359.
- Moore, T.R., J.L. Bubier and L. Bledzki. 2007. Litter decomposition in temperate peatland ecosystems: The effect of substrate and site. *Ecosystems* 10: 949-963.
- Moore, T.R., A. Heyes and N.T. Roulet. 1994. Methane emissions from wetlands, southern Hudson Bay lowland. *J. Geophys. Res.* 99: 1455-1467.
- Moore, T.R., N.T. Roulet and J.M. Waddington. 1998. Uncertainty in predicting the effect of climatic change on the carbon cycling of Canadian peatlands. *Clim. Change* 40: 229-245.
- Moore, T.R., J.L. Bubier, S.E. Frolking, P.M. Lafleur and N.T. Roulet. 2002. Plant biomass and production and CO₂ exchange in an ombrotrophic bog. *J. Ecol.* 90: 25-36.
- Moore, T.R., A. De Young, J.L. Bubier, E.R. Humphreys, P.M. Lafleur and N.T. Roulet. 2011. A multi-year record of methane flux at the Mer Bleue bog, southern Canada. *Ecosystems* 14: 646-657.
- Moore, T.R., J.A. Trofymow, M. Siltanen and L.M. Kozak. 2008. Litter decomposition and nitrogen and phosphorus dynamics in peatlands and uplands over 12 years in central Canada. *Oecologia* 157: 317-325.
- Munroe, J.S., J.A. Doolittle, M.Z. Kanevskiy, K.M. Hinkel, F.E. Nelson, B.M. Jones, Y. Shur and H.D. Matthews. 2007. Implications of CO₂ fertilization for future climate change in a coupled climate-carbon model. *Global Change Biol.* 13: 1068-1078.
- Muskett, R.R. and V.E. Romanovsky. 2011. Alaskan permafrost groundwater storage changes derived from GRACE and ground measurements. *Remote Sens.* 3: 378-397.
- Myers, B., K.L. Webster, J.W. McLaughlin and N. Basiliko. 2012. Microbial activity across a boreal peatland successional gradient: the role of fungi and bacteria in decomposition. *Wetlands Ecol. Manage.* 20: 77-88.
- Myers-Smith, I.H., A.D. McGuire, J.W. Harden and S. Chapin III. Influence of disturbance on carbon exchange in a permafrost collapse and adjacent burned forest. *J. Geophys. Res.* 112: G04017, doi:10.1029/2007JG000423.
- Nakai, Y., Y. Matsuura, T. Kajimoto, A.P. Abaimov, S. Yamamoto and O.A. Zyryanova. 2008. Eddy covariance CO₂ flux above a Gmelin larch forest on continuous permafrost in Central Siberia during a growing season. *Theor. Appl. Climatol.* 93: 133-147.

- Nakano, T., S. Kuniyoshi and M. Fukuda. 2000. Temporal variation in methane emission from tundra wetlands in a permafrost area, northeastern Siberia. *Atmos. Environ.* 34: 1205-1213.
- Nakano, T., W. Takeuchi, G. Inue, M. Fukuda and Y. Yasuoka. 2006. Temporal variations in soil-atmosphere methane exchange after fire in a peat swamp forest in West Siberia. *Soil Sci. Plant Nutr.* 52: 77-88.
- [NWWG] National Wetlands Working Group. 1988. *Wetlands of Canada*. Environ. Can., Polysci. Publ., Inc. Ottawa, ON. Ecol. Land Class. Ser. No. 24452 p.
- [NWWG] National Wetlands Working Group. 1997. *The Canadian Wetland Classification System*, 2nd ed. Warner, B.G. and Rubec, C.D.A. (eds.), Wetlands Res. Cent., Univ. Waterloo, Waterloo, ON. 68 p.
- Nelson, F.E. and S.I. Outcalt. 1987. A computational method for prediction and regionalization of permafrost. *Arctic Antarct. Alpine Res.* 19: 279-288.
- Neumann, H.H., G. DenHartog, K.M. King and A.C. Chipanshi. 1994. Carbon dioxide fluxes over a raised open bog at the Kinosheo Lake tower site during the Northern Wetlands Study (NOWES). *J. Geophys. Res.* 99: 1529-1538.
- Nykanen, H., J.E.P. Heikkinen, L. Pirinen, K. Tiilikainen and P.J. Martikainen. 2003. Annual CO₂ exchange and CH₄ fluxes on a subarctic peat mire during climatically different years. *Global Biogeochem. Cycles*. 17: 1018.
- Oechel, W.C., G.L. Vourlitis, S.J. Hastings and S.A. Bochkarev. 1995. Change in arctic CO₂ flux over 2 decades, effects of climate change at Barrow, Alaska. *Ecol. Appl.* 5: 846-855.
- Oechel, W.C., G.L. Vourlitis, S.J. Hastings, R.C. Zulueta, L. Hinzman and D. Kane. 2000. Acclimation of ecosystem CO₂ exchange in the Alaskan Arctic in response to decadal climate warming. *Nature* 406: 978-981.
- Oelke, C., T.J. Zhang and M.C. Serreze. 2004. Modeling evidence for recent warming of the Arctic soil thermal regime. *Geophys. Res. Lett.* 31: L07208, doi:10.1029/2003GL019300.
- Oelke, C., T. Zhang, M.C. Serreze and R.L. Armstrong. 2003. Regional scale modeling of soil freeze/thaw over the Arctic drainage basin. *J. Geophys. Res.* 108: 4314, doi:10.1029/2002JD002722.
- Ohta, T., T.C. Maximov, A. Johannes, T. Nakai, M.K. van der Molen, A.V. Kononov, A.P.T. Hiyama, Y. Iijima, E.J. Moors, H. Tanaka, T. Toba and H. Yabuki. 2008. Interannual variation of water balance and summer evapotranspiration in an eastern Siberian larch forest over a 7-year period (1998-2006). *Agric. For. Meteorol.* 148: 1941-1953.
- Oldfield, F., N. Richardson, and P.G. Abbleby. 1995. Radiometric dating (²¹⁰Pb, ¹³⁷Cs, ²⁴¹AM) of recent ombrotrophic peat accumulation and evidence for changes in mass balance. *The Holocene* 5: 141-148.
- [OMNR] Ontario Ministry of Natural Resources. 1993. *Ontario Wetland Evaluation System: Northern Manual*. Ont. Min. Nat. Resour., Wildl. Pol. Br., Toronto, ON. Northeast Sci. Technol., South Porcupine, ON. Techn. Man. TM-001173 p.
- O'Neill, K.P., E.S. Kasischke and D.D. Richter. 2003. Seasonal and decadal patterns of soil carbon uptake and emission along an age sequence of burned black spruce stands in interior Alaska. *J. Geophys. Res.* 108: 8155, doi:10.1029/2001JD000443.
- Osterkamp, T.E. 2005. The recent warming of permafrost in Alaska. *Global Planet. Change* 49: 187-202.
- Osterkamp, T.E. and V.E. Romanovsky. 1999. Evidence for warming and thawing of discontinuous permafrost in Alaska. *Permafrost Periglac.* 10: 17-37.
- Osterkamp, T.E., L. Viereck, Y. Shur, M.T. Jorgenson, C. Racine, A. Doyle and R.D. Boone. 2000. Observations of thermokarst and its impact on boreal forests in Alaska, USA. *Arctic Antarct. Alpine Res.* 32: 303-315.
- Ovenden, L. 1990. Peat accumulation in northern wetlands. *Quatern. Res.* 33: 377-386.
- Overduin, P.P., D.L. Kane and W.K.P. van Loon. 2006. Measuring thermal conductivity in freezing and thawing soil using soil temperature response to heating. *Cold Reg. Sci. Technol.* 45: 8-22.
- Paré, D., J.L. Banville, M. Gagneau and Y. Bergeron. 2011. Soil carbon stocks and soil carbon quality in the upland portion of a boreal landscape, James Bay, Québec. *Ecosystems* 14: 533-546.
- Parisien, M. A. and L. Sirois. 2003. Distribution and dynamics of tree species across a fire frequency gradient in the James Bay region of Québec. *Can. J. For. Res.* 33: 243-256.
- Parsekian, A.D., B.M. Jones, M. Jones, G. Grosse, K.M. Walter Anthony and L. Slater. 2011. Expansion rate and geometry of floating vegetation mats on the margins of thermokarst lakes, northern Seward Peninsula, Alaska, USA. *Earth Surf. Process. Landform.* 36: 1889-1897.
- Payette, S., L. Filion and A. Delwaide. 2008. Spatially explicit fire-climate history of the boreal forest-tundra (eastern Canada) over the last 2000 years. *Philos. Trans. R. Soc. Lond. Biol. Sci.* 363: 2301-2316.
- Payette, S., A. Delwaide, M. Caccianiga and M. Beauchemin. 2004. Accelerated thawing of subarctic peatland permafrost over the last 50 years. *Geophys. Res. Lett.* 31: L18208, doi:10.1029/2004GL020358.
- Pelletier, L., T.R. Moore, N.T. Roulet, M. Gagneau and V. Beaulieu-Audy. 2007. Methane fluxes from three peatlands in the La Grande Rivière watershed, James Bay lowland, Canada. *J. Geophys. Res.* 112: G01018, doi:10.1029/2006JG000216.
- Peltoniemi, J.I., J. Suomalainen, E. Puttonen, J. Näränen and M. Rautiainen. 2008. Reflectance properties of selected arctic-boreal land cover types: field measurements and their application in remote sensing. *Biogeosciences Discuss.* 5: 1069-1095.
- Penman, H.L. 1948. Natural evaporation from open water, bare soil and grass. *Proc. R. Soc. Lond. Ser. A.* 193: 120-145.
- Peñuelas, J., M. Estiarte and J. Llusia. 1997. Carbon based secondary compounds at elevated CO₂. *Photosynthetica* 33: 313-316.
- Peñuelas, J., I. Filella, L. Biel, Serrano and R. Save. 1993. The reflectance at the 950-970 nm region as an indicator of plant water status. *Int. J. Remote Sens.* 14: 1887-1905.
- Petrone, R.M., W.R. Rouse and P. Marsh. 2000. Comparative surface energy budgets in western Canada and central subarctic regions of Canada. *Int. J. Climatol.* 20: 1131-1148.
- Pflugmacher, D., O.N. Krankin and W.B. Cohen. 2007. Satellite-based peatland mapping: Potential of the MODIS sensor. *Global Planet. Change* 56:248-257.
- Pietroniro, A. and R. Leconte. 2000. A review of Canadian remote sensing applications in hydrology 1995-1999. *Hydrol. Process.* 14: 1641-1666.

- Pietroniro, A. and R. Leconte. 2005. A review of Canadian remote sensing and hydrology 1999-2003. *Hydrol. Process.* 19: 285-301.
- Pietroniro, A., J. Töyrä, R. Leconte and G. Kite. 2005. Remote sensing of surface water and soil moisture. Pp. 119-142 in Duguay, C.R and Pietroniro, A. (eds.). *Remote Sensing in Northern Hydrology: Measuring Environmental Change*, Geophys. Monogr. Ser., Vol. 163. Am. Geophys. Union, Washington, DC. 160 p.
- Pitkänen, A., J. Turunen and K. Tolonen. 1999. The role of fire in the carbon dynamics of a mire, eastern Finland. *Holocene* 9: 453-462.
- Ping, C. L., G.J. Michaelson, E.C. Packee, C.A. Stiles, D.K. Swanson and K. Yoshikawa. 2005. Soil Catena sequences and fire ecology in the boreal forest of Alaska. *Soil Sci. Soc. Am. J.* 69: 1761-1772.
- Pohl, S., P. Marsh and B.R. Bonsal. 2007. Modeling the impact of climate change on runoff and annual water balance of an arctic headwater basin. *Arctic* 60: 173-186.
- Prater, J.L., J.P. Chanton and G.J. Whiting. 2007. Variation in methane production pathways associated with permafrost decomposition in collapse scar bogs of Alberta, Canada. *Global Biogeochem. Cycles* 21: GB4004 doi:10.1029/2006GB002866.
- Prentice I.C., G.D. Farquhar, M.J.R. Fasham, M.L. Goulden, M. Heimann, V.J. Jaramillo, H.S. Keshgi, C. Le Quééré, R.J. Scholes, D.W.R. Wallace, D. Archer, M.R. Ashmore, O. Aumont, D. Baker, M. Battle, M. Bender, L.P. Bopp, P. Bousquet, K. Caldeira, P. Ciais, P.M. Cox, W. Cramer, F. Dentener, I.G. Enting, C.B. Field, P. Friedlingstein, E.A. Holland, R.A. Houghton, J.I. House, A. Ishida, A.K. Jain, I.A. Janssens, F. Joos, T. Kaminski, C.D. Keeling, R.F. Keeling, D.W. Kicklighter, K.E. Kohfeld, W. Knorr, E. Law, T. Lenton, K. Lindsay, E. Maier-Reimer, A.C. Manning, R.J. Matear, A.D. McGuire, J.M. Melillo, R. Meyer, M. Mund, J.C. Orr, S. Piper, K. Plattner, P.J. Rayner, S. Sitch, R. Slater, S. Taguchi, P.P. Tans, H.Q. Tian, M.F. Weirig, T. Whorf and A. Yool. 2001. The Carbon Cycle and Atmospheric Carbon Dioxide. Chapter 3. Pp 183-237 in Houghton, J.T., Ding, Y., Griggs, D.J., Noguer, M., Van der Linden, P.J., Dai, X., Maskell, K. and Johnson C.A. (eds.) *Climate Change 2001: The Scientific Basis*. Contribution of Working Group I to the Third Assessment Report of the Intergovernmental Panel on Climate Change. Cambridge Univ. Press, Cambridge, UK. 891 p.
- Preston, M.D., K.A. Smemo, J.W. McLaughlin and N. Basiliko. 2012. Peatland microbial communities and decomposition processes in the James Bay Lowlands, Canada. *Frontiers Microbiol.* 3: 1-15.
- Price, J.S. 1991. Evaporation from a blanket in a foggy coastal environment. *Bound.-Lay. Meteorol.* 57:391-406.
- Price, J.S. and M.K. Woo. 1988. Studies of subarctic coastal marsh: I. Hydrology. *J. Hydrol.* 103:275-292.
- Price, P.B. and T. Sowers. 2004. Temperature dependence of metabolic rates for microbial growth, maintenance, and survival. *Proc. Nat. Acad. Sci.* 101: 4631-4636.
- Price, J.S., D.A. Maloney and F.G. Downey. 1991. Peatlands of the Lake Melville Coastal Plain, Labrador. Pp. 293-302 in Prowse, T.D. and Ommanney, C.S.L. (eds.). *Northern Hydrology: Selected Perspectives Proceedings of the Northern Hydrology Symposium No. 6*. Environ. Can. Can. Gov. Publ. Cent., Suppl. Serv. Canada, Ottawa, ON.
- Priestley, C.H.B. and R.J. Taylor. 1972. On the assessment of surface heat flux and evaporation using large-scale parameters. *Mon. Weath. Rev.* 100: 81-92.
- Prokushkin, A.S., G. Gleixner, W.H. McDowell, S. Ruelow and E.D. Schulze. 2007. Source- and substrate-specific export of dissolved organic matter from permafrost-dominated forested watershed in central Siberia. *Global Biogeochem. Cycles* 21: GB4003. doi:10.1029/2007GB002938.
- Qian, H., R. Joseph and N. Zeng. 2010. Enhanced terrestrial carbon uptake in the Northern high latitudes in the 21st century from the coupled carbon cycle climate model intercomparison project model projections. *Global Change Biol.* 16: 641-656.
- Quinton, W.L. and N.T. Roulet. 1998. Spring and summer runoff hydrology of a subarctic patterned wetland. *Arctic Alpine Res.* 30: 285-294.
- Quinton, W.L., M. Hayashi and L.E. Chasmer. 2011. Permafrost-thaw-induced land-cover change in the Canadian subarctic: implications for water resources. *Hydrol. Process.* 25: 152-158.
- Quinton, W.L., M. Hayashi and A. Pietroniro. 2003. Connectivity and storage functions of channel fens and flat bogs in northern basins. *Hydrol. Process.* 17: 3665-3684.
- Quinton, W.L., R.K. Bemrose, Y. Zhang and S.K. Carey. 2009. The influence of spatial variability in snowmelt and active layer thaw on hillslope drainage for an alpine tundra hillslope. *Hydrol. Process.* 23: 2628-2639.
- Quinton, W.L., T. Shirazi, S.K. Carey and J.W. Pomeroy. 2005. Soil water storage and active-layer development in a sub-arctic tundra hillslope, southern Yukon Territory, Canada. *Permafrost Periglac.* 16: 369-382.
- Racine, M.J., M. Bernier and T. Ouarda. 2005. Evaluation of RADARSAT-1 images acquired in fine mode for the study of boreal peatlands: a case study in James Bay, Canada. *Can. J. Remote Sens.* 31: 450-467.
- Raich, J.W., E.B. Rasetter, J.M. Melillo, D.W. Kicklighter, P.A. Struedler, B.J. Peterson, A.L. Grace, B. Moore III and C.J. Vorosmarty. 1991. Potentail net primary production in South America: an application of a global model. *Ecol. Appl.* 1: 399-429.
- Railton, J.B. and J.H. Sparling. 1973. Preliminary studies on the ecology of peat mounds in northern Ontario. *Can. J. Bot.* 51: 1037-1073.
- Rapalee, G., L.T. Steyaert and P.G. Hall. 2001. Moss and lichen cover mapping at the local and regional scales in the boreal forest ecosystem of central Canada. *J. Geophys. Res.* 106: 33,551-33,563.
- Raymond, P.A., J.W. McClelland, R.M. Holmes, A.V. Zhulidov, K. Mull, B.J. Peterson, R.G. Striegl, G.R. Aiken and T.Y. Gurtovaya. 2007. Flux and age of dissolved organic carbon exported to the Arctic Ocean: A carbon isotopic study of the five largest arctic rivers. *Global Biogeochem. Cycles* 21: GB4011 doi:10.1029/2007GB002934.
- Reeve, A.S., D.I. Siegel and P.H. Glaser. 2000. Simulating vertical flow in large peatlands. *J. Hydrol.* 227: 207-217.
- Reeve, A.S., D.I. Siegel and P.H. Glaser. 2001. Simulating dispersive mixing in large peatlands. *J. Hydrol.* 242: 103-114.
- Reiche, M., G. Gleixner and K. Küsel. 2010. Effect of peat quality on microbial greenhouse gas formation in an acidic fen. *Biogeosciences* 7: 187-198.
- Riley, J.L. 1994. Peat and peatland resources of northeastern Ontario. *Ont. Geol. Surv. Toronto, ON. Open File Rep.* 153. 155 p.
- Riley, J.L. 2011. Wetlands of the Hudson Bay Lowland: An Ontario overview. *Nature Conserv. Can., Toronto, ON.* 156pp.
- Rinnan, R., A. Michelsen, E. Baath and S. Jonasson. 2007. Fifteen years of climate change manipulations alter soil microbial communities in a subarctic heath ecosystem. *Global Change Biol.* 13: 28-39.

- Riordan, B., D. Verbyla and A.D. McGuire. 2006. Shrinking ponds in subarctic Alaska based on 1950-2002 remotely sensed images. *J. Geophys. Res.* 111: G04002, doi:10.1029/2005JG000150.
- Riseborough, D.W. 2002. The mean annual temperature at the top of permafrost, the TTOP model, and the effect of unfrozen water. *Permafrost Periglac.* 13: 137-143.
- Riseborough, D., N. Shikomanov, B. Erzmuller, S. Gruber and S. Marchenko. 2008. Recent advances in permafrost modelling. *Permafrost Periglac.* 19: 137-156.
- Riutta, T., J. Laine and E.-S. Tuittila. 2007. Sensitivity of CO₂ exchange of fen ecosystem components to water level variation. *Ecosystems* 10: 718-733.
- Robinson, S.D. 2006. Carbon accumulation in peatlands, southwestern Northwest Territories, Canada. *Can. J. Soil. Sci.* 86: 305-319.
- Robinson, S.D. and T.R. Moore. 2000. The influence of permafrost and fire upon carbon accumulation in high boreal peatlands, Northwest Territories, Canada. *Arctic Antarct. Alpine Res.* 32: 155-166.
- Rochefort, L., D.H. Vitt and S.E. Bayley. 1990. Growth, production, and decomposition dynamics of Sphagnum under natural and experimentally acidified conditions. *Ecology* 71: 1986-2000.
- Rock, B.N., J.E. Vogelmann, D.L. Williams, A.F. Vogelmann and T. Hoshizaki. 1986. Remote detection of forest damage. *BioScience* 36: 439-445.
- Rodionov, A., H. Flessa, O. Kazansky and G. Guggenberger. 2006. Organic matter composition and potential trace gas production of permafrost soils in the forest tundra in northern Siberia. *Geoderma* 135: 49-62.
- Romanovsky, V.E. and T.E. Osterkamp. 2000. Effects of unfrozen water on heat and mass transport processes in the active layer of permafrost. *Permafrost Periglac.* 11: 219-239.
- Romanovsky, V.E., S.L. Smith and H. Christiansen. 2010. Permafrost thermal state in the polar northern hemisphere during the international polar year 2007-2009: synthesis. *Permafrost Periglac.* 21: 106-116.
- Ross, N., P.J. Brabham, C. Harris and H.H. Christiansen. 2007. Internal structure of open system pingos, Adventdalen, Svalbard: the use of resistively tomography to assess ground-ice conditions. *J. Environ. Eng. Geophys.* 12: 113-126.
- Roulet, N.T. 2000. Peatlands, carbon storage, greenhouse gases and the Kyoto Protocol: Prospects and significance for Canada. *Wetlands* 20: 605-615.
- Roulet, N.T. and J.W. McKenzie. 1998. Role of groundwater in determining the pattern of peatlands in the Hudson Bay lowlands. *Geol. Soc. Am. Ann. Meet. Abstr. with Programs* 30, A-119.
- Roulet, N.T. and M.-K. Woo. 1986. Hydrology of a wetland in the continuous permafrost region. *J. Hydrol.* 89: 73-91.
- Roulet, N., T. Moore, J. Bubier and P. Lafleur. 1992. Northern fens: methane flux and climate change. *Tellus B* 44: 100-105.
- Roulet, N.T., A. Jano, C.A. Kelly, L.F. Klinger, T.R. Moore, R. Protz, J.A. Ritter and W.R. Rouse. 1994. Role of the Hudson Bay lowland as a source of atmospheric methane. *J. Geophys. Res.* 99: 1439-1454.
- Roulet, N. T., P.M. Lafleur, P.J.J. Richard, T.R. Moore, E.R. Humphreys and J. Bubier. 2007. Contemporary carbon balance and late Holocene carbon accumulation in a northern peatland. *Global Change Biol.* 13: 397-411.
- Rouse J.W., R.H. Haas, J.A. Schell and D.W. Deering. 1974. Monitoring vegetation systems in the Great Plains with ERTS. *Proc. Third Earth Resources Technology Satellite-1 Symposium, NASA, Greenbelt, MD.* pp. 301-317.
- Rouse, W.R. 1998. A water balance model for a subarctic sedge fen and its application to climate change. *Clim. Change* 38: 107-234.
- Rouse, W.R. 2000. The energy and water balance of high-latitude wetlands: Controls and extrapolation. *Global Change Biol.* 6: 59-68.
- Rouse, W.R., S.G. Hardill and P. Lafleur. 1987. The energy balance in the coastal environment of James Bay and Hudson Bay during the growing season. *J. Climatol.* 7: 165-179.
- Rouse, W.R., R.L. Bello, A. D'Souza, T.J. Griffis and P.M. Lafleur. 2002. The annual carbon budget for fen and forest in a wetland at Arctic treeline. *Arctic* 55: 229-237.
- Rouse, W.R., A.K. Eaton, R.M. Petrone, L.D. Boudreau, P. Marsh and T.J. Griffis. 2003. Seasonality in the surface energy balance of tundra in the lower Mackenzie River Basin. *J. Hydrometeorol.* 4: 673-679.
- St. Amour, N.A., J.J. Gibson, T.W.D. Edwards, T.D. Prowse and A. Pietroniro. 2005. Isotopic time-series partitioning of streamflow components in wetland-dominated catchments, lower Laird River basin, Northwest Territories, Canada. *Hydrol. Process.* 19: 3357-3381.
- St-Hilaire, A., Courtenay, S. C., Diaz-Delgado, C., Pavey, B., Ouarda, T. B. M. J., Boghen, A and B. Bobee. 2006. Suspended sediment concentrations downstream of a harvested peat bog: Analysis and preliminary modelling of exceedances using logistic regression. *Can. Water Resour. J.* 31: 139-156.
- St-Hilaire, F., J. Wu, N.T. Roulet, S. Frolking, P.M. Lafleur, E.R. Humphreys and V. Arora. 2010. McGill wetland model: evaluation of a peatland carbon simulator developed for global assessments. *Biogeosciences* 7: 3517-3530.
- St. Jacques, J.-M. and D.J. Sauchyn. 2009. Increasing winter baseflow and mean annual streamflow from possible permafrost thawing in the Northwest Territories, Canada. *Geophys. Res. Lett.* 36: L01401, doi:10.1029/2008GL035822.
- Saito, K., M. Kimoto, T.M. Zhang, K. Takata and S. Emori. 2007. Evaluating a high-resolution climate model: Simulated hydrothermal regimes in frozen ground regions and their change under the global warming scenario. *J. Geophys. Res.* 34: F02S11, doi:10.1029/2006JF000577.
- Sannel, A.B.K. and P. Kuhry. 2008. Long-term stability of permafrost in subarctic peat plateaus, west-central Canada. *Holocene* 18: 589-601.
- Sannel, A.B.K. and P. Kuhry. 2009. Holocene peat growth and decay dynamics in sub-arctic peat plateaus, west-central Canada. *Boreas* 38: 13-24.
- Sannel, A.B.K. and P. Kuhry. 2011. Warming-induced destabilization of peat/thermokarst lake complexes. *J. Geophys. Res.* 116, G03035, doi:10.1029/2010JG001635.
- Saulnier-Talbot, E., M.L. Leng and R. Pienitz. 2007. Recent climate and stable isotopes in modern surface waters of northernmost Ungava Peninsula, Canada. *Can. J. Earth Sci.* 44: 171-180.
- Sazonova, T.S., E.V. Romanovsky, J.E. Walsh, and D.O. Sergueev. 2004. Permafrost dynamics in the 20th and 21st centuries along the East Siberian transect. *J. Geophys. Res.* 109: D01108, doi:10.1029/2003JD003680.

- Sazonova, T.S., V.E. Romanovsky, J.E. Walsh and D.O. Sergueev. 2004. Permafrost dynamics in the 20th and 21st centuries along the East Siberian transect. *J. Geophys. Res.* 109: D01108, doi:10.1029/2003JD003680.
- Schaefer, K., G.J. Collatz, P. Trans, A.S. Denning, I. Baker, J. Berry, L. Prihodko, N. Suits, and A. Philpott. 2008. Combined Simple Biosphere/Carnegie-Ames Stanford Approach (SiBCASA) Model. *J. Geophys. Res.* 113: G03034, doi:10.1029/2007JG000603.
- Schaefer, K., T. Zhang, L. Bruhwiler and A.P. Barrett. 2011. Amount and timing of permafrost carbon release in response to climate warming. *Tellus B* 63: 165-180.
- Schaepman-Strub, G., J. Limpens, M. Menken, H.M. Bartholomeus and M.E. Schaepman. 2009. Towards spatial assessment of carbon sequestration in peatlands: spectroscopy based estimation of fractional cover of three plant functional types. *Biogeosciences* 6: 275-284.
- Schell, D.M. and P. J. Ziemann. 1983. Accumulation of peat carbon in the Alaska arctic coastal plain and its role in biological productivity. Pp. 1105-1110 *in Proc. 4th Inter. Conf. on Permafrost in Fairbanks: Alaska*. Washington, DC. Natl. Acad. Press, Washington DC.
- Schneider, J., G. Grosse and D. Wagner. 2009. Land cover classification of tundra environments in the Arctic Lena Delta based on Landsat 7 ETM+ data and its application for upscaling of methane emissions. *Remote Sens. Environ.* 113: 380-391.
- Schramm, I., J. Boike, W.R. Bolton and L.D. Hinzman. 2007. Application of TopFlow, a spatially distributed hydrological model, to the Imnavait Creek watershed Alaska. *J. Geophys. Res.* 112: G04546, doi:10.1029/2006JGR000326.
- Schreader, C.P., W.R. Rouse, T.J. Griffis, L.D. Boudreau and P.D. Blanken. 1998. Carbon dioxide fluxes in a northern fen during a hot, dry summer. *Global Biogeochem. Cycles* 12: 729-740.
- Schulze, E.D., A. Prokuschkin, A. Arneith, N. Knorre and E.A. Vaganov. 2002. Net ecosystem productivity and peat accumulation in a Siberian aapa mire. *Tellus B* 54: 531-536.
- Schuur, E.A.G., J. Bockheim, J.G. Canadell, E. Euskirchen, C.B. Field, S.V. Goryachkin, S. Hagemann, P. Kuhry, P.M. Lafleur, H. Lee, G. Mazhitova, F.E. Nelson, A. Rinke, V.E. Romanovsky, N. Shiklomanov, C. Tarnocai, S. Venevsky, J.G. Vogel and S.A. Zimov. 2008. Vulnerability of permafrost carbon to climate change: Implications for the global carbon cycle. *BioScience* 58: 701-714.
- Schuur, E.A.G., K.G. Crummer, J.G. Vogel and M.C. Mack. 2007. Plant species composition and productivity following permafrost thaw and thermokarst in Alaskan Tundra. *Ecosystems* 10: 280-292.
- Schuur, E.A.G., J.G. Vogel, K.G. Crummer, H. Lee, J.O. Sickman and T.E. Osterkamp. 2009. The effect of permafrost thaw on old carbon release and net carbon exchange from tundra. *Nature* 459: 556-559.
- Seppälä, M. 1986. The origin of palsas. *Geogr. Ann.* 68: 141-147.
- Seppälä, M. 1990. Depth of snow and frost on a palsa mire, Finnish Lapland. *Geogr. Ann.* 72: 191-201.
- Seppälä, M. 2011. Synthesis of studies of palsa formation underlining the importance of local environmental and physical characteristics. *Quatern. Res.* 75: 366-370.
- Sheng, Y., L.C. Smith, G.M. MacDonald, K.V. Kremenetski, M.L. Konstantine, V. Kremenetski, K.E. Frey, A.A. Velichko, M. Lee, D.W. Beilman and P. Dubinin. 2004. A high-resolution GIS-based inventory of the west Siberian peat carbon pool. *Global Biogeochem. Cycles*. 18: GB3004, doi:10.1029/2003GB00021.
- Shiklomanov, N.I. and F.E. Nelson. 2002. Active-layer mapping at regional scales: A 13-year spatial time series for the Kuparuk region, north-central Alaska. *Permafrost Periglac.* 13: 219-230.
- Shimoyama, K., T. Hiayama, Y. Fukushima and G. Inoue. 2003. Seasonal and interannual variation in water vapour and heat fluxes in a west Siberian continental bog. *J. Geophys. Res.* 108: 4648, doi:10.1029/2003JD003485.
- Shuttleworth, W.J. and J.S. Wallace. 1985. Evaporation from sparse crops – and Energy combination theory. *Quart. J. Roy. Meteorol. Soc.* 111: 839-885.
- Siegel, D.I., P.H. Glaser, J. So and D.R. Janecky. 2006. The dynamic balance between organic acids and circumneutral groundwater in a large boreal peat basin. *J. Hydrol.* 320: 421-431.
- Siegel, D.I., A.S. Reeve, P.H. Glaser and E.A. Romanowicz. 1995. Climate driven flushing of pore water in wetlands. *Nature* 374: 531-533.
- Siltanen, R.M., M.J. Apps, S.C. Zoltai, R.M. Mair and W.L. Strong. 1997. A soil and organic carbon data base for Canadian forest and tundra mineral soils. *Nat. Resour. Can., Can. For. Serv., North. For. Cent., Edmonton, AB.* 50 p.
- Simard, M., P.Y. Bernier, Y. Bergeron, D. Pare and L. Guerin. 2009. Paludification dynamics in the boreal forest of the James Bay Lowlands: effect of time since fire and topography. *Can. J. For. Res.* 39: 546-552.
- Sitch, S., A.D. McGuire, J. Kimball, N. Gedney, J. Gamon, R. Engstrom, A. Wolf, Q. Zhuang, J. Clein and K.C. McDonald. 2007. Assessing the carbon balance of circumpolar arctic tundra using remote sensing and process modeling. *Ecol. Appl.* 17: 213-234
- Smith, L.C., T.M. Pavelsky, G.M. MacDonald, A.I. Shiklomanov and R.B. Lammers. 2007. Rising minimum daily flows in northern Eurasian rivers: A growing influence of groundwater in the high-latitude hydrologic cycle. *J. Geophys. Res.* 112: G04S47, doi:10.1029/2006JG000327.
- Smith, M.W. and D.W. Riseborough. 1996. Permafrost monitoring and detection of climate change. *Permafrost Periglac.* 7: 301-309.
- Smith, M.W. and D.W. Riseborough. 2002. Climate and the limits of permafrost: a zonal analysis. *Permafrost Periglac.* 13: 1-15.
- Smith, S. and M.M. Burgess. 2000. Ground temperature database for northern Canada. *Geol. Surv. Can., Open File Rep.* 3954. 57p.
- Smith, S. and M.M. Burgess. 2004. Sensitivity of Permafrost to climate warming in Canada. *Geol. Surv. Can., Bull.* 579. 24 pp.
- Smith, S.L., V.E. Romanovsky, A.G. Lewkowicz, C.R. Burn, A. Allard, G.D. Clow, K. Yoshikawa and J. Throop. 2010. Thermal state of permafrost in North America: a contribution to the international polar year. *Permafrost Periglac.* 21: 117-135.
- Søegaard, H. and C. Nordstrøm. 1999. Carbon dioxide exchange in a high-arctic fen estimated by eddy covariance measurements and modeling. *Global Change Biol.* 5: 547-562.
- Sofronov, M.A. and A.V. Volokitina. 1986. Ground/peat fires in the south of Western Siberia. *Lesn. Khoz.* 5: 56–58. [English summary in *For. Abstr.*]
- Sonnentag, O., J.M. Chen, D.A. Roberts, J. Talbot, K.Q. Halligan and A. Govind. 2007. Mapping tree and shrub leaf area indices in an ombrotrophic peatland through multiple endmember spectral unmixing. *Remote Sens. Environ.* 109: 342-360.

- Spence, S., W.R. Rouse, D. Worth and C. Oswald. 2003. Energy budget processes of a small northern lake. *J. Hydrometeorol.* 4: 694-701.
- Stadnyk, T., N. St. Amour, N. Kouwen, T.W.D. Edwards, A. Pietroniro and J.J. Gibson. 2005. A groundwater separation study in boreal wetland terrain: The WATFLOOD hydrological model compared with stable isotope tracers. *Isot. Environ. Health Stud.* 41: 49-68.
- Steinberg, M. 2003. Issues of carbon sequestration. *Science* 301: 1326-1326.
- Stendel, M. and J.H. Christensen. 2002. Impact of global warming on permafrost conditions in a coupled GCM. *Geophys. Res. Lett.* 29: doi:10.1029/2001GL014345.
- Stendel, M., V.E. Romanovsky, J.H. Christensen and T. Sazonova. 2007. Using dynamical downscaling to close the gap between global change scenarios and local permafrost dynamics. *Global Planet. Change* 56:203-214.
- Stevens, C.W., B.J. Moorman, S.M. Solomon and C.H. Hugenholtz. 2009. Mapping subsurface conditions within the near-shore zone of an Arctic delta using ground penetrating radar. *Cold Reg. Sci. Technol.* 56:30-38.
- Stewart, R.B. and W.R. Rouse. 1976. A simple method for determining the evaporation from shallow lakes and ponds. *Water Resour. Res.* 12: 623-628.
- Stocks, B. J., J. A. Mason, J. B. Todd, E.M. Bosch, B.M. Wotton, B.D. Amiro, M.D. Flannigan, K.G. Hirsch, K.A. Logan, D.L. Martell and W.R. Skinner. 2003. Large forest fires in Canada, 1959 – 1997. *J. Geophys. Res.* 108: 8149, doi:10.1029/2001JD000484.
- Striegl, R.G., G.R. Aiken, M.M. Dornblaser, P.A. Raymond and K.P. Wickland. 2005. A decrease in discharge-normalized DOC export by the Yukon River during summer through autumn. *Geophys. Res. Lett.* 32: L21413, doi:10.1029/2005GL024413.
- Striegl, R.G., M.M. Dornblaser, G.R. Aiken, K.P. Wickland and P.A. Raymond. 2007. Carbon export and cycling by the Yukon, Tanana, and Porcupine rivers, Alaska, 2001-2005. *Water Resour. Res.* 43: W02411, doi:10.1029/2006WR005201.
- Ström, L. and T.R. Christensen. 2007. Belowground carbon turnover and greenhouse gas exchanges in a sub-arctic wetland. *Soil Biol. Biochem.* 39: 1689-1698.
- Ström, L., M. Mastepanov and T.R. Christensen. 2005. Species-specific effects of vascular plants on carbon turnover and methane emissions from wetlands. *Biogeochemistry* 75: 65-82.
- Sushama, L., R. Laprise and M. Allard. 2006. Modeled current and future soil thermal regime for northeast Canada. *J. Geophys. Res.* 111: D18111, doi:10.1029/2005JD007027.
- Sushama, L., R. Laprise, D. Caya, D. Versegny and M. Allard. 2007. An RCM projection of soil thermal and moisture regimes for North American permafrost zones, *Geophys. Res. Lett.* 34, L20711, doi:10.1029/2007GL031385.
- Suyker, A.E., S.B. Verma and T.J. Arkebauer. 1997. Season-long measurement of carbon dioxide exchange in a boreal fen. *J. Geophys. Res.* 102: 29021-29028.
- Syed, K.H., L.B. Flanagan, P.J. Carlson, A.J. Glenn and K.E. Van Gaalen. 2006. Environmental control of net ecosystem CO₂ exchange in a treed, moderately rich fen in northern Alberta. *Agric. For. Meteorol.* 140: 97-114.
- Takata, K., S. Emori, and T. Watanabe. 2003; Development of the minimal advanced treatments of surface interaction and runoff. *Global Planet. Change* 38: 209-222.
- Tape, K., M. Strum and C. Racine. 2006. The evidence for shrub expansion in northern Alaska and the pan-arctic. *Global Change Biol.* 12: 686-702.
- Tarnocai, C. 1998. The amount of organic carbon in various soil orders and ecological provinces in Canada. Pp. 81–92 in Lal, R., Kimble, J.M., Follett, R.L.F. and Stewart, B.A. (eds.). *Soil Processes and the Carbon Cycle*. Adv. Soil Sci., CRC Press, New York, NY. 609 p.
- Tarnocai, C. 2006. The effect of climate change on carbon in Canadian peatlands. *Global Planet. Change* 53: 222-232.
- Tarnocai, C. and V. Stolbovov. 2006. Northern peatlands: their characteristics, development and sensitivity to climate change. Pp. 17-51 in Martini, I.P., Martinez Cortizas, A., Kessworth, W. (eds.). *Peatlands: Evolution and Records of Environmental and Climate Changes*. Elsevier, London, UK.
- Tarnocai, C., I.M. Kettles and B. Lacelle. 2000. Peatlands of Canada Map. *Nat. Resour. Can., Geol. Surv. Can., Ottawa, ON*. Open File 3834. Scale 1:6 500 000.
- Tarnocai, C., C.-L. Ping and J. Kimble. 2007. Carbon cycles in the permafrost region of North America. Pp. 127-138 in King, A.W., Dilling, L., Zimmerman, G.P., Fairman, D.M., Houghton, R.A., Marland, G., Rose, A.Z., Wilbanks, T.J. (eds.). *The First State of the Carbon Cycle Report (SOCCR): The North American Carbon Budget and Implications for the Global Carbon Cycle*. A Report by the U.S. Climate Change Science Program and the Subcommittee on Global Change Research National Oceanic and Atmospheric Administration, Natl. Climatic Data Cent., Asheville, NC. 239 p.
- Tarnocai, C., J.G. Canadell, E.A.G. Schuur, P. Kuhry, G. Mazhitova and S. Zimov. 2009. Soil organic carbon pools in the northern circumpolar permafrost region. *Global Biogeochem. Cycles* 23: GB2023, doi:10.1029/2008GB003327.
- Thibault, S. and S. Payette. 2009. Recent permafrost degradation in bogs of the James Bay area, Northern Québec, Canada. *Permafrost Periglac.* 20: 383-389.
- Thie, J. 1974. Distribution and thawing of permafrost in southern part of discontinuous permafrost zone in Manitoba. *Arctic* 27: 189-200.
- Thomas, V., P. Treitz, D. Jelinski, J. Miller, P. Lafleur and J.H. McCaughey. 2002. Image classification of a northern peatland complex using spectral and plant community data. *Remote Sens. Environ.* 84:83-99.
- Thompson, D.K. and M.-K. Woo. 2009. Seasonal hydrochemistry of a high arctic wetland complex. *Hydrol. Process.* 23: 1397-1407.
- Thormann, M.N., A.R. Szumigalski and S.E. Bayley. 1999. Aboveground peat and carbon accumulation potentials along a bog-fen-marsh wetland gradient in southern boreal Alberta, Canada. *Wetlands* 19: 305-317.
- Thornley, J.H.M. and M.G.R. Cannell. 2001. Soil carbon storage response to temperature: an hypothesis. *Ann. Bot.* 87: 591-598.
- Throop, J., A. G. Lewkowicz and S. L. Smith. 2012. Climate and ground temperature relations at sites across the continuous and discontinuous permafrost zones, northern Canada. *Can. J. Earth Sci.* 49: 1-12.
- Thurman, E.M. 1985. *Organic Geochemistry of Natural Waters*. Kluwer Academic Publishers Group, Dordrecht, NL.
- Toniolo, H., P. Kodial, L.D. Hinzman and K. Yoshikawa. 2009. Spatio-temporal evolution of a thermokarst in interior Alaska. *Cold Reg. Sci. Technol.* 56: 39-49.
- Touzi, R., A. Deschamps and G. Rother. 2007. Wetland characterization using polarimetric RADARSAT-2 capability. *Can. J. Remote Sens.* 33: S56-S67.
- Trettin, C. C., M. Davidian, M.F. Jurgensen and R. Lea. 1996. Organic matter decomposition following harvesting and site preparation of a forested wetland. *Soil Sci. Soc. Am. J.* 60: 1994-2003.

- Trumbore, S.E. and J.W. Harden. 1997. Accumulation and turnover of carbon in organic and mineral soils of the BOREAS northern study area. *J. Geophys. Res.* 102: 28817-28830.
- Turetsky, M.R. 2004. Decomposition and organic matter quality in continental peatlands: The ghost of permafrost past. *Ecosystems* 7: 740-750.
- Turetsky, M.F. and S. Ripley. 2005. Decomposition in extreme-rich fens of boreal Alberta, Canada. *Soil Sci. Soc. Am. J.* 69: 1856-1860.
- Turetsky, M.F. and R.K. Wieder. 2001. A direct approach to quantifying organic matter lost as a result of peatland wild fire. *Can. J. For. Res.* 31: 363-366.
- Turetsky, M. R., W.F. Donahue and B.W. Benscoter. 2011a. Experimental drying intensifies burning and carbon losses in a northern peatland. *Nature Communications* 1523: 1-5.
- Turetsky, M. R., B.D. Amiro, E. Bosch and J.S. Bhatti. 2004. Historical burn area in western Canadian peatlands and its relationship to fire weather indices. *Global Biogeochem. Cycles* 18: 1-9.
- Turetsky, M.R., S.E. Crow, R.J. Evans, D.H. Vitt and R.K. Wieder. 2008a. Trade-offs in resource allocation among moss species control decomposition in boreal peatlands. *J. Ecol.* 96: 1297-1305.
- Turetsky, M. R., E.S. Kane, J.W. Harden, R.D. Ottmar, K.L. Manies, E. Hoy and E.S. Kasischke. 2011b. Recent acceleration of biomass burning and carbon losses in Alaskan forests and peatlands. *Nat. Geosci.* 4: 27-31.
- Turetsky, M.R., M.C. Mack, T.N. Hollingsworth and J.W. Harden. 2010. The role of mosses in ecosystem succession and function in Alaska's boreal forest. *Can. J. For. Res.* 40: 1237-1264.
- Turetsky, M.R., C.C. Treat, M.P. Waldrop, J.M. Waddington, J.W. Harden and A.D. McGuire. 2008b. Short-term response of methane fluxes and methanogen activity to water table and soil warming manipulations in an Alaskan peatland. *J. Geophys. Res. – Biogeo.* 113: G00A10, doi:10.1029/2007JG000496.
- Turetsky, M.T., R. K.Weider, L. Halsey and D.H. Vitt. 2002a. Current disturbance and the diminishing peatland carbon sink. *Geophys. Res. Lett.* 29: 1526, 10.1029/2001GL014000.
- Turetsky, M.R., R.K. Wieder, C.J. Williams and D.H. Vitt. 2000. Organic matter accumulation, peat chemistry, and permafrost thawing in peatlands of boreal Alberta. *Ecoscience* 7: 379-392.
- Turetsky, M.R., R.K. Wieder, D.H. Vitt, R. Evans and K.D. Scott. 2002b. Boreal peatland C fluxes under varying permafrost regimes. *Soil Biol. Biochem.* 34: 907-912.
- Turetsky, M.R., R.K. Wieder, D.H. Vitt, R.J. Evans and K.D. Scott. 2007. The disappearance of relict permafrost in boreal North America: Effects on peatland carbon storage and fluxes. *Global Change Biol.* 13: 1922-1934.
- Turunen, J., N.T. Roulet and T.R. Moore. 2004. Nitrogen deposition and increased carbon accumulation in ombrotrophic peatlands in eastern Canada. *Global Biogeochem. Cycles* 18: GB3002, doi:10.1029/2003GB002154.
- Turunen, J., T. Tahvanainen and K. Tolonen. 2001. Carbon accumulation in west Siberia mires, Russia. *Global Biogeochem. Cycles* 15: 285-296.
- Uhlirova, E., H. Santruckova and S.P. Davidov. 2007. Quality and potential biodegradability of soil organic matter preserved in permafrost of Siberian tussock tundra. *Soil Biol. Biochem.* 39: 1978-1989.
- Ulrich, M., G. Grosse, S. Chabrillat and L. Schirmer. 2009. Spectral characterization of periglacial surfaces and geomorphological units in the Arctic Lena Delta using field spectrometry and remote sensing. *Remote Sens. Environ.* 113: 1220-1235.
- Urban, N.R., E.S. Verry and S.J. Eisenreich. 1995. Retention and mobility of cations in a small peatland: Trends and mechanisms. *Water Air Soil Pollut.* 79: 201-224.
- Valentine, D.W., E.A. Holland and D.S. Schimel. 1994. Ecosystem and physiological controls over methane production in northern wetlands. *J. Geophys. Res.* 99: 1563-1571.
- Vallée, S. and S. Payette. 2004. Contrasted growth of black spruce (*Picea mariana*) forest trees at treeline associated with climate change over the last 400 years. *Arctic Antarct. Alpine Res.* 36: 400-406.
- Vallée, S. and S. Payette. 2007. Collapse of permafrost mounds along a subarctic river over the last 100 years (northern Québec). *Geomorphology* 90: 162-170.
- van Bellen, S., P.L. Dallaire, M. Gameau and Y. Bergeron. 2011. Quantifying spatial and temporal Holocene carbon accumulation in ombrotrophic peatlands of the Eastmain region, Québec, Canada. *Global Biogeochem. Cycles* 25: GB2016, doi:10.1029/2010GB003877.
- van Bellen, S., M. Gameau, A.A. Ali, and Y. Bergeron. 2012. Did fires drive Holocene carbon sequestration in boreal ombrotrophic peatlands of eastern Canada? *Quatern. Res.* 78: 50-79.
- van Breemen, N. 1995. How *Sphagnum* bogs down other plants. *Trends Ecol. Evol.* 10: 270-275.
- van der Werf, G. R., J.T. Randerson, L. Giglio, G.J. Collatz, P.S. Kasibhatla and A.F. Arellano Jr. 2006. Interannual variability in global biomass burning emissions from 1997 to 2004. *Atmos. Chem. Phys.* 6: 3423-3441.
- Van Wijk, M.T., K.E. Clemmensen, G.R. Shaver, M. Williams, T.V. Callahan, F.S. Hapin III, J.H.C. Cornelissen, L. Gough, S.E. Hobbie, S. Jonsson, J.A. Lee, A. Michelsen, M.C. Press, S.J. Richardson and H. Reuth. 2003. Long-term ecosystem level experiments at Toolik Lake, Alaska, and at Abisko, northern Sweden: Generalizations and differences in ecosystem and plant type responses to global change. *Global Change Biol.* 10: 105-123.
- Vardy, S.R., B.G. Warner and T. Asada. 2005. Holocene environmental change in two polygonal peatlands, south-central Nunavut, Canada. *Boreas* 34: 324-334.
- Vardy, S.R., B.G. Warner, J. Turunen and R. Aravena. 2000. Carbon accumulation in permafrost peatlands in the Northwest Territories and Nunavut, Canada. *Holocene* 10: 273-280.
- Vitt, D.H. and W.-L. Chee. 1990. The relationships of vegetation to surface water chemistry and peat chemistry in fens of Alberta, Canada. *Vegetatio* 89: 87-106.
- Vitt, D.H., L.A. Halsey and S.C. Zoltai. 1994. The bog landforms of continental western Canada in relation to climate and permafrost patterns. *Arctic Alpine Res.* 26: 1-13.
- Vitt, D.H., L.A. Halsey and S.C. Zoltai. 2000a. The changing landscape of Canada's western boreal forest: the current dynamics of permafrost. *Can. J. For. Res.* 30: 283-287.
- Vitt, D.H., L.A. Halsey, I.E. Bauer and C. Campbell. 2000b. Spatial and temporal trends in carbon storage of peatlands of continental western Canada through the Holocene. *Can. J. Earth Sci.* 37: 683-693.

- Vitt, D.H., K. Wieder, L.A.Halsey and M. Turetsky. 2003. Response to *Sphagnum fuscum* to nitrogen deposition: a case study of Ombrogenous peatlands in Alberta, Canada. *Bryologist* 106: 235-245.
- Vitt, D.H., R.K. Wieder, K.D. Scott and S. Faller. 2009. Decomposition and peat accumulation in rich fens of boreal Alberta, Canada. *Ecosystems* 12: 360-373.
- Vogelmann, J.E. and B.N. Rock. 1986. Assessing forest decline in coniferous forests of Vermont using NS-001 Thematic Mapper Simulator data. *Int. J. Remote Sens.* 7: 1303-1321.
- Vourlitis, G.L. and W.C. Oechel. 1997. Climate change in northern latitudes: alterations in ecosystem structure and function and effects on carbon sequestration. Pp. 381-401 in Oechel, W.C., Callaghan, T., Gilmanov, T., Holten, J.I., Maxwell, B., Molau, U., Sveinbjörnsson, B. (eds.). *Global Change and Arctic Terrestrial Ecosystems*. Springer, Berlin. 493 p.
- Waddington, J.M. and N.T. Roulet. 2000. Carbon balance of a boreal patterned peatland. *Global Change Biol.* 6: 87-97.
- Waddington, J.M., T.J. Griffis and W.R. Rouse. 1998. Northern Canadian wetlands: Net ecosystem CO₂ exchange, and climatic change. *Clim. Change* 40: 267-275.
- Wagner, D., A. Lipski, A. Embacher and A. Gättinger. 2005. Methane fluxes in permafrost habitats of the Lena Delta: effects of microbial community structure and organic matter quality. *Environ. Microbiol.* 7: 1582-1592.
- Waldron, S., H. Flowers, C. Arlaud, C. Bryant and S. McFarlane. 2009. The significance of organic carbon and nutrient export from peatland-dominated landscapes subject to disturbance, a stoichiometric perspective. *Biogeosciences* 6: 363-374.
- Walker, D.A., G.J. Jia, H.E. Epstein, M.K. Reynolds, F.S. Chapin III, C. Copass, L.D. Hinzman, J.A. Knudson, H.A. Maier, G.J. Michaelson, F. Nelson, C.L. Ping, V.E. Romanovsky and N. Shiklomanov. 2003. Vegetation soil thaw depth relationships along a low Arctic bioclimate gradient, Alaska: Synthesis of information from the ATLAS studies. *Permafrost Periglac.* 14: 103-123.
- Wallén, B. and N. Malmer. 1992. Distribution of biomass along hummock-hollow gradients: a comparison between a North American and a Scandinavian peat bog. *Acta Soc. Bot. Pol.* 61: 75-87.
- Walter, K.M., S.A. Zimov, J.P. Chanton, D. Verbyla and F.S. Chapin. 2006. Methane bubbling from Siberian thaw lakes as a positive feedback to climate warming. *Nature* 443: 71-75.
- Walvoord, M.A. and R.G. Striegl. 2007. Increased groundwater to stream discharge from permafrost thawing in the Yukon River basin: Potential impacts on later export of carbon and nitrogen. *Geophys. Res. Lett.* 34: L12402, doi:10.1029/2007GL030216.
- Washburn, A.L. 1980. Permafrost features and evidence of climatic change. *Earth-Science Rev.* 15: 327-402.
- Watkins, L. 2011. The forest resources of Ontario. *Ont. Min. Nat. Resour., For. Br., For. Evaluat. Stand. Sect., Sault Ste. Marie, ON.* 307 p.
- Webster, K.L. and J.W. McLaughlin. 2010. Importance of water table in controlling dissolved carbon along a fen nutrient gradient. *Soil Sci. Soc. Am. J.* 74: 2254-2266.
- Webster, K.L. and J.W. McLaughlin. 2011. Carbon cycling. pp 311-321 in *Hudson Plains Ecozone⁺ Status and Trends Assessment*. Canadian Biodiversity: Ecosystem Status and Trends 2010, Technical Ecozone⁺ Report. *Compiled and edited by Abraham, K.M., McKinnon, L.M., Jumeau, Z., Tully, S.M., Walton, L.R., and Stewart, H.M. (lead coordinating authors and compilers). Can. Coun. Resour. Minist., Ottawa, ON.* 445 pp.
- Webster, K.L., J.W. McLaughlin, Y. Kim., M.S. Packalen and C. Li. 2013. Modelling carbon dynamics and respiration to environmental change along a boreal fen nutrient gradient. *Ecol. Model.* 248: 148-164.
- Welp, L.R., J.T. Randerson, J.C. Finlay, S.P. Davydov, G.M. Zimova, A.I. Davydova, and S.A. Zimov. 2005. A high-resolution time series of oxygen isotopes from the Kolyma River: Implications for the seasonal dynamics of discharge and basin-scale water use. *Geophys. Res. Lett.* 32: L14401, doi:10.1029/2005GL022857.
- Weltzin, J.F., S.D. Bridgman, J. Pastor, J. Chen and C. Harth. 2003. Potential effects of warming and drying on peatland community composition. *Global Change Biol.* 9: 141-151.
- Wessel, D.A. and W.R. Rouse. 1994. Modelling evaporation from wetland tundra. *Bound.-Lay. Meteorol.* 68: 109-130.
- Westin, B. and F.S. Zuidhoff. 2001. Ground thermal conditions in a frost crack polygon, a palsa and a mineral palsa (lithalsa) in the discontinuous permafrost zone, northern Sweden. *Permafrost Periglac.* 12: 325-335.
- Whiting, G.J. and J.P. Chanton. 2001. Greenhouse carbon balance of wetlands: Methane emission versus carbon sequestration. *Tellus* 53B: 521-528.
- Whitney, G. G. 1994. *From coastal wilderness to fruited plain: A history of environmental change in temperate North America from 1500 to the present.* Cambridge Univ. Press, New York, NY. 451 p.
- Wickland, K.P., R.G. Striegl, J.C. Neff and T. Sachs. 2006. Effects of permafrost melting on CO₂ and CH₄ exchange of a poorly drained black spruce lowland. *J. Geophys. Res.* 111: G02011, doi:10.1029/2005JG000099.
- Wieder, R. K., K.D. Scott, K. Kamminga, M.A. Vile, D.H. Vitt, T. Bone, B.W. Benscoter and J.A. Bhatti. 2009. Postfire carbon balance in boreal bogs in Alberta, Canada. *Global Change Biol.* 15: 63-81.
- Wilmking, M., J. Harden and K. Tape. 2006. Effect of tree line advance on carbon storage in NW Alaska. *J. Geophys. Res.* 111: GB2023, doi:10.1029/2005JG000074.
- Woo, M.-K. and P.D. DiCenzo. 1989. Hydrology of small tributary streams in a subarctic wetland. *Can. J. Earth Sci.* 26: 1557-1566.
- Woo, M.K. and X.J. Guan. 2006. Hydrological connectivity and seasonal storage change of tundra ponds in a polar oasis environment, Canadian High Arctic. *Permafrost Periglac.* 17: 309-323.
- Woo, M.-K. and K.L. Young. 2006. High arctic wetlands: Their occurrence, hydrological characteristics and sustainability. *J. Hydrol.* 320: 432-450.
- Woo, M.-K., D.L. Kane, S.K. Carey and D. Yang. 2008. Progress in permafrost hydrology in the new millennium. *Permafrost Periglac.* 19: 237-254.
- Wright, J.F., C. Duchesne, F.M. Nixon and M. Cote. 2001. Ground thermal modeling in support of terrain evaluation and route selection in the Mackenzie River Valley. *Geol. Surv. Can., CCAF Project Rep. A073, Nat. Resour. Can.* 53 p.

- Wright, N., M. Hayashi and W.L. Quinton. 2009. Spatial and temporal variations in active layer thawing and their implication on runoff generation in peat-covered permafrost terrain. *Water Resour. Res.* 45: W05414, doi:10.1029/2008WR006880.
- Wright, N., W.L. Quinton and M. Hayashi. 2008. Hillslope runoff from an ice-covered peat plateau in a discontinuous permafrost basin, Northwest Territories, Canada. *Hydrol. Process.* 22: 2816-2828.
- Wu T.H., Q.X. Want, M. Watanabe, J. Chen and D. Battogtokh. 2009. Mapping vertical profile of discontinuous permafrost with ground penetrating radar at Nalaikh depression, Mongolia. *Environ. Geol.* 56: 1577-1583.
- Yavitt, J.B. and M. Seidmann-Zager. 2006. Methanogenic conditions in northern peat soils. *Geomicrobiol. J.* 23: 119-127.
- Yavitt, J.B., C.J. Williams and R.K. Weider. 2000. Controls on microbial production of methane and carbon dioxide in three-Sphagnum-dominated peatland ecosystems as revealed by a reciprocal field or peat transplant experiment. *Geomicrobiol. J.* 17: 61-88.
- Yoshikawa, K., W.R. Bolton, V.E. Romanovsky, M. Fukuda and L.D. Hinzman. 2003. Impacts of wildfire on the permafrost in the boreal forests of interior Alaska. *J. Geophys. Res.* 108: 8148, doi:10.1029/2001JD000438.
- Yu, Z. 2006. Holocene carbon accumulation of fen peatlands in boreal western Canada: A complex ecosystem response to climate variation and disturbance. *Ecosystems* 9: 1278-1288.
- Yu, Z.C., 2012. Northern peatland carbons stocks and dynamics: A review. *Biogeosciences* 9: 4071-4085.
- Yu, Z., I.D. Campbell, C. Campbell, D.H. Vitt, G.C. Bond and M.J. Apps. 2003. Carbon sequestration in western Canadian peat highly sensitive to Holocene wet-dry climate cycles at millennial timescales. *Holocene* 13: 801-808.
- Zhang, K., J.S. Kimball, E.H. Hogg, M. Zhao, W.C. Oechel, J.J. Cassano and S.W. Running, S.W. 2008a. Satellite-based model detection of recent climate driven changes in northern high latitude vegetation productivity. *J. Geophys. Res. – Biogeo.* 113: G03033, doi:10.1029/2007JG000621.
- Zhang, T. 2005. Influence of the seasonal snow cover on the ground thermal regime: An overview. *Rev. Geophys.* 43: 1-23.
- Zhang, T., R.G. Barry and R.L. Armstrong. 2004. Application of satellite remote sensing techniques to frozen ground studies. *Polar Geogr.* 28: 163-196.
- Zhang, Y., W. Chen and J. Cihlar. 2003. A process-based model for quantifying the impact of climate change on permafrost thermal regimes. *J. Geophys. Res.* 108: 4695, doi:10.1029/2002JD003354.
- Zhang, Y., W. Chen and D.W. Riseborough. 2006. Temporal and spatial changes of permafrost in Canada since the end of the Little Ice Age. *J. Geophys. Res.* 111: D22103, doi:10.1029/2006JD007284.
- Zhang, Y., W. Chen and D.W. Riseborough. 2008b. Transient projections of permafrost distribution in Canada during the 21st century under scenarios of climate change. *Global Planet. Change* 60: 443-456.
- Zhang, Y., W. Chen, S.L. Smith, D.W. Riseborough and J. Cihlar. 2005. Soil temperature in Canada during the twentieth century: Complex responses to atmospheric climate change. *J. Geophys. Res.* 110: D03112, doi:10.1029/2004JD004910.
- Zhang, Y., C. Li, C.C. Trettin, H. Li, G. Sun. 2002. An integrated model of soil, hydrology, and vegetation for carbon dynamics in wetland ecosystems. *Global Biogeochem. Cycles* 16:17pp. doi:10.1029/2001GB001838.
- Zhao, L., Q.B. Wu, S. Marchenko and N. Sharkhuu. 2010. Thermal state of permafrost and active layer in central Asia during the international polar year. *Permafrost Periglac. Process.* 21: 198-207.
- Zhuang, Q., V.E. Romanovsky and A.D. McGuire. 2001. Incorporation of a permafrost model into a large-scale ecosystem model: Evaluation of temporal and spatial scaling issues in simulating soil thermal dynamics. *J. Geophys. Res.* 106: 33,649-33,670.
- Zhuang, Q.L., A.D. McGuire, K.P. O'Neill, J.W. Harden, V.E. Romanovsky and J. Yarie. 2002. Modeling soil thermal and carbon dynamics of a fire chronosequence in interior Alaska. *J. Geophys. Res.* 107: 8147 doi:10.1029/2001JD001244.
- Zhuang, Q. L., J.M. Melillo, M.C. Sarofim, D.W. Kicklighter, A.D. McGuire, B.S. Felzer, A. Sokolov, R.G. Prinn, P.A. Steudler and S.M. Hu. 2006. CO₂ and CH₄ exchanges between land ecosystems and the atmosphere in northern high latitudes over the 21st century, *Geophys. Res. Lett.* 33: L17403, doi:10.1029/2006GL026972.
- Zhuang, Q., A.D. McGuire, J.M. Melillo, J.S. Clein, R.J. Dargaville, D.W. Kicklighter, R.B. Myneni, J. Dong, V.E. Romanovsky, J. Harden and J.E. Hobbie. 2003. Carbon cycling in extratropical terrestrial ecosystems of Northern Hemisphere during the 20th century: a modeling analysis of the influences of soil thermal dynamics. *Tellus B* 55: 751-776.
- Zimmerman, R.W. and M.S. King. 1986. The effect of freezing on seismic velocities in unconsolidated permafrost. *Geophysics* 51: 1285-1290.
- Zimmermann, C. and C. Lavoie. 2001. A paleoecological analysis of a southern permafrost peatland, Charlevoix, Québec. *Can. J. Earth Sci.* 38: 909-919.
- Zimov, S.A., E.A.G. Schuur and F.S. Chapin. 2006a. Permafrost and the global carbon budget. *Science* 312: 1612-1613.
- Zimov, S.A., P. Davydov, G.M. Zimova, A.I. Davyova, E.A.G. Schuur, K. Dutta and F.S. Chapin. 2006b. Permafrost carbon: Stock and decomposability of a globally significant carbon pool. *Geophys. Res. Lett.* 33: L20502, doi:10.1029/2006GL02784.
- Zoltai, S.C. 1993. Cyclic development of permafrost in the peatlands of northwestern Alberta, Canada. *Arctic Alpine Res.* 25: 240-246.
- Zoltai, S.C. 1995. Permafrost distribution in peatlands of west-central Canada during the Holocene warm period 6000 years BP. *Géogr. Phys. Quatern.* 49: 45-54.
- Zoltai, S.C. and C. Tarnocai. 1971. Properties of a wooded palsa in northern Manitoba. *Arctic Alpine Res.* 8: 115-129.
- Zoltai, S.C., R.M. Siltanen and J.D. Johnson. 2000. A wetland database for the western boreal, subarctic, and arctic regions of Canada. *Nat. Resour. Can., Can. For. Serv., North. For. Cent. Edmonton, AB. Inf. Rep. NOR-X-368.* 30 p.
- Zoltai, S.C., L.A. Morrissey, G.P. Livingston and W.J. de Groot. 1998. Effects of fires on carbon cycling in North American boreal peatlands. *Environ. Rev.* 6: 13-24.

Climate Change Research Publication Series

Reports

- CCRR-01 Wotton, M., K. Logan and R. McAlpine. 2005. Climate Change and the Future Fire Environment in Ontario: Fire Occurrence and Fire Management Impacts in Ontario Under a Changing Climate.
- CCRR-02 Boivin, J., J.-N. Candau, J. Chen, S. Colombo and M. Ter-Mikaelian. 2005. The Ontario Ministry of Natural Resources Large-Scale Forest Carbon Project: A Summary.
- CCRR-03 Colombo, S.J., W.C. Parker, N. Luckai, Q. Dang and T. Cai. 2005. The Effects of Forest Management on Carbon Storage in Ontario's Forests.
- CCRR-04 Hunt, L.M. and J. Moore. 2006. The Potential Impacts of Climate Change on Recreational Fishing in Northern Ontario.
- CCRR-05 Colombo, S.J., D.W. McKenney, K.M. Lawrence and P.A. Gray. 2007. Climate Change Projections for Ontario: Practical Information for Policymakers and Planners.
- CCRR-06 Lemieux, C.J., D.J. Scott, P.A. Gray and R.G. Davis. 2007. Climate Change and Ontario's Provincial Parks: Towards an Adaptation Strategy.
- CCRR-07 Carter, T., W. Gunter, M. Lazorek and R. Craig. 2007. Geological Sequestration of Carbon Dioxide: A Technology Review and Analysis of Opportunities in Ontario.
- CCRR-08 Browne, S.A. and L.M. Hunt. 2007. Climate Change and Nature-based Tourism, Outdoor Recreation, and Forestry in Ontario: Potential Effects and Adaptation Strategies.
- CCRR-09 Varrin, R. J. Bowman and P.A. Gray. 2007. The Known and Potential Effects of Climate Change on Biodiversity in Ontario's Terrestrial Ecosystems: Case Studies and Recommendations for Adaptation.
- CCRR-11 Dove-Thompson, D. C. Lewis, P.A. Gray, C. Chu and W. Dunlop. 2011. A Summary of the Effects of Climate Change on Ontario's Aquatic Ecosystems.
- CCRR-12 Colombo, S.J. 2008. Ontario's Forests and Forestry in a Changing Climate.
- CCRR-13 Candau, J.-N. and R. Fleming. 2008. Forecasting the Response to Climate Change of the Major Natural Biotic Disturbance Regime in Ontario's Forests: The Spruce Budworm.
- CCRR-14 Minns, C.K., B.J. Shuter and J.L. McDermid. 2009. Regional Projections of Climate Change Effects on Ontario Lake Trout (*Salvelinus namaycush*) Populations.
- CCRR-15 Subedi, N., M. Sharma, and J. Parton. 2009. An Evaluation of Site Index Models for Young Black Spruce and Jack Pine Plantations in a Changing Climate.
- CCRR-16 McKenney, D.W., J.H. Pedlar, K. Lawrence, P.A. Gray, S.J. Colombo and W.J. Crins. 2010. Current and Projected Future Climatic Conditions for Ecoregions and Selected Natural Heritage Areas in Ontario.
- CCRR-17 Hasnain, S.S., C.K. Minns and B.J. Shuter. 2010. Key Ecological Temperature Metrics for Canadian Freshwater Fishes.
- CCRR-18 Scoular, M., R. Suffling, D. Matthews, M. Gluck and P. Elkie. 2010. Comparing Various Approaches for Estimating Fire Frequency: The Case of Quetico Provincial Park.
- CCRR-19 Eskelin, N., W. C. Parker, S.J. Colombo and P. Lu. 2011. Assessing Assisted Migration as a Climate Change Adaptation Strategy for Ontario's Forests: Project Overview and Bibliography.
- CCRR-20 Stocks, B.J. and P.C. Ward. 2011. Climate Change, Carbon Sequestration, and Forest Fire Protection in the Canadian Boreal Zone.
- CCRR-21 Chu, C. 2011. Potential Effects of Climate Change and Adaptive Strategies for Lake Simcoe and the Wetlands and Streams within the Watershed.
- CCRR-22 Walpole, A and J. Bowman. 2011. Wildlife Vulnerability to Climate Change: An Assessment for the Lake Simcoe Watershed.
- CCRR-23 Evers, A.K., A.M. Gordon, P.A. Gray and W.I. Dunlop. 2012. Implications of a Potential Range Expansion of Invasive Earthworms in Ontario's Forested Ecosystems: A Preliminary Vulnerability Analysis.
- CCRR-24 Lalonde, R., J. Gleeson, P.A. Gray, A. Douglas, C. Blakemore and L. Ferguson. 2012. Climate Change Vulnerability Assessment and Adaptation Options for Ontario's Clay Belt – A Case Study.
- CCRR-25 Bowman, J. and C. Sadowski. 2012. Vulnerability of Furbearers in the Clay Belt to Climate Change.
- CCRR-26 Rempel, R.S. 2012. Effects of Climate Change on Moose Populations: A Vulnerability Analysis for the Clay Belt Ecodistrict (3E-1) in Northeastern Ontario.
- CCRR-27 Minns, C.K., B.J. Shuter and S. Fung. 2012. Regional Projections of Climate Change Effects on Ice Cover and Open-Water Duration for Ontario Lakes
- CCRR-28 Lemieux, C.J., P. A. Gray, D.J. Scott, D.W. McKenney and S. MacFarlane. 2012. Climate Change and the Lake Simcoe Watershed: A Vulnerability Assessment of Natural Heritage Areas and Nature-Based Tourism.
- CCRR-29 Hunt, L.M. and B. Kolman. 2012. Selected Social Implications of Climate Change for Ontario's Ecodistrict 3E-1 (The Clay Belt).
- CCRR-30 Chu, C. and F. Fischer. 2012. Climate Change Vulnerability Assessment for Aquatic Ecosystems in the Clay Belt Ecodistrict (3E-1) of Northeastern Ontario.
- CCRR-31 Brinker, S. and C. Jones. 2012. The Vulnerability of Provincially Rare Species (Species at Risk) to Climate Change in the Lake Simcoe Watershed, Ontario, Canada
- CCRR-32 Parker, W.C., S. J. Colombo and M. Sharma. 2012. An Assessment of the Vulnerability of Forest Vegetation of Ontario's Clay Belt (Ecodistrict 3E-1) to Climate Change.
- CCRR-33 Chen, J, S.J. Colombo, and M.T. Ter-Mikaelian. 2013. Carbon Stocks and Flows From Harvest to Disposal in Harvested Wood Products from Ontario and Canada.

52718
(0.2k P.R., 13 05 27)
ISBN 978-1-4606-1438-9 (print)
ISBN 978-1-4606-1439-6 (pdf)